ESD-TDR-64-148
Vol. I

PROCEEDINGS OF THE THIRD TROPOSPHERIC REFRACTION EFFECTS MEETING

(in Two Volumes)

VOLUME I

Results and Status of Tropospheric Effects Measurement Programs

TECHNICAL DOCUMENTARY REPORT NO. ESD-TDR-64-148

NOVEMBER 1964

Prepared for

DIRECTORATE OF AEROSPACE INSTRUMENTATION
ELECTRONIC SYSTEMS DIVISION
AIR FORCE SYSTEMS COMMAND
UNITED STATES AIR FORCE
L. G. Hanscom Field, Bedford, Massachusetts

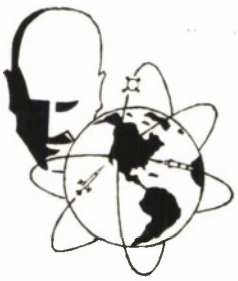

Project 705.1

Prepared by

THE MITRE CORPORATION
Bedford, Massachusetts

Contract AF19(628)-2390
ESD Task No. 5930.07 – 650A

ESD-TDR-64-148
Vol. I

PROCEEDINGS OF THE THIRD TROPOSPHERIC REFRACTION EFFECTS MEETING

(in Two Volumes)

VOLUME I

Results and Status of Tropospheric Effects Measurement Programs

TECHNICAL DOCUMENTARY REPORT NO. ESD-TDR-64-148

NOVEMBER 1964

Prepared for

DIRECTORATE OF AEROSPACE INSTRUMENTATION
ELECTRONIC SYSTEMS DIVISION
AIR FORCE SYSTEMS COMMAND
UNITED STATES AIR FORCE
L. G. Hanscom Field, Bedford, Massachusetts

Project 705.1

Prepared by

THE MITRE CORPORATION
Bedford, Massachusetts

Contract AF19(628)-2390
ESD Task No. 5930.07 – 650A

PROCEEDINGS OF THE THIRD TROPOSPHERIC REFRACTION EFFECTS MEETING

(In Two Volumes)

Volume I

Results and Status of Tropospheric-Effects Measurement Programs

Presented at

The MITRE Corporation
Bedford, Massachusetts

on

July 28, 29 and 30, 1964
(AF Task 5930.07 — 650A)

L. J. Galbiati
Technical Staff
The MITRE Corporation

Capt. E. G. Eames
Task Manager for the Air Force
Electronic Systems Division

FOREWORD

The collection of papers in this publication covers the presentations made at the Third Tropospheric Refraction Effects Meeting, sponsored by the Electronic Systems Air Force Systems Command of the Air Force. It should be noted that since the spcakers wcre limited in time, they would not cover all of the details on their work at that time. The papers contained in this document, in somc cases, extend the details of the oral presentations in that they much more comprehensively treat the topics. Furthermore, the results of the most rccent measurements data have been included where feasible.

The publication of these proceedings does not constitute official Air Force or MITRE endorsement, acceptance, or approval of the techniques proposed and used in the work, or of the results reported. Rather, it is a record of what work was covered, and provides a useful collection of basic data and measurement results to stimulate an exchange of ideas which will advance the state-of-the art. In addition, it serves as a ready reference of the most up-to-date thinking.

I wish to express my appreciation to the representatives of the various agencies for their excellent cooperation, to all the participants of the meeting, and to the Range Measurements Division of the Directorate of Aerospace Instrumentation for suggestions and assistance. I thank the members of the Technical Services and the Radar Systems and Techniques Departments of The MITRE Corporation for the excellent support they have given me during the meeting and in the preparation of this publication. The success of the meeting was greatly enhanced by their assistance. No acknowledgement would be complete without the mention of Mrs. Dorothy Pierce, who typed this document, of Miss Margy Lawlor, who spent many hours in the preparation of the artwork, and to Mrs. Patricia Chatta, who coordinated, planned, edited and guided this documcnt through all stages of its preparation.

L. J. Galbiati,
Chairman

PROCEEDINGS OF THE THIRD TROPOSPHERIC
REFRACTION EFFECTS MEETING

(in Two Volumes)

VOLUME I

Results and Status of Tropospheric Effects Measurement Programs

ABSTRACT

This publication covers the presentations made at the Third Tropospheric Refraction Effects Meeting, sponsored by the Electronic Systems Division of The Air Force Systems Command. The Meeting was held at The MITRE Corporation on July 28, 29 and 30, 1964. The proceedings are being published in two volumes for ease in handling; the papers covering the work on tropospheric refraction sponsored by the Electronic Systems Division in support of metric instrumentation on the national missile ranges, are contained in Volume 1. While these papers are complete in themselves, many of the specific details on the work covered in the proceeding of the second Refraction meeting (ESD-TDR-64-103) have not been repeated. The first volume also contains papers on the Findings and Recommendations of the National Academy of Science "Panel on Tracking Data Analysis" in the Area of Tropospheric Propagation and Refraction, Refractometer and Humidiometer Development of the Naval Research Laboratory, Spaced Refractometer Program of Eastern Test Range, and Canadian Tropospheric Measurement Activities.

Presentations on certain refraction activities at the Pacific Missile Range, the National Bureau of Standards, Ft. Huachuca, Ballistic Research Laboratory, M. I. T. Round Hill, Cold Lake Canada, on new measurement techniques, and on Tropospheric and Ionospheric Effects on Interferometer Systems have been included in Volume II.

REVIEW AND APPROVAL

Publication of this technical documentary report does not constitute Air Force approval of the reports findings or conclusions. It is published only for the exchange and stimulation of ideas.

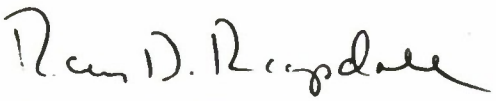

ROY D. RAGSDALE
Col, USAF
Director, Aerospace Instrumentation

CONTENTS

CONTENTS (CONTINUED)

AGENDA

THIRD TROPOSPHERIC REFRACTION EFFECTS MEETING

July 28, 29 and 30, 1964

Gaither Building, Room 1A-401
THE MITRE CORPORATION
Bedford, Massachusetts

DATE AND TIME	SUBJECT AND SPEAKER
July 28, 1964 Morning Session	Dr. L. J. Galbiati, Moderator
8:50	Opening Remarks Col. R. D. Ragsdale
8:55	Introduction Capt. E. G. Eames
9:00	Review of ESD Refraction Task Dr. L. J. Galbiati
9:15	Tropospheric Measurements of MISTRAM Site T. S. Weaver and D. L. Ringwalt
10:05	Digital Atmospheric Profile Generation Dr. R. M. Cunningham
10:25	Scale and Type of Atmospheric Refractive Index Anomalies J. H. Meyer
10:45	ESD Maui, Hawaii, Measurements Dr. M. C. Thompson
11:25	Field Test Results of Line Integral Refractometer H. M. Richardson

DATE AND TIME	SUBJECT AND SPEAKER
Afternoon Session	Dr. A. W. Straiton, Moderator
1:05	Findings and Recommendations of the National Academy of Science "Panel on Tracking Data Analysis" in the Area of Tropospheric Propagation and Refraction Dr. A. T. Waterman, Jr.
1:25	Comparison of Refraction Effects Correction Techniques C. Gardner
1:55	Spaced Refractometer Program at Eastern Test Range Dr. C. F. Martin
2:40	Fabry-Perot Refractometer and Precision Humidiometer Development at the Naval Research Laboratory D. L. Randall
3:15	Canadian Tropospheric Measurement Activities Dr. D. L. Hay
3:45	Response of Microwave Refractometer Cavities to Atmospheric Variations R. E. McGavin
4:00	Tropospheric and Ionospheric Effects on Interferometer Systems S. Newman

DATE AND TIME	SUBJECT AND SPEAKER
July 29, 1964 Morning Session	Dr. W. A. Dryden, Moderator
8:45	Multipath Effects Measurements Results E. W. Heinzerling
9:30	Results of Study of MISTRAM Data-Link Fading H. T. Dougherty
10:15	Some Comments on Microwave Link Characteristics and Problems B. Hadfield
10:30	Ft. Huachuca Atmospheric Refraction Effect Studies A. V. Carlson
11:00	Ballistic Research Laboratory Measurement Range G. Styles
11:25	Ray-Tracings in Cloud Cross Sections for a Long Baseline Interferometer R. K. Crane
12:10	Refraction Correction on C. W. Tracking Systems K. A. Norton

DATE AND TIME	SUBJECT AND SPEAKER
Afternoon Session	Dr. G. D. Sheckels, Moderator
1:20	Experiments at Cold Lake, Canada L. G. Rowlandson
1:50	M. I. T. Round Hill Measurement Results Dr. H. Cramer and J. Tillman
2:35	Refraction Measurements by Lunar Tracking P. Kalaghan
3:05	Progress on Long Path Absorption Refractometer W. G. Tank
3:35	Optical Depolarization and Scintillation Measurements over a Terrestrial Path Dr. J. R. Meyer-Arendt
4:00	Summary of Meeting Dr. L. J. Galbiati

July 30, 1964

Tours and Special Discussions: Arranged by J. T. Willis and T. E. Johnson

OPENING REMARKS: TROPOSPHERIC REFRACTION MEETING

Col. R. D. Ragsdale*

I'm Colonel Ragsdale, Director of Aerospace Instrumentation. I would like to welcome you men this morning to the Third Tropospheric Refraction Effects Meeting. One thing that has become very obvious during my briefings with General Davis of the National Range Division (NRD), and elsewhere around the country, is that everyone is very enthusiastic about the active refraction effects study programs we have at the Electronic Systems Division. Everytime we have briefed General Davis he has commented that this is one of the most important things we can do for him. The NRD staff is very interested in making sure that all the numbers derived by you folks are fed into their error models as soon as possible. They want to make sure that the refraction programs we undertake are related back to measurement accuracy.

I would like to say you are supported very well and at very high levels in your efforts in this refraction business; great things are expected from the effort in this area. I will now turn you over to Captain Eames, who is the Air Force head of the project, and let you get on with your business.

*Director, Aerospace Instrumentation, USAFSC, ESD, L. G. Hanscom Field, Bedford, Massachusetts

INTRODUCTION

Capt. E. G. Eames*

This three-day meeting is unclassified, and has been organized for the primary purpose of presenting you with information on the many significant activities in the area of tropospheric refraction effects. A second purpose is to provide you with the opportunity to meet each other in order to discuss the various aspects of the problem. We have limited the number of presentations at each session in order to provide discussion periods. The Proceedings of the second refraction meeting, held last November, have been distributed to all the attendees of that meeting. Extra copies will be made available in the lobby. Proceedings of this meeting will be distributed to all the attendees at these sessions.

The Directorate of Aerospace Instrumentation's interest in refraction is in line with its mission to support the National Ranges. We are presently funding a continuing comprehensive integrated program with the National Bureau of Standards (NBS), MITRE, and the Air Force Cambridge Research Laboratory (AFCRL).

The objectives are to develop techniques to minimize the refractive effects, determine the extent of the effects on optical systems, obtain real-time correction techniques, and develop noise predictors for tracking systems. Again, the emphasis is on feeding more of the data obtained as direct inputs into the error models in order to derive better corrections to the range systems.

* HQ ESD ESRIM, L. G. Hanscom Field, Bedford, Massachusetts

The program combines three separate approaches; namely, fixed-end point measurements, dynamic measurements at the Eastern Test Range (ETR), and a real-time correction device. I will now turn the meeting over to Dr. L. J. Galbiati, who will give you a more comprehensive description of each of these approaches.

REVIEW OF ESD REFRACTION TASK

L. J. Galbiati*

INTRODUCTION

The total effort under the refraction task at the Electronic Systems Division (ESD) has been divided into three parts; as shown in Fig. 1. While the individual work agents have specific, limited objectives, an effort is made to coordinate and direct tham so as to achieve composite results applicable to the operational problem of the National Range Division (NRD).

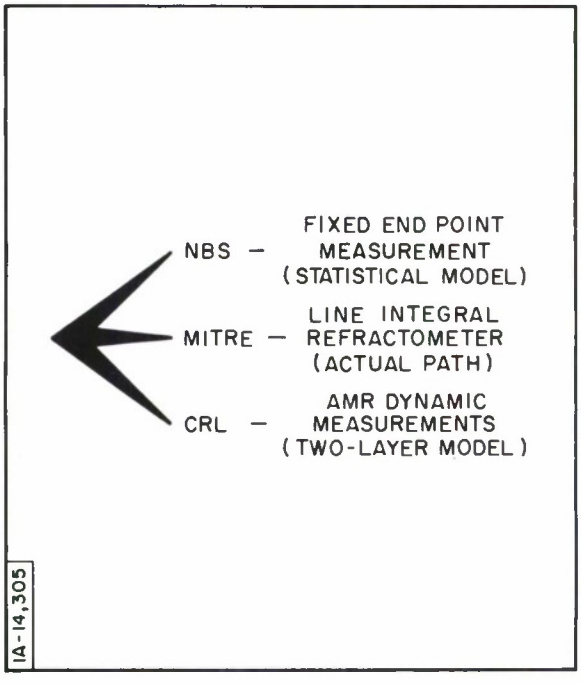

Fig. 1. Overall ESD Task Approach

*The MITRE Corporation, Bedford, Massachusetts

MEASUREMENTS AT THE EASTERN TEST RANGE

Dr. R. M. Cunningham is directing the work being performed for ESD by the Cloud Physics Branch of the Cambridge Research Laboratories (CRL). This effort involves obtaining dynamic meteorological measurements at the MISTRAM site of the Eastern Test Range (ETR), as well as analysis of the data. The data is obtained by use of special instrumented aircraft, radiosonde, wire-sonde, and ground-based meteorological instrumentation. (Fig. 2).

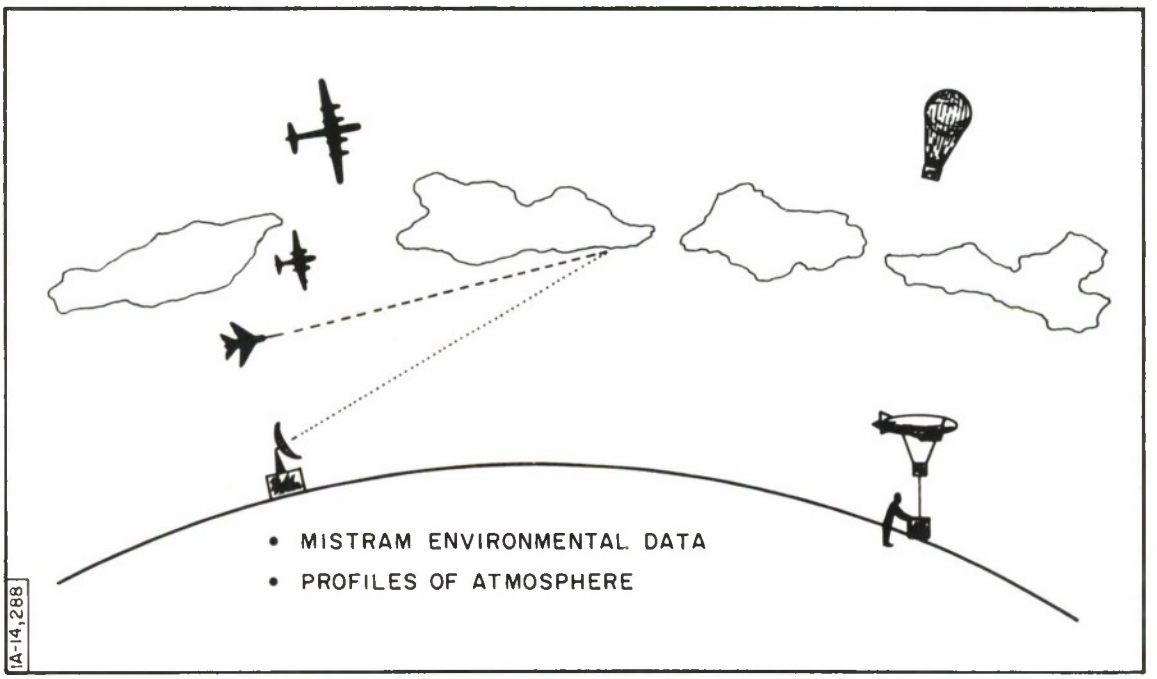

Fig. 2. Cambridge Research Laboratories – Dynamic Measurements

At the previous meeting (November 1963), I indicated that we were evaluating methods of presenting the data in a useful, meaningful fashion. During the past six months, we have concentrated on one unique method; the digital representation of the two-dimensional variations – in-refractivity

profile. The profiles are very difficult to generate in that they require extensive meteorological measurements over the specific terrain of interest, and interpretation of the data obtained by an experienced meteorologist. However profiles for three different days have been generated to date, and the way in which they are being utilized will be covered by R. K. Crane. With these representations, it is possible to use a computer to investigate such effects as the beam-sweeping movement resulting from tracking a moving target, different wind velocities, special meteorological conditions, and different environmental conditions for the individual rays of an interferometer system.

Dr. Dryden, in one of his studies, indicated the effect of a refractivity gradient along the legs of the MISTRAM system, and, from time to time. the validity of using one profile for correcting the entire interferometer system has been questioned. Little progress has been made resolving questions in this area to date; we have, therefore, endeavored to obtain data necessary in arriving at a solution by obtaining simultaneous vertical refractivity profile measurements at MISTRAM Central and MISTRAM end-points, some twenty miles distant, by using three instrumented aircraft. The details on this phase of the program will be covered by D. L. Ringwalt. Later, Dr. Cunningham will discuss the scales and types of atmospheric refractive index anomalies. J. H. Meyer will explain the mechanism of generating the profile, and R. K. Crane will show results of experiments utilizing the digital atmospheric profile. These papers summarize the ETR phase of our program.

FEASIBILITY TEST OF LINE INTEGRAL REFRACTOMETER

The feasibility field tests of the MITRE Line Integral Refractometer (LIR) have included measurements on a number of paths at different elevation angles between 0. 2 and 4. 9 degrees, as indicated by the top diagram in Fig. 3. In November 1963, preliminary results of the measurements on a level path, as

indicated by the bottom sketch in Fig. 3, were presented. This technique, as you may recall, involves the determination of the differential phase between two coherent signals (15. 6 and 31. 2 gc) transmitted over the actual path of interest. The differential phase shift is used to infer the differential transit time of the two signals and, therefore, provides desired information on the line integral of the refractivity; the line integral of refractivity is the correction one has to make to metric tracking system measurements.

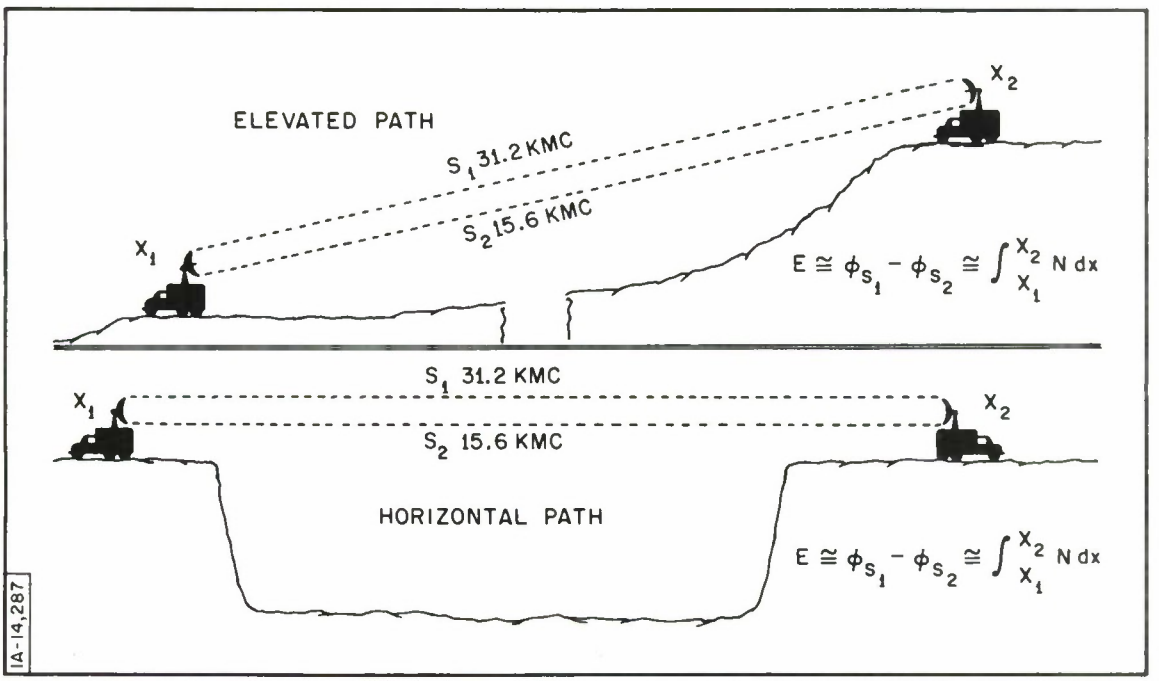

Fig. 3. MITRE – Line Integral Refractometer Technique

The sensitivity of the measurement instrumentation developed in this task has been very satisfactory, and the field measurements are the only ones of this type to my knowledge. H. M. Richardson will describe details of field tests. He will interpret the results in terms of tracking requirements and applicability to the general problem of the line-of-sight path corrections.

Future (early 1965) plans for this effort include measurements to determine the effect of the oxygen constituent in the transmission path. These will be obtained by measuring the differential phase of another pair (45 and 90 gc) of coherent signal frequencies bracketing the oxygen absorbtion region. The complete water vapor-oxygen refractometer should be tested sometime during the first-half of 1965.

One of the basic differences between the LIR measurement and the National Bureau of Standards (NBS) radio frequency phase measurements should be pointed out. The LIR measures the differential phase shift between two coherent signals at different frequencies (15. 6 and 31. 2 gc), whereas the NBS system measures the phase shift of a signal at one frequency (9. 4 gc). This difference in technique results in system where the end-points of the LIR do not have to be fixed and, therefore, can be mounted on an aircraft (see Fig. 4). No arrangements have been made to do so under the current

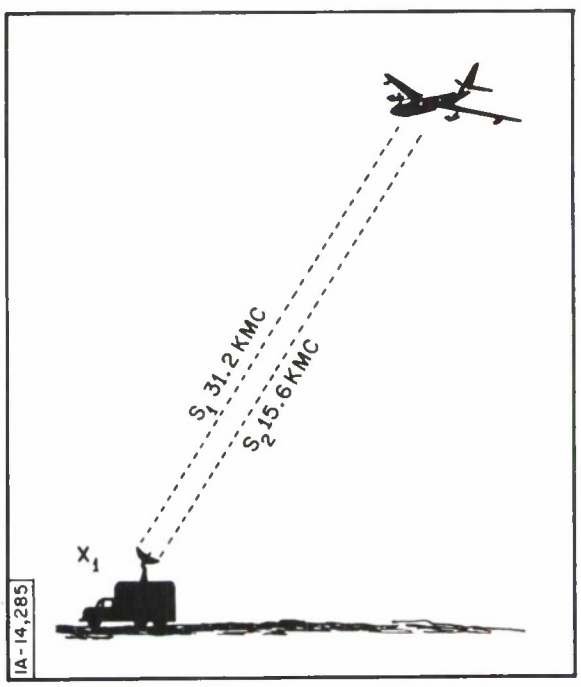

Fig. 4. MITRE – Line Integral Refractometer Technique

program. The NBS system, on the other hand requires fixed end-points to separate out a very small portion of the total effect. The LIR is the only potentially practical technique available for obtaining meaningful data on the actual microwave refractivity characteristics of the entire atmospheric path for a wide range of elevation angles.

OPTICAL AND RADAR FREQUENCY ACTIVITY

The ESD refraction activities at NBS includes work at both optical and radio frequencies (Fig. 5). We have consolidated the data requirements for different items of range instrumentation in which ESD is involved, and have outlined work statements which provide all the necessary information, but keep the number of separate measurement efforts at a minimum. That is, each phase of the NBS work does not necessarily reflect the problem associated with only one specific metric system.

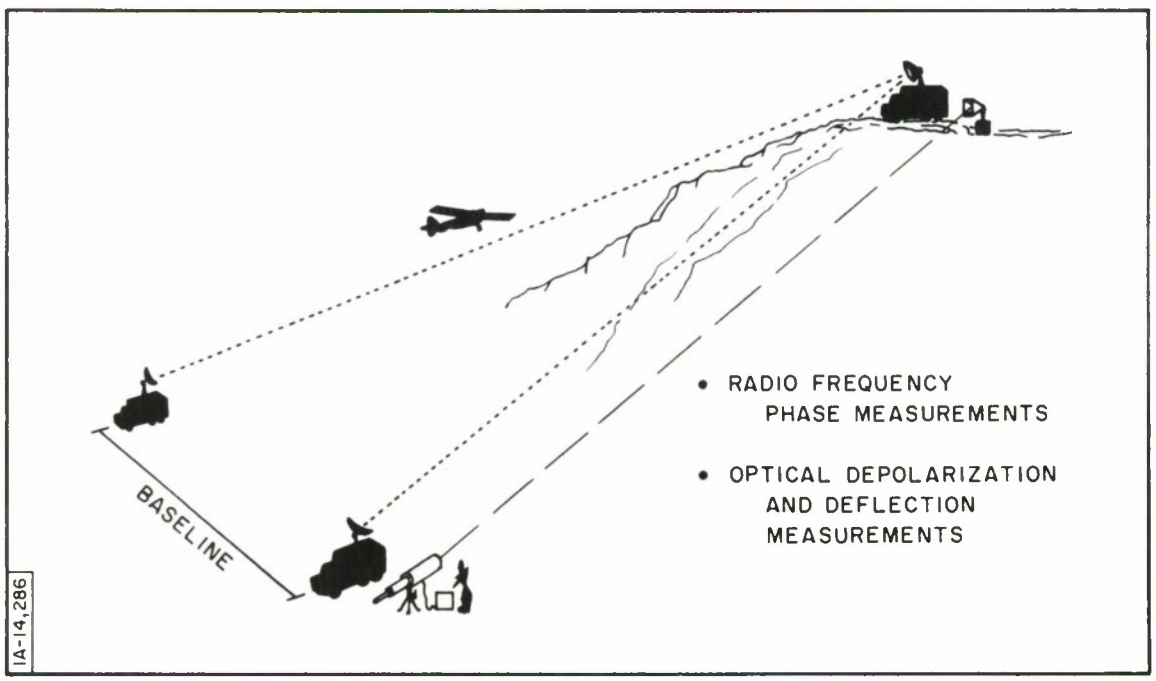

Fig. 5. National Bureau of Standards – Fixed End-Point Technique

The fixed end-point radio frequency phase measurement program field work at Maui, Hawaii has been completed and will be covered by Dr. M. C. Thompson. Optical depolarization measurements have been performed and will be reported on by Dr. J. R. Meyer-Arendt; this work was initiated about a year ago, and includes the literature survey report which is being published by NBS. The conclusions of this survey were published in the Proceedings of the second meeting. * Early this year, NBS was requested to study the problem of fading on the MISTRAM data links. They have been studying the MISTRAM records, and H. T. Dougherty will report their findings and recommendations.

SUMMARY

The details covering the history, objectives, and organization of the overall refraction task are covered in the Proceedings** of the second meeting, and will not be repeated in this publication. Papers on the results and progress achieved during the past six months on each phase of the ESD program will be presented by the individuals responsible for the work.

We have, in this short period of time, been able to instrument aircraft and collect valuable data at the Eastern Test Range. We have generated the first two-dimensional digital atmospheric profile, applied it to an operational system, and estimated atmospheric errors. The instrumentation for determining differential phase data between 15.6 and 31.2 gc signals has been developed, and the first long path field measurements have been completed. The feasibility testing of the line integral refractometer to date strongly indicates its high value as a calibration tool.

*See ESD-TDR-63-103, Vol. I, pages 1-131 to 1-142.

**ESD-TDR-64-103, Vols. I, II and III.

The comprehensive series of phase measurements at Maui, Hawaii, have been completed. These include the extensive set of measurements with refractometers spaced at considerable distances. Publications related to the work conducted under this program include:

Effects of Clouds and Moist Layer Roughness on Range Rate Errors of Radio Interferometer Tracking and Guidance Systems, AFCRL-63-706;

Instrumentation to Measure the Effect of Meteorological Parameters on the MISTRAM System and Preliminary Data Reduction, CRL Memo 11/3;

Line Integral Refractometer, MITRE Report SR-112;

Optical Scintillation, NBS Tech. Note No. 225; and

Proceedings of the Second Tropospheric Refraction Effects Meeting, ESD-TDR-64-103, Vols. I, II and III.

The investigators should be commended for the outstanding cooperation they have given me toward achievement of the overall technical objectives of this ESD task. We initiated a rather extensive measurement program, and have accumulated much experimental data directly related to the refraction problem. Hence, a continuous flow of results can be anticipated over the next year or so from the analysis of the data we have collected under this program.

SIMULTANEOUS REFRACTIVE INDEX MEASUREMENTS BY THREE AIRCRAFT

T. S. Weaver and D. L. Ringwalt*

INTRODUCTION

On 16 and 17 June 1964, three aircraft, equipped with refractometers, obtained simultaneous refractive index measurements in the MISTRAM area while flying a tight V-formation, and also while separated by about 20 miles. These measurements were obtained in preparation for and in order to determine the problems involved in more extensive tests planned for early August. This work, carried out at Patrick Air Force Base (PAFB), is part of an atmospheric research program aimed specifically toward improving the tracking accuracy of MISTRAM. The data to be presented has not been completely checked and consequently, the results should be considered as preliminary.

PURPOSE

The primary purpose of these tests was to determine the feasibility of airborne intercomparison and calibration of the refractometers aboard three separate aircraft. This intercomparison and calibration is necessary if accurate simultaneous refractive index measurements are to be obtained in the MISTRAM area by the three aircraft during the planned intensive measurements in August. The August measurements will be used as inputs to MISTRAM error model computations.

*Electromagnetic Research Corporation, College Park, Maryland

A secondary purpose was to obtain soundings, at MISTRAM Central and at the outlying 100 K. West and 100 K. South sites, of the type that will be obtained in August, to learn of possible operational or technical difficulties.

EQUIPMENT

Three aircraft were used for the tests:

(a) Aircraft No. 30133, a C-130, equipped with a Texas-type refractometer and extensive meteorological equipment;

(b) Aircraft No. 37802, a C-131, equipped with an ASH-14 refractometer; and

(c) Aircraft No. 37794, a C-131, equipped with a Texas-type refractometer and other meterological equipment.

In addition to the three aircraft, the facilities of the Pan American Airways (PAA) weather station at MISTRAM Central were used for radiosonde and wire-sonde measurements.

EXPERIMENTS

A number of experiments or calibrations were conducted. The aircraft maneuvers are described in the next section. Each of the experiments listed on the following page, along with the results, is discussed later in the report. The experiments consisted of refractive index measurements in the three aircraft as they

(a) made simultaneous ascents and descents while flying in a V-formation,

(b) made simultaneous ascents over MISTRAM Central, 100 K. West and 100 K. South, and

(c) flew in a level flight in V-formation.

FLIGHT PLAN

The same flight plan was used on both days. All three aircraft departed form PAFB. The C-130 aircraft (133) climbed to 25,000 feet, while both C-131 aircraft (794 and 802) climbed to 15,000 feet. About 16 miles ENE of MISTRAM Central, 133 descended to 15,000 feet to join the other two aircraft.

After approximately 5 minutes of level flight at 15,000 feet, 802 took the lead of a V-formation, with 794 to port and 133 to starboard. The aircraft commenced a 4-minute holding pattern, with standard rate turns, on a heading of 340/160 degrees and at a position about 16 miles ENE of MISTRAM Central. While maintaining this pattern, all aircraft descended in formation to 500 feet, at approximately 1000 feet per minute, with 802 calling out altitude on the VHF radio at 1000-foot intervals.

All aircraft maintained the 500-foot altitude for 5 minutes and then started to ascend at 500 feet per minute, maintaining the 4-minute holding pattern during the ascent until an altitude of 15,000 feet was reached. The 802 continued to call out altitude at 1000-foot intervals. Maintaining 15,000 feet, 133 proceeded to 100 K. West, 794 to MISTRAM Central, and 802 to 100 K. South.

At a time indicated by 133, each aircraft began to descend at 1000 feet per minute, using a figure-eight pattern centered on the respective MISTRAM stations. The figure-eight track was centered on a 340/160-degree line, with turns beginning 2 minutes after the aircraft passed over the MISTRAM stations. After reaching an altitude of 500 feet over the MISTRAM sites, all aircraft proceeded to a point approximately 10 miles downwind from MISTRAM Central while climbing to 2000 feet.

With 802 as the lead aircraft in a V-formation, and with 794 to port and 133 to starboard, the aircraft flew toward the wiresonde balloon (at MISTRAM

Central) which was flying at about 2000 feet. The 794 and 802 turned left approximately one-half mile from the balloon, while 133 passed as close as practical to the balloon. All aircraft rendezvoused at a point 10 miles downwind from MISTRAM Central to repeat the run.

MISTRAM Central reported winds at 2000 feet as light and variable on both days. As a result, the following tracks were flown:

June 16

Track No. 1 — 240 degrees to MISTRAM Central at 1900 feet;

Track No. 2 — 252 to 240 degrees to MISTRAM Central at 1900 feet;

Track No. 3 — 340 degrees to MISTRAM Central at 1900 feet;

Track No. 4 — 45 degrees to MISTRAM Central at 1900 feet.

June 17

Track No. 1 — 30 degrees to MISTRAM Central at 2000 feet;

Track No. 2 — 270 degrees to MISTRAM Central at 2000 feet;

Track No. 3 — 40 degrees to MISTRAM Central at 2000 feet.

OPERATIONS

No serious operational problems were encountered in flying the three aircraft in the tight V-formation, or in making simultaneous descents with the aircraft about 20 miles apart. The greatest difficulty was in the post-flight correlation of the data. A better method, either manual or automatic, is needed to mark all recordings simultaneously with, for instance, time, for future correlation of events.

FORMATION ASCENTS AND DESCENTS

The formation ascents and descents of the three aircraft between 15,000 and 500 feet were made at sea about 16 miles ENE of MISTRAM Central, where atmospheric conditions were relatively stable and where good correlation of the refractive index data from the three aircraft could be expected. If the atmosphere is assumed homogeneous over at least the volume in which the three aircraft are flying, then any lack of correlation between the values of refractive index recorded in the three aircraft may be ascribed to instrumentation differences.

The air temperature difference between 15,000 and 500 feet was about 27 degrees C. By first descending to warmer air and then ascending to the colder air, temperature effects upon the refractometer measuring cavity are cycled. Assuming the 15,000-foot value of refractive index does not vary in the time between the descent from and the return to 15,000 feet, then any difference in the indicated value of refractive index before the descent and after the ascent is a measure of the hysteresis of the measuring cavity.

Aircraft barometric type altimeters "lag" the actual altitude during ascents and descents, depending upon the rate of ascent or descent. During an ascent, the altimeter will indicate an altitude lower than actual pressure altitude, with greater differences being indicated for rapid ascents. Similarly, the altimeter will indicate a higher altitude than actual pressure altitude during descent, with greater differences being indicated for more rapid descents.

Corrections for altimeter lag have not been made in the data to be shown in the figures. Since 802 announced the altitude at 1000-foot intervals, the data for each aircraft has been plotted to the same scale. However, it should be noted that, because of the altimeter lag problem, any particular altitude as plotted will not only differ from the true pressure altitude, but will also differ

for the ascent and descent. The overall effect of this is to shift, in indicated altitude, a particular refractive index perturbation between ascent and descent.

Although corrections for altimeter lag have not been made in the data plots, such corrections are possible and will be made at a later date in the following manner: Both 133 and 794 made comparisons of the altitude, as indicated on both the barometric altimeter and the radar altimeter, during the ascents and descents. Since the radar altimeter has no lag characteristics, it is thus possible to correct all altitudes to a common and true altitude scale.

The 133 and 794 have refractometer systems modified in a manner described by Shaw. This modification removes, almost entirely, drifts in the system output, except those due to cavity characteristics. The modification also includes provisions for precision calibration in 25 N-unit steps. The calibration of the 802 refractometer is accomplished by noting the difference in the indicated refractive index while adjustments are made to a calibrated micrometer tuning screw on the reference cavity.

Inspection of the 802 records for 17 June immediately after the flight indicated that an obvious and large change in calibration had occurred. A new scale (N-units/unit recorder deflection) was constructed by comparison with the 133 data. No claim is made that this correction is proper, only that the corrected scale is "reasonable." This fact must be kept in mind during inspection of the data.

Figures 1 and 2 show the over-water descents and ascents of each aircraft. The following procedure was used in plotting these descents and ascents: In all plots, the absolute value of refractive index at 15,000 feet was normalized to the radiosonde value obtained at MISTRAM Central nearest the time of the flight. The radiosonde data is plotted at the right in Figs. 1 and 2.

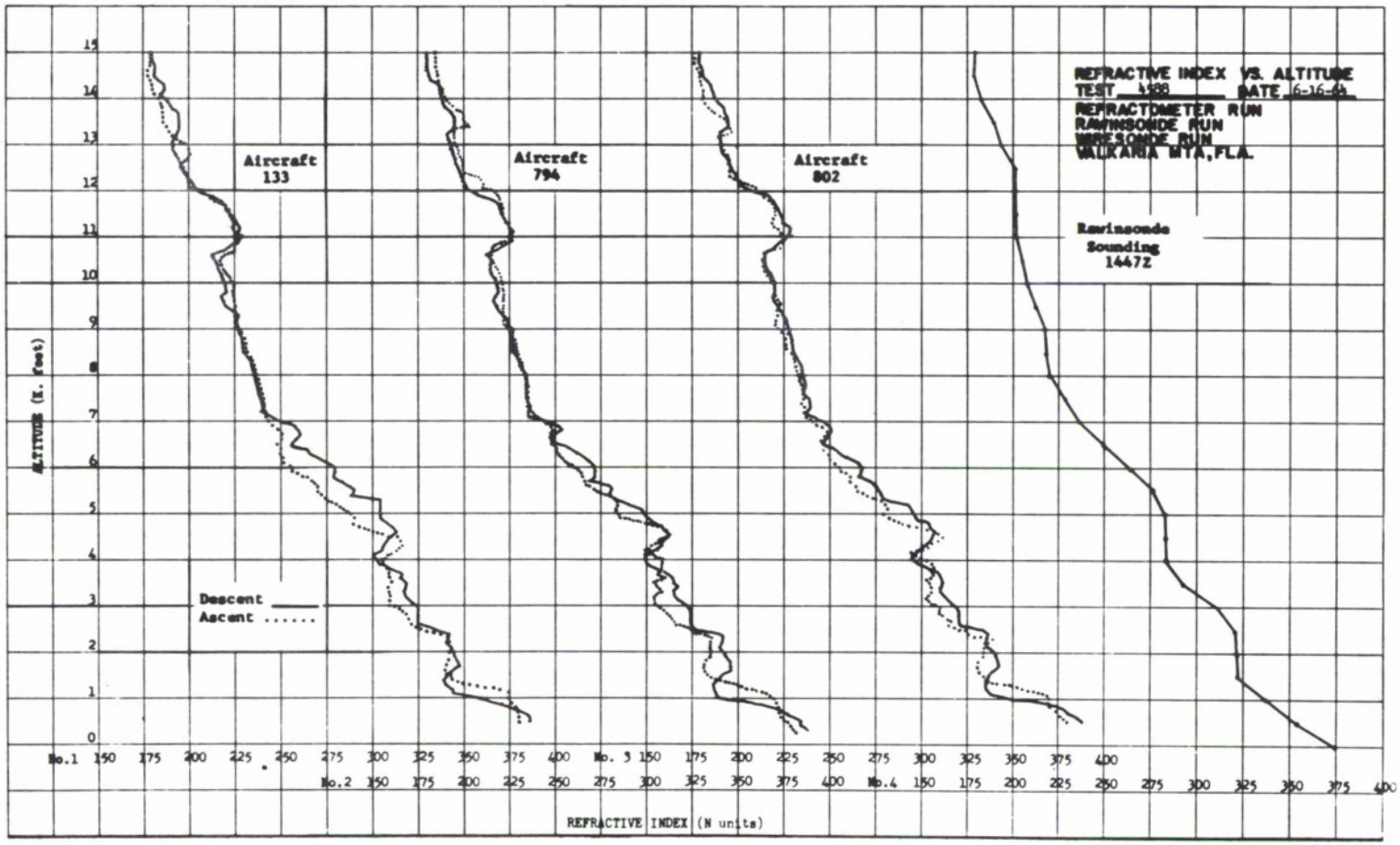

Fig. 1. Ascents vs. Descents, 16 June 1964

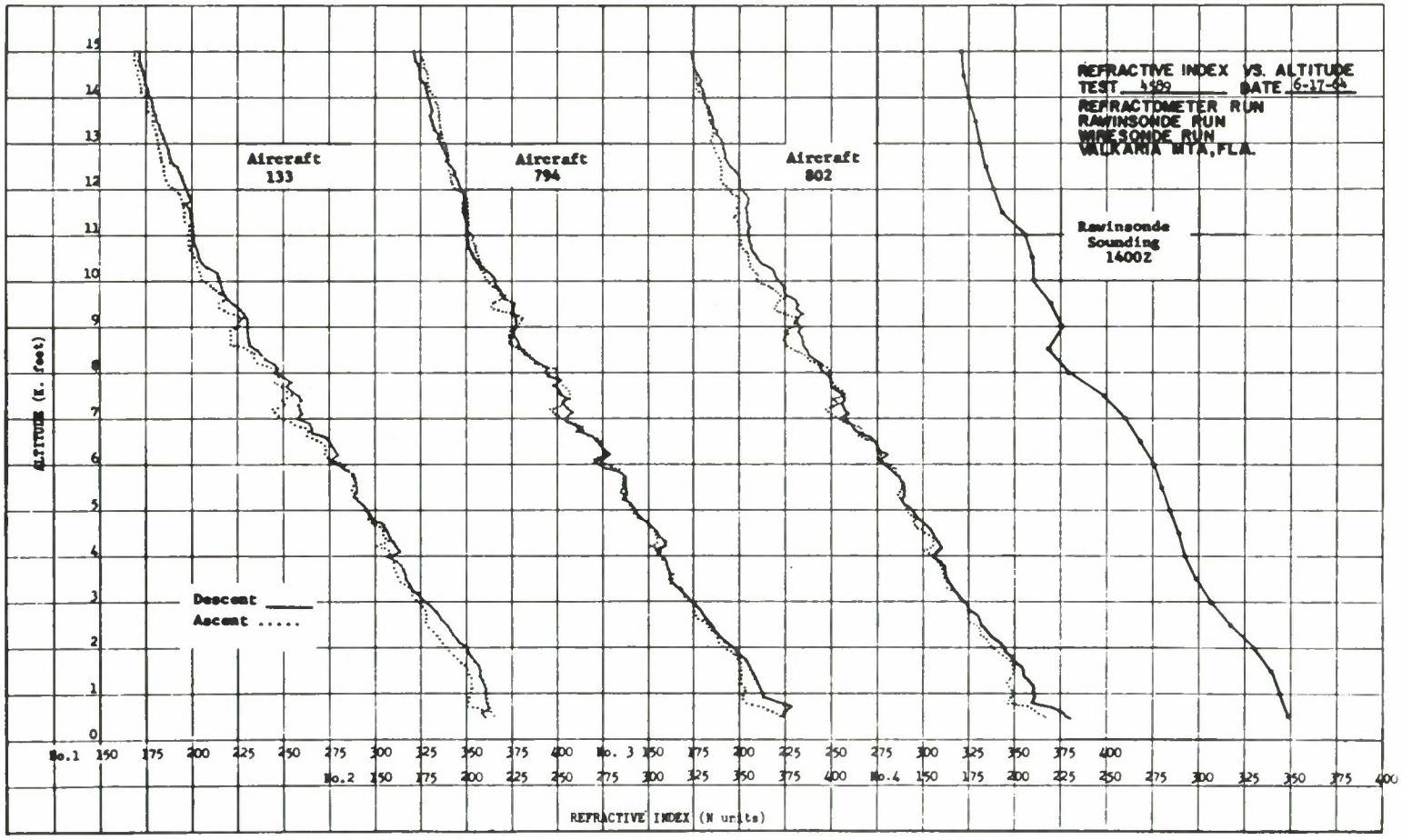

Fig. 2. Ascents vs. Descents, 17 June 1964

Because of separation between MISTRAM Central and the operating area, no particular detailed correlation with the aircraft data is expected. The aircraft descents were plotted and then, without changing the scale, the ascents were plotted. If it is assumed that the atmosphere did not change, the refractive index indication should return to the initial value at 15,000 feet. It is seen that the refractive index value at 15,000 feet does return to the initial value within 3 to 4 N-units for all aircraft on both days of operation.

Inspection of the profiles for 16 June shows first that this was not a particularly good day for the measurements. This kind of test requires a "smooth" atmosphere, and the profiles show that this was not the situation, particularly below about 7000 feet. Considering that no corrections have been made to the data for either cavity or altimeter characteristics and that the atmosphere was not "smooth," the ascents and descents for the three aircraft compare quite well. Note particularly the region between about 6000 feet and 12,000 feet. In this region, all three aircraft retraced their profiles within 3 to 4 N-units.

Deviations between ascents and descents below 7000 feet are often correlated among the three aircraft. The indicated roughness of the atmosphere probably is responsible for some of the differences between aircraft, even though they were flying in a tight V-formation. The profiles obtained on 17 June show somewhat better agreement between ascents and descents, since the atmosphere was appreciably smoother on that day than on 16 June. When altimeter lag corrections are made to the data, their effect will be to "lift" the whole trace for the ascent and to "lower" the whole trace for the descent.

A better comparison of the data from the three aircraft, is shown in Fig. 3. The plots of the data obtained while the three aircraft made ascents and descents in formation are superimposed. Figures 1 and 2 might be considered

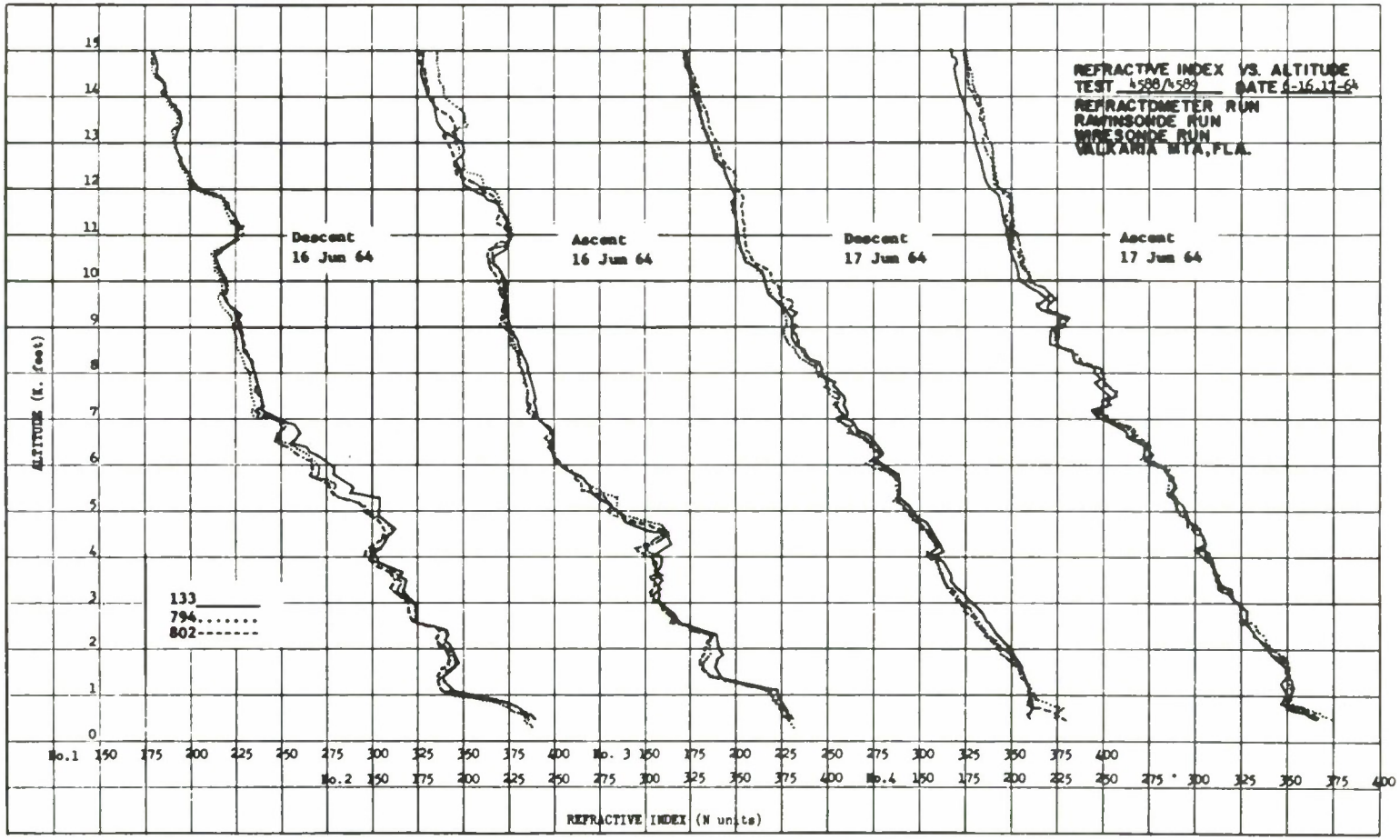

Fig. 3. Formation Ascents and Descents, 133 vs. 794, vs. 802

as internal comparisons, while Fig. 3 is a true comparison of the three aircraft installations. Altimeter lag, due to the method of logging altitude in each aircraft, will not affect the comparisons of Fig. 3.

As explained earlier, the 802 data used the 133 data for calibration, and, for this reason, better correlation should be expected between 133 and 802 than between 133 and 794. This, however, is not obvious in Fig. 3. The tendency for 794 to indicate lesser values of refractivity than 133 might be due to the method of normalizing the data to the radiosonde value at 15,000 feet on descents.

The differences between the various profiles are displayed in Fig. 4; some features already noted are shown clearly. The differences between the 133 data and that for the 794 and 802 have been plotted against altitude for the descents on both days. The differences are less at the higher altitudes where the atmosphere is smoother. The plots suggest that the 794 and 802 data are better correlated than the 133 and 794 or the 133 and 802 data. This observation is made by noting the similarity in the shapes of the two plots for 16 June and the two plots for 17 June.

It must be kept in mind that this experiment and these data reductions have been performed to determine the problems involved in obtaining several simultaneous profile measurements, using several aircraft. These profiles will then be used in MISTRAM error model calculations. The profile data shown in Figs. 1 to 3 should be compared in a manner directly applicable to this problem. The error model will make use of the propagation delay of a radio signal, relative to propagation in a vacuum, through the atmosphere, as described by refractivity profiles. Table 1 lists the delays for vertical propagation to an altitude of 15,000 feet. Delays for propagation to the same altitude at other elevation angles may be determined by multiplying the indicated values by the cosecant of the elevation angle.

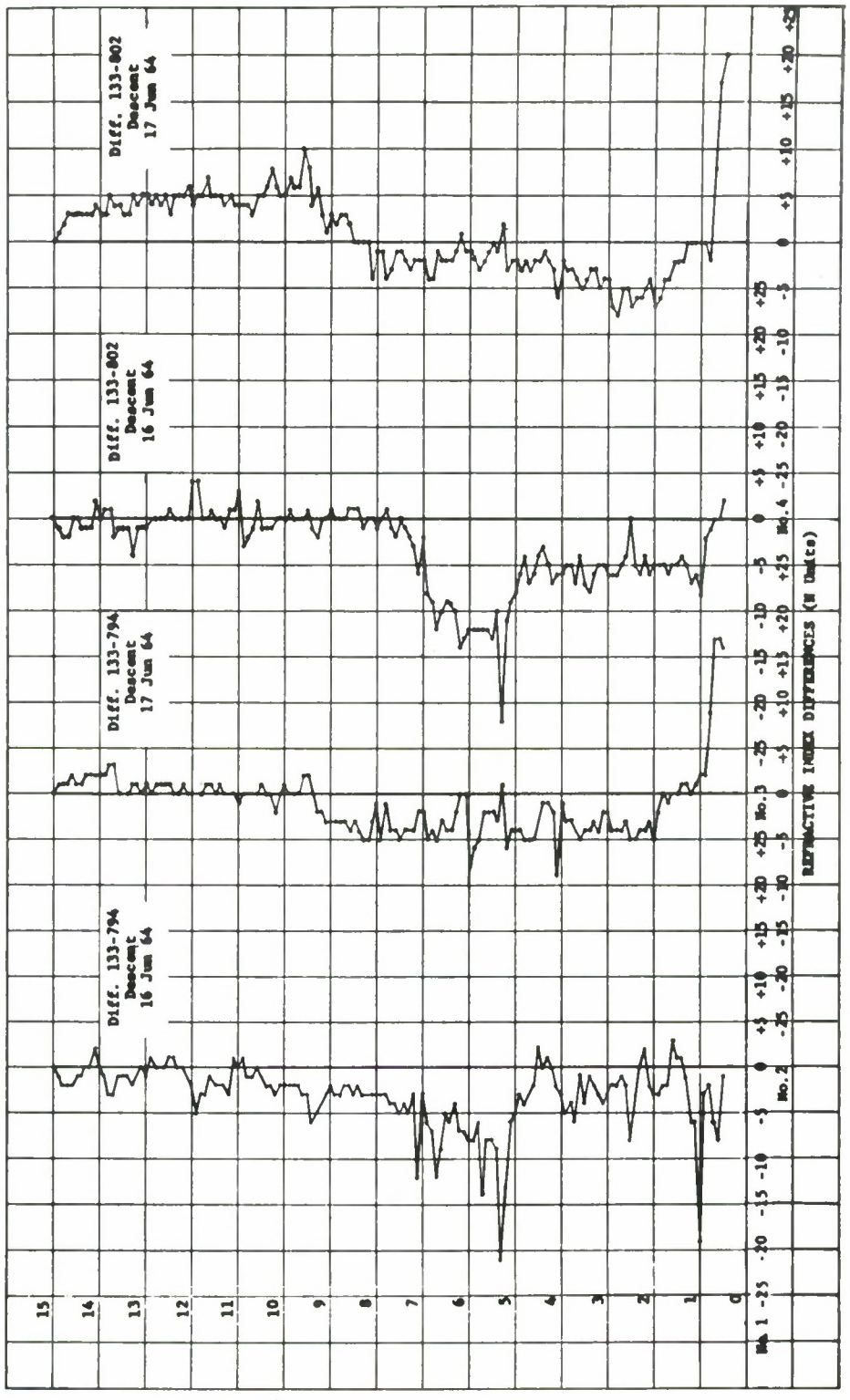

Fig. 4. Sounding Differences 133 vs. 794 and 802

Table 1

Vertical Propagation Delays to 15,000-Foot Altitude

	Descent (D_D) and Ascent (D_A) Delays (ft.)	Aircraft No.			Difference (ft.)		
		133	794	802	133 vs. 794	133 vs. 802	794 vs. 802
16 June	D_D	3.78	3.73	3.73			
	D_A	3.76	3.73	3.70			
	$D_D - D_A$	0.02	0.00	0.03			
	$D_D - D_D$				0.05	0.05	0.00
	$D_A - D_A$				0.03	0.06	0.03
17 June	D_D	3.75	3.74	3.76			
	D_A	3.68	3.74	3.71			
	$D_D - D_A$	0.07	0.00	0.05			
	$D_D - D_D$				0.01	-0.01	-0.02
	$D_A - D_A$				-0.06	-0.03	0.03

Assuming homogeneity of the atmosphere in at least the volume in which the three aircraft are flying, the differences in the three right-hand columns of Table 1 might be considered as "errors" due to instrumentation in the three aircraft. The maximum error is seen to be 0.06 foot.

As will be seen more clearly later in this report, the atmosphere is not homogeneous in the volume occupied by the three aircraft. This was first suggested by inspection of Figs. 1 to 4; Fig. 4, perhaps, indicates this most clearly. It will be remembered that the differences between aircraft were greater at the lower altitudes, where the atmosphere was more turbulent, than at the higher altitudes, where the atmosphere was smoother. Thus, if it were necessary to use the three simultaneous profiles in a particular calculation, there is good reason to use an average of the three profiles as the "true" or "representative" profile.

INDIVIDUAL SOUNDINGS OVER MISTRAM CENTRAL, 100 K. WEST, AND 100 K. SOUTH SITES

Simultaneous measurement of the refractivity profiles over the individual MISTRAM stations is a goal of the August tests. These refractivity profiles will be used in MISTRAM error model calculations to see if they result in improved MISTRAM accuracy.

Individual soundings were obtained over MISTRAM Central, 100 K. West, and 100 K. South, to obtain some preliminary data, as well as to determine the problems of gathering and reducing this type of data.

In Figs. 5 and 6, the simultaneous descents by the three aircraft over MISTRAM Central, 100 K. West, and 100 K. South, are first shown separately, and are then superimposed in the right-hand plot in each figure. These profiles were plotted directly from the raw data, with no corrections except for the scale correction to 802 as explained earlier.

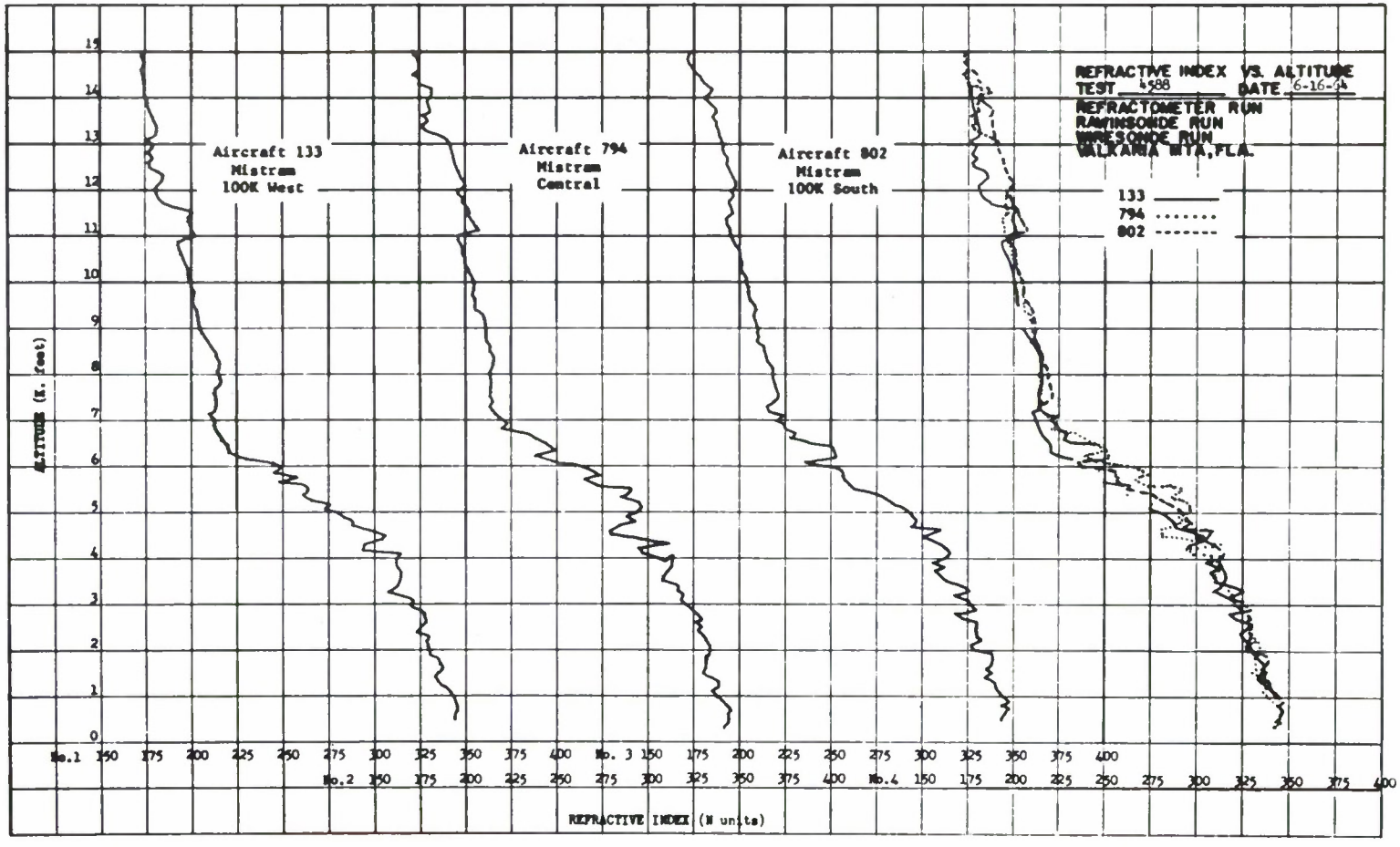

Fig. 5. Simultaneous Soundings: MISTRAM Central, 100 K. West, and 100 K. South

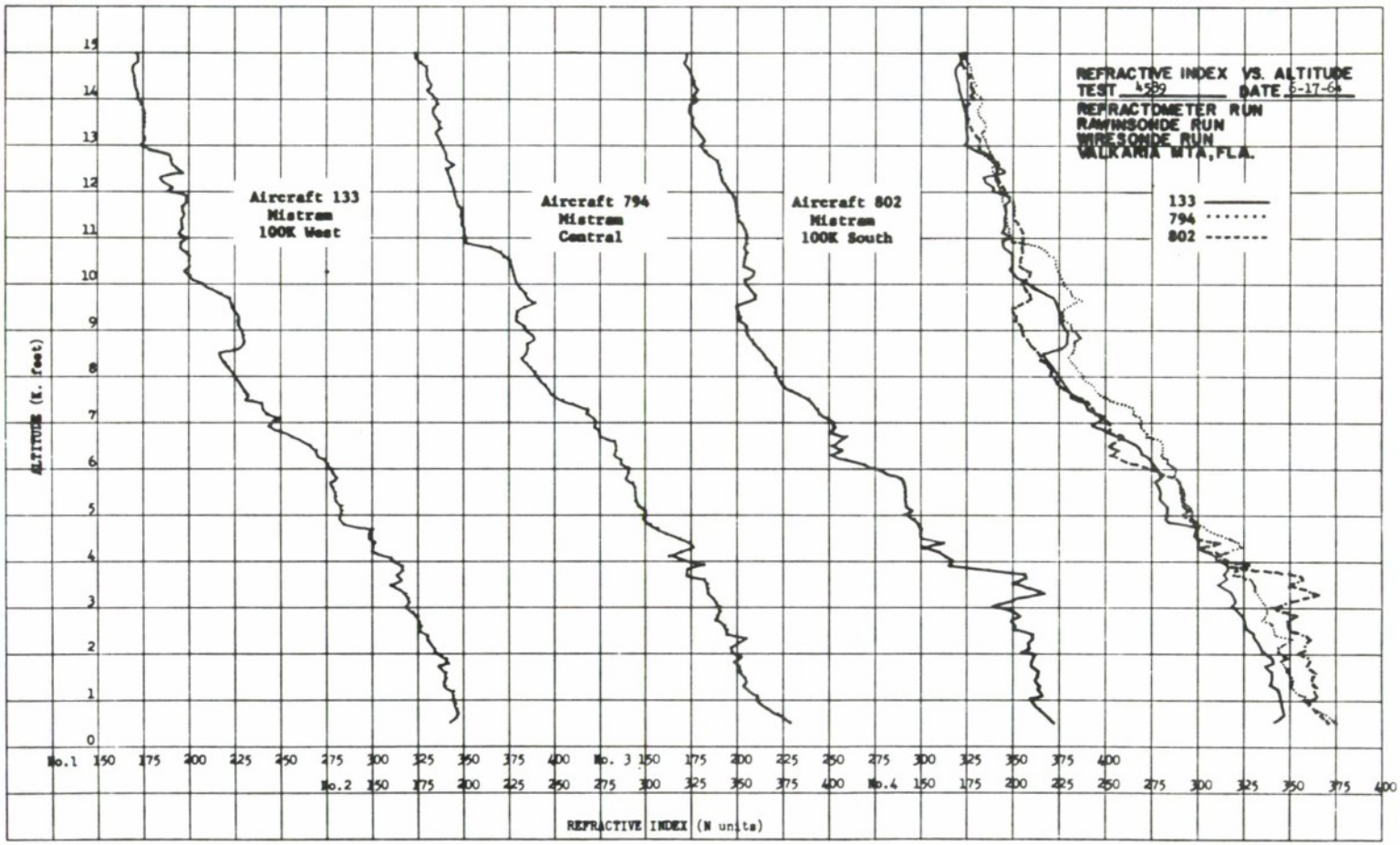

Fig. 6. Simultaneous Soundings: MISTRAM Central, 100 K. West, and 100 K. South

It is immediately apparent that the differences in profile at the three MISTRAM stations, as shown on the right in Figs. 5 and 6, are greater than the differences in profile shown in Figs. 1 to 3. This was expected, of course, since about 20 miles separate MISTRAM Central and 100 K. West and 100 K. South. If it is assumed that the total differences in profile in Figs. 5 and 6 are due to the atmosphere (and not to instrumentation), then a calculation of the propagation delay of a radio wave through the atmosphere, described by these refractivity profiles, is information pertinent to the determination of MISTRAM bias errors.

Table 2 tabulates the delays for vertical propagation of a radio wave to an altitude of 15,000 feet as calculated from the refractivity profiles shown in Figs. 5 and 6. As mentioned earlier, the delay to the same altitude for other elevation angles may be determined by multiplying the values in Table 2 by the cosecant of the elevation angle.

If the profile at MISTRAM Central (Fig. 5 or 6) had been assumed to be present over all of MISTRAM, and if it had further been assumed that the beams from each station operate principally in the profile taken over that station, then the delays in Table 2 (rows 4, 5, and 6), appropriately modified for elevation angle, indicate the range-difference errors that would be produced by the first 15,000 feet of the atmosphere. That these differences are large in relation to MISTRAM expectations points out the seriousness of the meteorological effects upon MISTRAM.

FORMATION LEVEL RUNS

The three aircraft made a total of seven level runs in a tight V-formation at 2000 feet from various directions into MISTRAM Central during the two days of tests. Two runs from 16 June and one run from 17 June have been converted to common scales and plotted in Figs. 7, 8, and 9.

Table 2

Vertical Propagation Delays of a Radio Wave to a 15,000-Foot Altitude

	Aircraft			
	Difference	No.	Location	Delay (ft.)
16 June		794	MISTRAM Central (MC)	3.61
		133	100 K. West (KW)	3.51
		802	100 K. South (KS)	3.58
	$DM_C - D_{KW}$			0.10
	$D_{MC} - D_{KS}$			0.03
	$D_{KW} - D_{KS}$			-0.07
17 June		794	MISTRAM Central (MC)	3.84
		133	100 K. West (KW)	3.63
		802	100 K. South (KS)	3.72
	$D_{MC} - D_{KW}$			0.21
	$D_{MC} - D_{KS}$			0.12
	$D_{KW} - D_{KS}$			-0.09

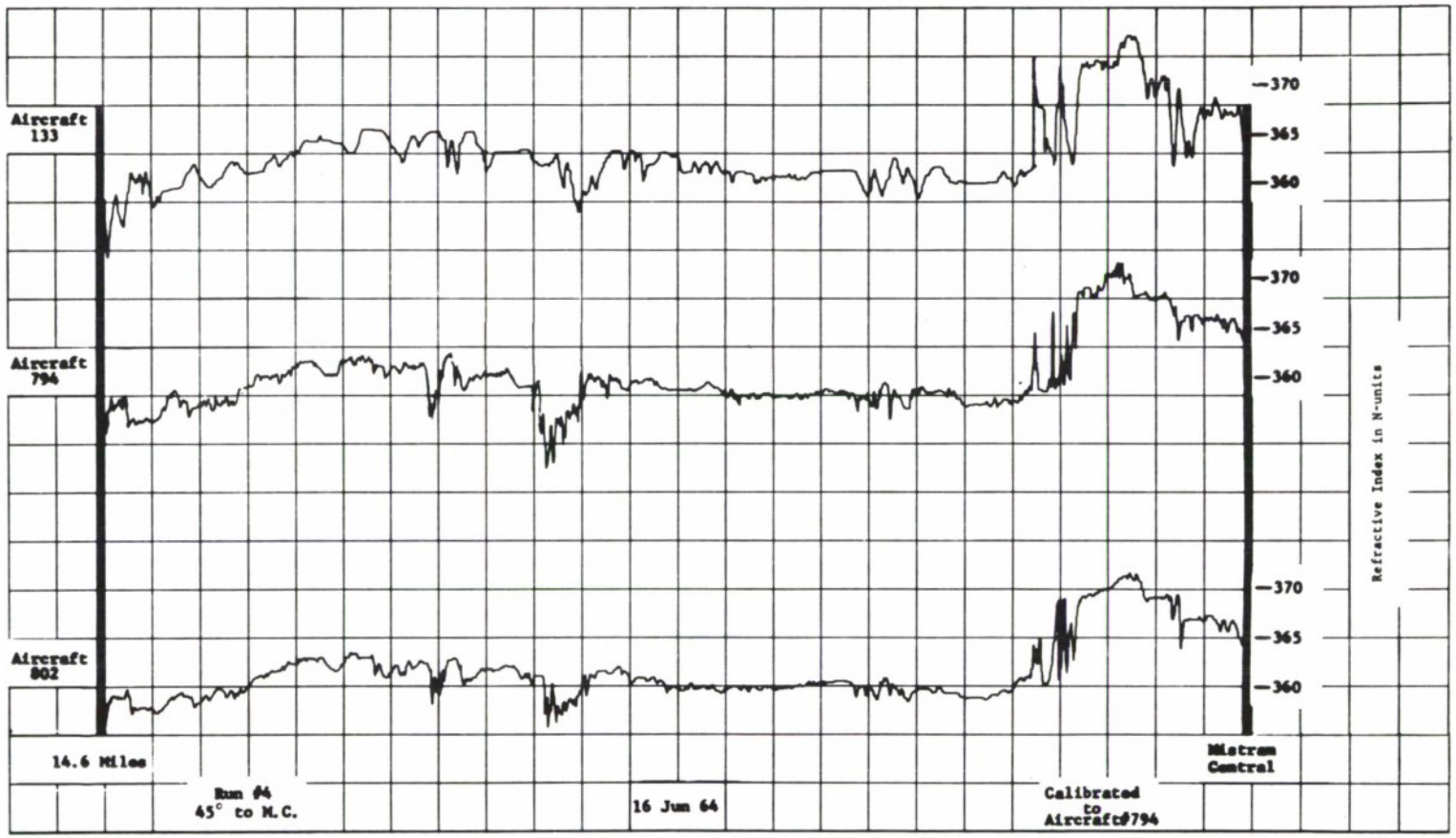

Fig. 7. Formation Level Runs, Three Aircraft, 2000 Feet

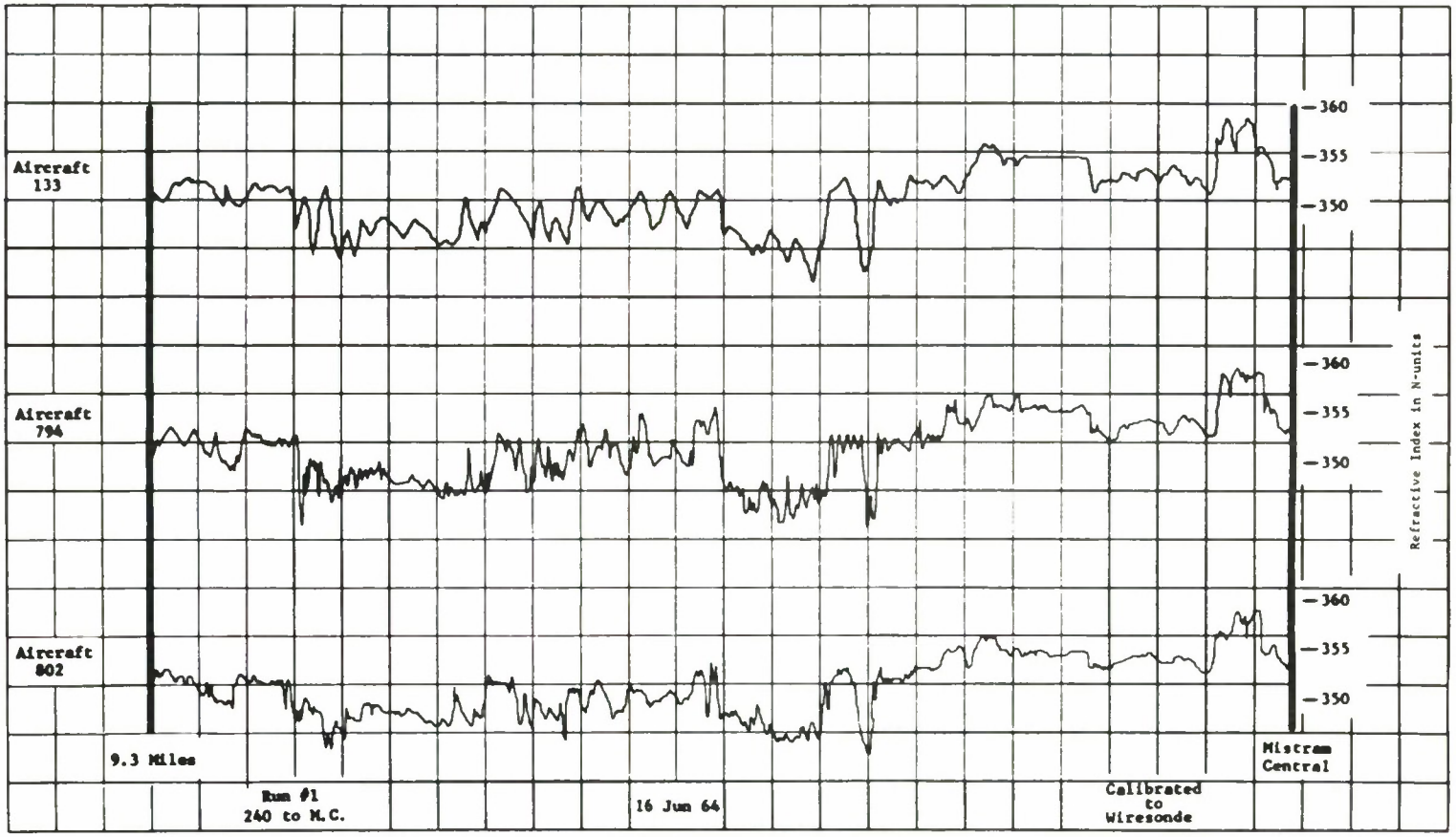

Fig. 8. Formation Level Runs, Three Aircraft, 2000 Feet

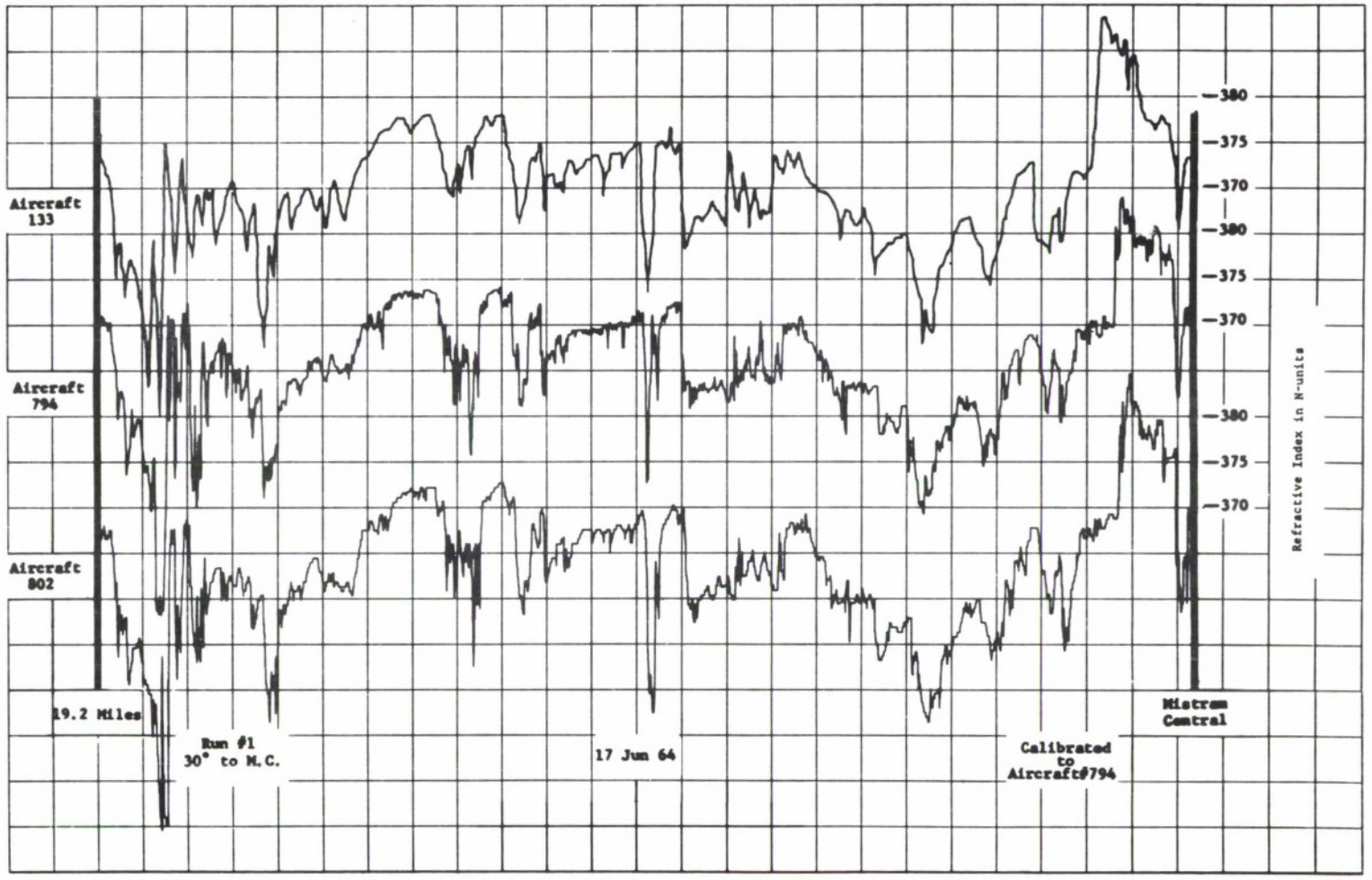

Fig. 9. Formation Level Runs, Three Aircraft, 2000 Feet

These plots were obtained by using the Gerber Model GDDRS-3B Digital Data Reduction System, modified to drive a plane x - y plotter. The 802 record compressed 80 N-units into about 1.5 inches of curvilinear deflection while the 794 record had a scale of 25 N-units per 2.5 inches. The 133 record, made with a 100 pen recorder, was difficult to read in fine detail, and this fact is evidenced in the generally smoother character of the 133 plots in Figs. 7, 8, and 9. The accurate reduction of these records to a common scale is difficult.

The records from the three aircraft appear to agree quite well in gross detail on all three runs. No conclusions should be drawn from the fine detail, since the data reduction process depends heavily upon the interpretation and skill of the GDDRS operator.

These records also give a crude indication of the lack of homogeneity of refractivity in the volume occupied by the three aircraft. The run in Fig. 7 was about 9.3 nautical miles (n. m.) in length. Thus, the vertical lines in Fig. 7 represent about 2500 feet of aircraft travel. If we assume a 250-foot separation between 802 and 794, the two outside aircraft in the V-formation, then the variations of refractive index shown in Fig. 7, for distances corresponding to one-tenth the distance between vertical lines, might be present between 794 and 802 in the 2000-foot altitude ranges during their descents and ascents.

It was intended to compare this data with the wiresonde data obtained at MISTRAM Central during the time the wiresonde was flown at a constant altitude. If it is assumed that, on some time scale, temporal variations of refractivity are spatial variations drifting with the wind, this process should allow the separation of temporal and spatial variations which are combined in the aircraft data. It should also produce an absolute calibration point for the aircraft refractometers when they fly by the wiresonde balloon.

Since the winds at 2000 feet were light and variable on both operating days, the first goal was not attained. The wiresonde value of refractive index at 2000 feet determined the vertical scales of Fig. 7. The comparable wiresonde value for Figs. 8 and 9 was not obtained because of instrumentation difficulties. Accordingly, on these figures, the vertical scales were determined from the 794 data.

SCALE AND TYPE OF ATMOSPHERIC REFRACTIVE INDEX ANOMALIES

R. M. Cunningham*

We outlined the Air Force Cambridge Research Laboratory's part in ESD's refractive index project last November.** D. L. Ringwalt''s paper describes the problems involved with the accurate measurement of refractive index profiles and bias corrections. I will illustrate the scale and type of atmospheric refractive index anomalies we will be talking about, from those that appear as bias in the present interferometer systems to those that produce noise. J. H. Meyer and R. K. Crane, in their presentations, will show how this type of data, along with aircraft and ground measurements, can be quantitized in terms of numbers familiar to those handling data from long baseline radio interferometer systems.

The atmospheric anomalies I will be talking about are those made visible by clouds (Fig. 1). A cloud of the cumulus family often develops in regions of relatively dry air. We see the common result in terms of the refractive index. This type of trace is commonly obtained in flight through the upper-half of a growing cumulus cloud. A map showing the distribution of cumulus clouds, therefore, is, to a large extent, a map of this scale of refractive index anomaly.

I will show a number of figures pertaining to 7 August 1963. In Fig. 2, we see the peninsula of Florida from the Tyros satellite. The clouds shown, which are largely cumulus cloud groups, can be considered as areas of high refractive index or high bias to an interferometer system. Note the sharp differences along the coast lines, as well as the effects of lakes, and of the gulf stream. Note also the occurrence of cloud patches and cloud lines.

---

*Cloud Physics Branch, Cambridge Research Laboratory, Bedford, Massachusetts

**See ESD-TDR-64-109, Vol. I, p. 1-15.

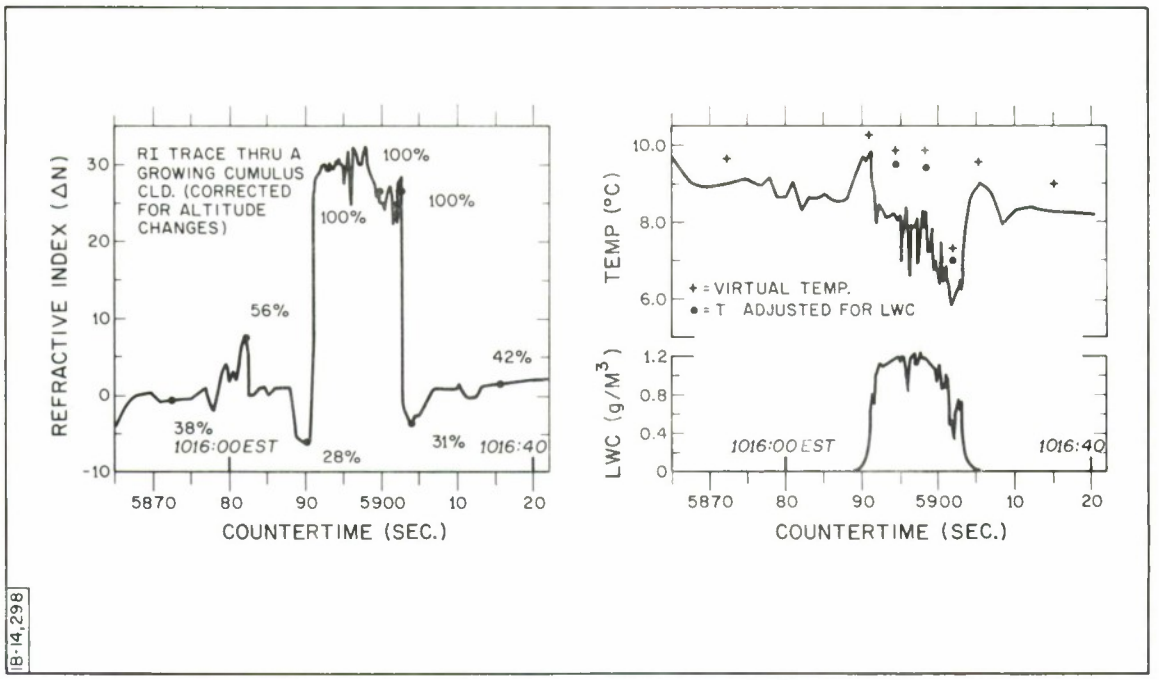

Fig. 1. Atmospheric Anomalies Through a Cloud Section

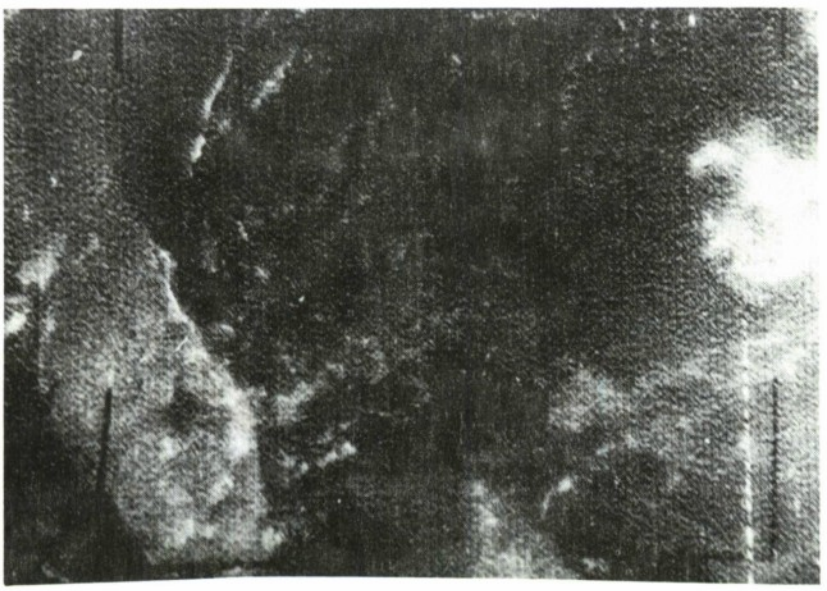

Fig. 2. Florida Peninsula Cloud Structure As Seen From A Tyros Satellite

Interferometer systems with baselines of 10 miles and up are obviously affected by such atmospheric structures. This scale of cloud distribution and its climatology should be considered before locating any future large baseline system.

Descending from the satellite level of 100 miles to the U-2 level, we can examine the same sea breeze clouds over MISTRAM in more detail. In Fig. 3, we can see the MISTRAM short legs; the left cross denotes the MISTRAM Central (MC) site, and the right cross the 100 K. West (KW) site. Various cloud sizes and cloud groups are visible. The clouds inland are moving with the wind, while the semi-permanent cloud "front" remains almost stationary at the sea breeze convergence line shown by the surface wind pattern of Fig. 4.

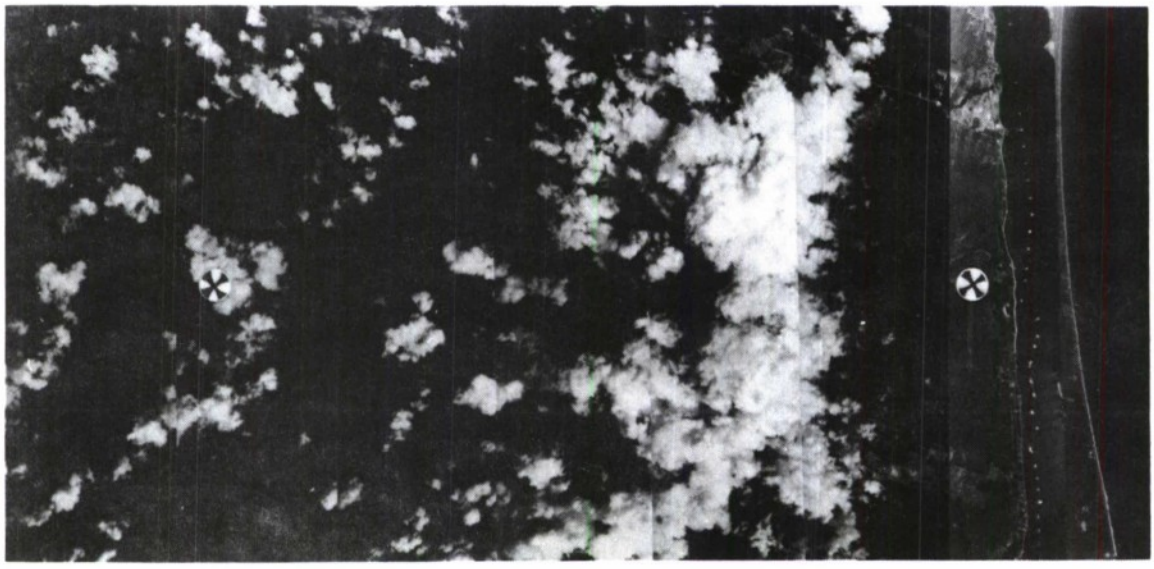

Fig. 3. MISTRAM Site Sea-Breeze Clouds as Seen in a U-2 Aircraft (7 August 1963; 10:31 EST)

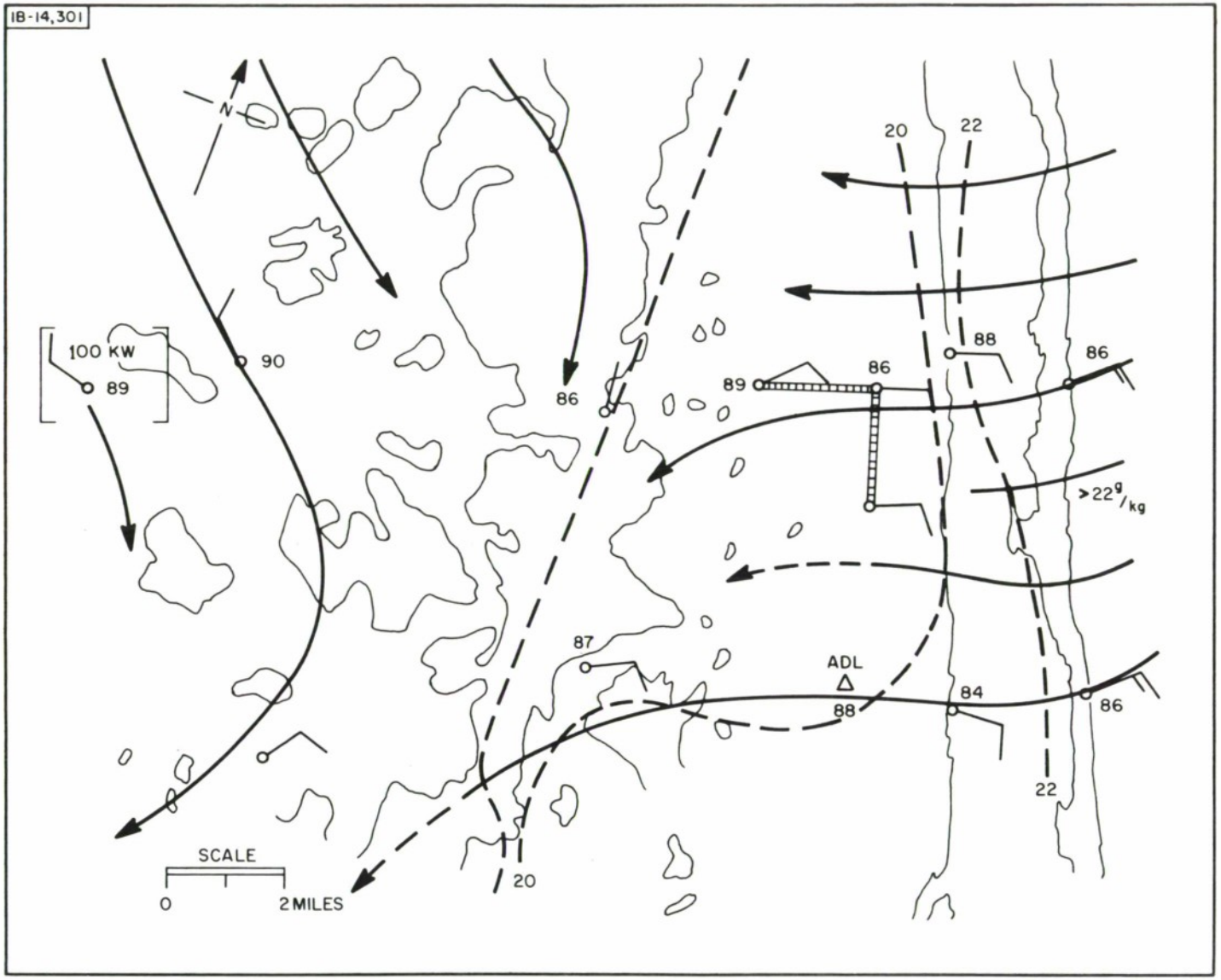

Fig. 4. Typical MISTRAM Site Surface Wind Pattern (7 August 1963; 10:30 EST)

A more familiar type of view of this cloud line is shown in Figs. 5 and 6. MISTRAM Central and the 10 KW and 10 K. South (KS) are just visible in the upper center of the picture of Fig. 5. The vertical dark band covering part of the clouds over cape Kennedy is a propeller blade of the aircraft. Note that Cape Kennedy and Merritt Island are just large enough to produce fairly large single cloud masses. Figure 6 is a ground observers' view of the same cloud line. This picture was taken looking north from the airport visible in the lower center of Fig. 5. Figure 7, which is one scale size smaller than the mesocale, shows a close-up of one of the sea breeze clouds pictured previously. The scale of refractive index, irregularly illustrated in the figure, is given by the roughness of the cloud edge. Turbulent eddies in the cloud show at the edge as round bumps of the order of 500 feet or so in size. This is the scale which has been treated and described most successfully by statistical methods, by the micro-meteorologist and by those studying radio propagation. At the moment, we will not include this scale in the papers to follow (J. H. Meyer, R. K. Crane), although it may be included in a statistical fashion at a later date.

We have looked at the mesoscale of cloud and associated refractive index for this typical summer day over MISTRAM; now let us look at the time scale of these features. Before we look, however, we should note the two following definitions: a bias error, as the term is used in connection with MISTRAM errors, can be considered a constant error over the time MISTRAM is tracking a missile, say 5 to 6 minutes, while a noise might be considered a fluctuating error at any period less than 5 to 6 minutes.

Figures 8 and 9 show two U-2 mosaics, photographed 19 minutes apart. Figure 10 shows a history of individual cloud turrets measured from time-lapse ground photography. The ground camera was placed on the outer beach SE of MISTRAM Central. The cloud histories shown on the top graph in solid line belong to the cloud group along the sea breeze line at the bottom of the two U-2

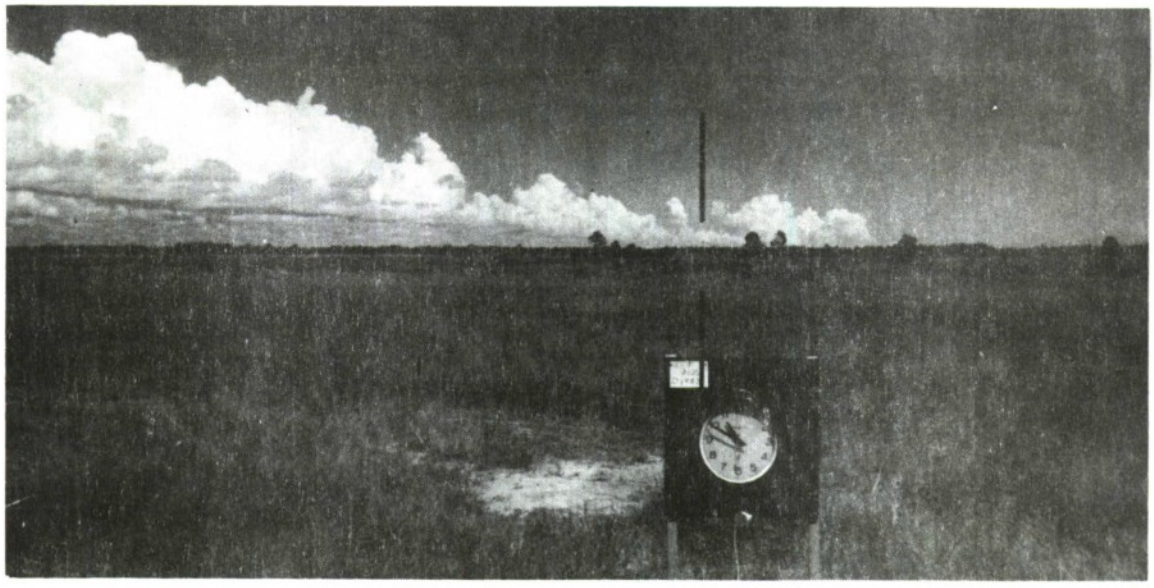

Fig. 5. Florida Coast Cloud Line Observed from Ground

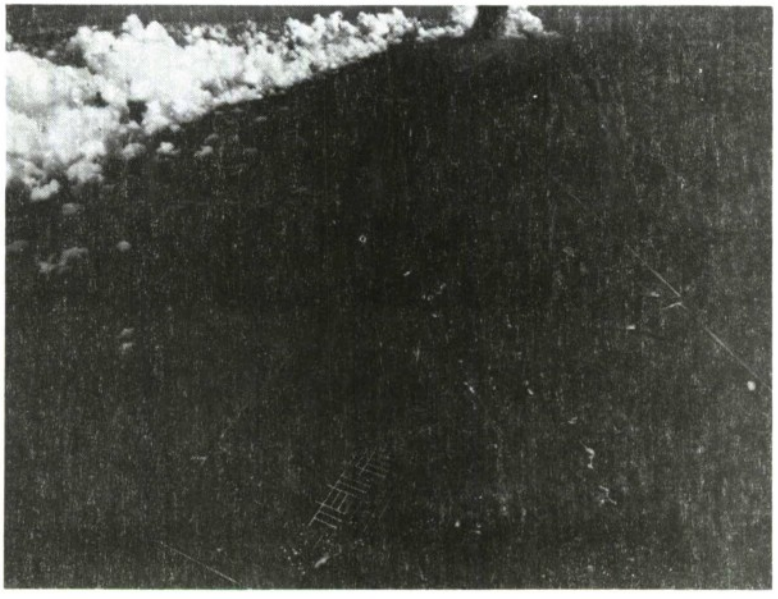

Fig. 6. Florida Coast Cloud Line Observed from Aircraft

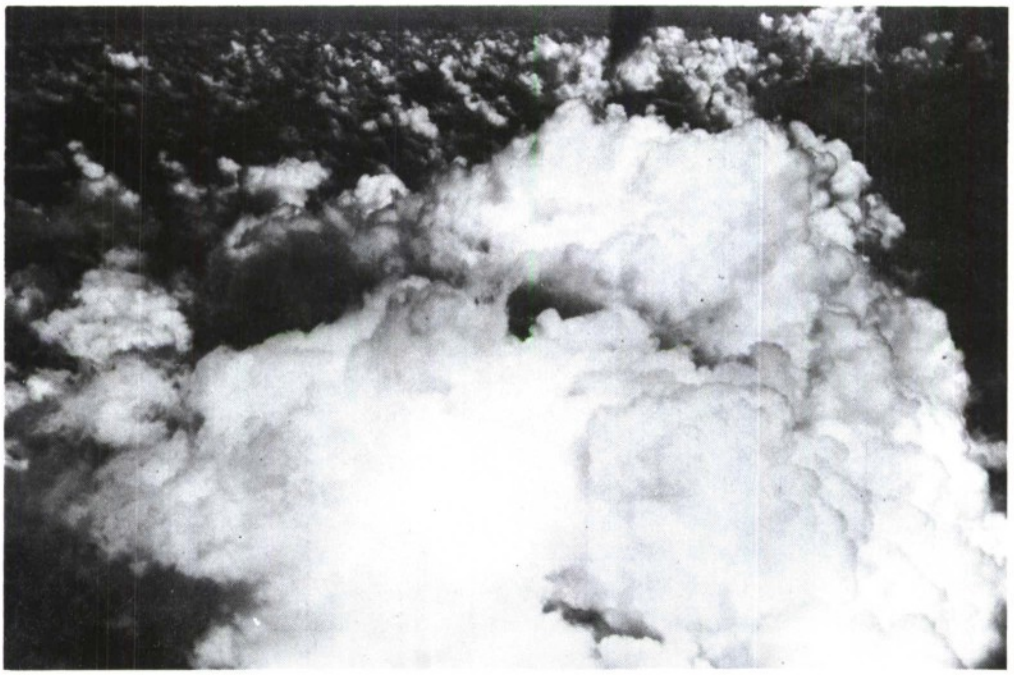

Fig. 7. Fine Structure of Sea Breeze Clouds

derived mosaics. The dashed line represents the early history of the developing group just below the midpoint of the long E-W leg at MISTRAM. The bottom graph depicts the history of the large cloud group 5 miles west of MISTRAM Central. (A map scale can be derived from the visible two mile short baseline legs of MISTRAM. The main roads are on a N-S, W-E grid, so that MISTRAM legs are actually close to WSW and SSE.) It appears, when one compares the two successive U-2 mosaics, that this cloud group collapsed as a whole. Its detailed history shows, however, that the individual turrets making up the group were less and less successful in reaching the size of their previous turrets.

The time scale and space scale of cloud dimension and history are positively correlated. In this case, for instance cloud turrets have dimensions of about 1 mile and life histories above the more general lower cloud masses of 4 to 7 minutes, while major cloud groups have dimensions of about 5 miles and life histories of 1/2 to 1 hour or more.

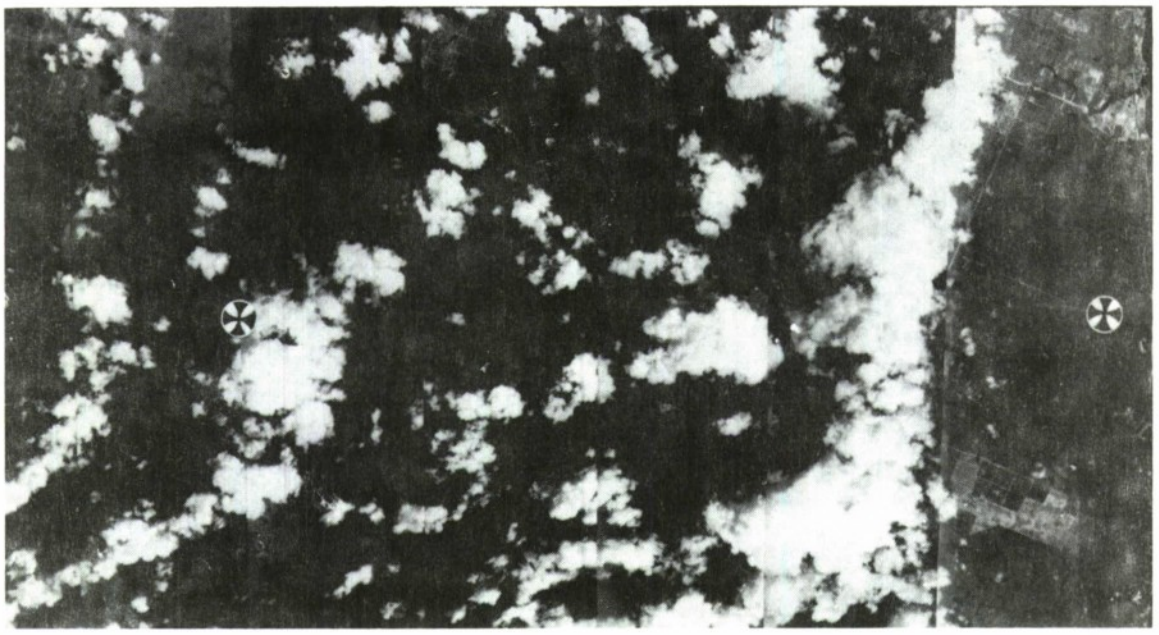

Fig. 8. MISTRAM Site Sea Breeze Cloud Pattern (7 August 1963; 10:49 EST)

Fig. 9. MISTRAM Site Sea Breeze Cloud Pattern (7 August; 11:08 EST)

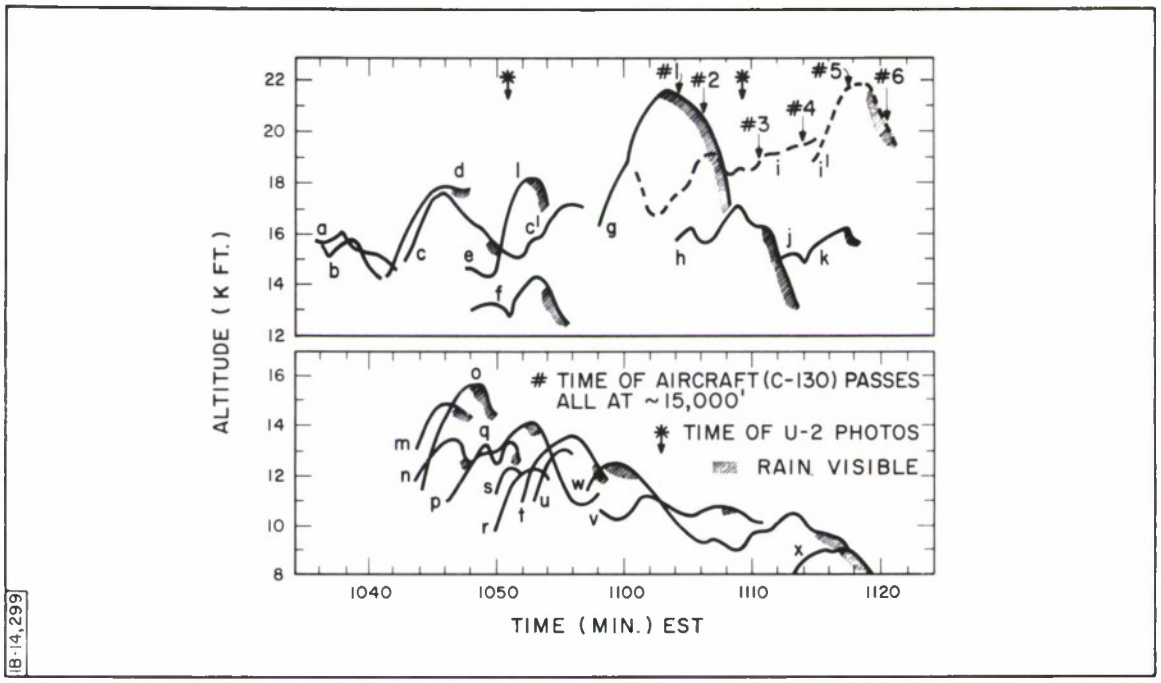

Fig. 10. Cloud Growth History

In summary, then: Clouds of the cumulus variety allow us to see various scales of refractive index anomaly. This fact permits the meteorologist skilled in mesoscale weather phenomena to contribute a nonstatistical partial answer to the radio propagation problems limiting the accuracy of radio interferometer systems. At a scale of a mile or so, the time rate of change of these cloud features is slow enough that a bias and a very low frequency noise correction could be made to the MISTRAM data in post-flight analysis. This would be done with the aid of cloud mosaics (on days with the proper cloud types) for the time of a shot and a sample of cloud-to-clear-air refractive index taken shortly before or after the same shot. A real-time correction could also be estimated from cloud observation and previous cloud-clear air ΔN measurements. A cloud climatology related to geographic features would help in locating future systems to minimize large bias and large low frequency noise errors of the above type.

DIGITAL ATMOSPHERIC PROFILE GENERATION

J. H. Meyer*

Dr. R. M. Cunningham discussed, through the use of cloud photographs taken at different altitudes, some of the various atmospheric scale sizes which exist in the troposphere. In this paper, the mesoscale meteorology along the E-W leg of the Valkaria, Florida, MISTRAM site and the method used to describe a particular realization of the atmosphere at a given instant of time are discussed.

At the second refractivity conference, held at The MITRE Corporation in November 1963, Dr. Cunningham discussed some of the refractive index data gathered in Florida the previous August. The analysis of the data presented by Dr. Cunningham was in the form shown in Fig. 1. Since then, further analysis of the data has been completed. However, before proceeding, a review of the refractive index data and cloud cross section shown in Fig. 1 is in order.

Level-run airborne refractive index measurements versus altitude, taken at different altitudes along a flight path over the E-W leg of MISTRAM, are shown. The flight path extended eastward several miles over the ocean and approximately one to two miles west of the 100 K. West (KW) site. Representation of the level-run refractive index data in the manner shown in Fig. 1 allows one to associate discontinuities measured at a particular altitude with those measured at the other altitudes. Each level run is plotted versus time so that the distance between MISTRAM Central (MC) and 100 KW decreases with altitude. This is because the aircraft was flown at a constant indicated airspeed. At a constant indicated airspeed, true airspeed or ground speed increases with

*Technical Operations, Inc., Burlington, Massachusetts

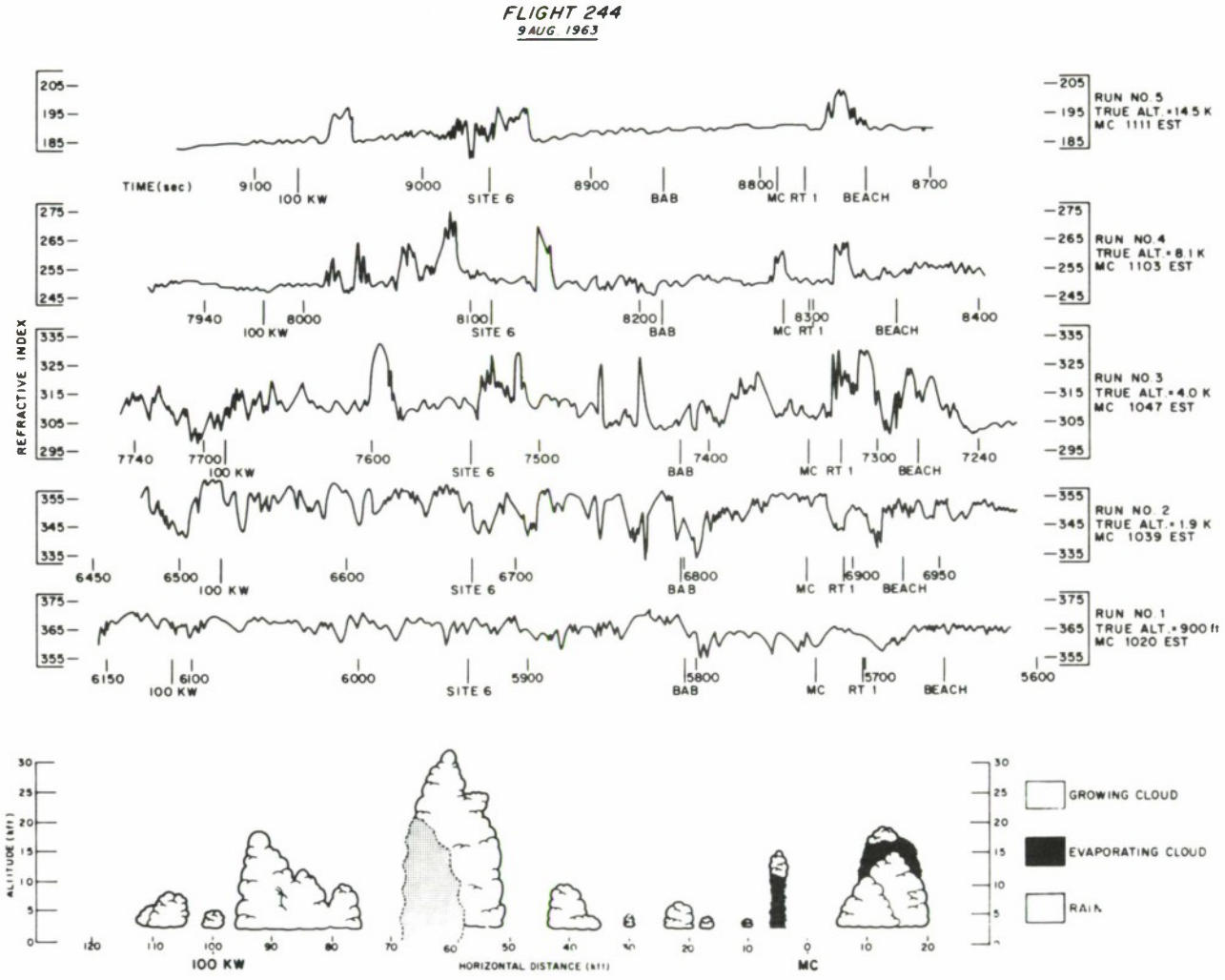

Fig. 1. Level-Run C-130 Refractive Index Traces At Various Altitudes and Cloud Cross Section Roughly Corresponding to Conditions on Run Five From A Synthesis of Data Shown Above and U-2 and C-130 Photographs

altitude and, therefore, the distance between MC and 100 KW decreases with altitude. The cloud cross section shown at the bottom of Fig. 1 was constructed to correspond roughly to the refractive index discontinuitics shown on Run No. 5 from a synthesis of the level-run data and photographs taken by the C-130 and U-2 aircraft.

The next step in the analysis was a check on the agreement between the aircraft data and the most representative radiosonde data for the time period over which the flight took place. A mean was found for a 50-second data sample over MISTRAM Central for each level run. Refractive index discontinuities caused by clouds were discounted in computing the mean. The mean values for the aircraft level runs were than compared with (Fig. 2) with the radiosonde values for the height at which the level run was made. The solid curve in Fig. 2 is the computed radiosonde refractive index N_A profile, and the dashed curve is the computed radiosonde saturated refractive index (N_S) profile. The solid

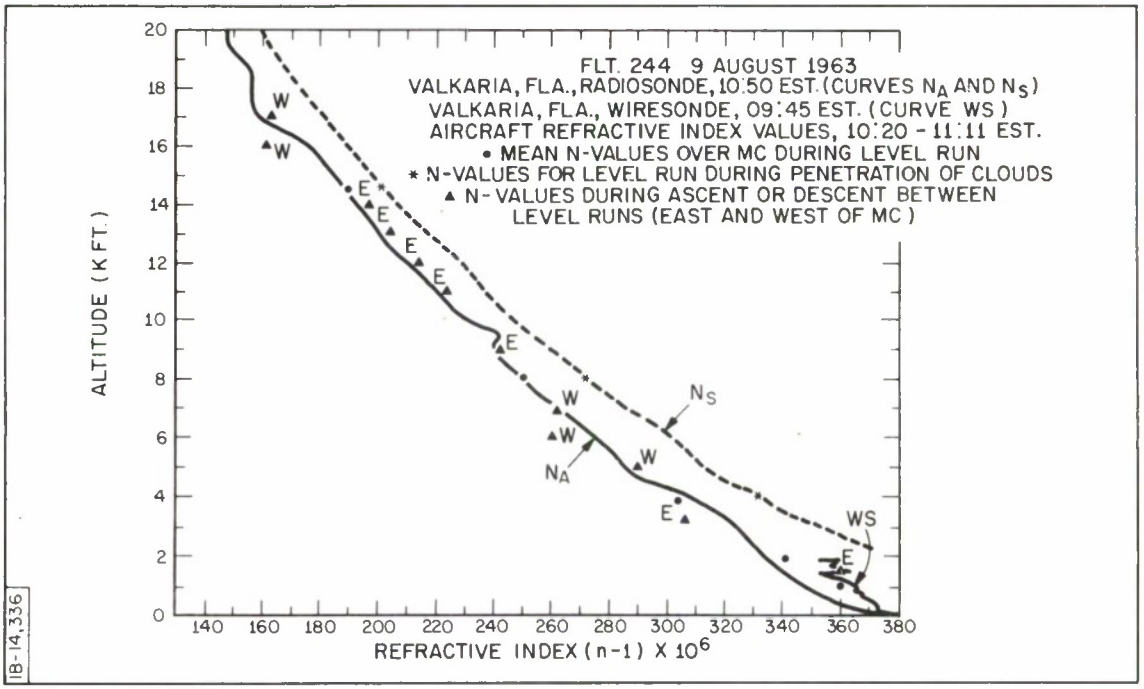

Fig. 2. Comparison of the AFCRL C-130 Refractive Index Values with the Most Representative Valkaria, Fla., Radiosonde N-Profile for 9 August 1963

circles are the 50-second mean aircraft values of refractive index over MISTRAM Central. The solid triangles are the refractive index aircraft values sampled during ascent or descent between the level runs, and are measurements made east and west of the E-W leg of MISTRAM.

There is good agreement between the aircraft and radiosonde refractive index values, except below 2000 feet. At those altitudes, the aircraft values have better agreement with the wiresonde-computed refractive index values. This difference, found between the radiosonde, wiresonde and aircraft data, was present in all the data gathered during August 1963. The exact cause for this disagreement is unknown, and should be investigated. A further check on the agreement between the aircraft and radiosonde refractive index data is made by comparison of the refractive index values measured during aircraft penetration of growing clouds with the computed radiosonde-saturated refractive index. The asterisks in Fig. 2 are the aircraft saturated refractive index values. One can easily see there is good agreement.

Using the 50-second refractive index means computed for each of the level runs over MISTRAM Central for the data shown in Fig. 1, refractive index differences (ΔN's) were abstracted from the level-run index data. Combining the ΔN data with surface ΔN data computed from meteorological measurements taken at sites along the E-W leg of MISTRAM and using the cloud cross section shown in Fig. 1 as a model, the ΔN data was adjusted for time and space variations. Iso ΔN contours were then drawn for the adjusted data.

The ΔN cross section and cloud cross section for 9 August 1963 are shown in Fig. 3. The ΔN cross section shown in Fig. 3 is a particular realization of the atmosphere at a given instant of time, which allows one to use ray-tracing techniques to determine the effects of such an atmosphere on the propagation of

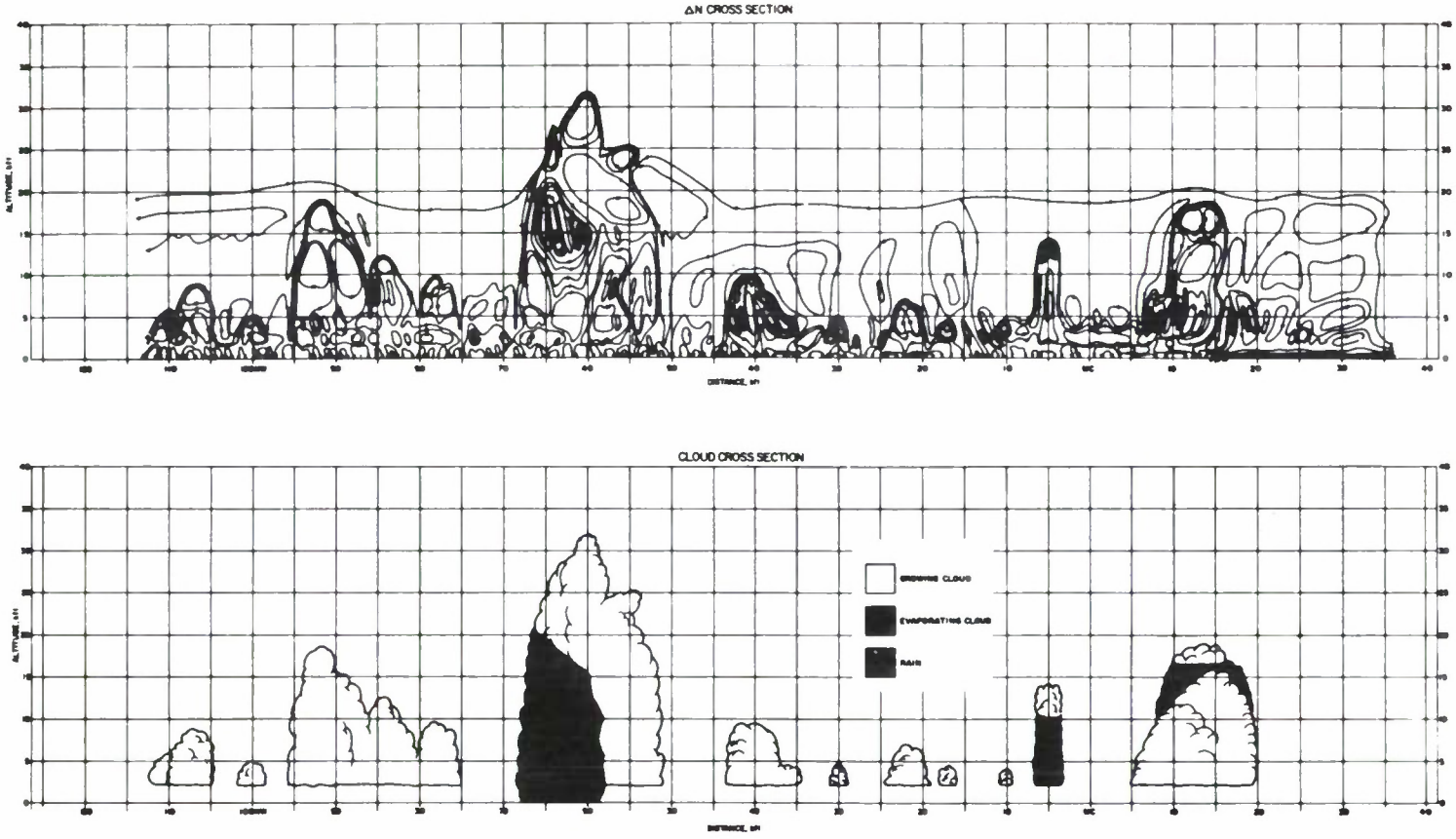

Fig. 3. Cloud Cross Section for 9 August 1963, Flight 244, Along the E-W Leg of MISTRAM with the Corresponding N-Cross Section.

electromagnetic waves through it. Some of the more significant features of the ΔN cross section shown in Fig. 3 are:

(a) the shallow moist layer of air, associated with the sea breeze, near the surface at approximately 15 to 20 kilofeet east of MISTRAM Central;

(b) the clouds associated with the sea breeze front at approxiamately 10 to 15 kilofeet east of MISTRAM Central;

(c) the large changes in ΔN as one goes from ambient air into a cloud;

(d) the difference in the magnitude of ΔN for a growing cloud and one that is dissipating or evaporating (some differences in magnitude can range as high as 30 N-units); and

(e) the general change of the ambient ΔN values from plus to minus as one follows the cross section from east to west.

With respect to the features shown in the ΔN cross section for 9 August 1963 (Fig. 3), it is obvious that the three tracking sites, MISTRAM Central, 10 KW and 100 KW, would experience different propagation conditions. In this particular case, MISTRAM Central tracking at very low angles would probably experience the effects of the shallow moist layer to the east.

Airborne refractive index measurements and meteorological measurements at the ground sites along the E-W leg of MISTRAM taken on the 7^{th} and 8^{th} of August 1963 were analyzed in the same manner. Figures 4 and 5 show, respectively, the level-run refractive index data versus altitude and the associated cloud cross sections for 7 August and 8 August. Figures 6 and 7 show the comparison of the level-run, 50-second means and other aircraft refractive index values with this computed radiosonde N-profiles, respectively, for

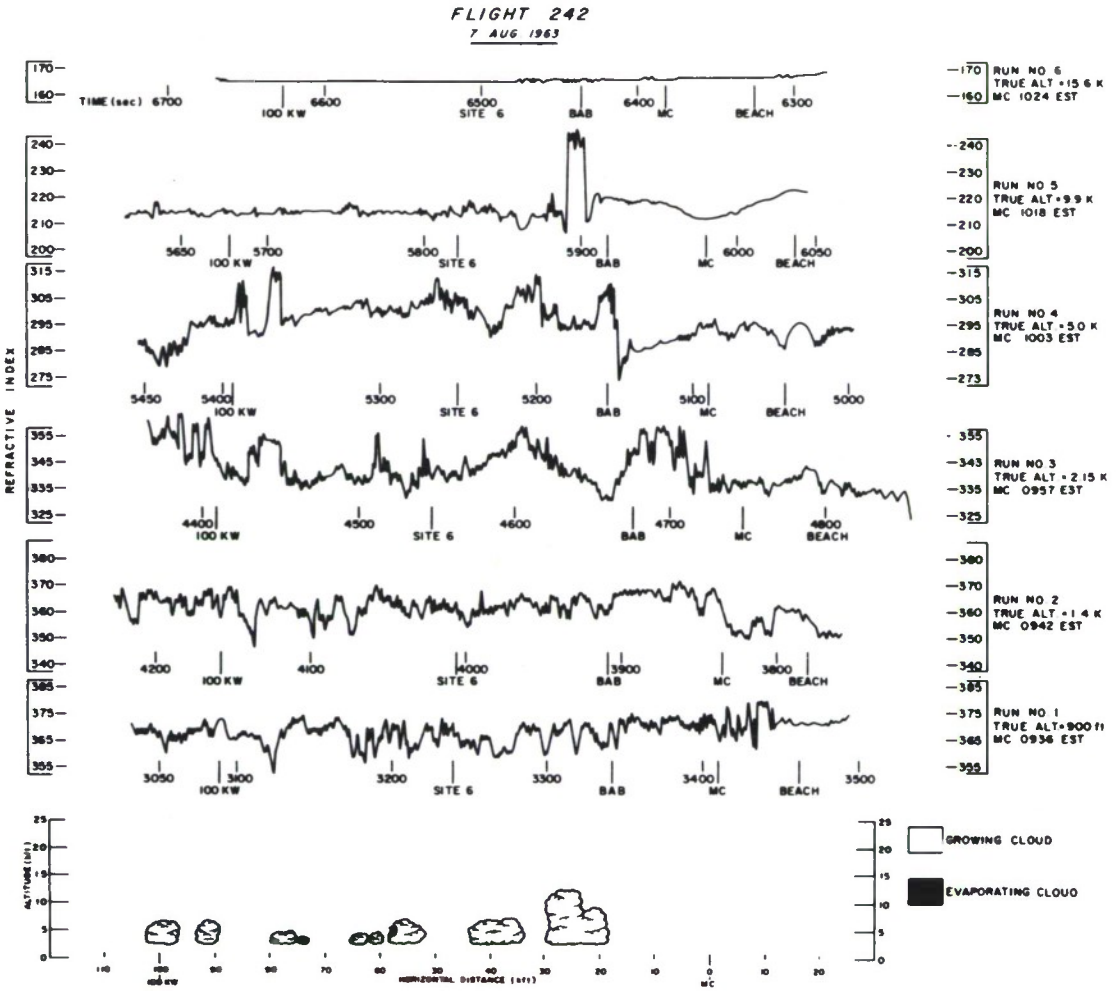

Fig. 4. Level Run C-130 Refractive Index Traces at Various Altitudes and Cloud Cross Section Roughly Corresponding to Conditions on Runs 4 and 5 from a Synthesis of Data Shown Above and U-2 and C-130 Photographs

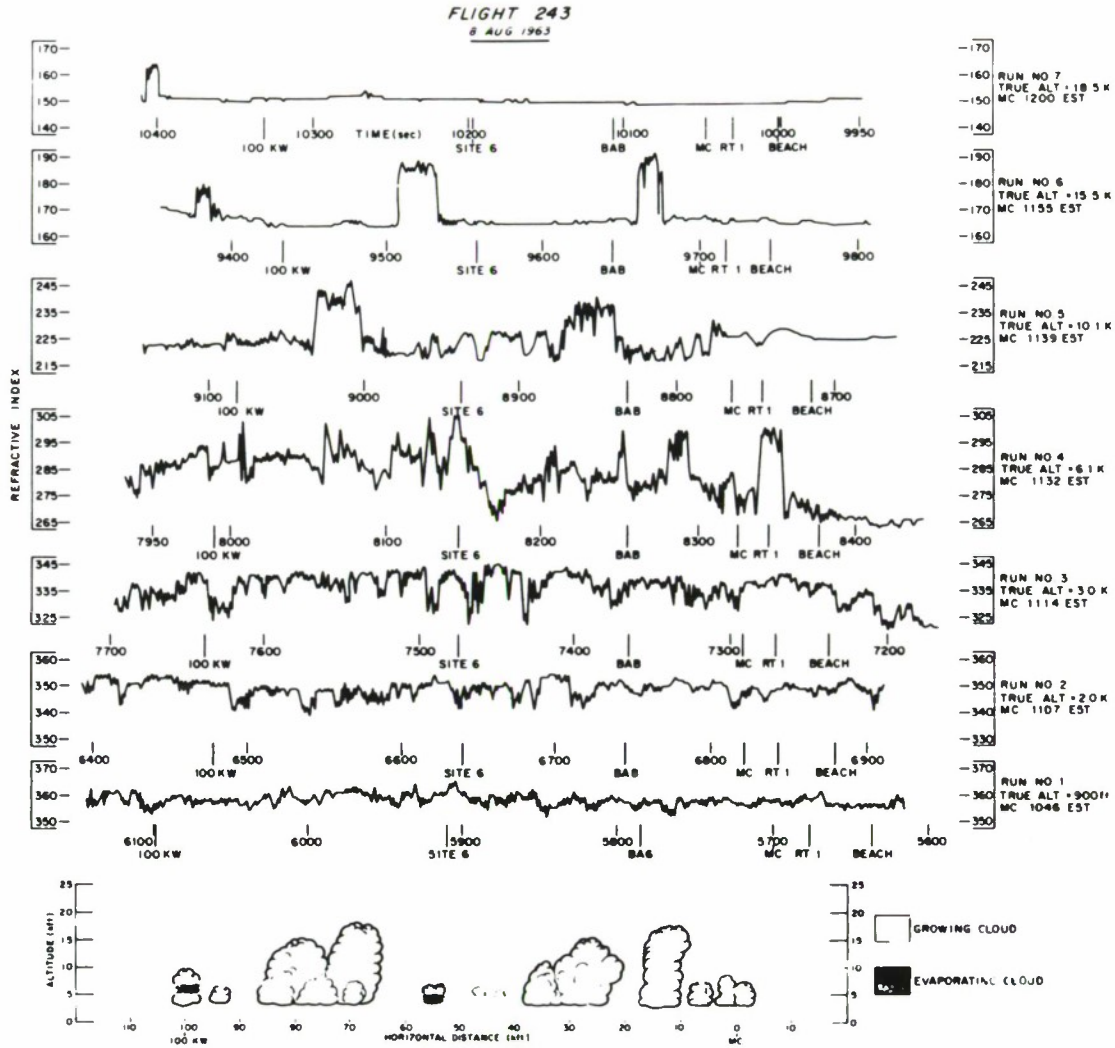

Fig. 5. Level-Run C-130 Refractive Index Traces at Various Altitudes and Cloud Cross Section Roughly Corresponding to Conditions on Runs 5 and 6 from a Synthesis of Data Shown Above and U-2 and C-130 Photographs

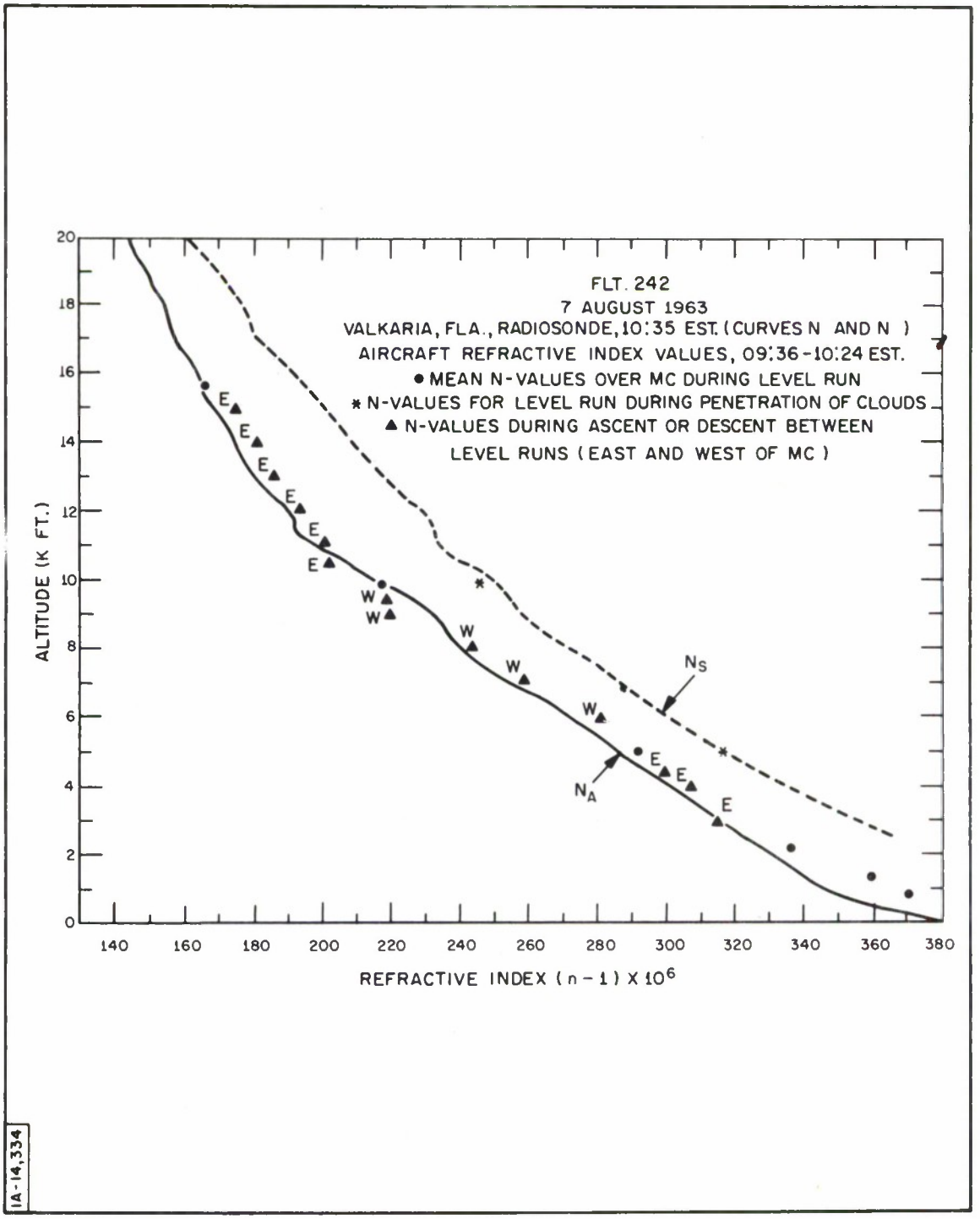

Fig. 6. Comparison of the AFCRL C-130 Refractive Index Values with the Most Representative Valkaria, Fla., Radiosonde N-Profile for 7 August 1963

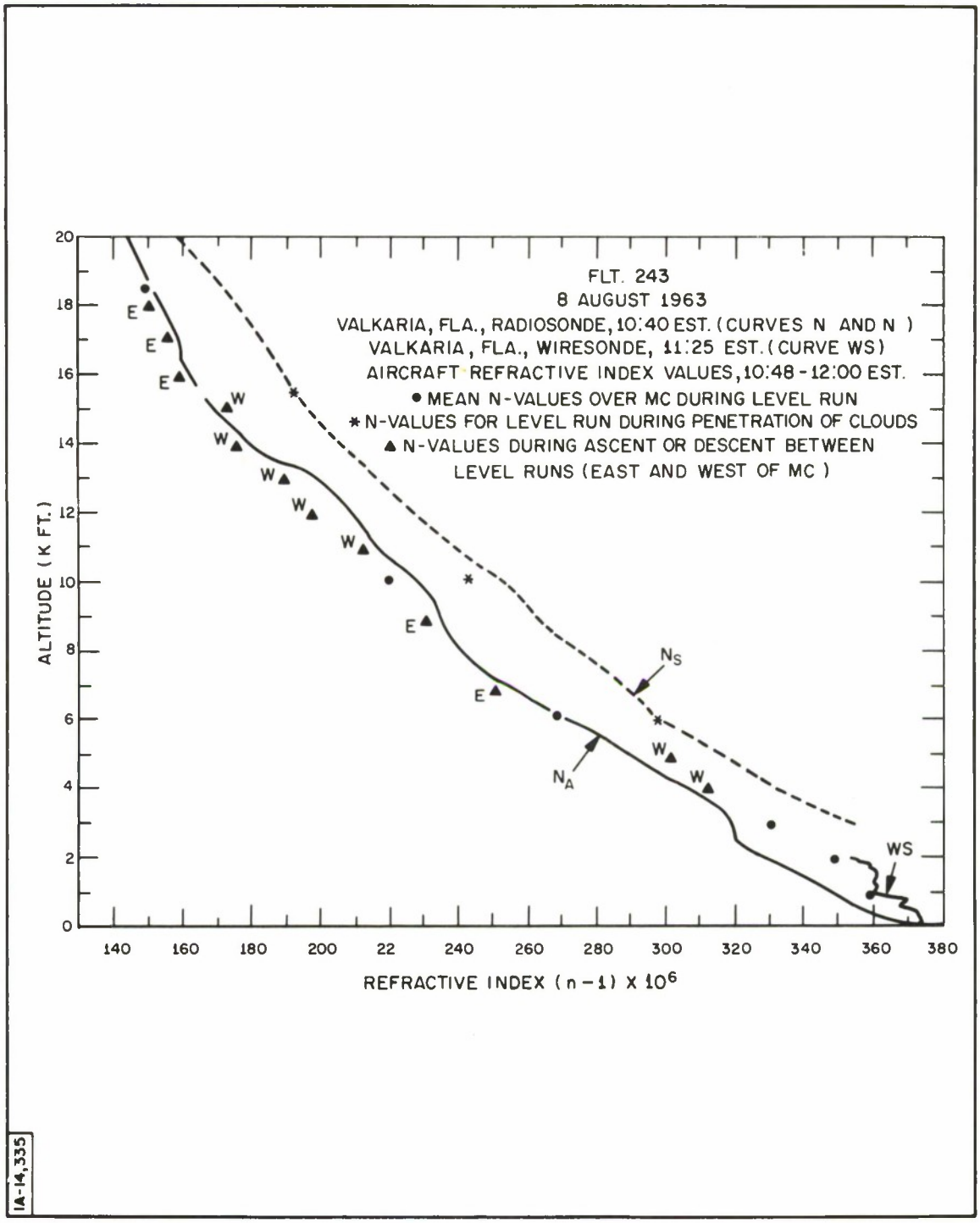

Fig. 7. Comparison of the AFCRL C-130 Refractive Index Values with the Most Representative Valkaria, Fla., Radiosonde N-Profile for 8 August 1963

7 August and 8 August 1963. Again, there is good agreement between the aircraft and radiosonde refractive index values, except below the altitude of 2000 feet on 7 August and 3000 feet on 8 August.

The cloud and ΔN cross sections for 7 August and 8 August 1963 are shown in Figs. 8 and 9, respectively. The significant features of these two ΔN cross sections are similar to those mentioned for the 9 August ΔN cross section; however, on the 7^{th} and 8^{th} of August, the cross sections show a difference in the location of the clouds associated with the sea breeze front. Notice should be given to the fact that the shallow moist layer next to the surface is present in both the ΔN cross sections; however, it extends inland a little further than in the case of 9 August.

On 7 August, which is the day Dr. Cunningham described, the line of building cumulus clouds along the sea breeze front, and ΔN pattern on the cross section show some of the effects of the topographical features along the E-W leg of the MISTRAM system. The rather disorganized ΔN pattern associated with the clouds, (Fig. 8) between 30 and 85 kilofeet west of MISTRAM Central reflects the effects of the swamp-type terrain over this particular part of the MISTRAM system. Convective heating, which is producing the well defined ΔN pattern associated with the clouds over the 100 KW site, is not evident over the above mentioned area. By considering the propagation of electromagnetic energy through the atmospheres shown in Figs. 8 and 9, one can easily note that the propagation conditions are different for any one of the tracking sites located along the E-W leg of the MISTRAM system.

The ΔN data for the three days were quantized, using a 500-foot grid, to determine what effects the three ΔN cross sections presented would have on the tracking capability of the MISTRAM system. R. K. Crane, of The MITRE

Corporation talks about the ray-tracing program used to compute the range, range difference and range-rate errors caused by the particular realized atmospheres constructed for 7, 8, and 9 August (see page 87).

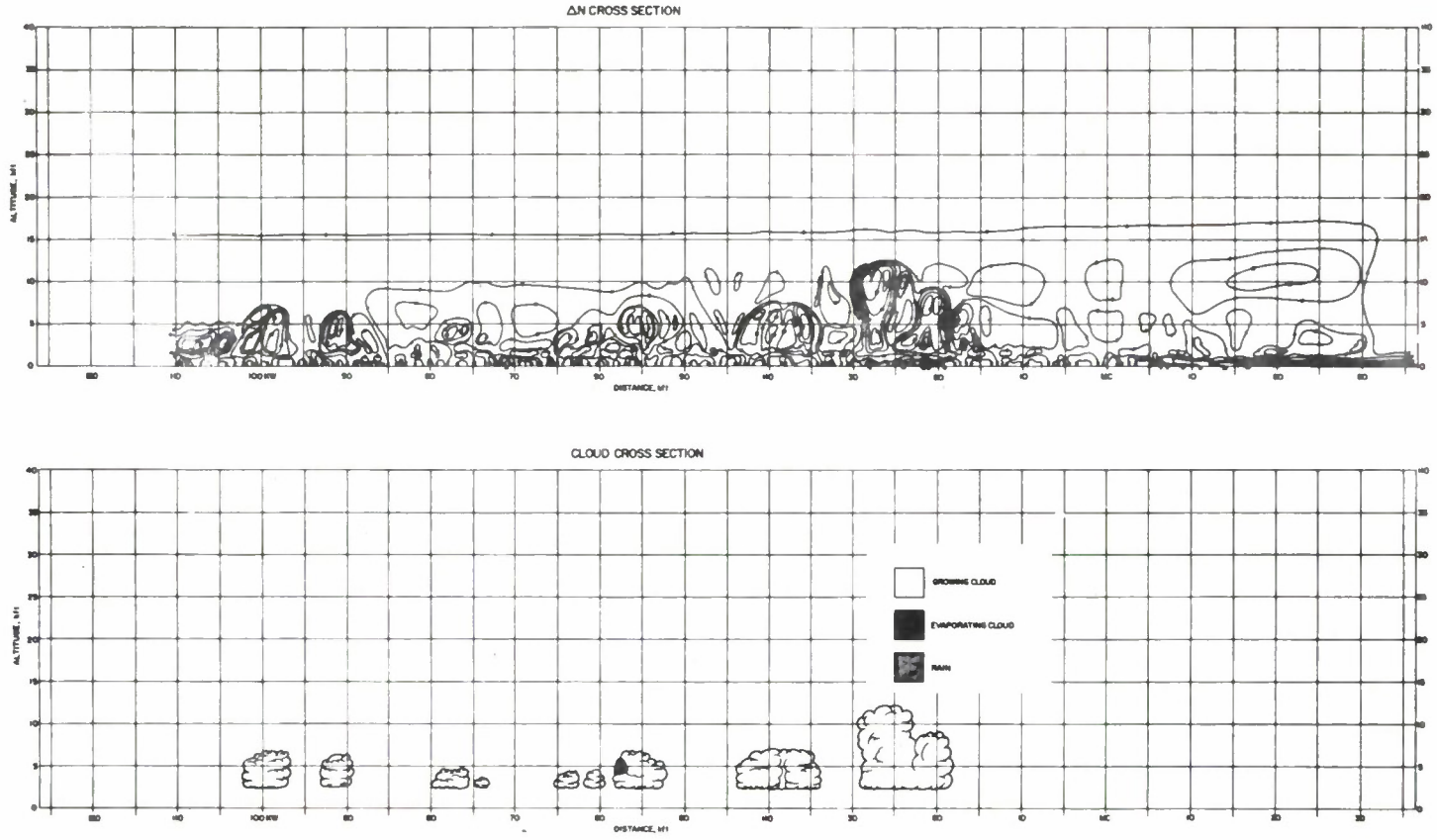

Fig. 8. Cloud Cross Section for 7 August 1963, Flight 242, Along the E-W Leg of MISTRAM with the Corresponding N-Cross Section

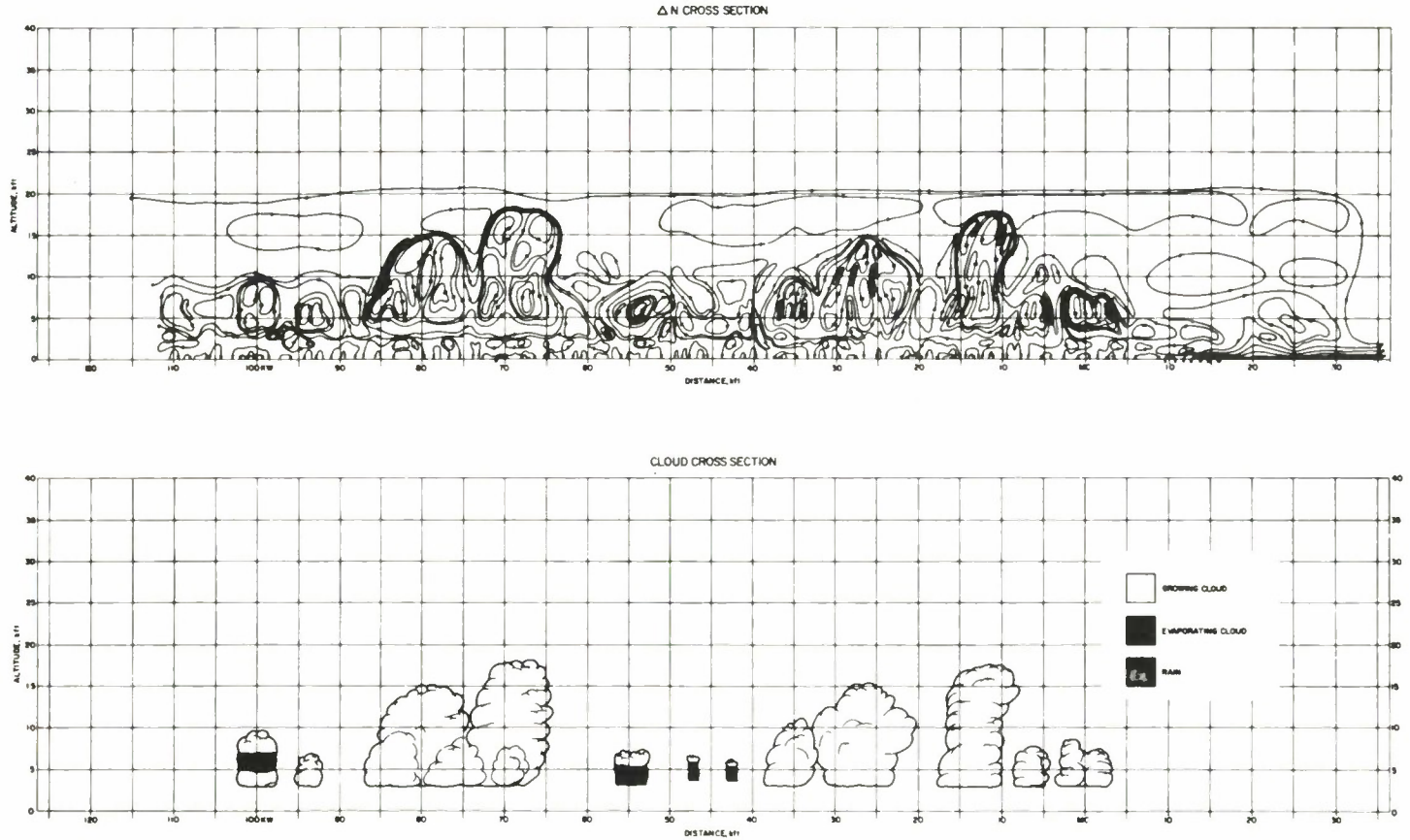

Fig. 9. Cloud Cross Section for 8 August 1963, Flight 243, along the E-W Leg of MISTRAM with the Corresponding N-Cross Section

RAY-TRACINGS IN CLOUD CROSS SECTIONS FOR A LONG BASELINE INTERFEROMETER

R. K. Crane*

INTRODUCTION

Presentations by R. M. Cunningham and J. H. Meyer (see pages 33 and 43 , respectively) describe the mesoscale refractive index cross sections along the E-W leg of the Valkaria, Florida, MISTRAM site. In this paper, the range, range difference, range rate, and range difference rate errors, caused by the refractive index variations described by the cloud cross sections, are presented for the MISTRAM interferometer system.

METHOD OF ANALYSIS

The variation of refractive index in the troposphere occurs over many scale sizes, ranging from the turbulent to the synoptic scales. Two ranges of scale sizes are considered for this analysis: those that contribute to a refractive index distribution that does not vary over the spatial extent of the cross section, and those that cause refractive index variations over distances ranging from 500 feet to the largest dimension of the cross section. The first of these scale size ranges contributes to the bias error; the second, to the cross-sectional error. For convenience, these scale size ranges are labeled bias and cross section.

The refraction-induced errors are computed using the methods of geometric optics. The scale sizes being considered imply that the changes of refractive index, over the dimensions of a wave length, are small, and that the

*The MITRE Corporation, Bedford, Massachusetts

ray-tracing equations are valid. The ray equations used are simplifications of Hamilton's Canonical Equations, valid for a variation of refractive index with height above a spherical earth. The position of a ray in space is computed using the spherically symmetric ray equations. The modification of the ray position by the variation of refractive index, as described by the cross section, is assumed to be negligible. The only effect of the cross section is to cause small changes in the phase velocity along the ray.

For ease of computation, the bias variation of refractive index, or bias profile, is considered to be composed of a number of layers, each layer having a linear change in m, where m is defined as the product of the index of refraction and the distance from the center of the coordinate system. With this assumption, the ray equations may be integrated directly in terms of trigonometric functions.

This approximate description of the bias profile describes the change of refractive index with height in almost the same manner as the familiar linear change in refractive index description, the maximum difference between the two approximate descriptions being $0.1N$ for the profiles considered.

Using the linear m description, the ray equations are:

$$\theta = \theta_i + \Delta\theta ;$$

$$m = nr = \left(1 + N \times 10^{-6}\right)\left(R_0 + h\right) ;$$

$$\Delta\theta = \int_{h_i}^{h} \frac{\cot \alpha \, dh}{R_0 + h} = \theta - \theta_i \text{ in the } i^{th} \text{ layer.*}$$

*Subscript i indicates value at the lowest height in the i^{th} layer.

Conditions on C_i^2

If $C_i^2 > 0$, then

$$\left.\begin{aligned} \Delta\theta &= v_i \log_e\left(\frac{\omega_i}{\omega}\right) \\ r &= 2C_i\,\omega_i e - \frac{\Delta\theta}{v_i}\left[\left(\omega_i e - \frac{\Delta\theta}{v_i} - f_i\right)^2 - A_1^2\right] - 1 \\ \omega &= \frac{a + e_i + (1+r) f_i}{1+r} \end{aligned}\right\} .$$

If $C_i^2 = 0$, then

$$\left.\begin{aligned} \Delta\theta &= \frac{1+s}{D_i}\left(\frac{a_i}{1+r_i} - \frac{a}{1+r}\right), \\ r &= 2D_i\left[\left(\frac{a_i}{1+r_i} - \frac{D_i\,\Delta\theta}{1+s}\right)^2 - A_i^2\right] - 1 \end{aligned}\right\} .$$

If $C_i^2 < 0$, then

$$\left.\begin{aligned} \Delta\theta &= v_i \cdot \tan^{-1}\left(\frac{\omega_i - \omega}{1 + \omega\,\omega_i}\right) \\ r &= \frac{\sqrt{|C_i^2|}}{z} \cdot \left(\pm \frac{\sqrt{A_i^2 + f_i^2}}{1+u^2} - f_i\right) - 1 \\ \omega &= \frac{(1+r)\,f_i - \sqrt{|C_i^2|}}{a} , \end{aligned}\right\}$$

where

$$u = \frac{1 - \omega_i \tan \frac{\Delta\theta}{v_i}}{\omega_i + \tan \frac{\Delta\theta}{v_i}} \quad ,$$

$$z = \frac{A_i^2 - u^2 f_i^2}{1 + u^2} \quad ,$$

$$r = \frac{h}{R_0} \quad ,$$

$$A_i = \frac{\Delta M \times 10^{-6}}{\Delta^h} \cdot R_0 = \left(R_0 + h\right) \times 10^{-6} \frac{dN}{dh} + 1 + N \times 10^{-6} \quad ,$$

$$M = N + \frac{h \times 10^6}{R_0} + \frac{Nh}{R_0} \simeq N + \frac{h \times 10^6}{R_0} \quad ,$$

$$N = (n - 1) \times 10^6 \, , \quad n = \text{index of refraction} \quad ,$$

$$D_i = A_i \left(1 + e_i\right) \, ,$$

$$e_i = M_i \times 10^6 - A_i \left(1 + \frac{h_i}{R_0}\right) j \quad ,$$

$$C_i^2 = e_i \left(2 + e_i\right) - S \left(2 + S\right) \, ,$$

$$S = \left(1 + N \times 10^{-6}\right)\left(1 + \frac{h}{R_0}\right)\cos \alpha_0 - 1$$

$$a = \sqrt{\left(M \times 10^{-6}\right)\left(2 + M \times 10^{-6}\right) - S\left(2 + S\right)}$$

$$f_i = \frac{D_i}{\sqrt{|C_i|^2}} \quad ,$$

$$v_i = \frac{1 + S}{\sqrt{|C_i|^2}} \quad ,$$

The terms θ, h, R_0 and α are defined in Fig. 1.

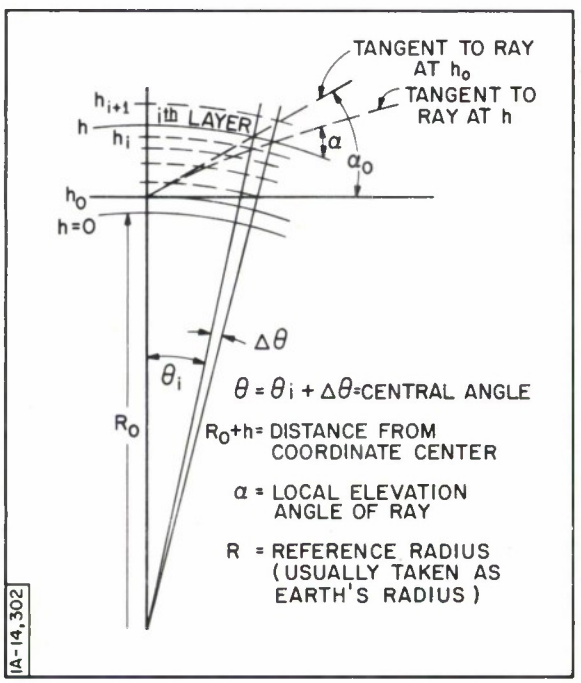

Fig. 1. Geometry for Ray Tracing

Using these equations, the central angle for the point of intersection of the ray with an arc of constant height or the point of intersection of the ray with the radius vector for a given central angle may be computed. The cross section description of refractive index variation consists of a table of ΔN values, one value for each intersection of an arc of constant height, and a radius vector as shown in Fig. 2. The value ΔN specifies the difference between the measured refractive index at a point in space and the value of refractive index for that point specified by the bias profile. The electrical range along the ray, as determined by a transit time measured, is given by $R_E = C\Delta_t$, where

$$\Delta_t = \int_{\text{along ray}} \frac{ds}{v}$$

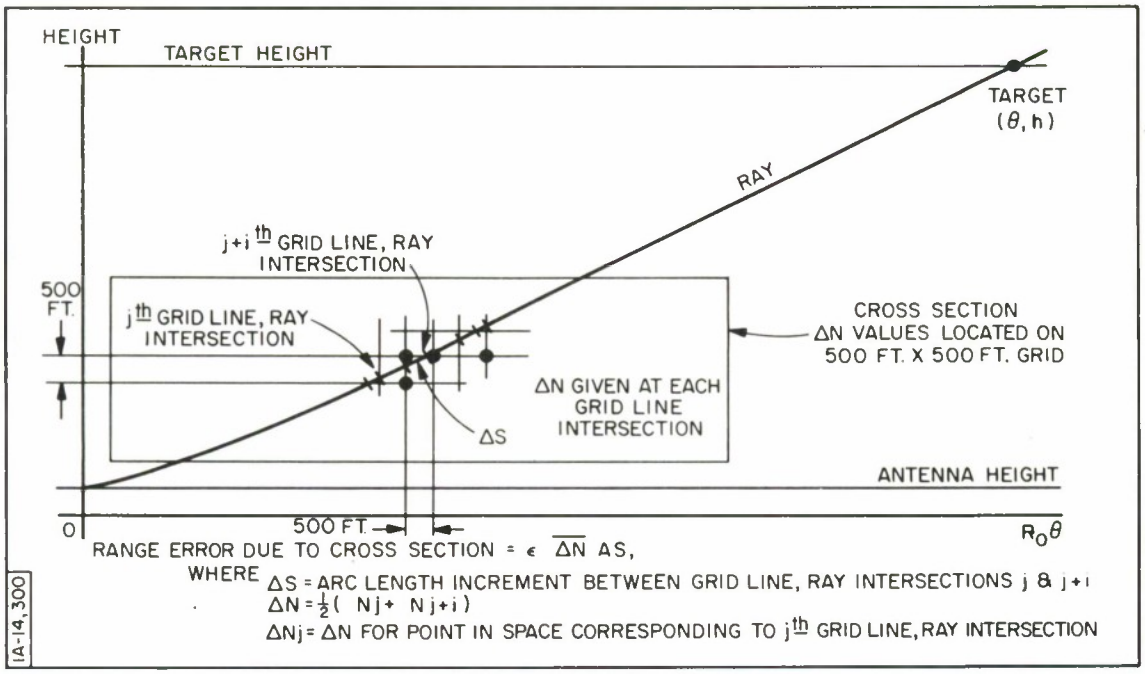

Fig. 2. Geometry for Ray in the Cross Section

$$R_E = c \int_{\text{along ray}} \frac{ds}{v} = \int_{\text{along ray}} \left(\frac{c}{v}\right) ds = \int_{\text{along ray}} nds$$

$$= \int_{\text{along ray}} \left(n_{\text{bias}}\right) ds + \int_{\text{along ray}} \left(n_{\text{cross section}}\right) ds$$

$$= \left(R_B\right)_{\text{bias}} + \left(\Delta R_C\right)_{\text{cross section}}$$

where

c = velocity of light in free space,

n = velocity of light in the medium, and

s = arc length along ray.

The range error produced by the cross section, ΔR_C, is found by determining the line integral of ΔN for the ray in the cross section. The position of the ray is assumed to be determined solely by the bias profile. The incremental arc length, ΔS between each ray grid line intersection can be computed using the integral for ΔS for a linear m profile for each layer.

$$\Delta S = \int_{1 + r_i}^{1 + r} \csc \alpha \, d\left(1 + r\right) = \int ds$$

$$= R_0 \left(\frac{a - a_i}{A_i} \right) \quad A_i \neq 0$$

$$= R_0 \left[\frac{\left(1 + e_i\right)\left(r - r_i\right)}{|C_i|} \right] \quad A_i = 0$$

where the variables are as defined above.

The cross sectional range error is calculated by assuming that the equation may be approximated as:

$$\Delta R_C = \int_{\text{along ray}} \left(\Delta N \times 10^{-6} \right) ds \quad \sum \int_{\text{along ray between grid lines}} \Delta N \; ds$$

$$\simeq \sum \bar{\Delta N} \; \Delta S$$

where ΔN is taken as one-half the sum of the values of ΔN for each end of the incremental segment of arc, ΔS.
The value of ΔN for each grid line ray intersection is calculated by linearly interpolating between values of ΔN for adjacent grid lines.

The bias range error ΔR_0 is calculated by subtracting the true range to the target from the electrical range. The equation used to compute R_B is given by:

$$R_B = \sum_{\text{layers}} \int n_B \, ds$$

$$= R \sum \left[a_{i+1} - a_i + (1 + e_i) \log_e \left(\frac{a_{i+1} + 1 + M_{i+1} \times 10^{-6}}{a_{i+1} + M_i \times 10^{-6}} \right) \right.$$

$$\left. + \frac{(1 + e_i (2 + e_i))}{1 + S} \Delta\theta_i \right]$$

where $\Delta\theta_i = \theta_{i+1} - \theta_i$ and the remaining variables are as defined above

The range error for a given ray is computed as a function of the initial elevation angle and the ray end-point heights. The initial elevation angles for two rays that intersect at the true target position must be calculated, see Fig. 3 in order to determine the range difference error for an interferometer measurement. The method of calculation used was to assume a value of initial elevation angle α_{0A} calculated θ for the end-point height, and compare the results with the given target position. The initial elevation angle was then corrected using the difference between the result and the given value, α_{0A} as:

$$\Delta\theta = \frac{R_0 (\theta_c - \theta_r) \sin \alpha_{0A}}{S}$$

This process was iterated until the difference between θ_r and θ_c was less than 5.0×10^{-9} milliradians. The computations were performed using an IBM 7030 Stretch computer, and the resultant accuracy of the refraction effects for a given linear profile is shown in Table 1. These accuracies relate only to

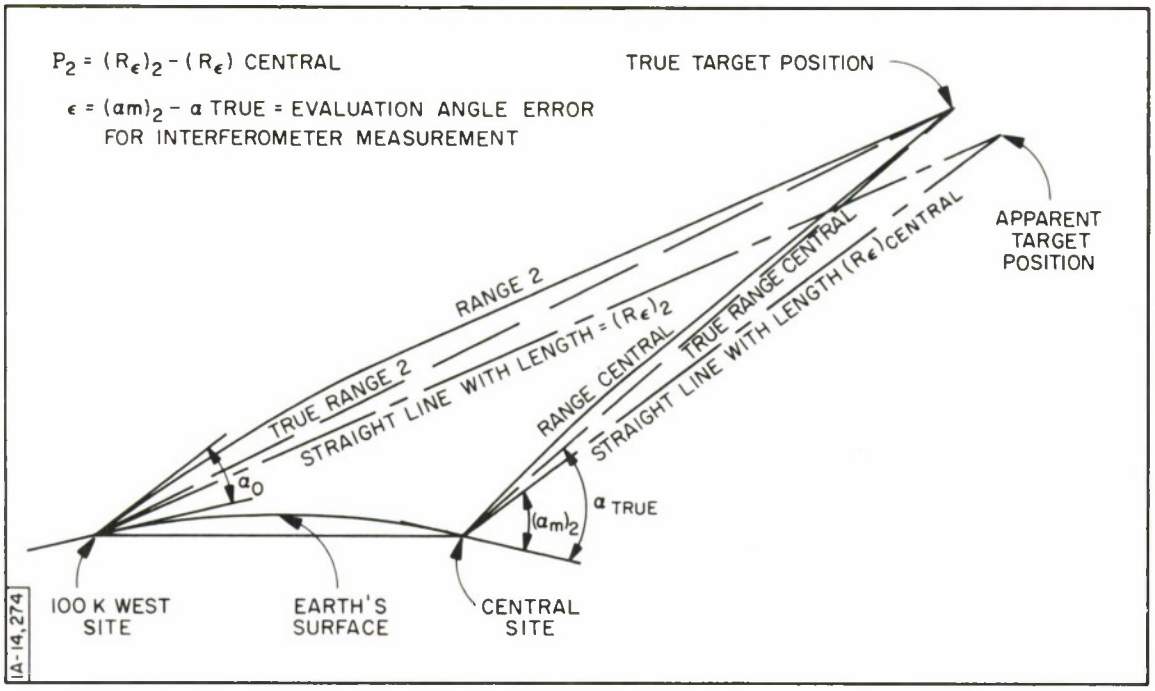

Fig. 3. Geometry for Interferometer Calculation

computations based on the bias approximation to the refractive index variations in space. They do not include the uncertainties associated with using the bias profile to model the atmosphere.

Table 1

Computation Accuracy for a Given Linear m Profile

For $h < 1 \times 10^6$ ft., $\alpha_0 > 10$ mr.			
$\theta(h)$	error	$<10^{-9}$	mr.
$h(\theta)$	error	$<10^{-2}$	ft.
R(h)	error	$<10^{-5}$	ft.
S(h)	error	$<10^{-5}$	ft.

CALCULATED RANGE ERRORS

The refractive index cross-sections, prepared by J. Meyer, describe the N-variations over a horizontal distance of 150,000 feet and a vertical distance of 32,000 feet. The deviation of refractive index from the bias profile value is assumed to be zero outside of the given cross section. The cross-sectional errors were calculated for elevation angles between 10 and 35 degrees for a target at 32,808 feet (10 kilometers). These errors apply for all heights above 32,808 feet for the indicated elevation angles, because the cross section has zero values above this height. The cross-sectional range errors plotted, for three different antenna locations in the cross section, are shown in the figures on pages 68 and 72. These ray path starting points correspond to the location of the three MISTRAM sites along the E-W leg. The interferometer calculations were performed using the assumption that the target trajectory lies in the plane of the three sites or in the plane for which the cross section is valid.

7 August 1963

The bias profile, rawinsonde profile, and aircraft measurements of refractive index for 11:00 EST for 7 August 1963 are shown in Fig. 4. The bias profile was generated, using a best fit approximation, to the data points below 20,000 feet, the rawinsonde data from 20,000 to 40,000 feet, and the IACO standard atmosphere (dry term only) above 40,000 feet. The cross section representative of this particular time is pictured in Fig. 6. The cross sectional range errors for each of the MISTRAM sites are given in Fig. 5. One percent of the bias range error for a target at 32,808 feet is plotted for reference.

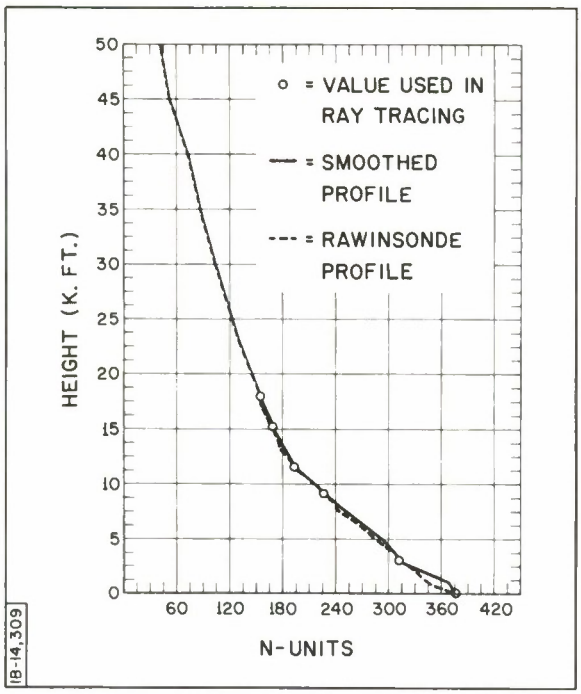

Fig. 4. Refractive Index Profile, 7 August 1963, Valkaria, Florida

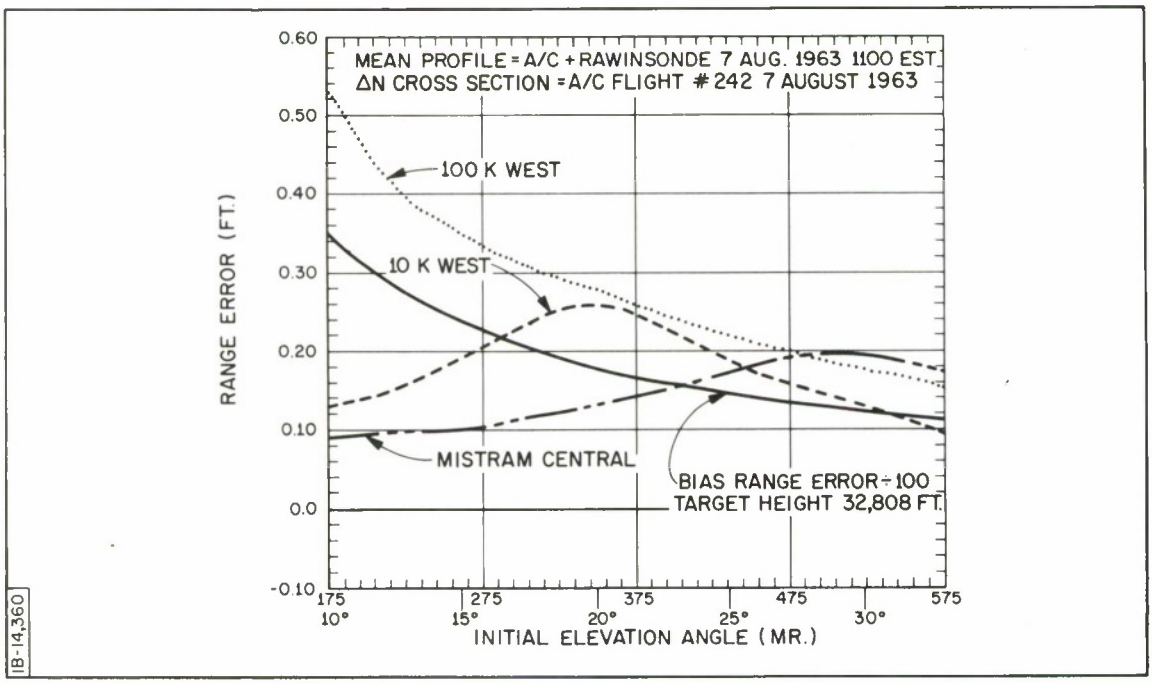

Fig. 5. Cross-Sectional Range Error, 7 August 1963, MISTRAM Central, Valkaria, Florida

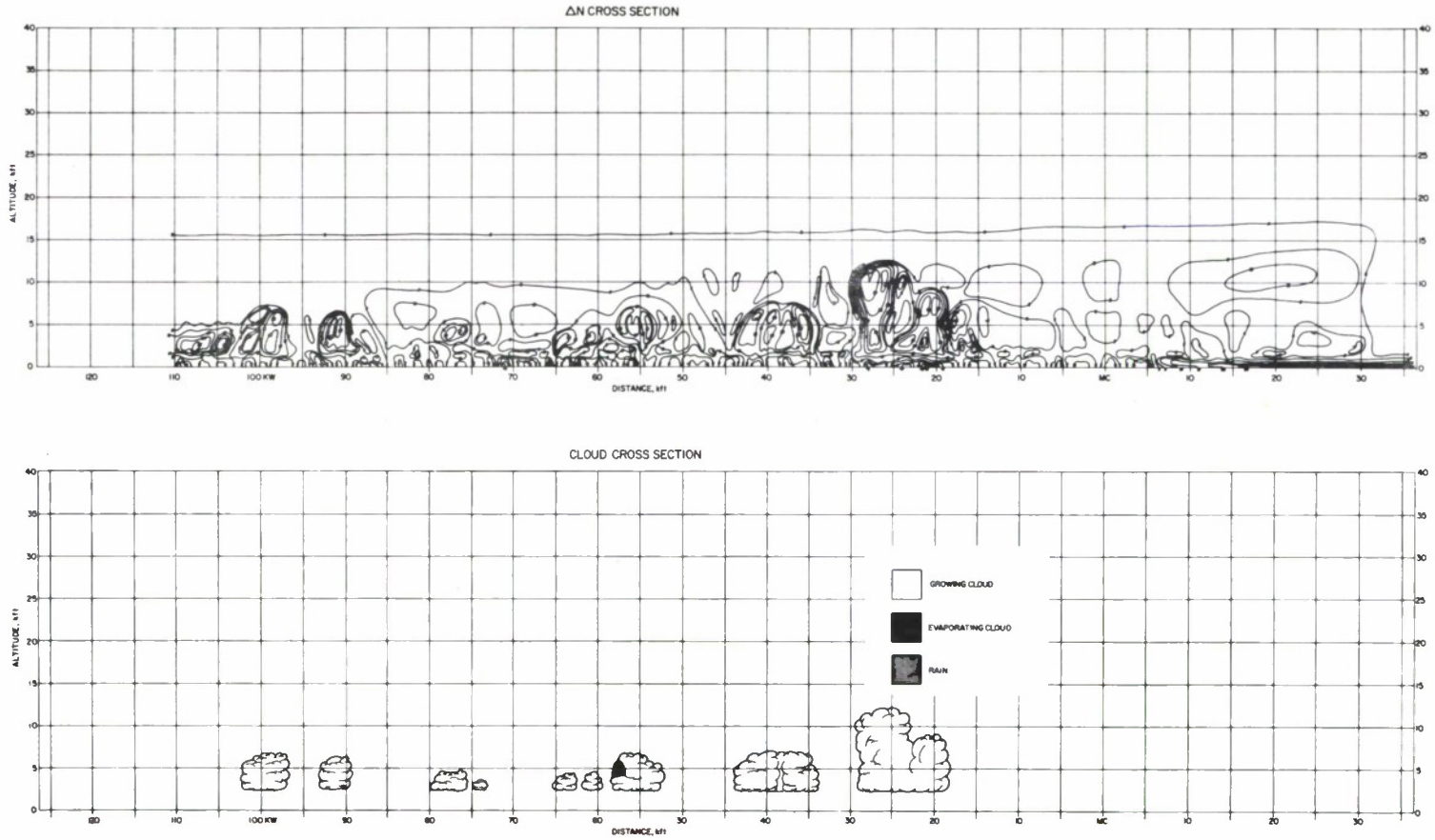

Fig. 6. ΔN and Cloud Cross Sections, 7 August 1963, Valkaria, Florida

The rays from both the MISTRAM Central and the 10 K. West (KW) sites lie in the clear (cloud-free) region over the range of elevation angles shown. At elevation angles between 10 to 20 degrees, the 10 KW ray is sweeping up into region of space with $\Delta N = +10$; this region contributes to the peak in the range error curve at an elevation angle of about 10 degrees. The 100 KW ray passes through the sea breeze-induced clouds at about 25,000 feet west of MISTRAM Central. As the ray sweeps up, it gets above the cloud with the high ΔN–values, and the cross-sectional range error drops.

8 August 1963

The bias profile, ΔN cross section and cross sectional errors are shown in Figs. 7, 8, and 9. The MISTRAM Central rays, for elevation angles less than 18 degrees, and the 10 KW rays, for elevation angles less than 13 degrees, pass under the sea breeze-induced clouds. The cross-sectional range errors increase for higher elevation angles as the ray passes through the clouds.

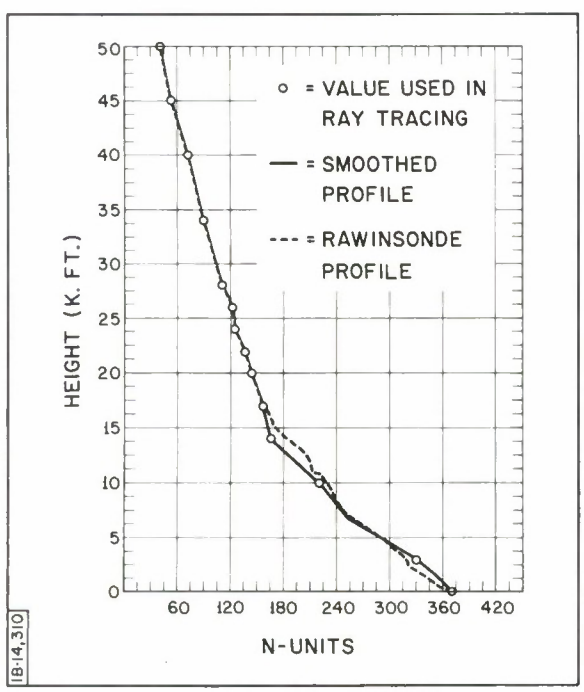

Fig. 7. Refractive Index Profile, 8 August 1963, Valkaria, Florida

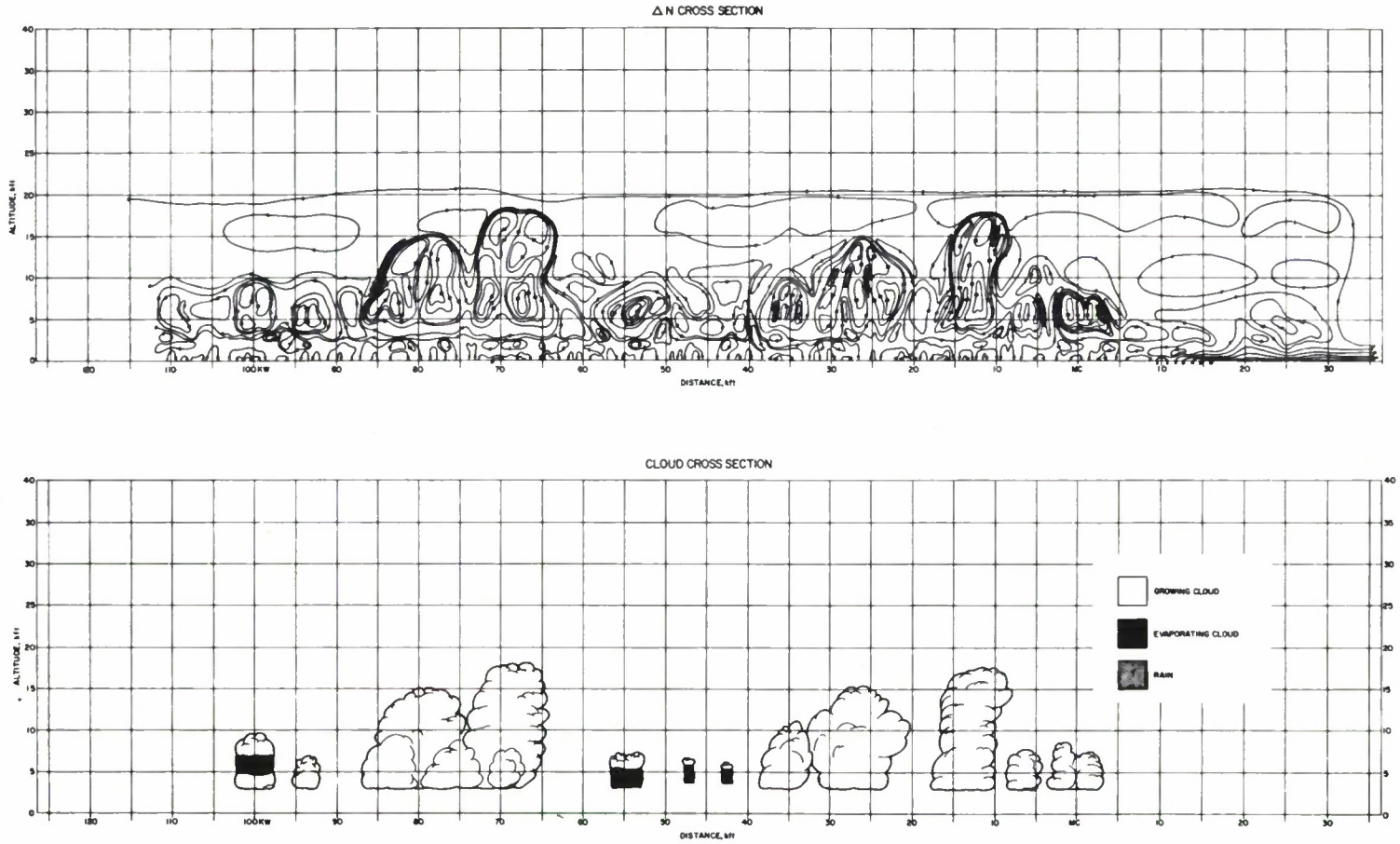

Fig. 8. ΔN and Cloud Cross Sections, 8 August 1963, Valkaria, Florida

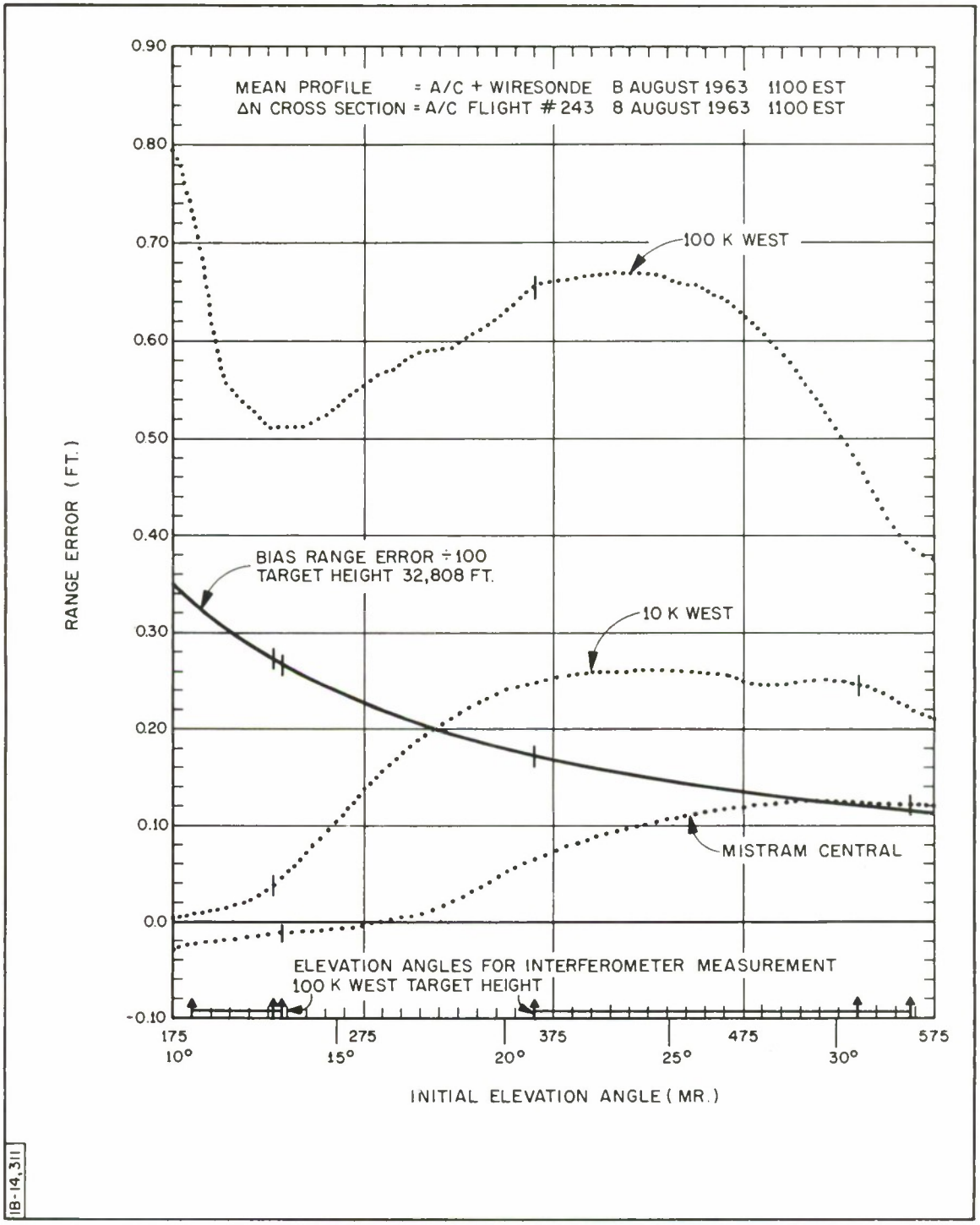

Fig. 9. Cross-Sectional Range Error, 8 August 1963, MISTRAM Central, Valkaria, Florida

The 100 KW rays pass through the clouds about 70,000 feet west of the Central site for elevation angles near 25 degrees. The result is the rapid change in cross-sectional range error for increasing elevation angle.

9 August 1963

The bias profile, ΔN cross section, and cross-sectional range errors are given in Figs. 10, 11, and 12. The 10 KW rays pass through the sea breeze clouds for elevation angles greater than 10 degrees. For elevation angles above 20 degrees, the ray passes through a region of low ΔN in the center of the clouds. The sea breeze clouds are closer to the beach than they were on either the seventh or eighth of August. This results in an increase in the MISTRAM Central cross-sectional errors at lower elevation angles than on the other two days.

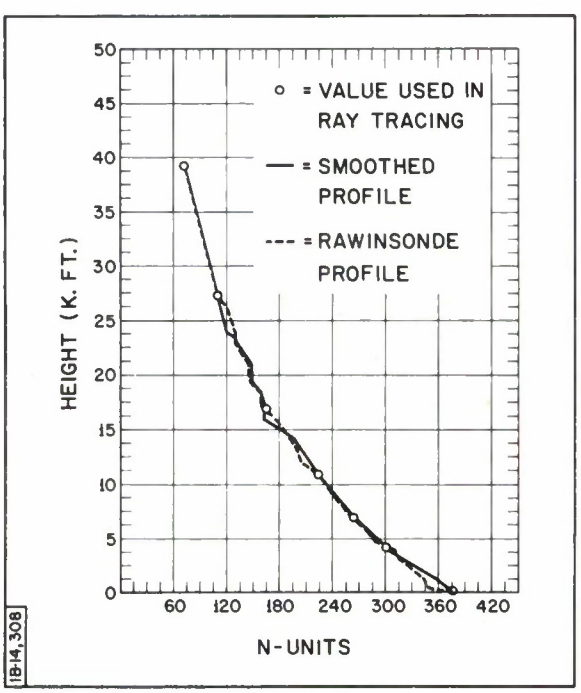

Fig. 10. Refractive Index Profile, 9 August, 1963, Valkaria Florida

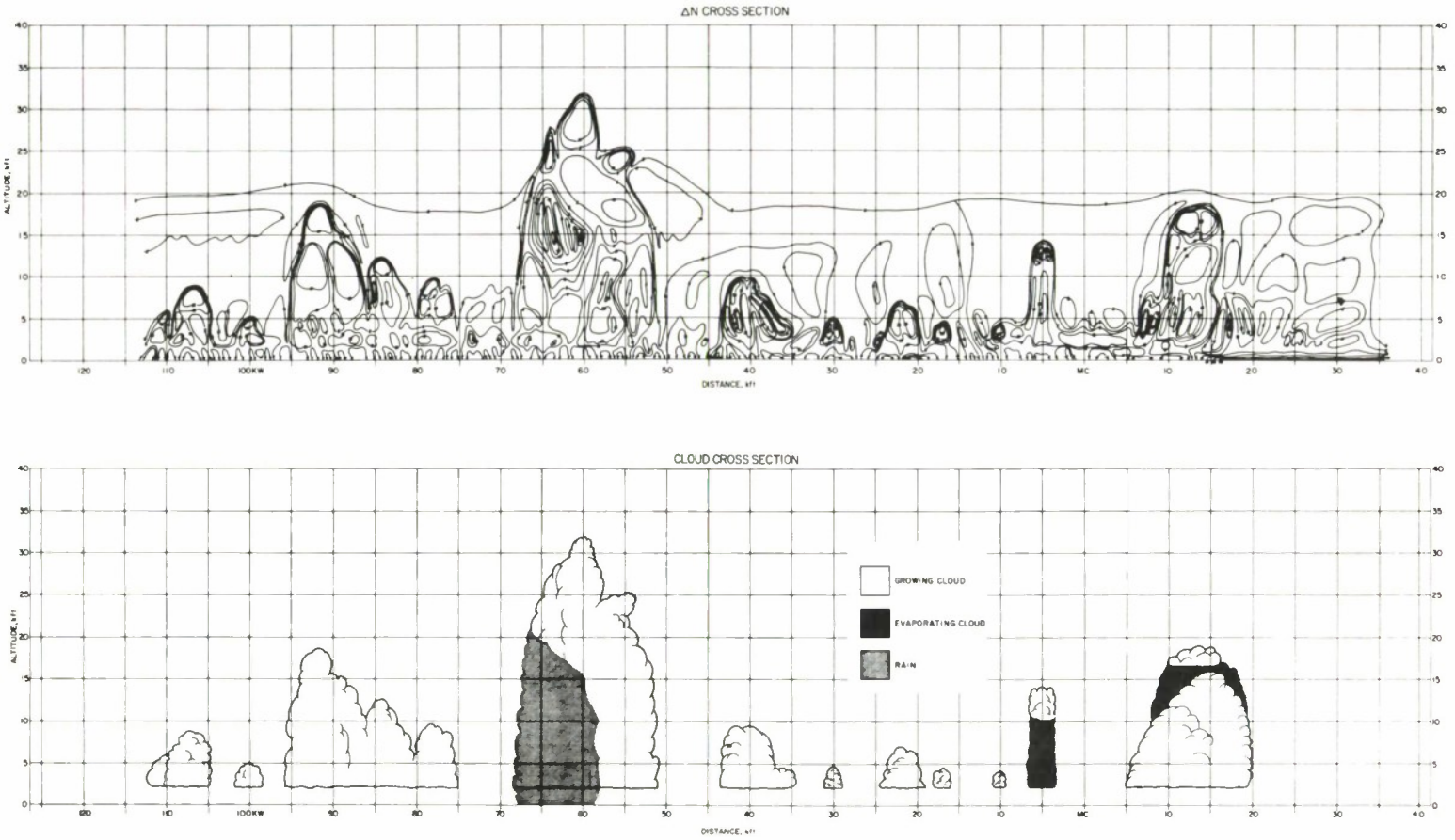

Fig. 11. Δ N and Cloud Cross Sections, 9 August 1963, Valkaria, Florida

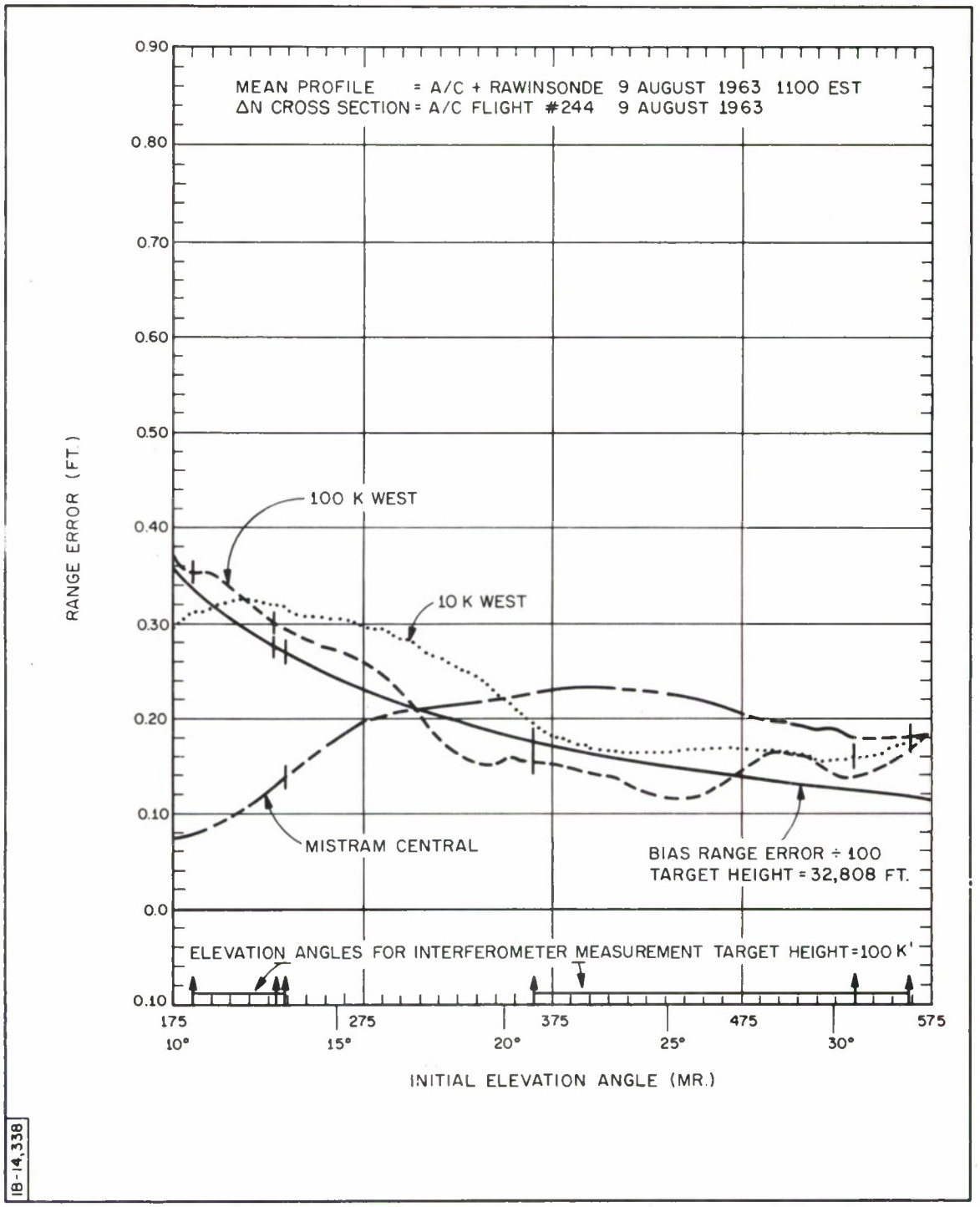

Fig. 12. Cross-Sectional Range Error, 9 August 1963, MISTRAM Central Valkaria, Florida

Interferometer Errors for 7 August 1963

The preceding data gives the cross-sectional range error as a function of elevation angle for a single ray. For an interferometer measurement, two rays are combined, each at a different elevation angle. The correct elevation angles for rays intersecting at both 100,000 and 999,999 feet were computed to determine the errors for interferometer measurements. The results are given in Figs. 13 to 22. The elevation angle error is defined in Fig. 3. The baseline comparison value,

$$\delta\rho = P_1 - \frac{1}{10} P_2 \quad ,$$

is given in Figs. 22; this Figure also compares the range difference errors ($\delta\rho$) for each of the three days for which data was processed.

On 7 August, it can be seen that the cross-sectional range error meets specifications for angles above 10 degrees, while the range difference error for the short baseline does not. The comparison of errors between the two baselines does not conclusively show that a long baseline system is better than a short one. The actual errors strongly depend upon target position. The range difference rate error alone does not meet specifications for the long baseline at angles less than 13 degrees. The short baseline range rate error meets specifications over the range of values of elevation angle that have been plotted. These rate errors are strongly affected by the target trajectory and velocity; the assumed rate of change of initial elevation angles at the 100 KW site was 1 milliradian/second.

An actual target trajectory would have to be used to compute the range, range difference, range rate, and range rate difference errors for comparison with Cape Kennedy data. The results discussed in this report pertain to a simple constant-height trajectory.

It should be noted that the range difference rate errors for actual missile trajectories may differ from those indicated above. The purpose of using a simple trajectory was to enable us to present an example of how the profile can be used to study a problem area of an operational system. Now that the technique has been developed and the necessary computer program written, it is certainly a simple matter to continue using this approach for other similar investigations on the MISTRAM system.

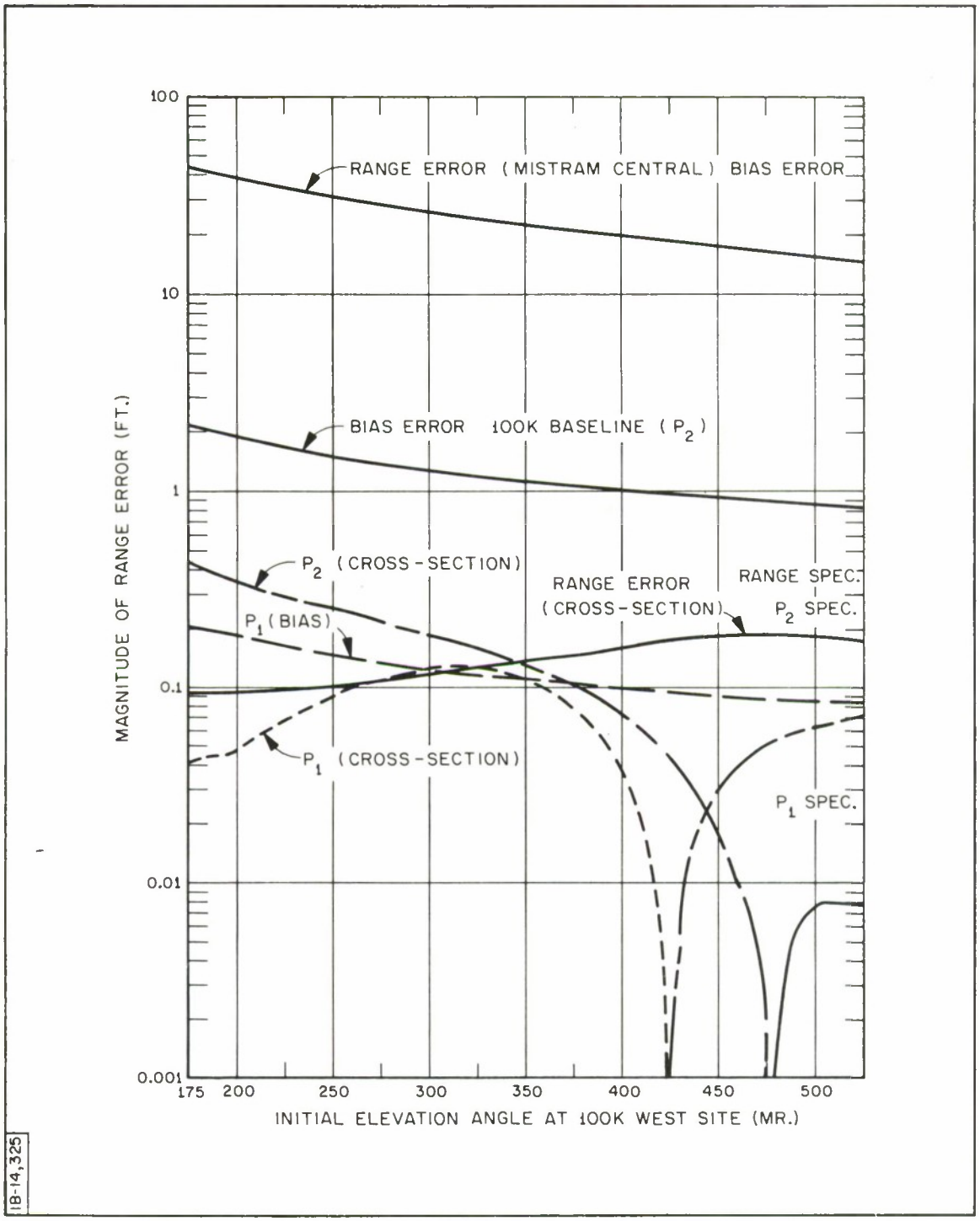

Fig. 13. MISTRAM System Profile and Cross Section, 7 August 1963; Target Height: 999,999 Feet

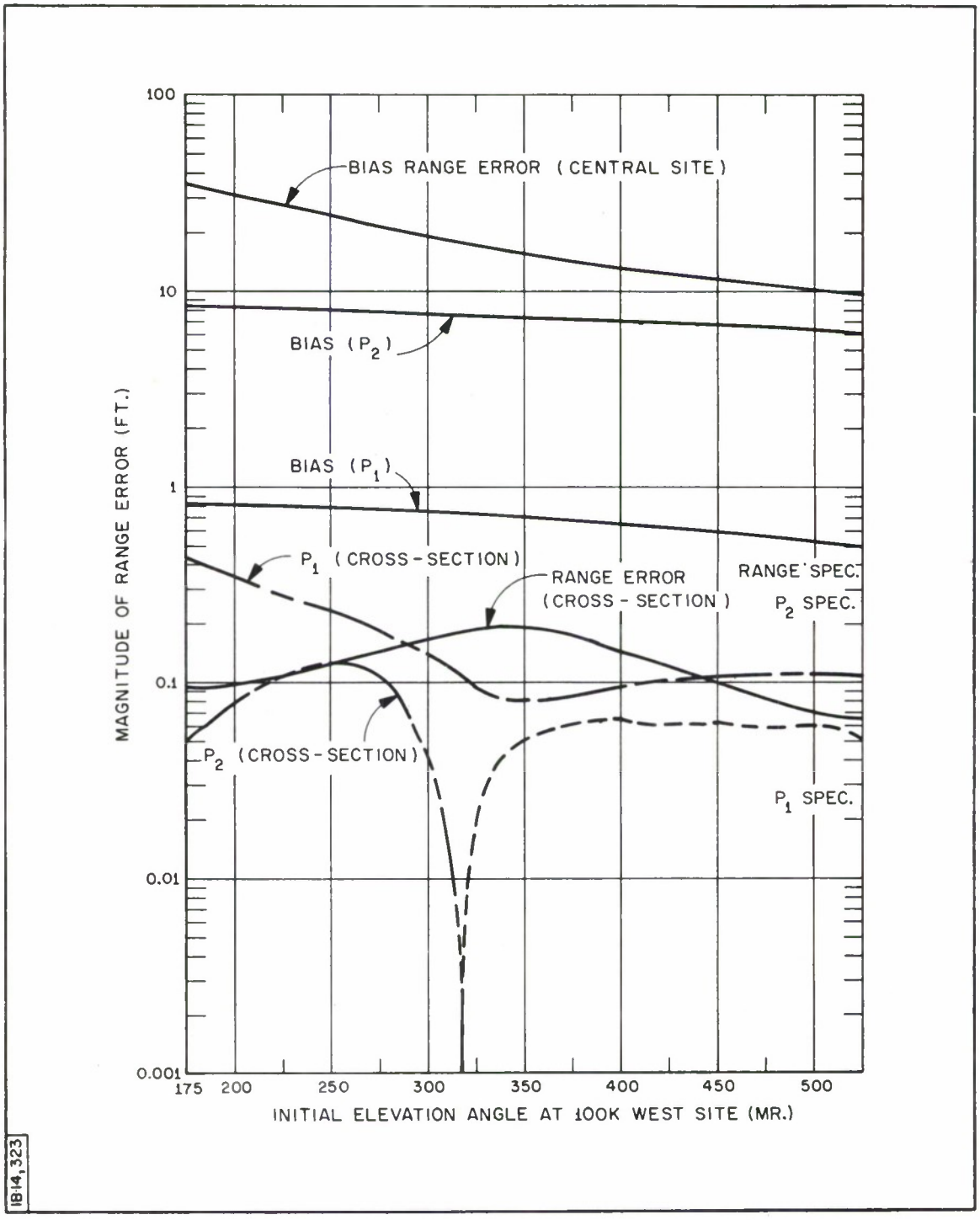

Fig. 14. MISTRAM System Profile and Cross Section, 7 August 1963; Target Height: 100,000 Feet

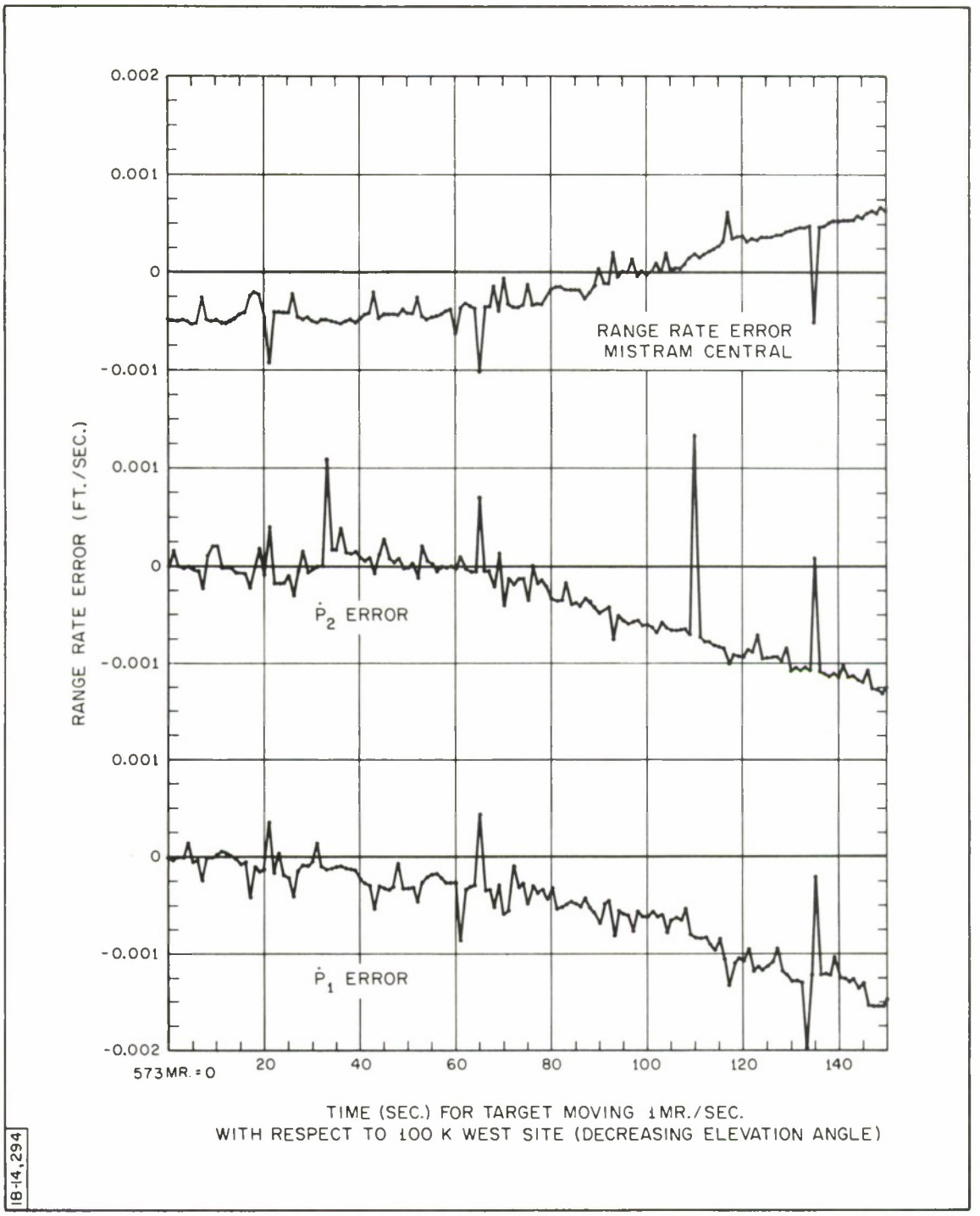

Fig. 15. Range Rate Error and Range Difference Rate Errors Due to Cross Section, 7 August 1963, MISTRAM System; Target Height: 999,999 Feet

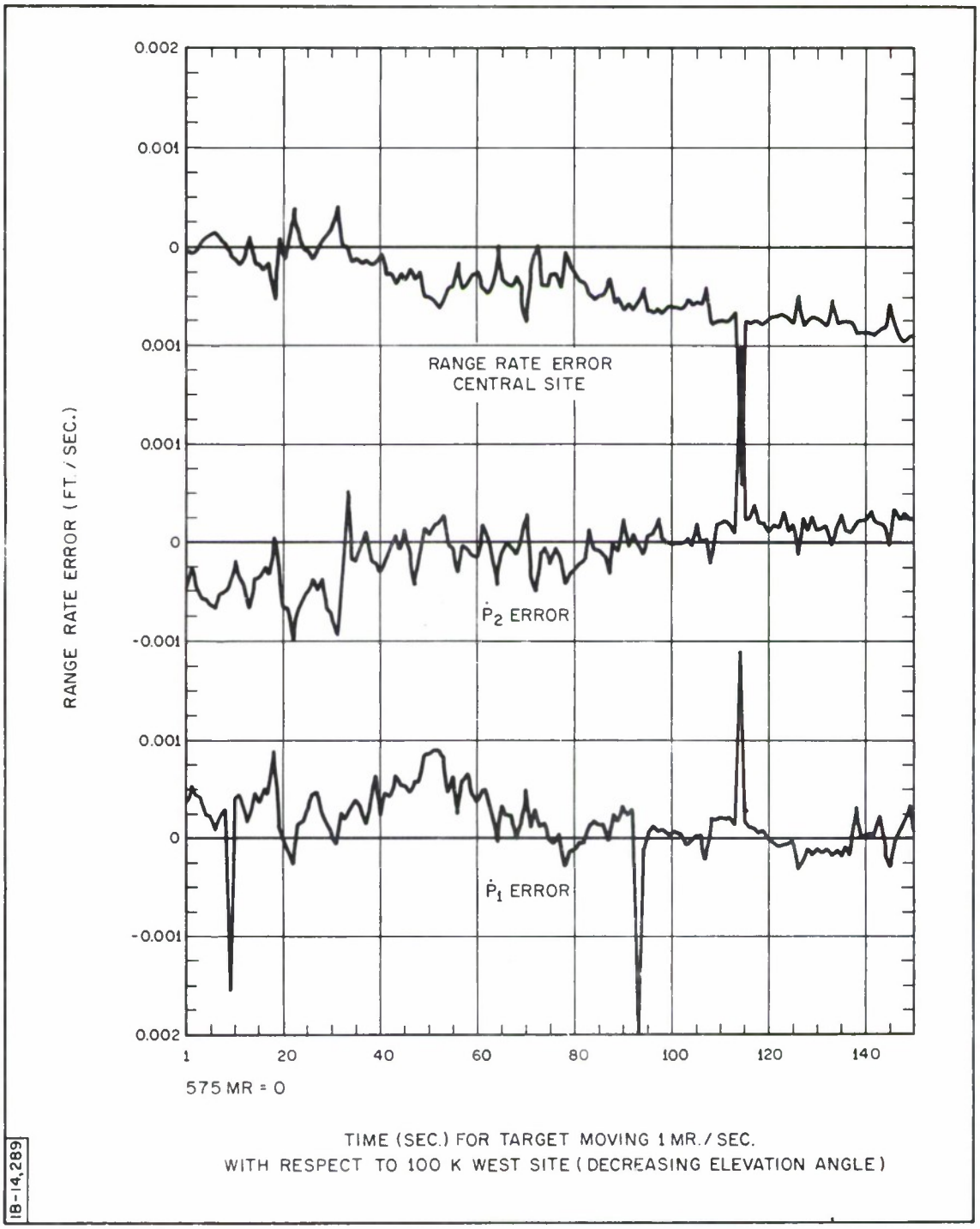

Fig. 16. Range Rate Error and Range Difference Rate Errors Due to Cross Section, 7 August 1963, MISTRAM System; Target Height: 100,000 Feet

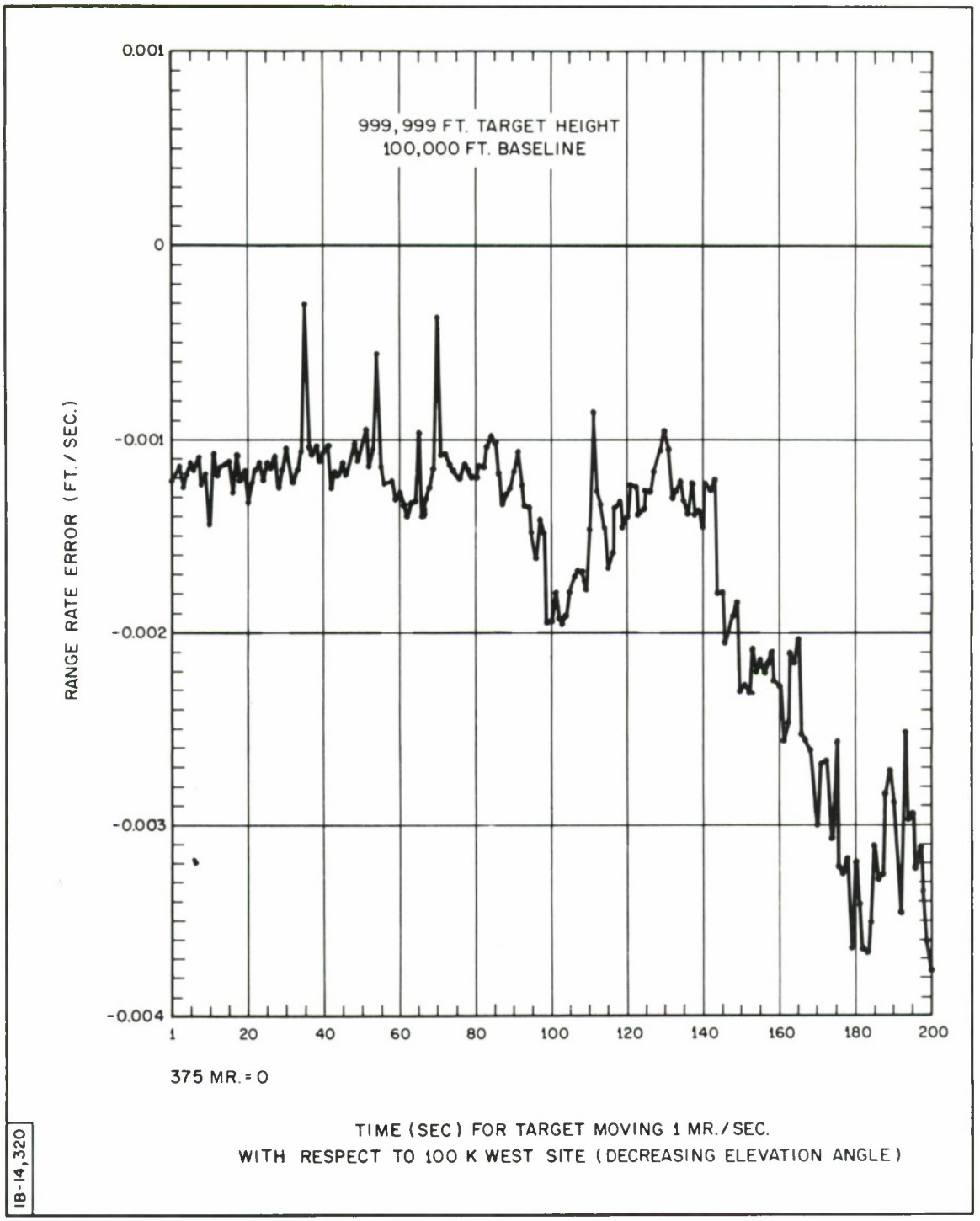

Fig. 17. Range Difference Rate Error, 7 August 1963; Target Height: 999,999 Feet, Baseline: 100,000 Feet

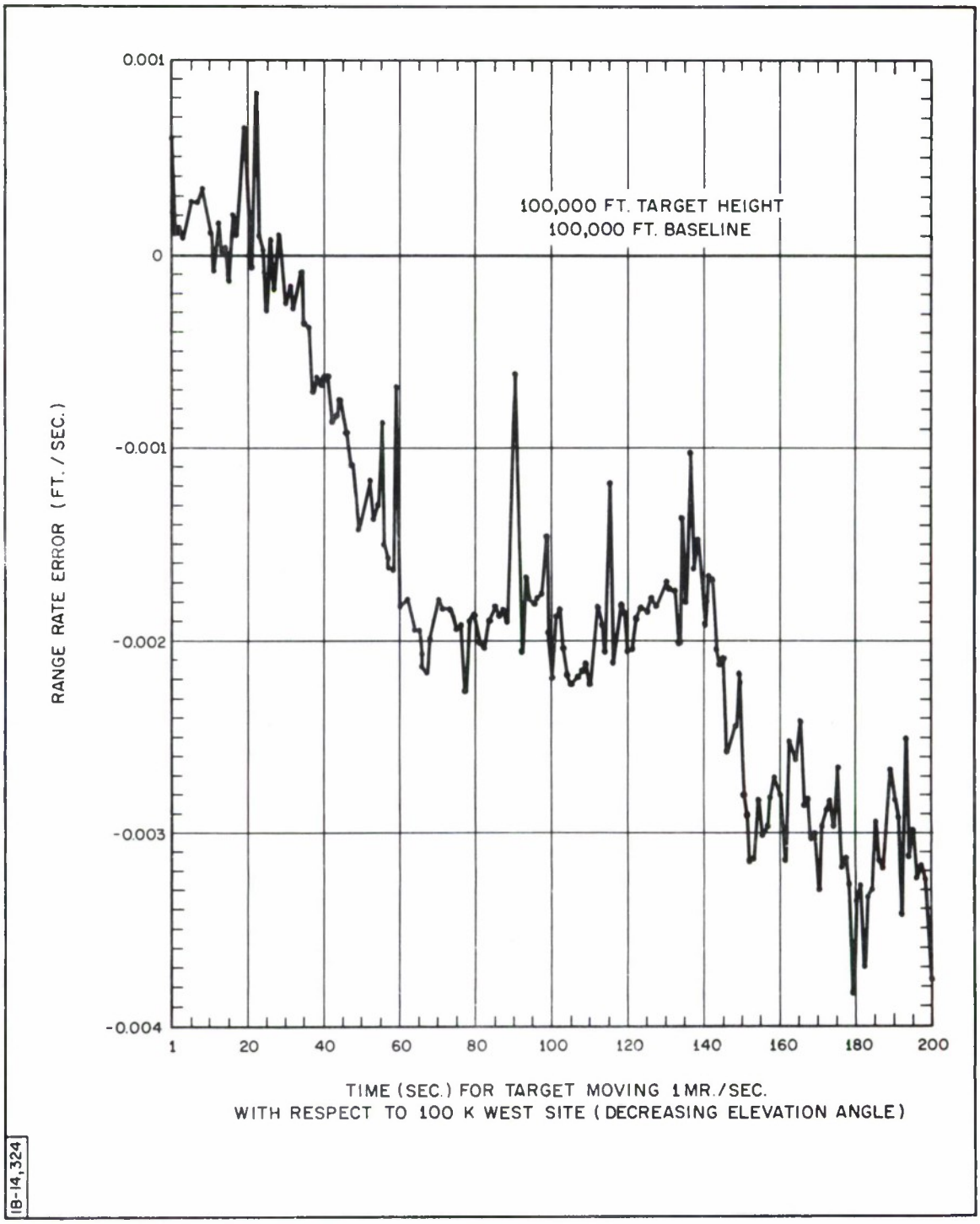

Fig. 18. Range Difference Rate Error, 7 August 1963; Target Height: 100,000 Feet, Baseline: 100,000 Feet

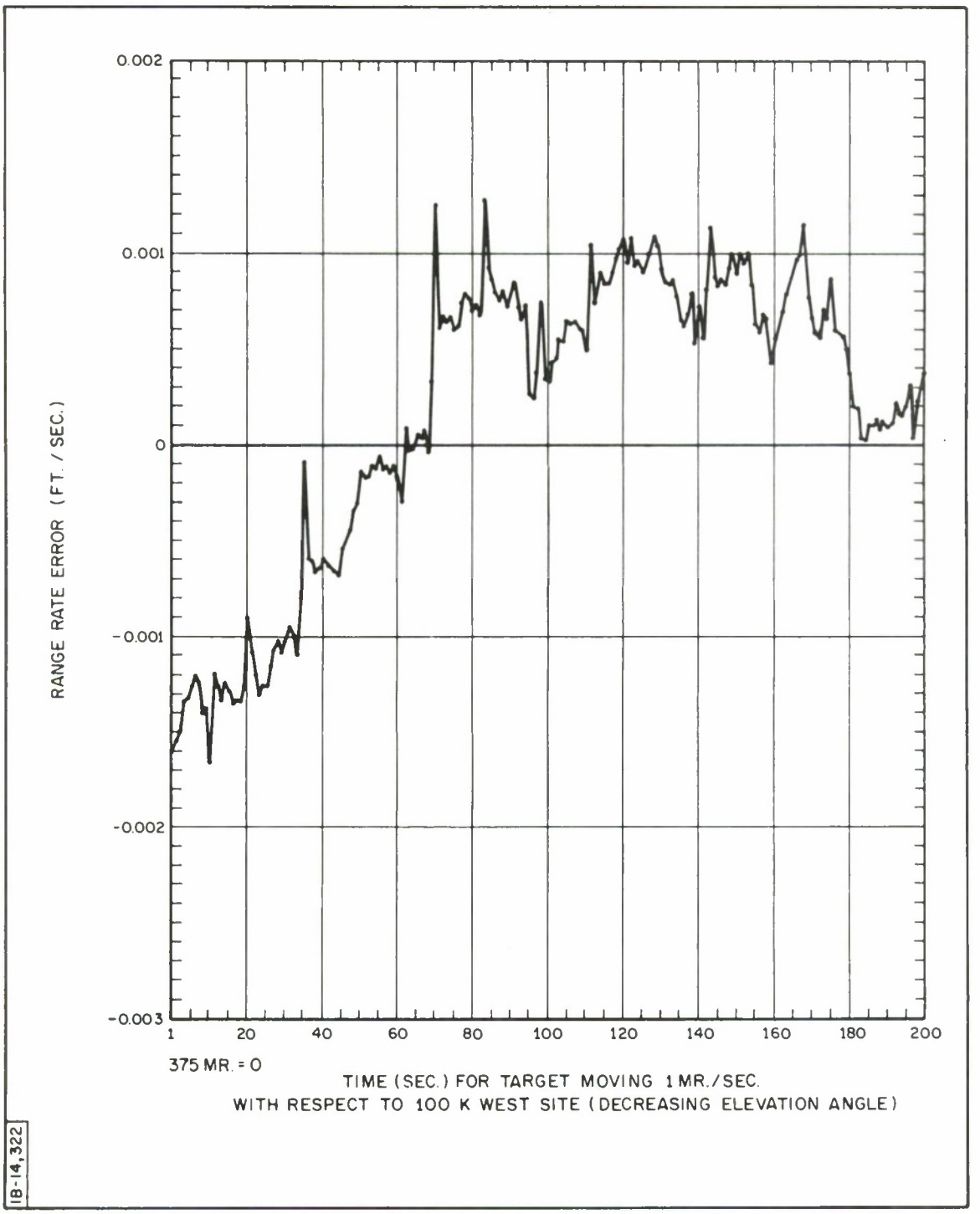

Fig. 19. Range Difference Rate Error, 7 August 1963; Target Height: 100,000 Feet, Baseline: 10,000 Feet

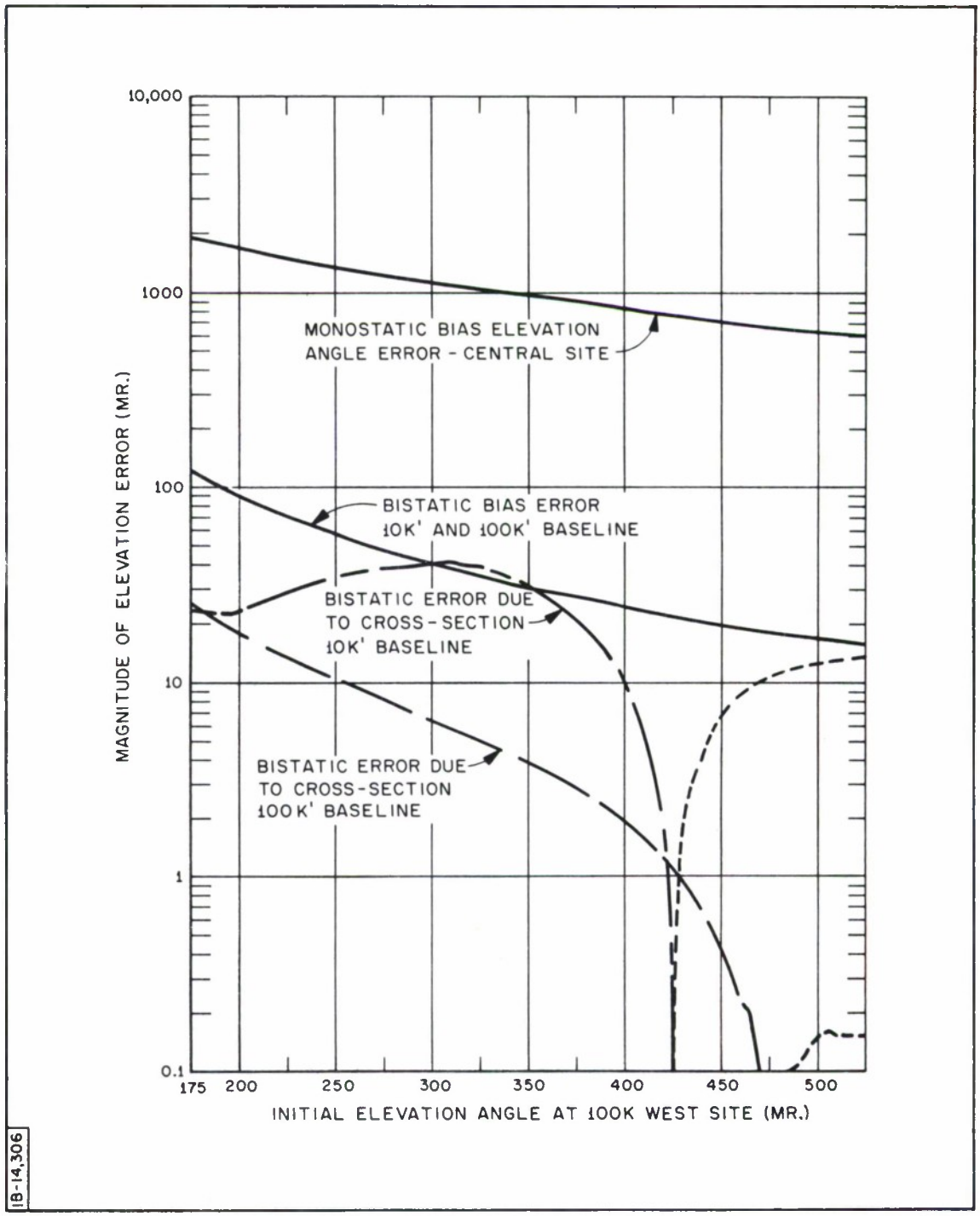

Fig. 20. Elevation Angle Errors, Profile and Cross Section, 7 August 1963; Target Height: 999,999 Feet

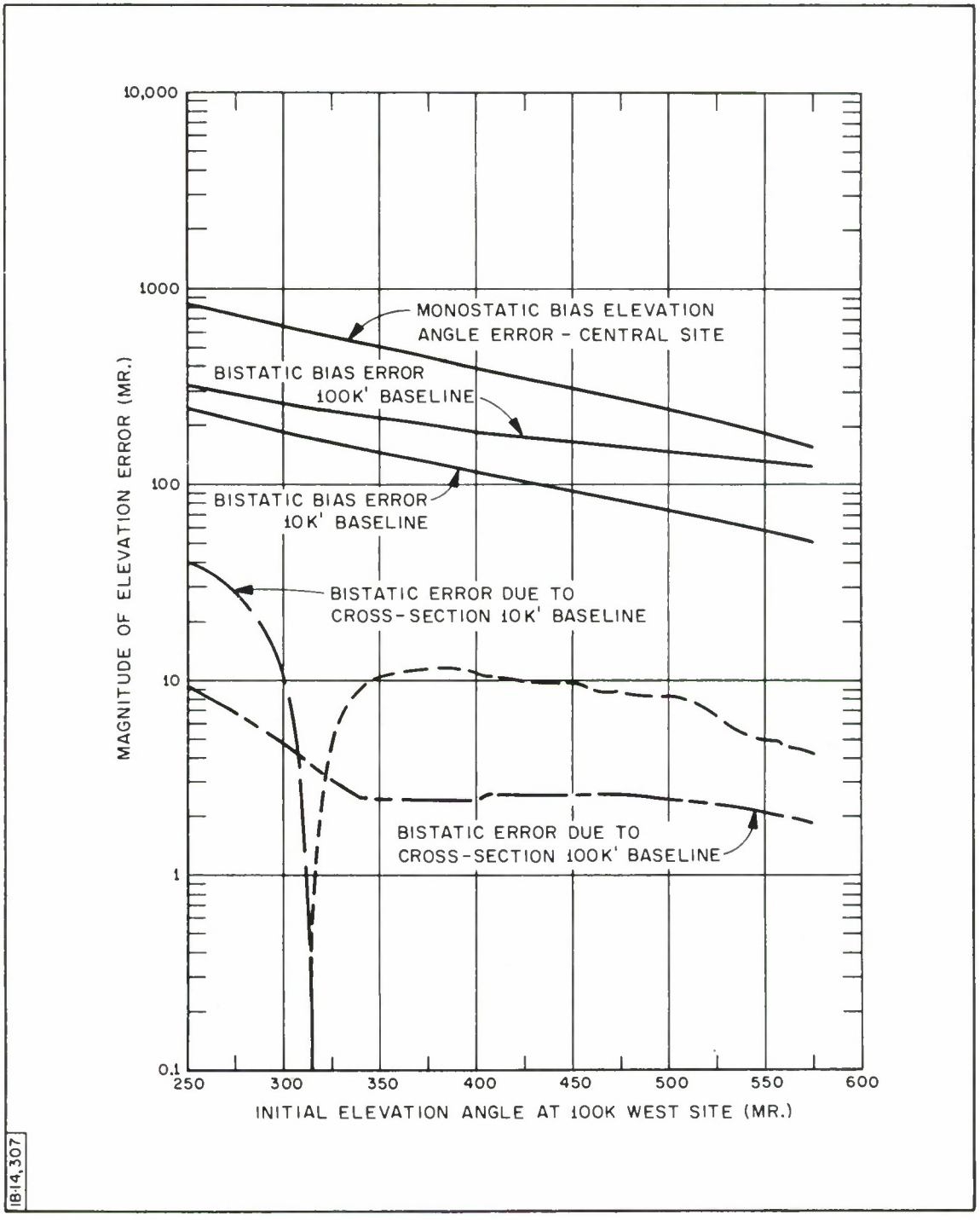

Fig. 21. Elevation Angle Errors, Profile and Cross Section, 7 August 1963; Target Height: 100,000 Feet

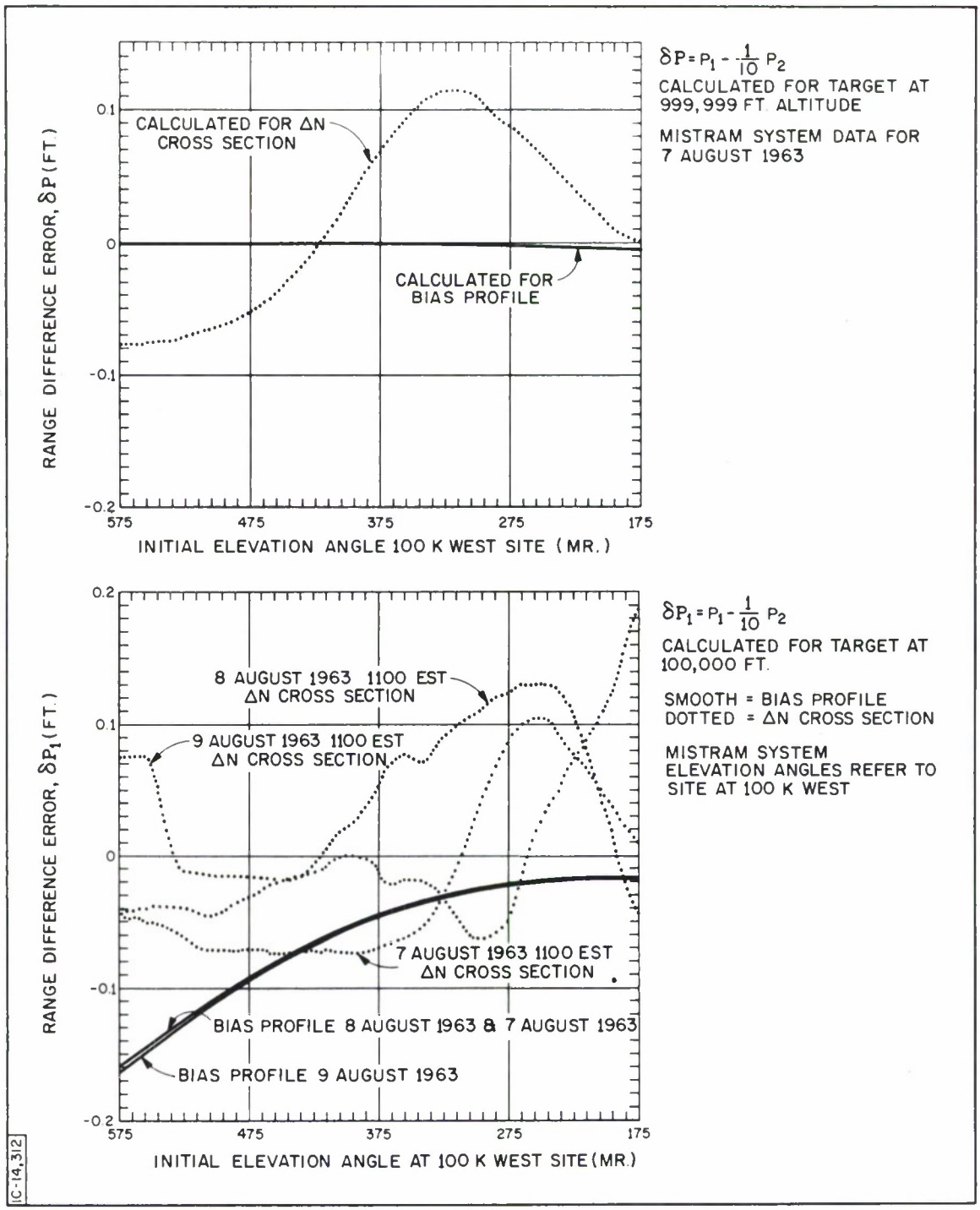

Fig. 22. Range Difference Errors as a Function of Elevation Angle

ESD MAUI, HAWAII, MEASUREMENTS

M. C. Thompson, Jr. *

INTRODUCTION

The installation of the 9.4-gc transmitter and receiver for the X-band, fixed end-point phase measurements at Maui, Hawaii, was started in November 1963; the first data run was performed in January 1964, and the field measurements were scheduled for completion in mid-July 1964. Current plans are to return the equipment to Boulder, Colorado.

The following outline summarizes the various test conditions for which data was obtained. The location and the profile of the propagation path on Maui are given in Vol. 1 of the previous Proceedings. ** The location of the instrumentation on the airstrip is shown in Fig. 1.

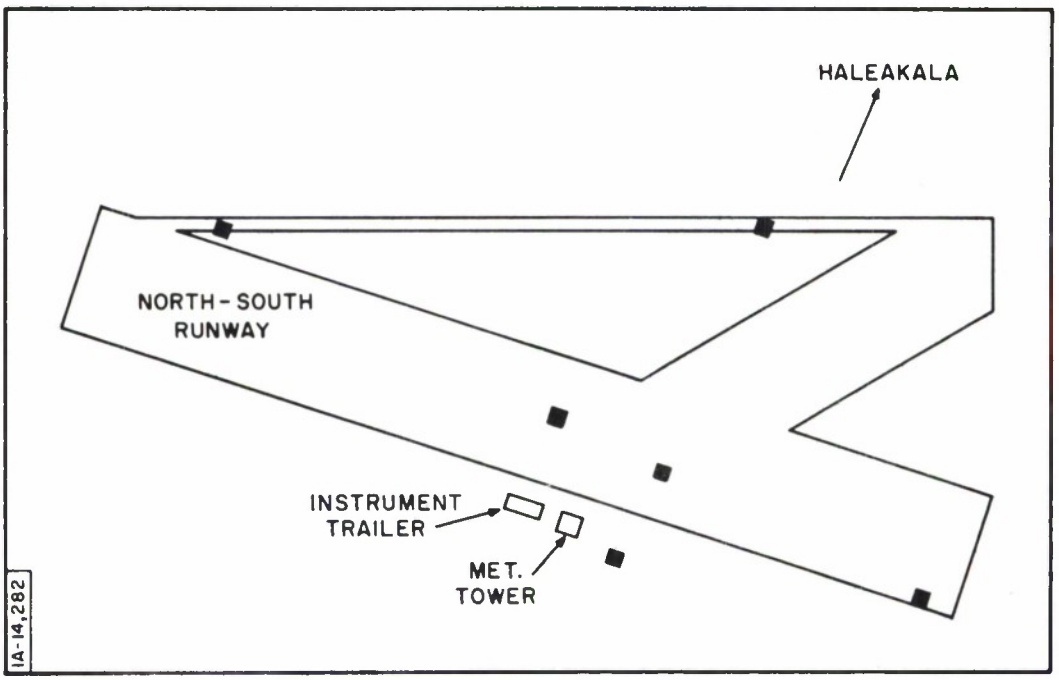

Fig. 1. Location of Instrumentation on Runways (Puuene, Hawaii, Naval Air Station)

* National Bureau of Standards, Boulder, Colorado

**See ESD-TDR-64-103, Vol. 1, p. 129, Figs. 1-8(a) and 1-8(b).

MEASUREMENT OUTLINE

Antenna Aperture Smoothing

Recorded range variations simultaneously, over paths using 3- and 0.5-meter antennas, mounted side-by-side, during January 6, 7 and 8, and 14, 15 and 16. (See Fig. 1-9 (c) Page 1-130 for ESD-TDR-64-103.)

Comparison of Range Difference Between a Horizontal In-Line Baseline and an Equivalent Vertical Baseline

Recorded ranges and range differences simultaneously, using a 30-meter vertical baseline and a corresponding horizontal in-line baseline, during February 11, 12 and 13. (See Fig. 1-9d of above reference.)

Short Horizontal In-Line Baselines

Recorded range differences simultaneously, using baselines of 40-, 100- and 250- meters, on March 4, 5, and 6 (see Fig. 2).

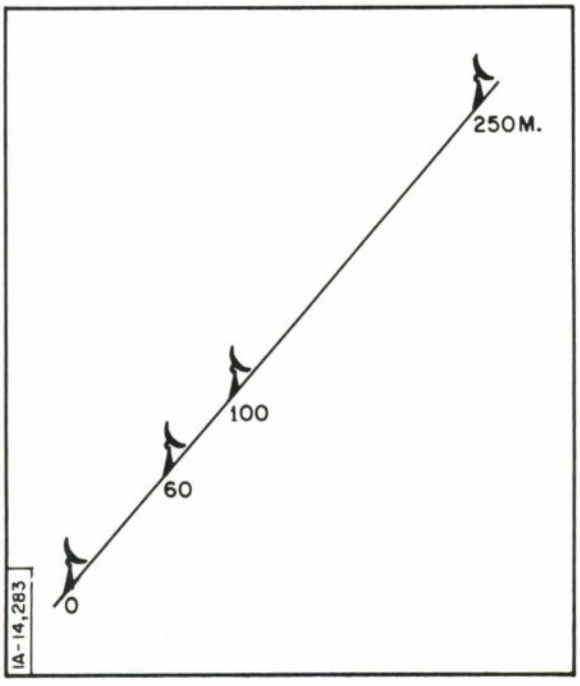

Fig. 2. Horizontal Short In-Line Antenna Arrangement

Long Horizontal In-Line Baselines

Recorded range differences using baselines of 250-, 400-, 855- and 1255-meters, from March 18 to 24, and from April 10 to 17 (see Fig. 3).

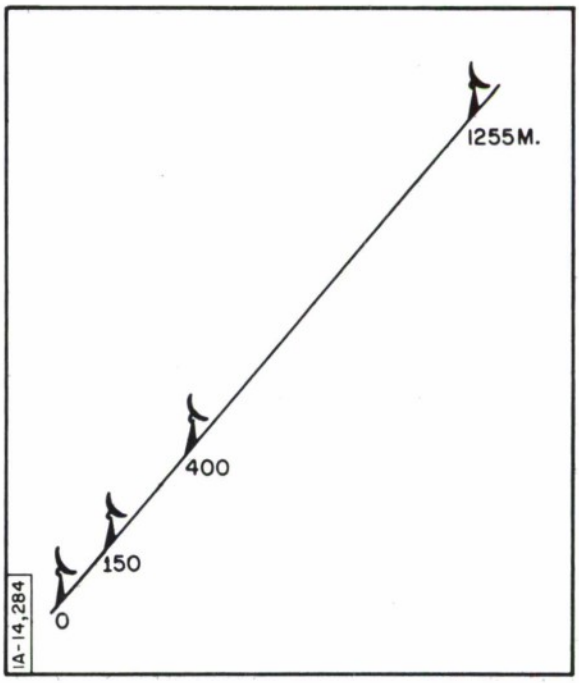

Fig. 3. Horizontal Long In-Line Antenna Arrangement

Short Azimuth Baselines

Recorded range differences simultaneously, using baselines of 4.5-, 31.5- and 201.5- meters, normal to the propagation path, from May 7 to 13 (see Fig. 4).

Long Azimuth Baselines

Recorded range differences simultaneously, using baselines of 201.5-, 598.5-, 800- and 1700-meters, from May 21 to 28 (see Fig. 5).

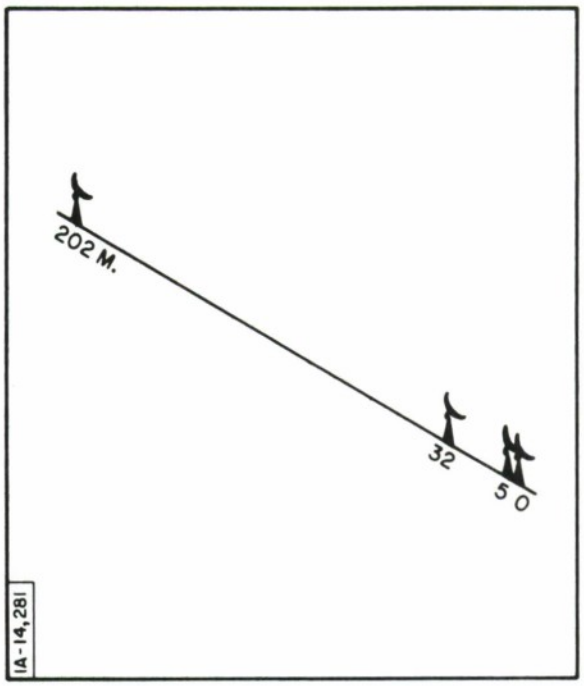

Fig. 4. Antenna Arrangement for Short Azimuth Baseline

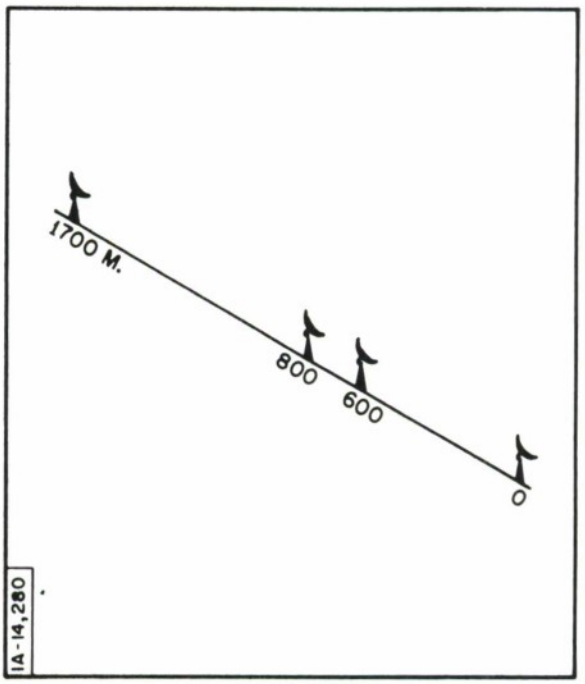

Fig. 5. Antenna Arrangement for Long Azimuth Baseline

Comparison of Surface and Airborne Index Measurements for Range Corrections

Recorded one range and surface index at six points distributed around the lower antenna. Recorded index along vicinity of path, using airborne refractometer, from June 10 to 17.

FUTURE PLANS

The data from these experiments will be analyzed in terms of the spectra of the various range and range difference fluctuations. Both these spectra and the variables will be examined for correlation with other parameters, such as the index, for possible application of the index for prediction or correction of range errors.

FIELD TEST RESULTS OF THE LINE INTEGRAL REFRACTOMETER

Harold M. Richardson*

INTRODUCTION

The molecular resonances of water vapor and oxygen molecules have been the subject of theoretical and experimental investigations because of the practical importance of the effect with regard to microwave attenuation. The theory predicts that there will be a slight dispersion, or change of refractive index with frequency, associated with these resonances. The dispersion, which can be calculated from the known physical constants of the molecules, is so small that it is very difficult to measure with current laboratory techniques.

These dispersive regions cause a differential in the propagation transit time of two signals at different frequencies as the waves traverse an atmospheric path. With a suitable choice of frequencies, a measurement of transit time differentials provides information on the total tropospheric refractivity, integrated over the path. This measurement could provide a direct correction to precision microwave distance-measuring equipment to compensate for the slowing effects of the clear air troposphere, as well as a means of gaining some insight into meteorological and propagation parameters. **

PRINCIPLE OF OPERATION

When the scale of the propagation path inhomogeneities permits the approximation of geometric optics, the transit time (t) may be expressed as

---

*The MITRE Corporation, Bedford, Massachusetts

**Background information and prior testing results on the MITRE Line Integral Refractometer (LIR) may be found in ESD-TDR-64-103, Vol. I, pp. 1-77 to 1-106.

$$t = \frac{1}{c} \int_S n \, ds = \frac{S}{c} + \frac{1}{c} \int_S N \, ds \qquad (1)$$

where

c is the vacuum velocity of light,

ds is an elemental arc length,

S is the curved ray path over which the integration is performed.

The integrated refractivity over the path $\left(\int_S N \, ds\right)$ may be recognized as a measure of the slowing effect caused by the presence of the material atmosphere on the electromagnetic waves. This quantity is the first-order correction to inferences of distance from transit time measurements. Ray bending produced by refractivity gradients causes the arc length S to differ from the straight-line distance. However, this difference is a second-order effect, provided the angle between the ray and the refractivity gradient does not approach 90 degrees, and can be neglected for atmospheric paths at elevation angles greater than a few degrees.

The differential transit times, phases, and refractivities for two coherent frequencies $\left(f_1 , f_2\right)$, transmitted over the same path, are related as follows:

$$t_1 - t_2 = \frac{\psi_1}{2\pi f_1} - \frac{\psi_2}{2\pi f_2} = \frac{1}{c} \int (N_1 - N_2) \, ds = \frac{1}{c} \int D_{1,2} \, ds \quad . \qquad (2)$$

where

ψ_1 and ψ_2 are the phase angles corresponding to the transit times, and

$D_{1,2}$ is the dispersivity.

This equation shows that a special kind of phase measurement is proportional to the line integral of differential refractivity (dispersivity). The differential phase is

$$[(f_2/f_1)\,\psi_1 - \psi_2] \text{ at } f_2 \ .$$

FIELD TESTS

A transmitter and two identical receivers for a measurement of water vapor have been constructed and mounted in truck vans for field tests. This apparatus (or portions thereof) have been operated over the seven paths listed in Table 1.

The Bald Knob to Mt. Rowe, N. H., path, of 0.2-degree elevation, 12.8-mile length, was used for calibration-testing of phase versus humidity during October and November, 1963. The presence of strongly variable fluctuations* in the phase readings from this horizontal path led to an acceleration of the slanted path testing program. The Southern Appalachians provided the next four paths, elevated 2.6, 1.9, 3.2, and 4.9 degrees, and with lengths as indicated in the Table. The Toll House Gap, N. C., to Johnson City, Tenn., path was slightly vignetted in the lower side of the main lobe of the 15.6-gc pattern, and was used primarily for checkout prior to operation on the Toll House Gap to Pinnacle Peak, Tenn., path. The paths from Camp Creek Bald to Tusculum Airport, Tenn., and from Camp Creek Bald to Moncier cow pasture, also in Tennessee, were used in a beam-switching experiment prior

*See ESD-TDR-64-103, Vol. I, Figs. 1-12 and 1-13.

to utilization of the latter path for long-term (24-hour) test. The two paths were used primarily for checkout operations and antenna phase pattern measurements.

Table 1

Test Paths

Paths	Elevation Angle (deg)	Length (miles)	Date	Remarks
Bald Knob to Mt Rowe, N. H.	0.2	12.8	Oct. to Nov. '63	Phase-Humidity Comparison
Toll House Gap, N. C. to Johnson City, Tenn.	2.6	18.3	Apr. '64	Slanted Path (Vignetted)
Toll House Gap, N. C. to Pinnacle Peak, Tenn.	1.9	15.3	Apr. '64	Slanted Path
Camp Creek Bald to Tusculum Airport, Tenn.	3.2	10.0	May '64	Beam Switching
Camp Creek Bald to Moncier Cow Pasture, Tenn.	4.9	6.5	May '64	Long-Term Power Spectra
Clay Pit Hill to Boston Hill, Mass.	0.1	1.15	Apr. to June '64	Near-Field Phase versus Distance
Boston Hill Parking Lot	0	0.02	Apr. to June '64	Near-Field Phase

The path profiles are illustrated in Fig. 1. The dashed lines represent the position of the first antenna null which clears all obstructions to the mid-point (from either end), except for the Toll House Gap to Johnson City path.

The stability of the apparatus taken into the field, as illustrated in Fig. 2, is within 0.1-degree, 1-second time and 1-decibel changes in the 15.6- and 31.2-gc carriers.

TEST RESULTS

The elevated path testing results indicated the presence of strongly variable fluctuations. The peak-to-peak fluctuations (Fig. 3) were determined from the first 2.8 minutes of a 40-minute test record, ultimately used to determine the long-term power spectra. The data were obtained over a 6.5-mile, 4.9-degree elevated path.

The fluctuations, as the figure shows, become small around sunset on 5 May, and then increase for the period from midnight of 5 May to about sunrise of 6 May. The fluctuations near sunset of 6 May were again relatively small before becoming alternately noisy and quiet from near midnight 6 May to almost noon of 7 May. These fluctuations have been observed to change from approximately 2 degrees peak-to-peak to 10 degrees peak-to-peak in approximately 5 minutes.

On 5, 6 and 7 May, all the data was obtained under atmospheric conditions of warm, clear, stable, high-pressure air, with calm to very light surface winds. Variable direction 15 mile/hour-winds were present at the transmitter site on Camp Creek Bald (elevation 4440 feet). During the test period, a marked dip and subsequent return to normal in water vapor content occurred at the 5000-foot level, as indicated by Nashville, Tenn., and Greensboro, N.C., rawinsonde, but no change was discernible at either van site.

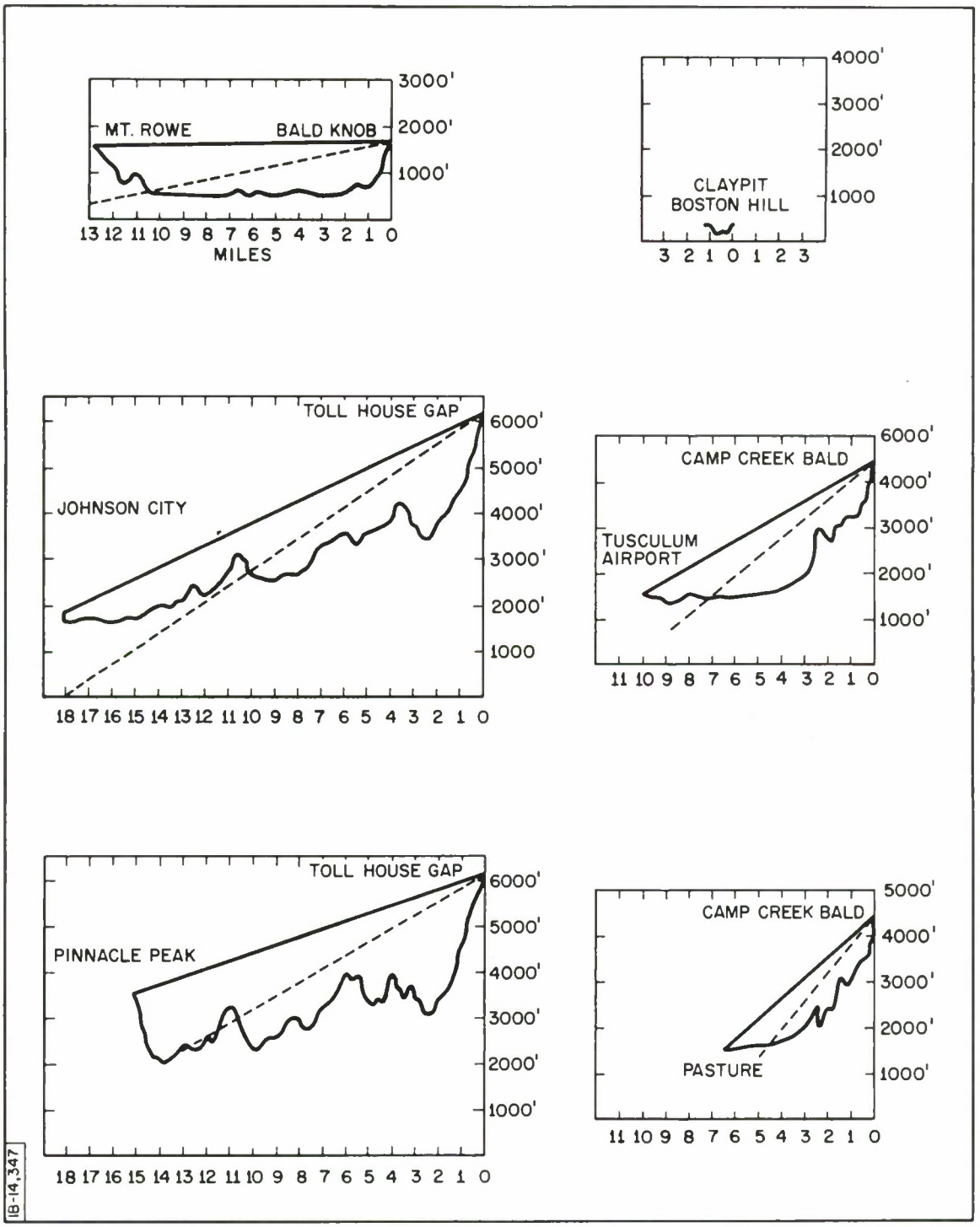

Fig. 1. Refractometer Test Site Profiles

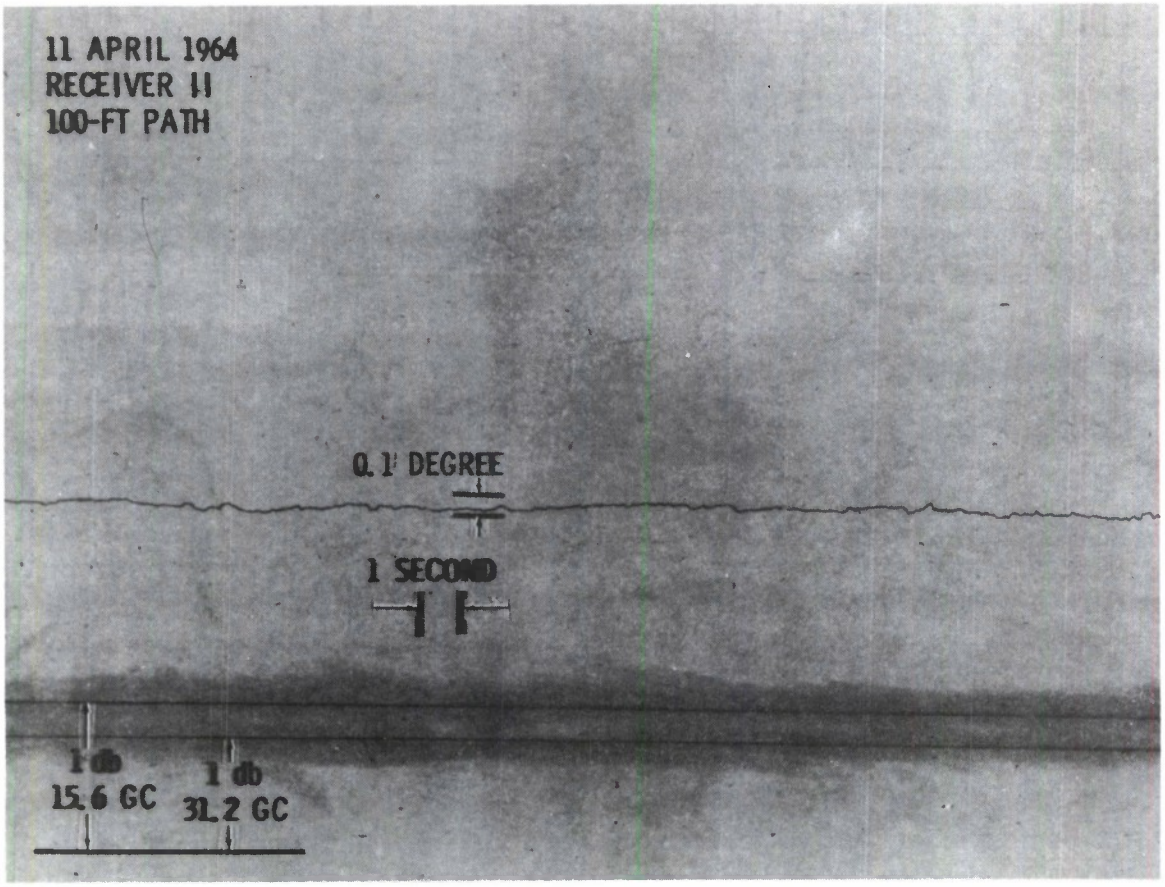

Fig. 2. Apparatus Stability

Power Spectra

Ten power spectra, as determined from 40-minute runs, have been computed for the Camp Creek Bald to the Moncier cow pasture path; in addition, two long-term power spectra have been derived by piecing the serial, individual runs with some interpolations. Five spectra have been obtained for the Toll House Gap to Pinnacle Peak path, two spectra for the Toll House Gap to Johnson City path, and three spectra of the apparatus with 100-foot paths.

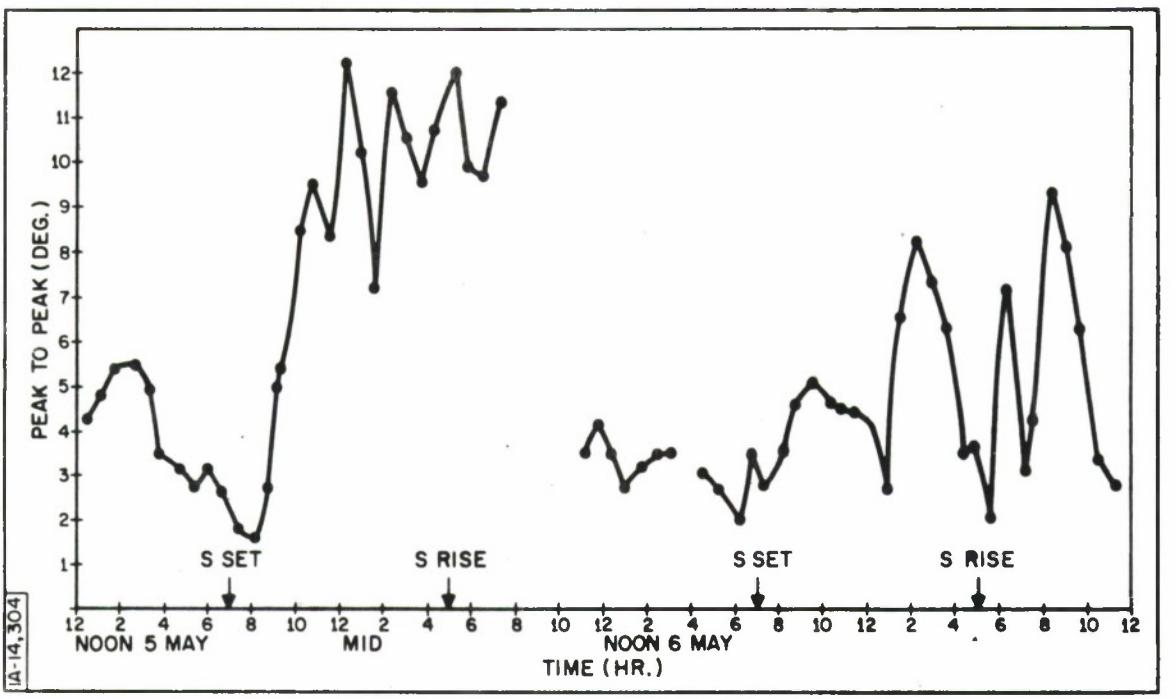

Fig. 3. Variable Signal Fluctuations for Slanted Paths

Some typical, early spectra are shown in Fig. 4 for the 6.5-mile, 4.9-degree elevated path. They are characterized by a relatively flat region, a break point between 10^{-1} and 10^{0} cycles/second, and a rapid fall off at the higher frequencies. The power densities of the spectra vary considerably in the flat region and to a lesser degree in the slope after the break point. The characteristic shape of the spectra was similar to that obtained during the initial testing over Lake Winnipesaukee, N. H.

The 11 April, 100-foot curve in Fig. 4 indicates the spectrum characteristic of the apparatus. Autocorrelation functions have been obtained for all the spectra. with typical results, as shown in Fig. 5, for no atmosphere (100 feet) and with atmosphere (6.5 miles) as indicated.

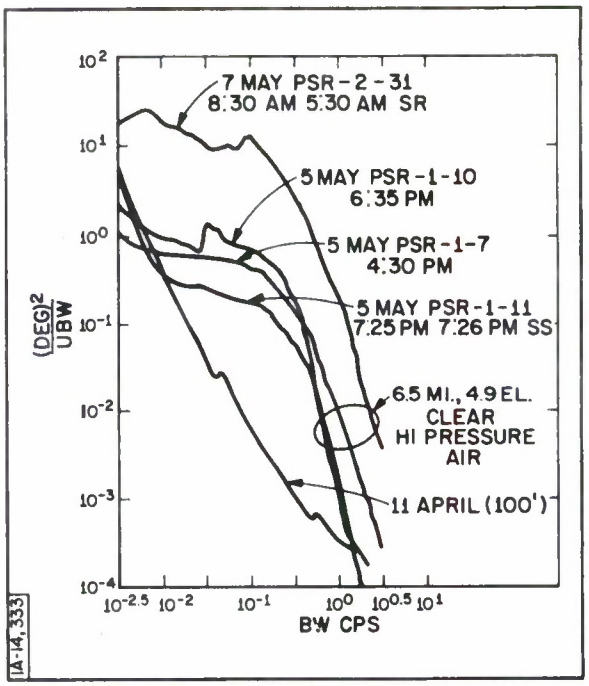

Fig. 4. Characteristic Spectra

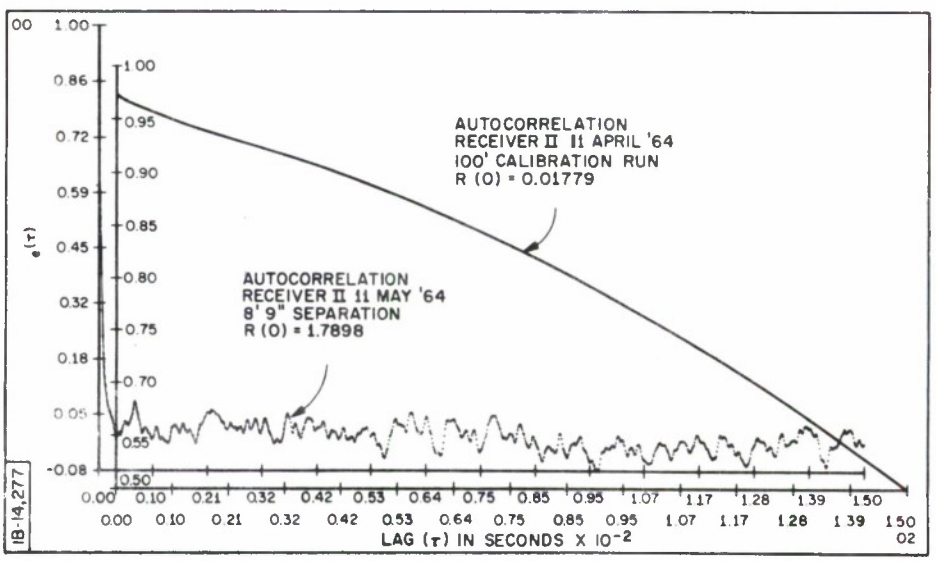

Fig. 5. Autocorrelation Curve of Signals

Figure 6 shows two interesting spectra; the low-frequency power densities are approximately equivalent, but the break point is significantly different. The wind at the receiver was essentially nil at both times of data collection, but the wind at the transmitter was approximately 20 miles/hour for the 6 May spectrum and about 10 miles/hour for 7 May. The path average wind is unknown, but these spectra and wind observations tend to indicate wind effects.

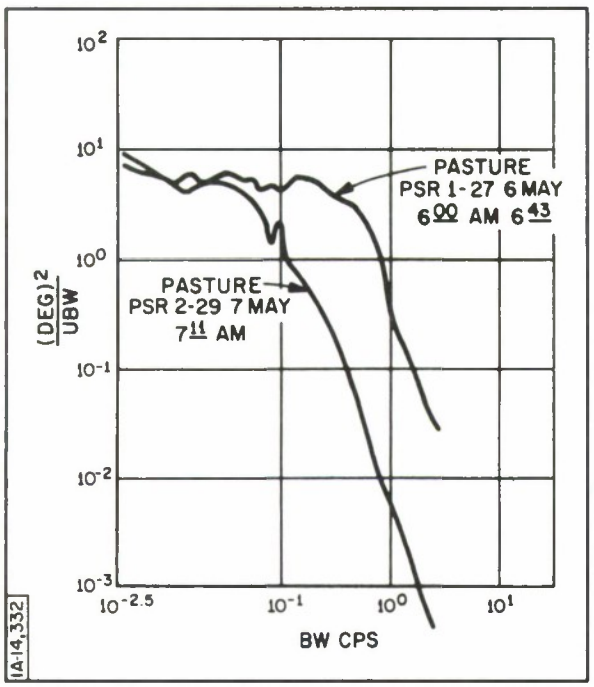

Fig. 6. Comparative Spectra

Baseline Experiments

A very limited set of data was taken over three small baselines, 8.75, 16.3 and 184 feet. The two power spectra for the 8.75-foot baseline are shown in Fig. 7. Inspection shows common features in the spectra from $10^{-2.5}$ to 10^{-1} cycles/second. In spectroscopic terms, there appear to be some common "absorption lines" in the spectra. Similar spectra have been computed for the other baselines, the cospectra, coherency matrix, etc., are currently being calculated.

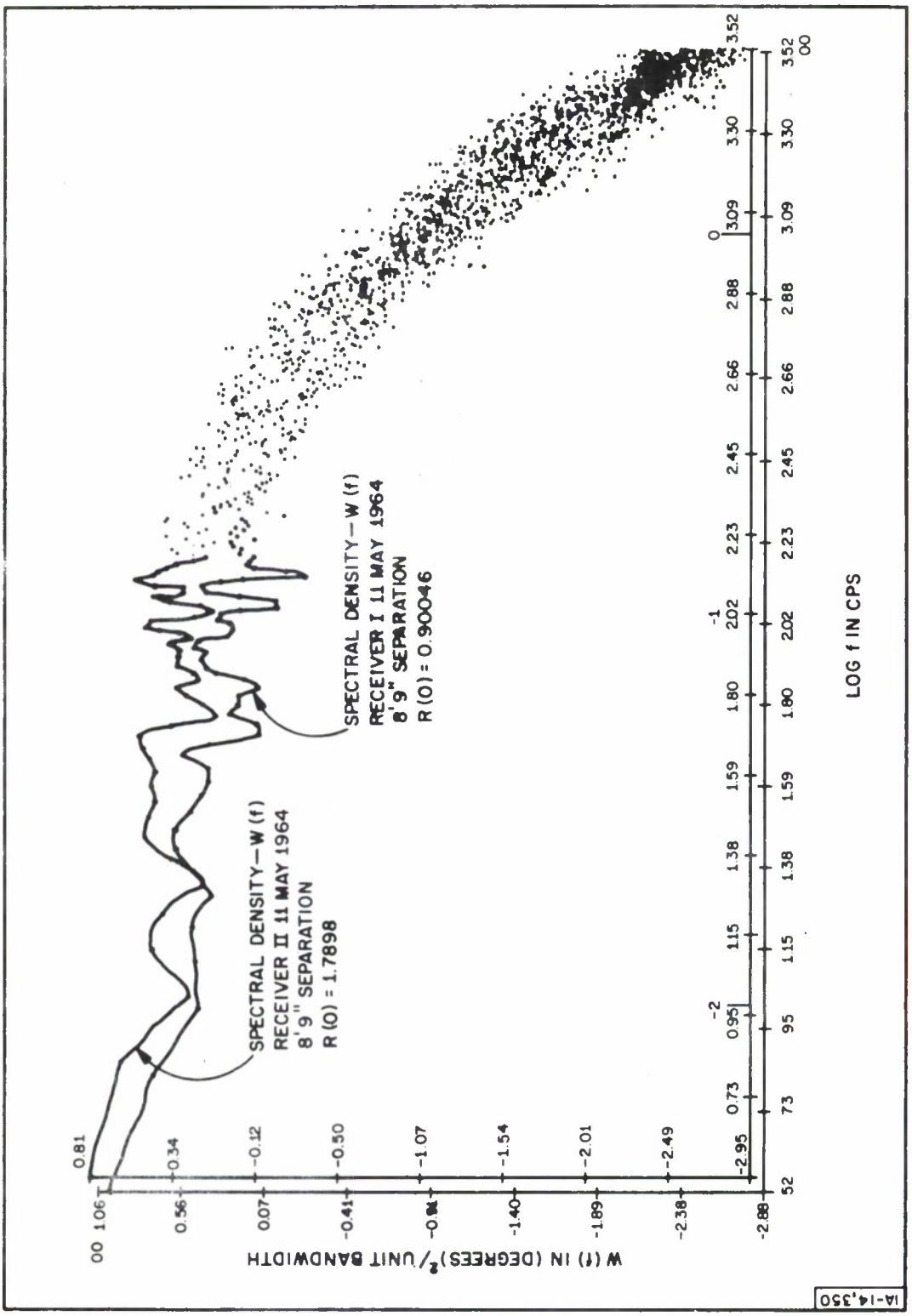

Fig. 7. Baseline Spectra (8.75-Foot Separation)

The analog records of rectified carrier amplitude monitors for the 184-foot separation are shown in Fig. 8. The monitors in each receiver show the usual degree of correlation, with little correlation apparent from receiver to receiver; Fig. 9 illustrates significantly more correlation from receiver to receiver. Close examination of the details of the recordings, illustrated in Fig. 10, reveal a relatively high degree of correlation of all monitors but with a delay in time, for Receiver I relative to Receiver II, of approximately 1 second. This delay agrees well with the observed cross wind at the receiver and the "frozen-in" structure model.

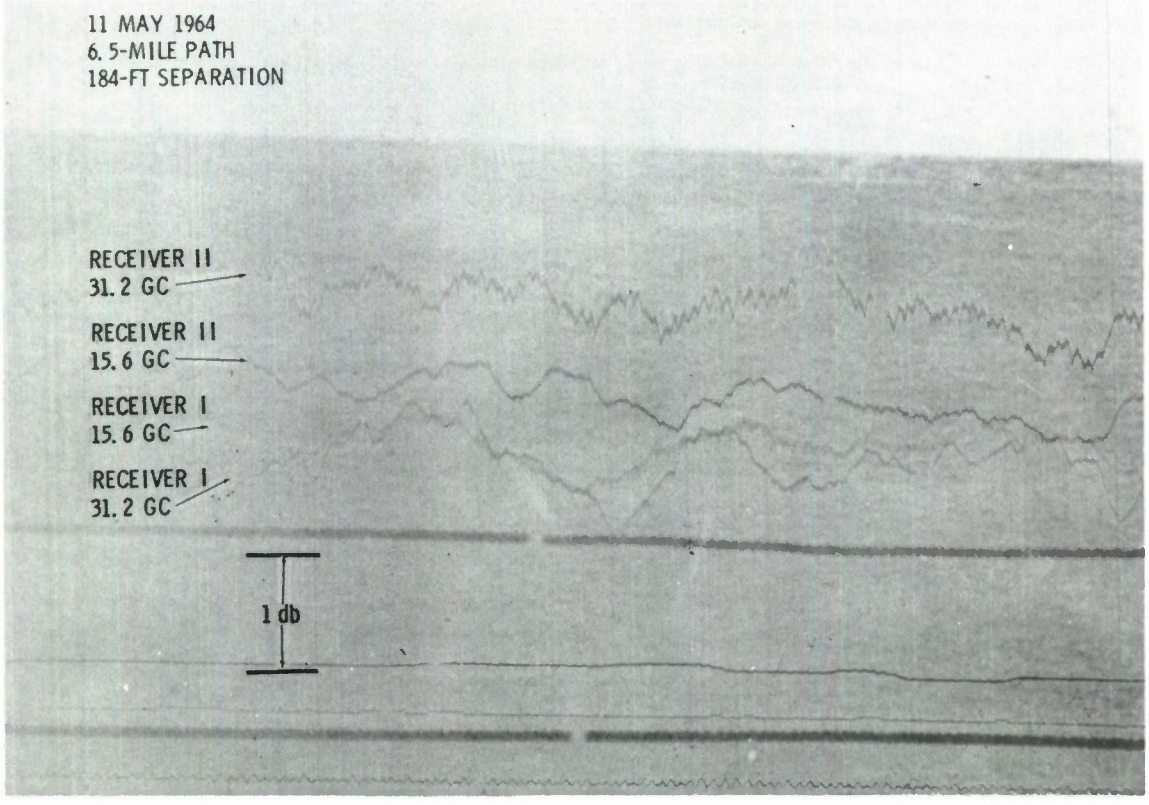

Fig. 8. Carrier Amplitude

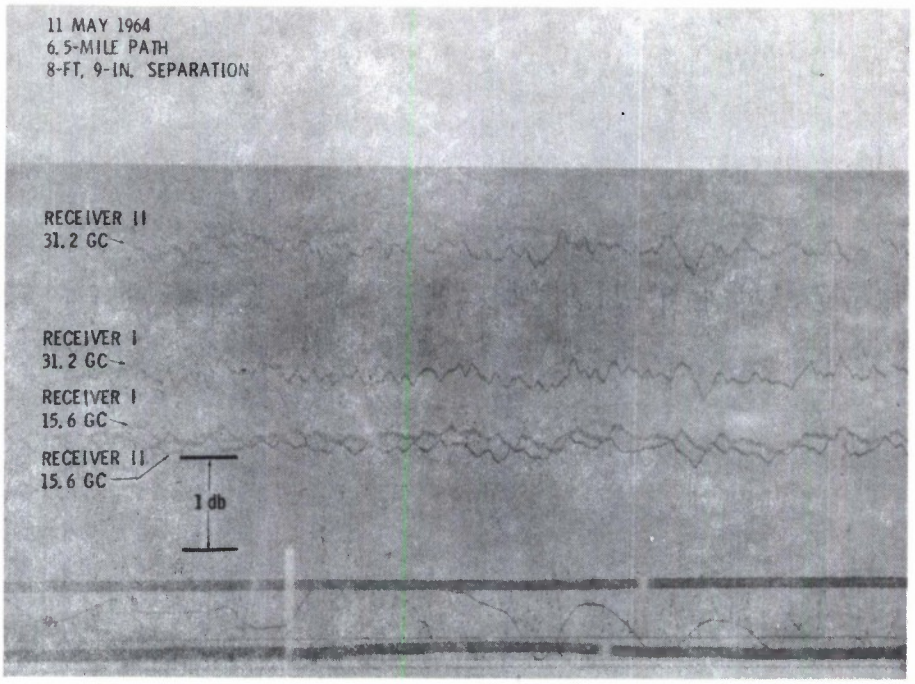

Fig. 9. Comparison of Receiver Signal

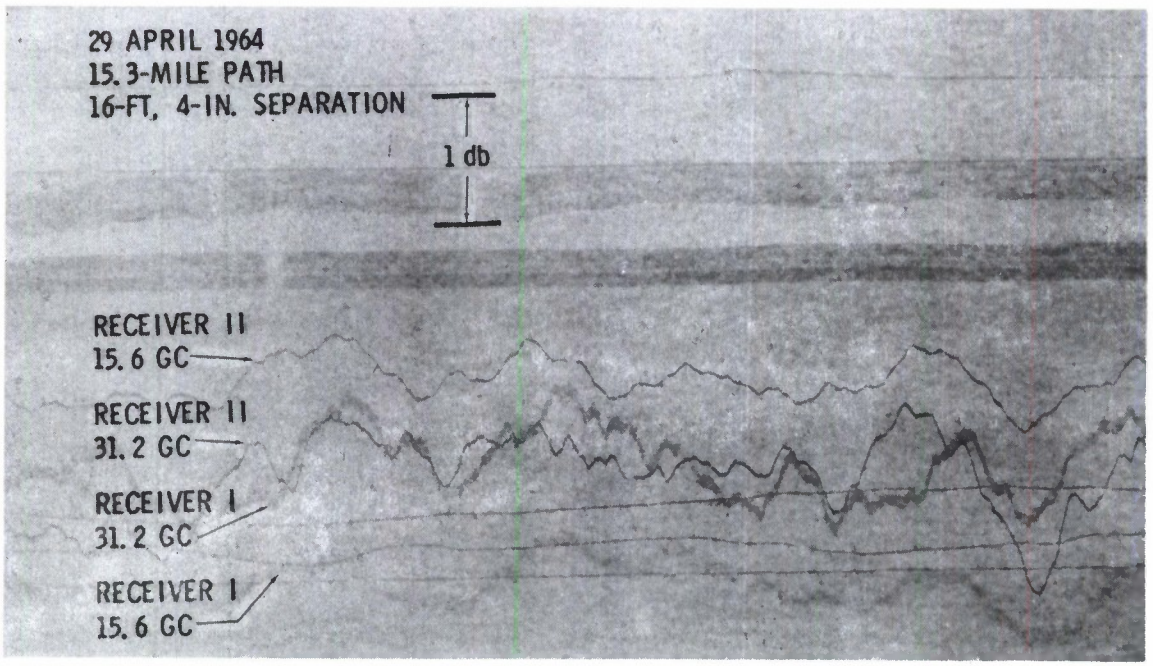

Fig. 10. Comparison of Carrier Amplitude Signals

Beam-Switching

The main purpose of the expedition to Tennessee was to determine the influence of elevation angle on the variable fluctuations, over and above atmospheric changes. The continued presence of the fluctuations precluded path-to-path comparison, except for near-simultaneous or extensive observations. The near-simultaneous observation was made in the transmitter beam-switching (manual) experiment, with Receiver I located in the cow pasture (6.5-mile path, 4.9-degree depression) and Receiver II located at Tusculum airport (10-mile path, 3.2-degree depression). The results of the experiment conducted over a 40-minute period, are shown in Fig. 11. The received signals experienced

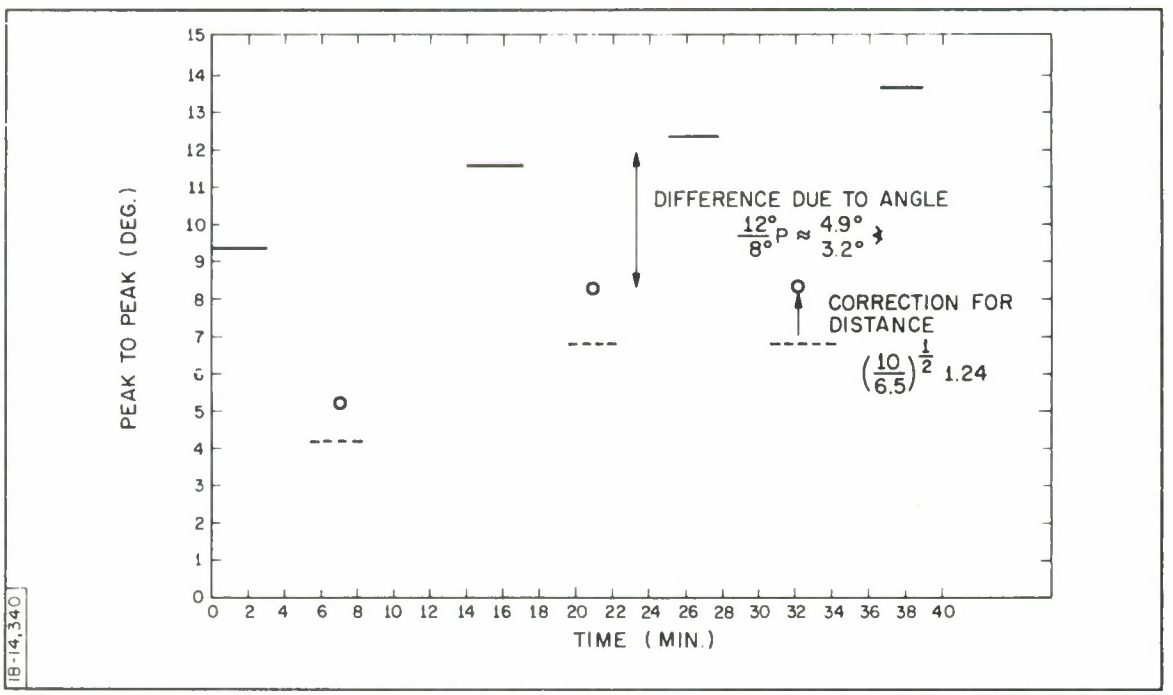

Fig. 11. Peak-To-Peak Signal Variation

phase fluctuations of 9.4 degrees, peak-to-peak, in Receiver II during the first three minutes of the run; Receiver I measured 4.2-degree phase fluctuations from 5 to 9 minutes from start; Receiver II then measured 11.6 degree fluctuations from 13 to 17 minutes, etc. After scaling the short-path values for comparison with those of the longer path, the effect of elevation was inversely proportional to angle, i.e., $(\psi_1/\psi_2) = (\theta_1/\theta_2)$, or 12 degree/8 degree phase $\simeq \frac{4.9}{3.2^\circ}$ elevation angle. The data is too limited to devise a general low which describes the dependence of elevation angle on phase fluctuations, but it does indicate that elevation angle is a parameter to be considered.

The following equations are the basis for the scaling ratio and is given for measurements of $N = 60\ N$ units for 10 gm/m^3 water vapor and $N_1 - N_2$ is determined by the second equation for the same density:

$$N = \frac{4\pi N_m}{\Sigma_e - \frac{W_l^\circ}{KT}} \sum \frac{\nu |p|^2 l - \frac{W_l^\circ}{KT}}{h(\nu l l^2 - \nu^2)} f(T, P) = N_m F_1(T, P) \simeq \frac{C_1 N_m}{T} ,$$

$$N_1 - N_2 = \frac{4\pi N_m}{\Sigma_e \frac{W_l^\circ}{KT}} \left[\sum \frac{\nu |p|^2 l - \frac{W_l^\circ}{KT}}{h(\nu l l^2 - \nu_1^2)} f(T, P) - \sum \frac{\nu |p|^2 l - \frac{W_l^\circ}{KT_f}}{h(\nu l l^2 - \nu_2^2)} (T, P) \right]$$

$$= N_m F_2(T, P) \simeq \frac{C_2 N_m}{T^{0.48}} ,$$

$$\frac{N}{N_1 - N_2} = \frac{F_1(T, P)}{F_2(T, P)} \simeq \frac{C_3}{T^{0.52}} ,$$

$$N = C_4 (N_1 - N_2), \quad C_4 = \frac{60}{0.038} = 1580 .$$

The microwave portion of the LIR is shown in Fig. 12 and the digital phase shifter portion of a complete LIR including the oxygen phase shifter is shown in Fig. 13. The oxygen microwave hardware for the LIR is currently under development.

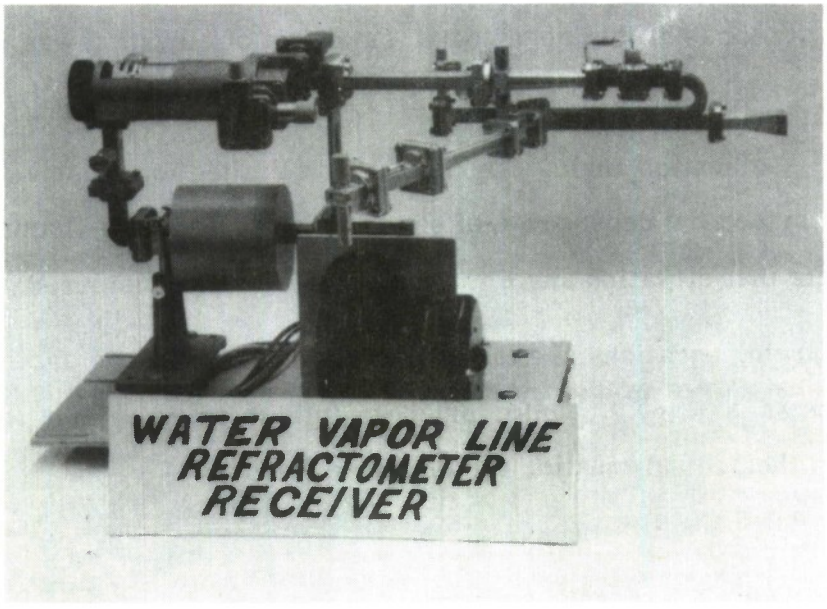

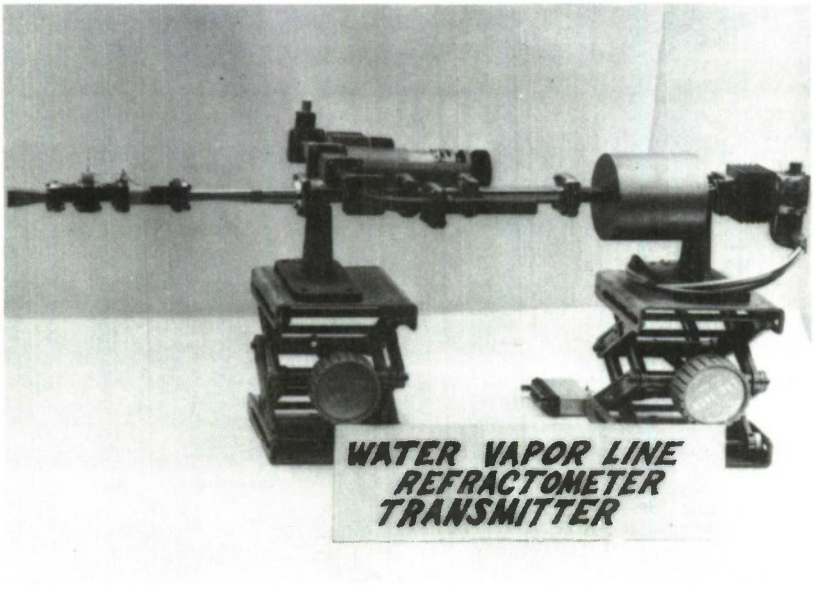

Fig. 12. Microwave Electronics

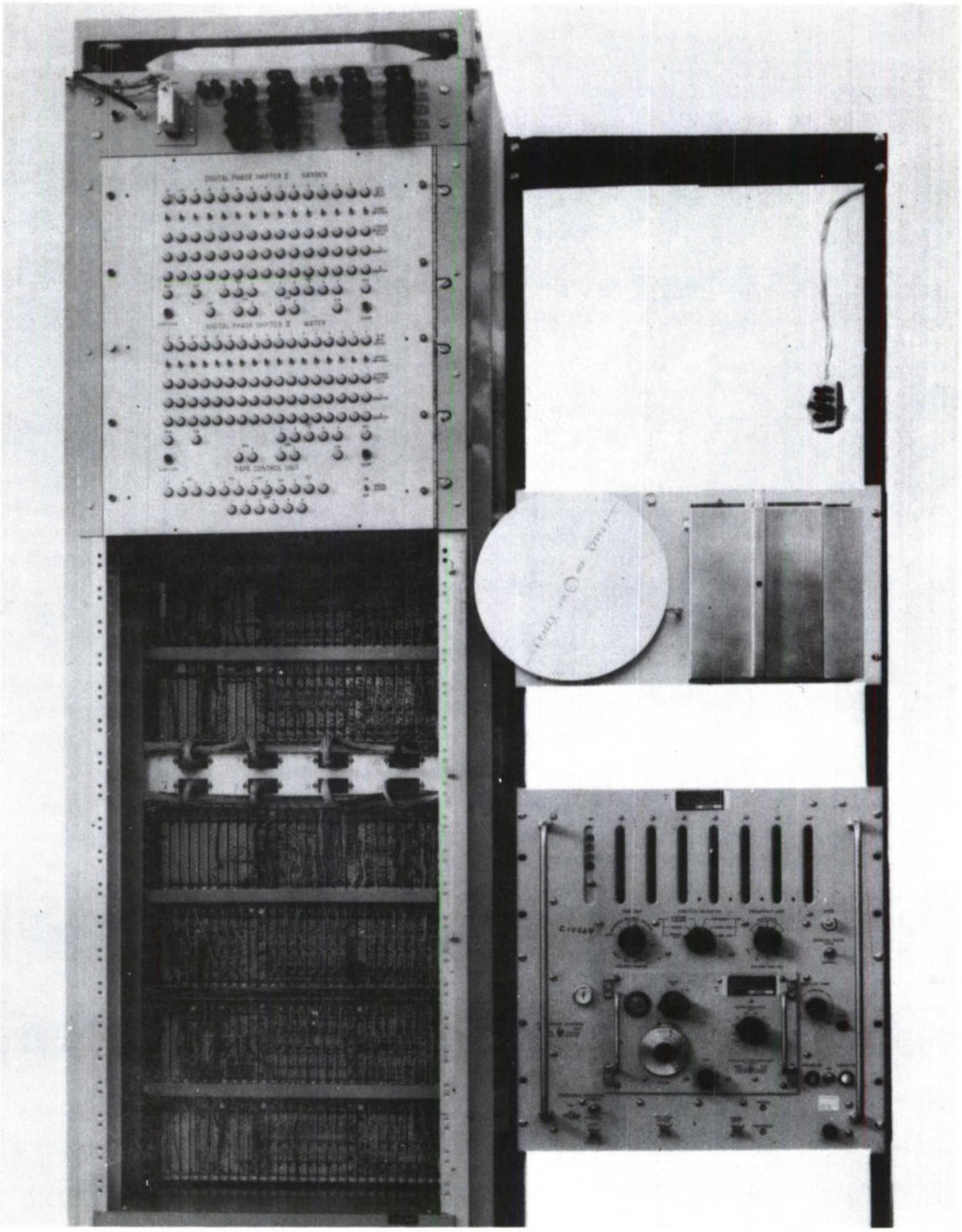

Fig. 13. Digital Phase Shifter

Smoothing Times

The early testing* demonstrated that the LIR responded to atmospheric changes when the fluctuations were smoothened by an averaging process. Considerations of the magnitude of the fluctuations and the stability of the atmosphere lead to the conclusion that the short-time fluctuations are caused by some propagation mechanism not representative of density or refractive variations. This is graphically shown in Fig. 14, where the long-term and short-term power spectra are represented along with the power spectra developed by the National Bureau of Standards (NBS). The two straight lines of slope -8/3 bracket the

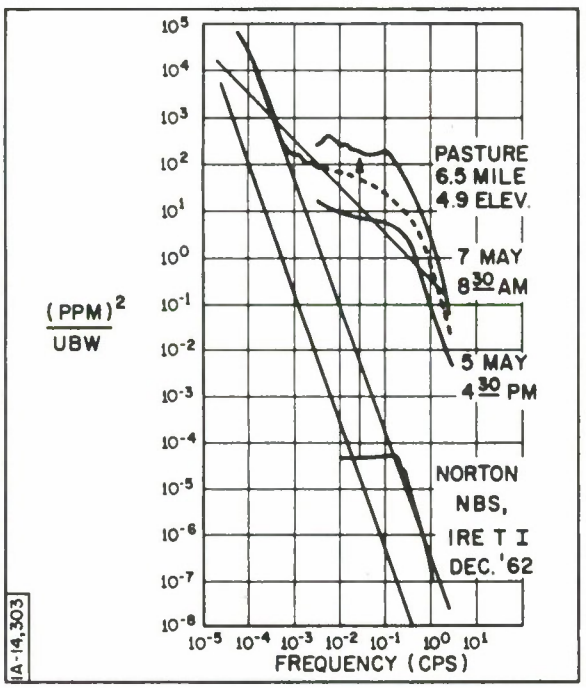

Fig. 14. Measurement Spectra Results

variable levels observed by NBS, and are considered to represent the atmospheric fluctuations (scaled to 6.5-mile path). The LIR long-term spectra compare well with this spectra in the 10^{-4} to 10^{-3} cycles/second region before breaking away into a plateau region whose level is highly variable (as indicated by two

*See ESD-TDR-64-103, Vol. I, Figs. 1-15 and 1-16.

typical short-term spectra). See Fig. 14. Thus, the difference between the plateau and the (-8/3) regeion represents "free" or unwanted signal over and above what may be considered true atmospheric data.

Since power spectra do not show the direct current component of the atmosphere, which is of primary interest to us, it is desirable to compare the variable component to the average level. This data was taken under conditions of approximately 10 gm/m^3 of water vapor, or 60 N-units of refractivity in the path. A 1 percent measurement of this quantity would yield 0.6 N-unit accuracy. For the sake of simplicity, the plateau region may be approximated as a constant power per unit bandwidth, up to a complete cutoff frequency representative of the break point. A locus of such plateau values and break point frequencies is given by the line of slope -2 for a 0.6 N unit fluctuation.

It can be seen that the plateau region can exceed the 0.6 N-fluctuation at frequencies as low as 10^{-3} cycles per second and as high as 10^{-1} cycles per second. (One spectra had a plateau lower than the lowest shown in Fig. 14).

The LIR spectra have been scaled upward, from phase measurements of dispersivity, to represent the path refractivity by the ratio of refractivity to dispersivity, 1580. Without this scaling, the data occur in the vicinity of the Norton* and Barrows explanation of the spectra. ** The length of the arrow (Fig. 14) is representative of the scaling factor. While the agreement is good, the effect of elevation angle on the fluctuations and the observation of extremely large amplitude fluctuations in the presence of visible striations indicate that mechanisms in addition to "wave optics" must be considered.

*See ESD-TDR-64-103, Vol. I, pp 1-143 to 1-153.
**Ibid., pp. 1-155 to 1-193.

STATUS OF FEASIBILITY TESTING

The status of feasibility testing of the LIR may be stated as follows:

(1) smoothing of the data is necessary at low-elevation angles (5 degrees);

(2) range from 10 to 1000 seconds for (1 percent precision), 100-second smoothing is typical;

(3) attainable accuracy has not been demonstrated experimentally because of the inherent difficulty of measurement over 10-mile atmospheric paths;

(4) instrument precision of 0.13-degree root-mean-square corresponds to a 1 percent measurement of nominal humidity (10 gm/m^3) over a 6-mile path; and

(5) a nominal humidity measurement of 1 percent corresponds to a 0.6 N-unit measurement of a 0.2 percent refractivity measurement.

Comparison with other Techniques

A comparison with other methods of line-of-sight radio path correction can be made as follows:

(1) end-point measurements require long-term averaging time of approximately 3 hours, and highly averaged spatial models. This method yields residuals of 1-3 percent.

(2) Meteorological profile and ray-tracing methods may yield 3 x 1.6 percent correction accuracy with an estimated time-constant of about 1 hour.

(3) The LIR determines an average over a path, requires 10-to 1000-seconds smoothing, with a potential accuracy of 0.6 N-unit or 0.2-percent accuracy.

OPTICAL DEPOLARIZATION AND SCINTILLATION MEASUREMENTS OVER A TERRESTRIAL PATH

Jurgen R. Meyer-Arendt*

The experiments described concern scintillation and polarization phenomena observed over a 25-km. long, single terrestrial path and over a double-path of twice that length. Both types of phenomena were studied using a scintillation-polarization monitor that can be operated in two ways (Fig. 1). These are

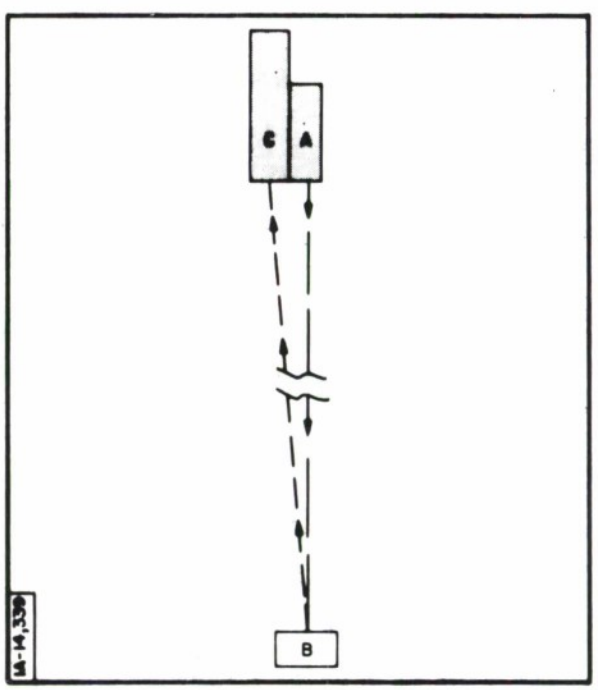

Fig. 1. Single-Path Scintillation – Polarization Monitor

*National Bureau of Standards, Boulder, Colorado

referred to as Single Path arrangement and Return Path arrangement. In the single-path, light source (B) and receiver (C) are located at opposite ends of the test path. In the return path arrangement, light source (A) and receiver (C) are both placed at the same terminal. The light is returned by a mirror or other type of reflector (B). We have used both a plane, first-surface mirror (practical only for short-path lengths), a corner cube reflector of 35 cm cross-sectional diameter, and a special array of corner reflectors which form part of a geodimeter.

A schematic diagram, and a photograph of the instrument set up for return path experiments, are shown in Figs. 2 and 3. The telescope, denoted (1), has a 7.5-cm. aperture achromatic objective (d) of 114-cm focal length. A prismatic member (2), located near the focal plane, has a divergent lens cemented to its front face and a plane mirror cemented to its rear face. A hole, about 6 mm. in diameter, is drilled through the prism and the mirror. The light then passes through a polarizing filter (3) with a central hole, through an iris diaphragm (e), a rotating polarizing filter or a Glan-Thompson prism (5), and a ground glass (6), and is incident on the light-sensitive surface of a photomultiplier tube (7). The light comes from a high-pressure mercury arc (a) and passes through a collimating lens (b) on to the target (c). Part of the light can reach the photo-tube directly via the window (4). A large-diameter polarizing filter is placed in front of the collimating lens (b); the other part of the light falling directly, without traversing the path, on the photo surface is polarized by the outer portion of the filter (3).

The experiments were carried out from 9 to 19 June 1964 on Maui, Hawaii, using the same path that had been used for radio refraction measurements by Norton and his coworkers[1] *, and which is currently being used again by

*Numbers in brackets designate References on page 122.

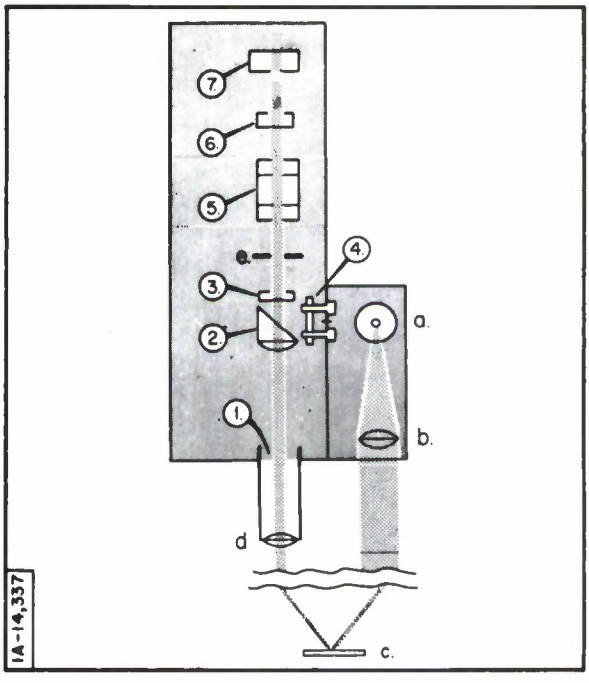

Fig. 2. Polarization Monitor, Schematic

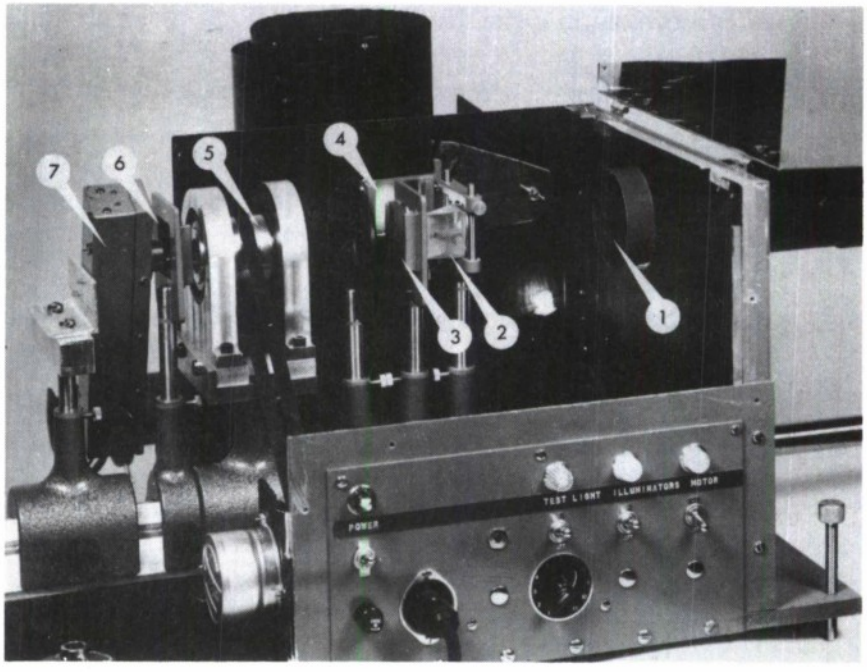

Fig. 3. Polarization Monitor, Control Panel

Two Representations of Double-Path Scintillation

M. C. Thompson, Jr., and his group. The island of Maui offers both a semi-tropical humid climate, (easily accessible by car, on the top of Mt. Haleakala (3055 m.)) an arid climate where subfreezing temperatures sometime prevail. Between these two regions there are heavy air turbulence and hazy-to-dense clouds moving into and out of the path, smoke from burning sugar cane fields, and almost-constant strong winds (the trade wind, blowing mostly in a northerly direction), normal to path of observation. The length of the path (one way) is 24.88 km.

The results of our experiments can be briefly described as follows:

(a) The single path recordings show strong scintillation, i.e., intensity fluctuations, with occasional high spikes or flashes of light of short duration.

(b) Single-path polarization records show a well discernible sinusoidal curve on which scintillation fluctuations are superimposed.

(c) In all return path experiments, the noise level is higher because much light is back scattered in the path. The reflectors act as a (stationary) secondary light source, producing essentially the same, and sometimes even less pronounced, scintillation, an effect that might be the result of the larger cross section of the reflectors as compared to the primary light source.

(d) In the return path polarization experiments, the influence of back scatter is rather distracting. It can easily be shown that the sinusoidal curve ordinarily obtained is, in no small part, produced by the polarized light returned by scatter from the initial light beam. This is evident from the fact that moving clouds which completely block out the return signal only moderately reduce the sinusoidal signal

recorded (see the last one-third in the upper tracing in Fig. 4). In order to minimize this effect, an iris diaphragm was placed in the prime focus of the telescope objective and carefully adjusted so as to admit light forming the reflector image only. The result is shown in the lower portion of Fig. 4.

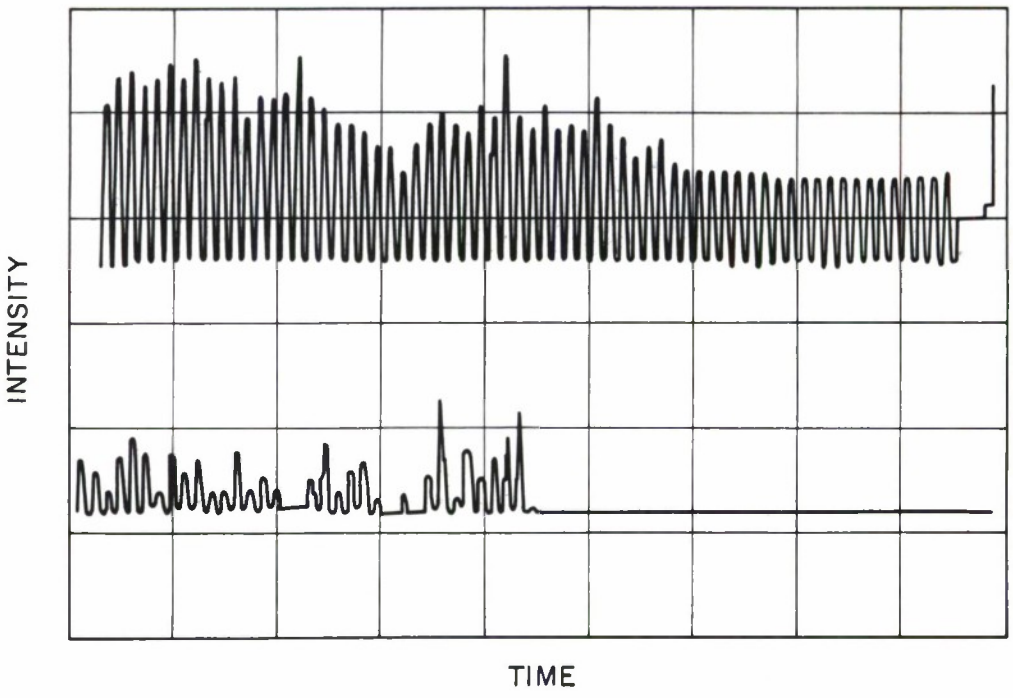

Fig. 4. Return Path Polarization

In summary, we come to the following conclusions:

(a) Based on the experiments performed, there is no evidence of depolarization produced by atmospheric turbulence. Attenuation, caused by haze, limits the signal transmission before any depolarization becomes evident. Polarization phenomena caused by aerosols[2] or by background skylight[3] are excluded in this study.

(b) Scintillation is a major limitation to optical telecommunication. Its influence increases with the distance traversed, the characteristics of the atmosphere traversed (turbulence, etc.), and with the degree of collimation of the light source (higher collimation is less favorable).

(c) Any receiver for optical information transmittal based on polarization must have provision for compensation of scintillation fluctuations. This can be accomplished, for instance, by a beam-splitter, two-photocell arrangement. (An interesting proposal for a photoelectric method for simultaneously measuring all four Stokes parameters is found in Reference 4.)

Finally, it should be mentioned that the results presented in this paper are preliminary in nature, and that they will be further analyzed. It appears probable that some kind of turbulence might arise from thermal expansion produced by a very strong laser beam. This possibility is currently being explored at the National Bureau of Standards, Boulder Laboratories, in a series of experiments in which a laser pulse is directed into one arm of a Mach-Zehnder interferometer (Fig. 5). Local perturbations would then show as distortions of the interference pattern produced in the interferometer by light from another, auxiliary light source.

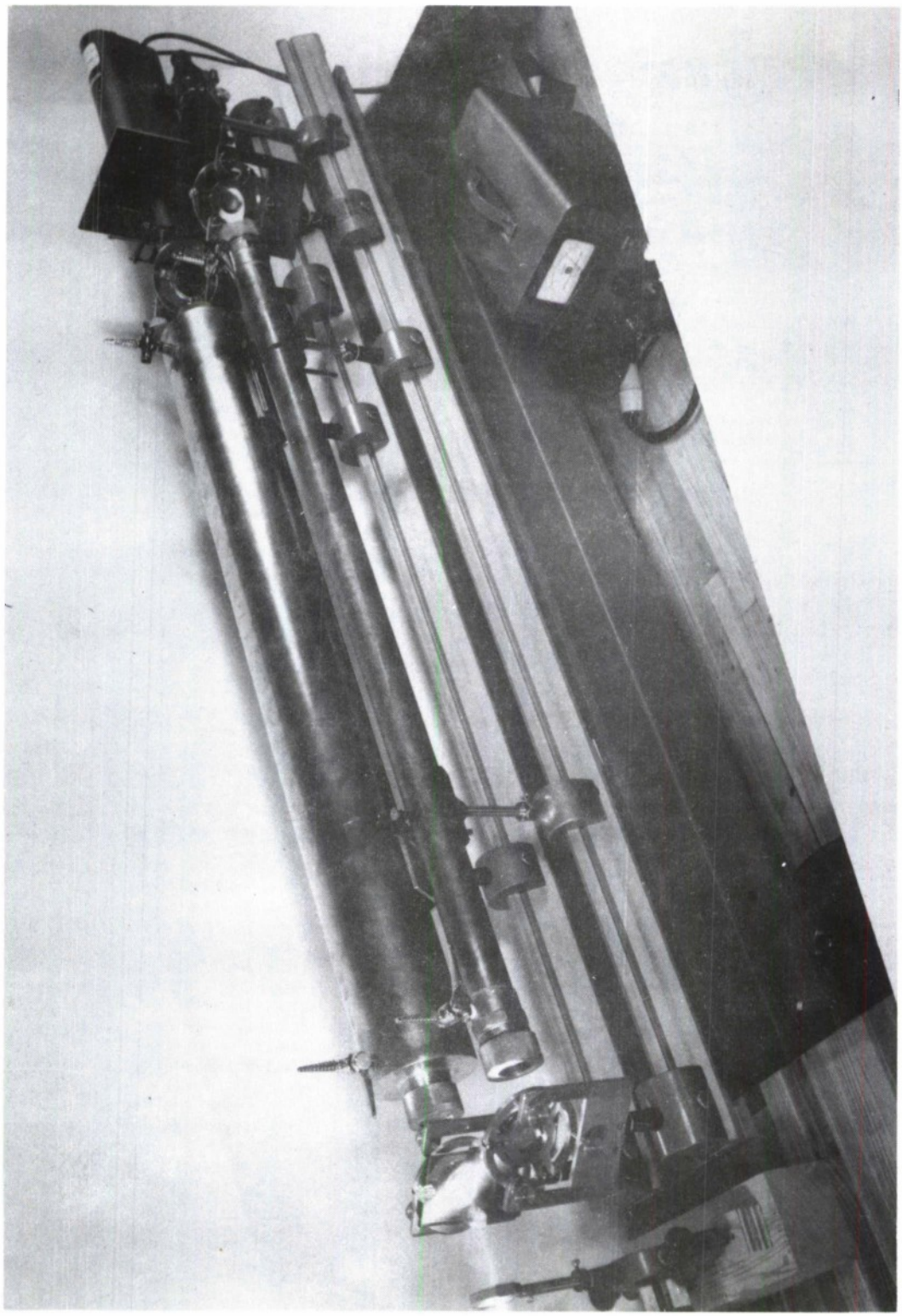

Fig. 5. Mach-Zehnder Interferometer

REFERENCES

1. Norton, K.A., Herbstreit, J.W., Janes, H.B., Hornberg, K.O., Peterson, C.F., Barghausen, A.F., Johnson, W.E., Wells, P.I., Thompson, M.C., Jr., Vetter, M.J., and Kirkpatrick, A.W. An Experimental Study of Phase Variations in Line-of-Sight Microwave Transmissions. National Bureau of Standards Monograph 33, 1961.

2. Stamov, D.G. "The Special Importance of the Polarimetric Method of Determining and Studying the Turbidity of the Earth Atmosphere as Compared with Actinometric and Diaphanoscopic Methods," (in Russian). Akad. Nauk Kazakhskoi SSSR, Alma-Ata, Trudy 3, pp. 163-170, 1962.

3. Dietze, G., "Einführung in die Optik der Atmosphäre," Akad. Verlagsgesellschaft Geest & Portig., pp. 168-171, 187-191 Leipzig, 1957.

4. Ioshpa, B.A., and Obridko, V.N., "Photoelectric Analysis of Polarized Light," Optics and Spectroscopy, 15, pp. 60-62, 1963.

FADING ON MICROWAVE LINE-OF-SIGHT PATHS

H. T. Dougherty*

INTRODUCTION

The received signals for line-of-sight propagation paths tend to vary with time because of the refractive index gradient variations along the propagation ray path. Although this is experienced at lower frequencies, the effect can become particularly severe at microwave frequencies; fading can result, which reduces the reliability of the system below an acceptable value. This fading can be considered under two general categories.

1. Multipath or phase interference fading.

   This effect, the result of refractive index gradient variations, is generated by the interference between the direct wave and (a) the specular component of the ground-reflected wave; (b) nonspecular components of the ground-reflected wave; (c) partial reflections from elevated layers or atmospheric sheets; or (d) additional direct wave paths produced by horizontally distributed changes in refractive index. These are illustrated in Fig. 1.

2. Fading caused by attenuation or defocusing

   This results from partial isolation of the transmitting and receiving antennas because of (a) intrusion of the earth's surface into the propagation path (diffraction fading); partially reflecting

*National Bureau of Standards, Boulder, Colorado

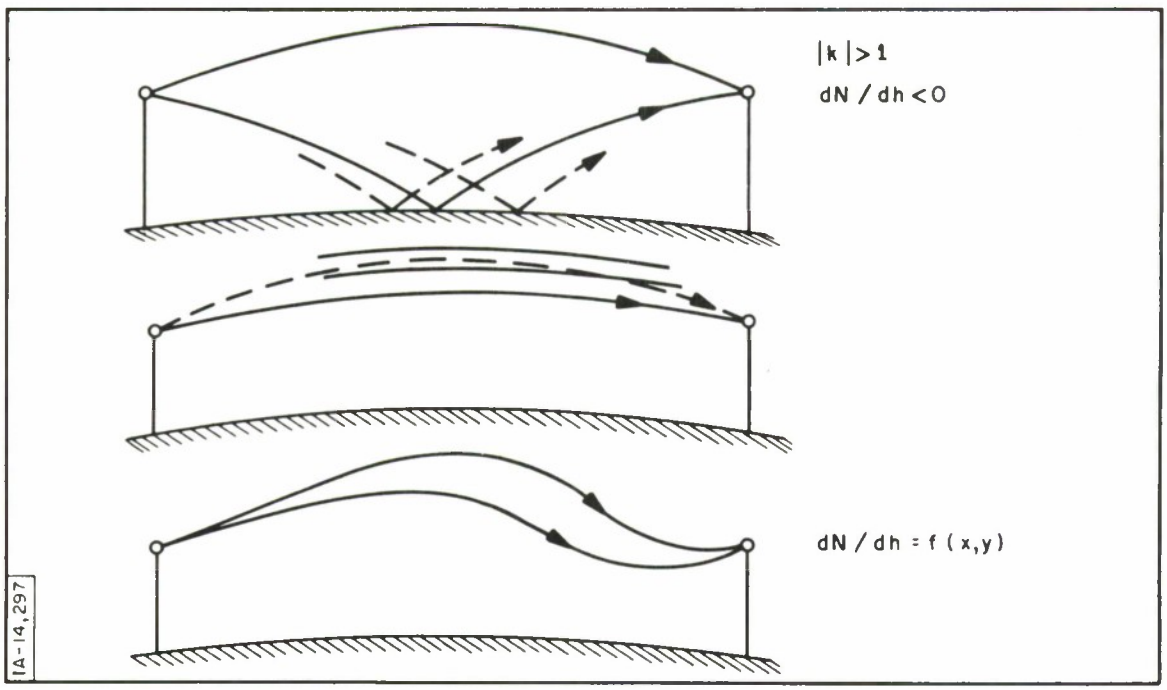

Fig. 1. Effects of Refractive Index Gradient Variations

elevated layers interpositioned between the terminal antenna elevations; or (c) ducting formations containing only one of the terminal antennas. These are illustrated in Fig. 2. A comprehensive description of the foregoing and additional fading mechanisms is given by Bechmann and Spizzichino[1]*

FADING CHARACTERISTICS

When fading is observed on microwave line-of-sight paths, it is useful to characterize the fading. This may be done in terms of the duration and depth of the fades, their diurnal variation, and any selectivity with respect to

*Numbers in brackets designate References on page 135.

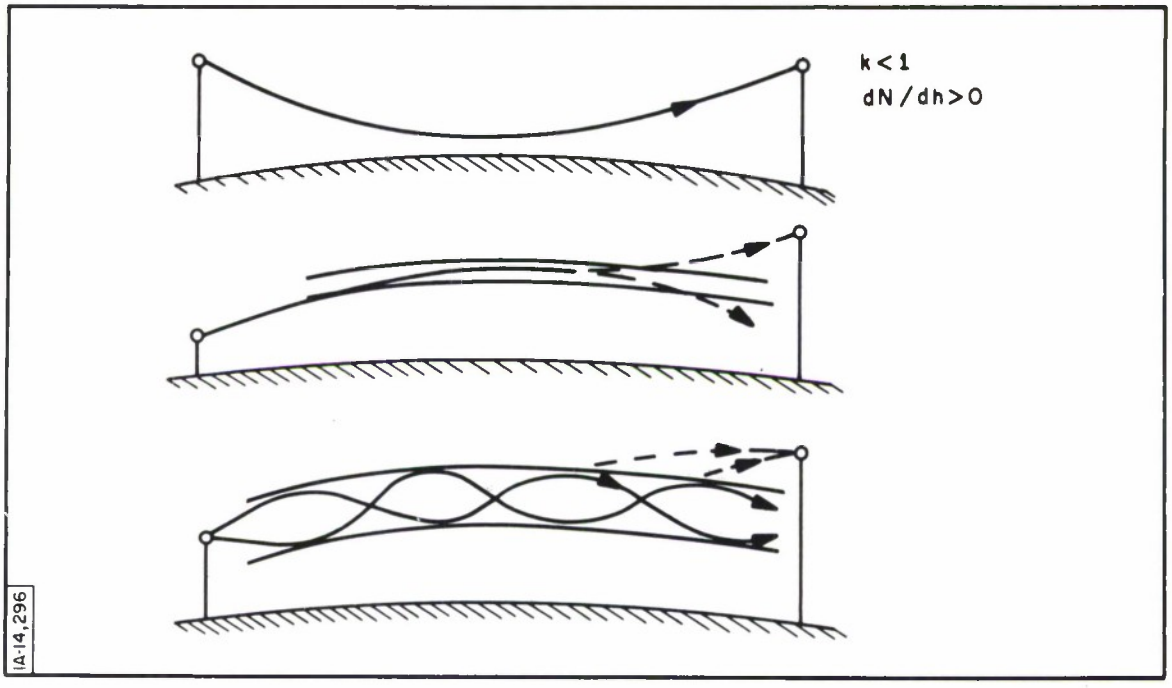

Fig. 2. Fading Mechanisms

space or frequency. The characterization may then permit identification of the fading mechanism (s) and suitable techniques to reduce their effects.

The depths of the fades encountered in multipath phenomena can be quite severe, depending, of course, upon the effective reflection coefficients or the relative amplitudes of the component waves. The interference between the direct wave and the reflected wave from ground or elevated layer can produce fades persisting from minutes to hours. During such fades, the nonspecular component, normally small for grazing angles, can cause additional interference resulting in deeper, more rapid fades whose durations are of the order of seconds. The multipath fades tend to be less frequent during the afternoon hours when conditions more closely approach the "standard atmosphere" for which most paths are designed.

These fades are selective in space and frequency so that their effects can be reduced substantially by space or frequency diversity.[2, 3, 4, 5] Other techniques are also available. For example, the Japanese have employed anti-reflective wave antennas[6] to reduce the contribution of ground-reflected waves. Furthermore, for propagation over rough terrain, the proper choice of antenna sites can also reduce or eliminate the ground-reflected wave.

Attenuation fading caused by diffraction of the earth can persist for several hours and to depths of up to 20 or 30 db. The depth of fading is space and frequency selective, and tends to be less frequent during the afternoon hours. This may be avoided by antenna heights which provide clearances of several Fresnel zones for the standard atmosphere. Deep fades, up to 16 db, lasting for hours or days (fadeouts), characterize the attenuation produced by ducts and elevated layers. These are selective in space but not in frequency, and tend to be less prevalent during the daylight hours. These fadeouts can, therefore, be encountered, to a degree, by space diversity.

MISTRAM I OBSERVATIONS

The multipath phenomenon has been observed as a source of fading on the MISTRAM I System of the Atlantic Missile Range (AMR). This has been particularly troublesome for that part of the communication link subsystem which consists of microwave relay circuits transmitting all signals, including data and timing synchronization between stations in the System. Signal recordings at approximately 7 gc, obtained from 17 September 1963 through 20 April 1964, were provided by the Pan American Technical Staff of the Air Force Eastern Test Range (AFETR) for two of the overland links.

The following is the result of the analysis by the National Bureau of Standards (NBS). Both paths were similar, 30.5 km. in length with effective antenna heights of 41.1 and 47.7 meters. A portion of the recorded signal exhibiting deep fades is presented in Fig. 3. The numerous fades of the first

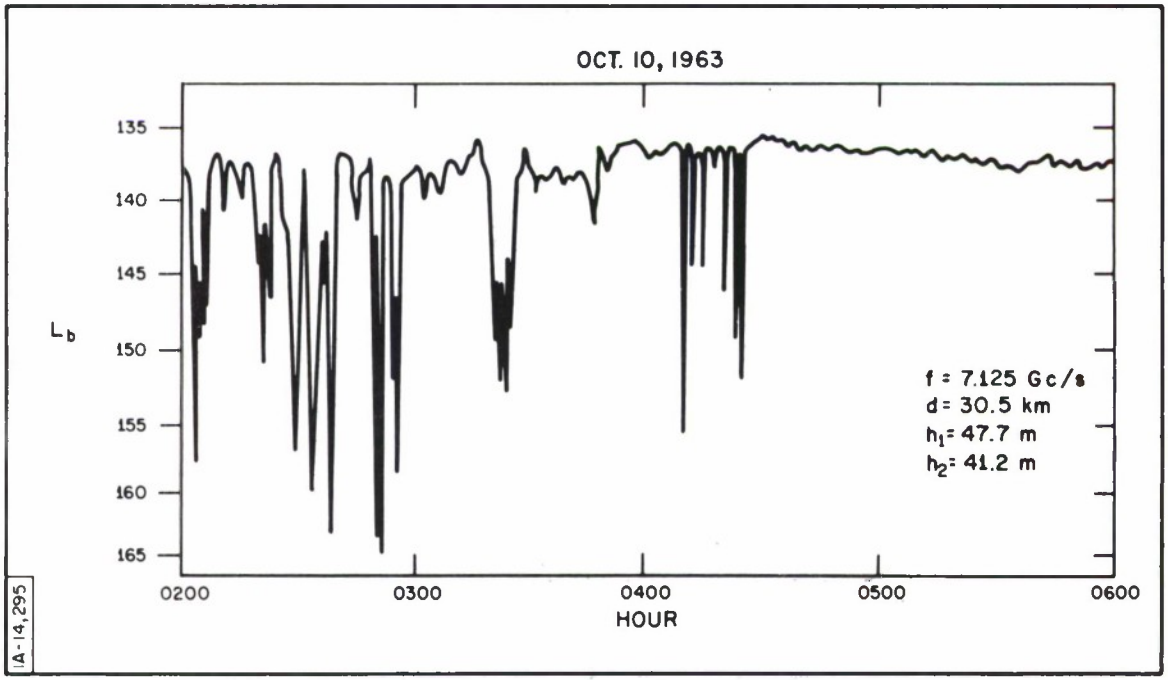

Fig. 3 Deep Fades on MISTRAM System

hours or so shown are typical of about 1.4 percent of the observation period. The signal during the next hour shown is representative of about 5.6 percent of the period, and the last hour is typical of the other 93 percent of the time. Even during the hours when fading was experienced the signal generally returned to, or above, the free-space value (a basic transmission loss of approximately 139 db) -- the behavior that is characteristic of a direct plus ground-reflected wave type of phase interference. The occurrence of the fading was not predictable,

since it exhibited no definite diurnal pattern; that is, there were many days for which no fading occurred. When fading did occur, it occasionally extended into daytime hours.

These particular links employed frequency diversity reception for which Δf was 250 mc. A comparison of the recorded signals for the two frequencies is shown for a period of several hours in Fig. 4. The strong similarity in the signal variation pattern is as expected for multipath fading. The "lag" between the two patterns is generally not constant because it is a function not only of the frequency spacing and the gradient of refractive index involved, but also of the time rate of change of the gradients encountered. For certain strong negative gradients, the lag will go to zero, making the frequency diversity ineffective.

This effect was illustrated with a film* following the oral presentation; the film showed the results of an experimental study[5] of a 48.3-km over-water, microwave line-of-sight propagation path. By employing a frequency sweeping technique for both the transmitter and the receiver local oscillator, Lewin obtained, for two vertically spaced receiving antennas, an oscilloscopic comparison of the two multipath lobing patterns. The transmitter frequency, 4.3 gc was swept ± 300 mcs. The local oscillator (IF = 60 mc, BW = 10 mc,) was swept at a much slower rate. The height of the transmitting antenna was 198 meters and the heights of the receiving antennas were 169.8 and 164 meters. The film, representing six days of observations sampled at one-minute intervals, showed the relative displacement of the two patterns as the atmospheric conditions changed.

*Film based on L. Lewin's experimental results.

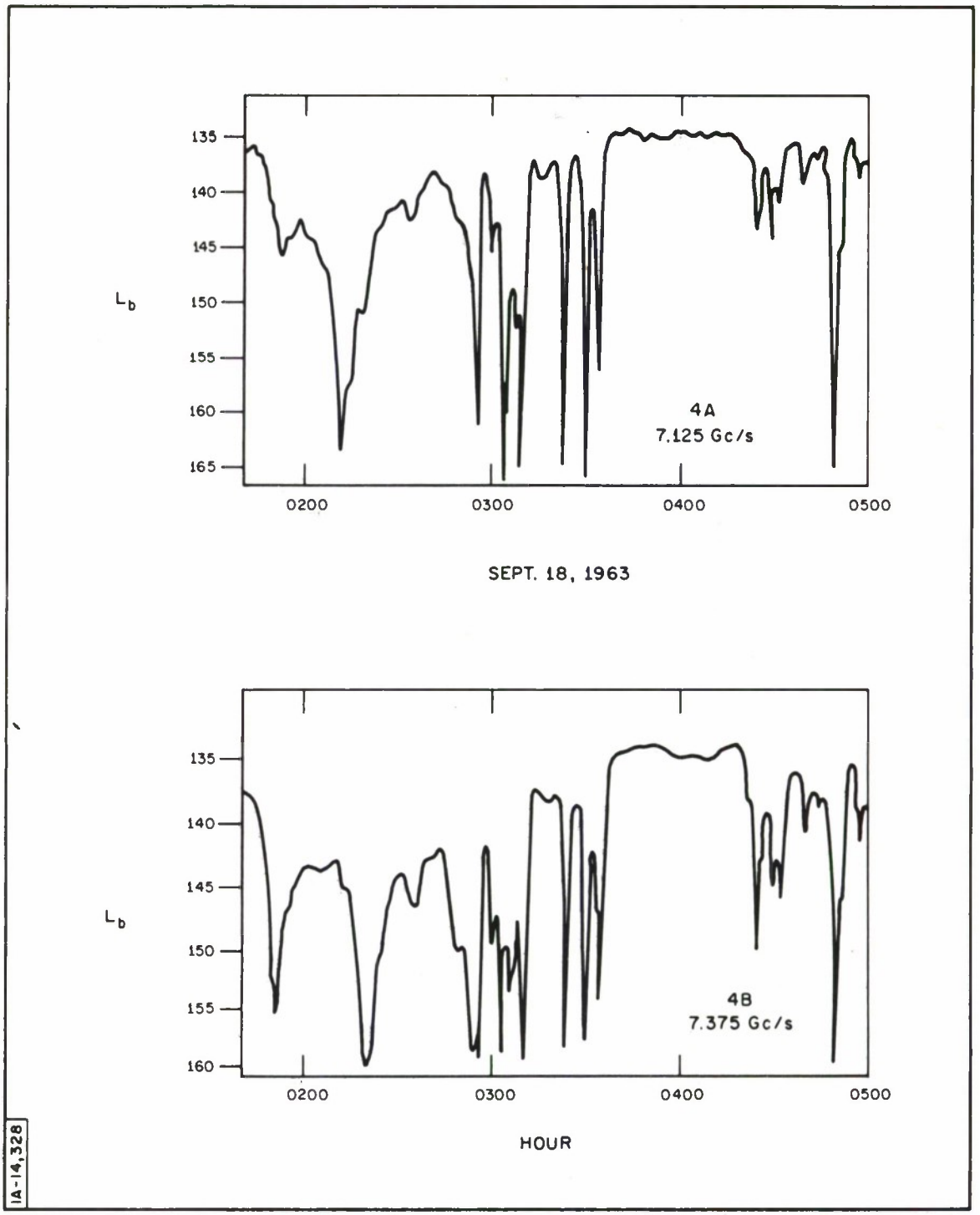

Fig. 4 Comparison of Signals at Two Frequencies

Figure 5 indicates a few of the situations shown in the film. The plots of E_1 and E_2 versus f represent the envelopes of the oscilloscope traces for the upper and lower antennas, respectively. The oscilloscope sweep was synchronized with the sweep frequency of the transmitter. The plot at the top of the slide is representative of the condition which was generally observed for optimum spacing between antennas. The plot at the center of the figure represents the observed comparison for an excessive antenna spacing. The plot at the bottom shows the effect of attenuation of the field at the lower antenna possibly due to partial isolation of the lower antenna. Sample illustrations have been given by Lewin.[5]

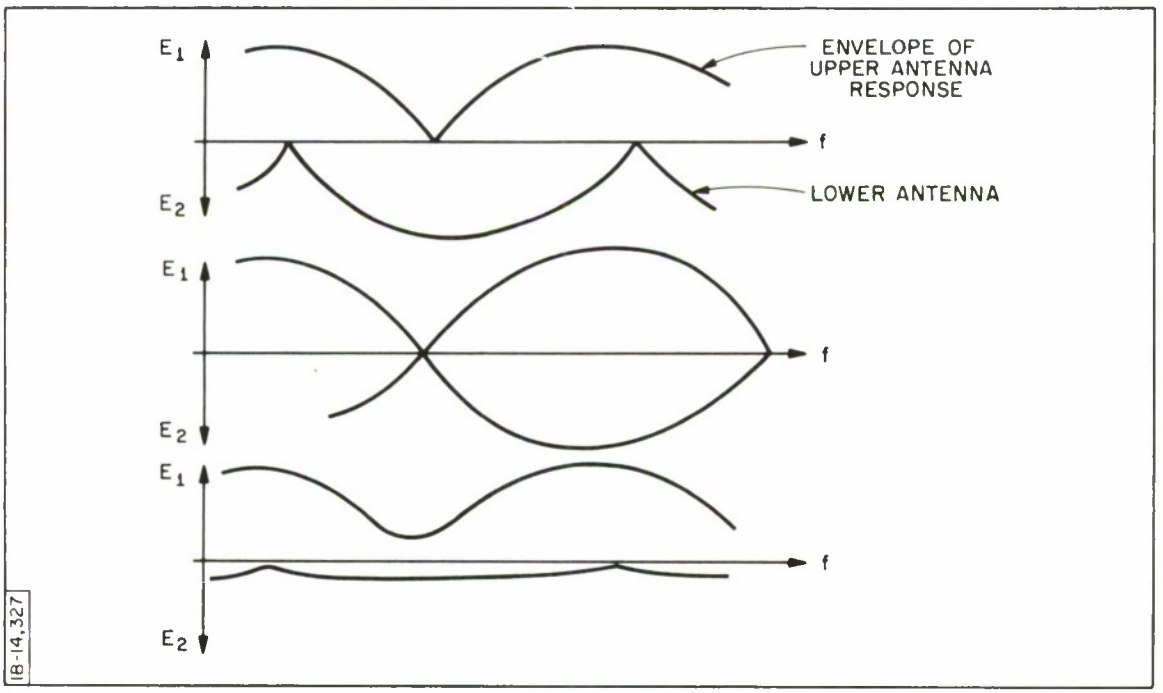

Fig. 5 Envelopes of Signals from Spaced Antennas

DIVERSITY RECEPTION

The signal recordings mentioned above, and those illustrated in Fig. 4, indicate that a substantial improvement would be expected for a diversity reception system which provides for wide variations in the gradients of refractive index. Lewin[5] describes a procedure for determining the optimum antenna or frequency spacing for such a situation. Briefly, the procedure consists of determining:

(a) the terminal antenna heights required to provide, for a given path length and operating frequency, a specified protection (a 20-db fade margin, for example) against diffraction fading for those extreme positive values of refractive index gradients that might be encountered, and

(b) the diversity spacing required to provide the specified protection against multipath fading for those extreme negative refractive index gradients that might be encountered.

The MISTRAM I paths, described previously, can be used to illustrate the results of applying such a procedure. The present terminal heights are adequate to provide a 20-db fade margin for positive gradients up to approximately +200 N units/km.

An examination of the wiresonde data available at various times during the period of the MISTRAM I signal recordings indicates refractive index gradients generally of the order of -75 N units/km, which corresponds to an effective earth's radius factor, k, of 1.9. The average gradient for the first 100 meters or so above the surface ranged from -206 to +75 N units/km. This corresponds to a range of k-values from approximately -3.1 to 0.68. To insure a

20-db fade margin for gradients of -314 N units/km or greater, a diversity spacing of approximately 11 meters, or 1150 mc, would be required.

Either the antenna or the frequency spacing would provide the required 20 db fade margin for diffraction fading or multipath (direct plus ground-reflected wave) fading for these particular paths. In general, however, the possibility of attenuation fading because of elevated layers or ducting conditions would suggest that the antenna spacing provides a preferable form of diversity reception. In addition, the use of spaced antennas permits addition of the two received signals at RF by means of a phase combiner.[5] This technique has been employed successfully both in England[7] and Japan.[4]

CONCLUSIONS

The experimental data shows that frequency diversity spacing of 250 mc is inadequate for the paths described. The author expects that diversity reception by means of vertically spaced antennas will provide a substantial improvement in system performance for the fading mechanisms commonly encountered over the microwave line-of-sight paths for the flat, maritime terrain of MISTRAM I. Although the effects of elevated layers and ducting conditions, if encountered, may be partially offset by the diversity reception with spaced antennas, their most severe effects would require increased antenna gains, more sensitive receiving systems, or increased transmitter power.

REFERENCES

1. Beckmann, P. and Spizzichino, A. The Scattering of Electro Magnetic Waves from Rough Surfaces, New York, The MacMillan Company, 1963.

2. Cabess, R. "The Achievement of Reliable Radio Communication Links on Over-Water Paths in Greece," (in French), L'Onde Electrique, 35, pp. 724-727, 1955.

3. Gudmandsen, P. and Larsen, B. F. "Statistical Data for Microwave Propagation Measurements on Two Oversea Paths in Denmark," Trans. IRE, AP-5, pp. 255-259, 1957.

4. Kakita, K. "Space Diversity Reception in Microwave Relay Systems," Proc. Microwave Seminar, Tokyo, I, Doc. No. 9, pp. 102-120, 1961.

5. Lewin, L. "Diversity Reception and Automatic Phase Correction," Proc. IEE, 109 B, pp. 295-303, July 1962.

6. Kawazu, S., Kato, S. and Morito, K. "Over-Sea-Propagation of Microwave and Anti-Reflected-Wave Antenna," Reports of ECL, Japan, 7, pp. 171-191, June 1959.

7. Dawson, G. "A Space Aerial Diversity Reception Technique for Microwave Radio Relay Systems," Proc. Microwave Seminar, Tokyo, I, Doc. No. 4, pp. 86-101, 1961.

SOME COMMENTS ON MICROWAVE LINK CHARACTERISTICS AND PROBLEMS

B. M. Hadfield*

GENERAL

All methods of radio communication between two points on the earth's surface suffer from defects, but the variety and degree diminish as the transmitted frequency is raised. This is true primarily because reasonably sized directive antennas become feasible, so that the transmitter energy can be concentrated into a narrow beam directed at the receiving point. Hence, microwave links operate roughly above 1000 mc, are strictly line-of-sight, and require reasonably high masts to elevate the antennas above the earth's curvature and any intervening hills.

Microwave links owe their existence, as highly competitive alternates for overhead wires and underground cables, to commercial exploitation on the basis of equal or greater reliability, higher channel capacity, and lower maintenance costs with comparable initial costs. By comparison with other forms of radio link, microwave methods have been refined until there is literally no comparison in terms of reliability. For example, 99.9 percent reliability is accepted as conventional practice in this field. The equipment needs to attain this performance are well known, and are obtainable from many manufacturers on a production basis.

A narrow beam line-of-sight link provides, in effect, an invisible cable between the terminals, whose power loss between isotropic antennas is given by $22 + 20 \log_{10} d/L$ db (where d is distance and L is wavelength), or 6 db/octave

*The MITRE Corporation, Bedford, Massachusetts

of distance or frequency. External noise has a relatively minor effect on design, because of the narrow beam and the high frequency. Hence, the only basic design factors are

(1) the generation of sufficient power to overcome the overall attenuation and provide a sufficient signal-to-noise (S/N) ratio at the receiver, and

(2) the effects generated because the beam is not ideally narrow and has to traverse a medium which causes it to deviate from a straight line between the terminals.

While the following sections will stress the problems associated with setting up and maintaining a microwave link, it must be emphasized that many of these problems exist in other methods of point-to-point communication to an even greater degree, together with other difficulties more or less incapable of being overcome except by a usually expensive tradeoff. Microwave links are not expensive, and some additional figures will be given later as to their extreme reliability, when properly installed.

LIMITING FACTORS DEPENDENT ON LINK DISTANCE

Free-Space Loss (Between Isotropic Antennas)

The 6 db/octave of distance effect is small compared to the "basic" loss at, say, 1 mile. This "basic" loss, often termed the launching loss, is 100 to 120 db at 1 nautical mile (n.m.) and for frequencies between 1000 and 10,000 mc. Between 5 and 60 miles and 1000 to 10,000 mc, the loss varies between 114 and 154 db. This is not a highly significant change if about 80 db of the "basic" 114 db loss can be neutralized by antenna gains, since the receiver sensitivity can be less than 0.1 microwatt (2700 uv on 75 ohms). At 10,000 mc, antennas of 4-foot diameter will give a total gain of 80 db, and at 3000 mc,

the diameter would be 13 feet. Distances of up to 50 miles have been achieved, on a 99 percent reliability basis, with not more than 1 watt of generated power.

Mast (Antenna) Height

The link distance is limited primarily by how high a mast can be tolerated, or engineered, to withstand the elements with minimum twist or sway. If a maximum of 150 feet is decided on, then the link length can be 18 n. m. at 1000 mc, 23 n. m. at 3000 mc, and 26 n. m. at 10,000 mc, assuming that the intervening terrain is smoothly curved.

The required antenna height is the sum of a component proportional to the square of distance ($d^2/4.5$, d measured in nautical miles), and a component proportional to distance and inversely proportional to transmitter frequency. The latter component becomes negligibly small at distances of about 50 miles.

Antenna height for line-of-sight over obstacles, more than any other factor, limits the use of microwave beamed links to around 30 to 50 miles for permanent installations where some choice can be made in the relative disposition of the sites.

Microwave Link Fading, Signal Strength Margin and Design Criteria

Normal propagation losses, at 6 db/octave of distance, occur mainly in the daytime, when the lower atmosphere is thoroughly mixed by rising currents and winds. Alternatively, normal propagation losses occur when the humidity content of the lower atmosphere is low, as in winter months.

Abnormal propagation losses are caused either by abnormal refraction index gradients, reflection from some midpath surface, or absorption by water vapor, rain or snow. Whereas absorption gives a steady decrease in signal strength for the duration of the cause, refraction index changes and reflections give rise to variable decreases known as fading.

In regards to absorption losses, it is sufficient to say that they are proportional to distance, to the density of the water content, and to the square of frequency. At around the usual microwave link distance of 20 to 30 miles, absorption can be a serious matter for frequencies above 3000 mc. In any event, absorption losses should always be allowed for, since any relatively steady depression of signal strength only tends to enhance the fading losses.

Signal variations caused by reflections are primarily the result of overall bending or twisting of the beam path between the antennas, because of refraction index changes, and only occasionally the result of a dense atmospheric layer above the line-of-sight. The effects of beam-edge reflection from the ground in the midpath, are normally avoided by stipulating an additional height to the antennas over and above that for insuring a line-of-sight. The additional height is proportional to distance and inversely proportional to frequency, i.e., about 60 feet at 20 miles for 3000 mc.

For the main cause of fading, namely refractive index gradient changes, the variable loss in signal strength is produced by the partial cancellation of energy between beam ray paths that have travelled different distances. This is the well known multipath effect. Almost all fading levels of more than 15 db below normal daytime signal level are caused by this interference between direct and indirect ray path lengths within the normal beamwidth.

Even under normal conditions, the beam is bent downward by the normal decrease in atmosphere dielectric constant with height. This is allowed for in design by assuming that the earth's radius is multiplied by 4/3, thus giving basic antenna heights somewhat less than would be required for a tangential line-of-sight path.

Changes in humidity, pressure and temperature cause both local and widespread changes in dielectric constant, and even inversions of the normal

gradient. Thus, the received signal may come successively from various parts of the beam lobe structure, or from two or more different ray paths. In addition, the overall bending of the beam may occasionally cause it to hit a highly reflective midpath surface, such as water or marshy land. With the lower portion of the beam being reflected and the upper still going direct, conditions are similar to VHF space wave propagation in which the propagation loss is 12 db/octave of distance.

Thus, if the fading is attributed to multiple ray paths generated by changes in the vertical refractive index gradients, then vertical space diversity of antennas should help to overcome fading. But if the fading is the result of a midpath reflection or to mere bending at the beam, space diversity is unlikely to help. Frequency diversity will also help in those cases produced by multiple ray paths. There is always a very fine structure associated with fading, and where this is important, frequency diversity is the only help. Fine structure fading can produce short fades of more than 45 db below the normal level.

When the normal reduction of atmosphere dielectric constant with height becomes inverted, then the beam will be deflected up off the receiving antenna, and only a weak signal will be received by diffraction from the intervening ground. This is particularly true if the design has not allowed enough initial beam clearance from the intervening terrain, with a late-evening radiation-type ground fog, and in late summer.

Alternatively, it is possible to get abnormally high signal strengths, especially when the atmosphere is still and the earth is hotter than the air, because of the formation of a waveguide atmosphere duct which prevents the beam from spreading normally.

In general, there is always a diurnal change of signal level, and use of too narrow a beam or insufficient path clearance very much enhances multipath fading. Multipath fading level variations of between + 15 and - 30 db over 30 miles are liable to occur.

A specimen design allowance for fading at 2000 mc would be small or zero for short distances up to 10 miles, since beam deviations clearly increase with distance. From 10 to 20 miles, the design allowance increases to 20 db. Above 25 miles, however, it is not found that proportionally larger allowances are required; a margin to cope with signals 30 to 35 db below normal is usually quite adequate.

The fading rate tends to increase with frequency, but the integrated duration of low signal levels is about the same at all frequencies between 1000 and 10,000 mc.

One of the most reliable microwave systems, the Bell TD-2 between the East and West coasts, uses 20 to 30 mile links (sited on mountains), and is designed to accommodate fading from +5 to -25 db, with average rates of fade of 10 db/second.

The long-term reliability of a single 30-mile link, without diversity, is about 90 percent for a 10-db fading margin, 99 percent for a 20-db margin, and 99.9 percent for a 30-db margin, at frequencies of about 2000 mc.

In general, abnormal fading, caused by abnormal climatic conditions or to a difficult route, is usually compensated for by diversity transmission and reception, using spaced antennas, frequencies or different polarizations. Diversity reception, of one term or another, is found to be imperative for over-water paths, if high reliability is desired.

Attenuation Due to Atmospheric Absorption or Scattering

This problem is peculiar to microwave links, since it is significant for frequencies above 1000 mc. Its magnitude is also a function of distance. Snow or heavy rainfall are the only conditions which produce absorption at frequencies up to 10,000 mc, and a reasonable formula is $\frac{10R}{(\text{wavelength})^2}$ db/mile, where R is the rainfall in inches/hour, and the wavelength is in centimeters. This attenuation is only significant for frequencies above 3000 mc, amounting to 20 db at 10,000 mc, for 20 n. mi., and 1 inch/hour of rainfall. This is of the same order as multipath fading at 20 miles and 10,000 mc.

Attenuation caused by this condition is a serious matter because it can result in complete outage for the duration of the storm. It is primarily caused, however, by the use of frequencies above 5000 mc and by the lack of a system design margin. Users of frequencies above 5000 mc rely on the normal design fading margin to compensate for this effect, since it is true that normal fading is not present during rainfall because of the turbulent condition of the atmosphere. Also, the probability of a prolonged storm of 1 inch/hour over the whole of a microwave system is not very great, according to present operating experience in this country. However, in other parts of the world, for example, the monsoon regions, outages attributable to these conditions would be very probable.

In general, then, although rainstorm and snowstorm attenuation is possible on microwave links, in practice it need not be a limiting factor, provided frequencies below 5000 mc are used with link lengths less than 30 miles, and provided the design is engineered with an adequate margin for fading all descriptions.

OTHER DESIGN FACTORS NOT PRIMARILY DEPENDENT ON DISTANCE

Route Survey and Terminal Siting

In common with all point-to-point communication systems, but more particularly on account of the line-of-sight requirement, beamed microwave links have to be readily adaptable to the terrain between the terminals, and to the available terminal sites which are economically situated with respect to the user.

Much has been written on the subject of how to survey such links, most of which reduces to a requirement that the designer should have a complete picture both in plan and cross section of the terrain between the desired terminals, during both winter and summer (due to the changing foliage). By normal "hand and foot" methods, this sort of survey can be an exhausting process, requiring perhaps several visits if the early assumptions based on survey maps prove inaccurate, as is often the case.

However, aerial photographic surveys in depth, plus aerial contour mapping, plus trial propagation tests (with proper regard for the prevailing atmospheric conditions) between helicopters equipped with standard transmitters and receivers hovering over the proposed sites at the proposed mast heights, all reduce the time element for the geographic system design to a matter of days rather than weeks.

In general, then, the main requirement in designing a microwave system (such as operating frequency, power generated, receiver sensitivity, channel usage, antenna sizes and mast heights) is to have acquired sufficient experience of operating microwave links in the designated area. There is plenty of such experience for links anywhere in the United States, and a fair amount for other latitudes and climates.

Mast Rigidity, and the Use of Reflectors

Because the mast heights for links of 20 miles or more are greater than 100 feet for a smooth curved earth, and because thay have to support antennas (or reflectors) weighing some 400 to 1000 pounds, with beamwidths of 4 degrees or less, mast rigidity is an important factor in overall long-period system performance. A twist of more than 2 degrees will clearly give received-signal level variations comparable to normal multipath fading.

Normal atmospheric loading conditions are 1/2-inch of ice and 85 m. p. h. winds, for installations in the United States, and usually the mechanical design permits 2-1/2 degrees angular beam deflection for antennas mounted at the mast head. For designs using a ground-based antenna beamed upward to a reflector at the mast head, the usual permissible mast deflection is 1-1/2 degrees, since the resulting beam deflection is twice this amount.

A typical permanent steel mast construction uses a triangular trussed beam weighing 620 pounds/20-foot section, and can be erected to a height of 340 feet. An aluminum mast is similar in design, weighs 50 pounds/10-foot section, and can be errected to 200 feet.

Portable or mobile masts are now available, which are erectable on a small baseplate, by means of an integral winch. A typical example is a 100-foot mast telescoping into a 12-foot package which can be erected by 4 men on a 3-foot square baseplate, in 2 hours, including guying. The total weight of the mast plus reflector is about 800 pounds. Its rigidity is such as to limit beam deflections to -0. 75 degree in elevation and 1. 5 degrees in azimuth, under the normal ice and wind loading conditions.

It is sometimes possible, and necessary, to use passive reflectors situated along the link and sited so as to get around or over some obstruction

which would otherwise demand prohibiting mast heights. However, such reflectors are really permanent, since to intercept a reasonable portion of the beams, they have to be large (20 feet x 24 feet, say), very rigid (not more than 0.14 degree twist), and very flat (to 0.5 inch). They also reduce the beam-width to about 0.5 degree, and although they thereby contribute gain, the net result is an enhancement of multipath fading.

Operating Reliability and Maintenance Costs of Commercial Equipment and Systems

The American Gas and Electric Company has a 5-link system, one link of which uses a passive reflector on a hilltop, which has been in operation for 2 years. They have kept records of outages for any cause, including regular maintenance and some initial troubles while learning the maintenance techniques. Their measured system reliability is 99.89 percent, and they expect to improve this to 99.95 percent.

Southern California Edison Company operate 40,000 miles of private wire lines and 7000 miles of microwave circuits. The maintenance costs of their private wire lines is $0.68/mile/month, while the microwave system varies between $0.32 and $0.51/mile/month. They confirm the high reliability of microwave systems, and say that the best possible wire line reliability has been found to be 98.2 percent.

Cleveland Electric Illumination Company has an extensive microwave system for transfer-trip relaying, which is considered to require the most reliable type of communications channel. Their preliminary tests over 5 months, including summer fading, showed a reliability of 99.98 percent over a distance of 19 miles during which no false signals at all were received.

From the above, and other evidence too long to be incorporated here, there can be no doubt that properly engineered beamed microwave links have

reliabilities as good as, and probably better than, private wire and cable links, with much lower maintenance costs and probably lower initial or amortization costs.

OBSERVATIONS ON THE MISTRAM FADING PROBLEM

While we have not had enough time to look at all the recorded signal level charts in detail, it would seem that there are at least two types of fading; one which is of short period with deep excursions, and the other which is slower and superposed on a general reduction in signal level.

Frequency diversity should compensate for the short-period deep fades, but the general depression of received level is indicative of midpath trouble, and is more likely to be overcome by increasing the antenna height than by vertical diversity with the present masts.

It is pertinent to inquire whether any propagation tests were run over a period of a year between the baseline sites and against various antenna heights. The whole subject of microwave link siting is very involved and very important to successful operation. The designer should have a complete picture in plan and cross section of the terrain, during summer and winter, and tests using a pair of helicopters are quite common.

No mention has been made in the presentations, or the discussions, of a design fading allowance in the MISTRAM baseline links (30 db is a common allowance for fading). Furthermore, in a well-designed microwave link, even when all such allowances have been made, an operating margin of 20 db is usually still available. This surplus margin, more than anything else, is what accounts for the very high reliability of conventional, commercial microwave links. It would be interesting to have available a typical breakdown of the transmitter, propagation and reception losses and margins, for the MISTRAM baseline microwave links.

REFERENCE BIBLIOGRAPHY

Bachynski, M. P. "Microwave Propagation over Rough Surfaces, "RCA Review 20, 308-335; June 1959.

Barrow, B. B. "Diversity Combination of Fading Signals with Unequal Mean Strengths," Trans, IRE, CS-11, 73-78, March 1963.

Barsis, A. P. and Johnson, M. E. "Prolonged Space-Wave Fadeouts in Tropospheric Propagation," NBS J. Res., 66D, 681-694, 1962.

Barsis, A. P., Barghausen, A. F. and Kirby, R. S. "Studies of Within-the-Horizon Propagation at 9300 Mc," Trans. IEEE, AP-11, 24-38, January 1963.

Bateman, R. "Elimination of Interference Type Fading at Microwave Frequencies with Spaced Antennas," Proc. IRE, 34, 662-676; May 1946.

Bean, B. R. "Climatology of Ground-Based Radio Ducts," NBS J. Res., 63D, 29-34; 1959.

Bean, B.R., Horn, J. D. and Ozanich, A. M. Jr. Climatic Charts and Data of the Radio Refractive Index for the United States and the World, NBS Monograph 22, 178 pp, November 1960.

Beard, C. I., and Katz, I. "The Dependence of Microwave Radio Signal Spectra on Ocean Roughness and Wave Spectra," Trans. IRE, AP-5, 183-191, April 1957.

Beard, C. I. "Coherent and Incoherent Scattering of Microwaves from the Ocean," Trans. IRE, AP-9, 470-483, 1961.

Beckmann, P. and Spizzichino, A. The Scattering of Electromagnetic Waves from Rough Surfaces, Vol. 4 of the International Series of Monographs on Electromagnetic Waves, The MacMillan Company, New York.

Beckmann, P. "Statistical Distribution of the Amplitude and Phase of a Multiply Scattered Field," NBS J. Res., 66D, 231-240, 1962

Bogle, A. G. "Some aspects of Microwave Fading on an Optical Path over Sea," Proc. IEE, Part B, 99, 236, 1952.

Brekhorskikh, L. W. Waves in Layered Media, Academic Press, New York and London, 1960.

Bremmer, H. "Propagation of Electromagnetic Waves," Encylopedia of Physics, XVI, "Electric Fields and Waves," Sec. 97, 596-601, 1958.

Brennan, D. G. "Linear Diversity Combining Techniques," Proc. IRE, 47, 1075-1102, June 1959.

Brilliant, M. "Fading Loss in Diversity Systems," Trans. IRE, CS-8 173-176, September 1960.

Burns, W. R. "Some Statistical Parameters Related to the Nakagami-Rice Probability Distribution, NBS J. Res., 68D, 429-434, 1964.

Bussey, H. E. "Reflected Ray Suppression Proc. IRE, 38, 1453, December 1950.

Cahn, C. R. "Combined Digital Phase and Amplitude Modulation Communication Systems," Trans. IRE, CS-8, 150-155, September 1960.

Chavance, P. "Etude de Propagation des Ondes Centimétriques dans le Nord de la France," Ann. Télécomm., 7, 254-261, 1954.

Clarke, K. K., and Cohn, J. "Carrier-to-Noise Statistics for Various Carrier and Interference Characteristics," Proc. IRE, 46, Part I, 889-895, May 1958.

Crawford, A. B., and Jakes, W. C. "Selective fading of microwaves," Bell Sys. Tech. J., 31, 68-103, (1952).

Day, J. P., and Trolese, L. G. "Propagation of Short Radio Waves over Desert Terrain," Proc. IRE, 38, 165-175, February 1950.

Dawson, G. "A Space-Aerial Diversity Reception Technique for Microwave Radio-Relay Systems," Proc. ITU Microwave Seminar, Vol. 1, Doc. No. 4, p 86-101, Tokyo, 1961.

De Lange, O. E. "Propagation Studies at Microwave Frequencies by Means of Very Short Pulses," Bell Sys. Tech. J., 31, 91-103, January 1952.

Dougherty, H. T. and Maloney, L. J. "Application of Diffractions by Convex Surfaces to Irregular Terrain Situations," NBS J. Res., 68D, 239-250, February 1964.

Durkee, A. L. "Results of Microwave Propagation Tests on a 40-Mile Overland Path," Proc. IRE, 36, 197-205, February 1948.

Dutton, E. J. "On the Climatology of Ground-based Radio Ducts and Associated Fading Regions," NBS Tech. Note 96, 38, June 1961.

Du Castel, F., Misme, P. and Voge, J. "Partial Reflections in the Atmosphere and Long Distance Propagation," Ann. Telecomm., 13, 209-214, 1958.

Englund, C. R., Crawford, A. B. and Mumford, W. W. "Ultra-Short-Wave Transmission over a 39-Mile "Optical" Path", Proc. IRE, 28, 360-369, August 1940.

Flock, W. L., Mackey, R. C. and Hershberger, W. D. "Propagation at 36,000 Mc in the Los Angeles Basin," Trans. IRE, AP-8, 235-241, May 1960.

Franceschetti, G. "An Approach to Tropospheric Duct Propagation," Proc. IEEE, 51, 1481-1486, November 1963.

Funakawa, K. and Kato, J. "Experimental Studies of Propagational Characters of 8.6 mm Wave on the 24-km Path," J. Radio Res. Labs., 9, 351-367, September 1962.

Gilman, G. W., and Willis, F. H. "Experience with Space and Frequency Diversity Fading on New York-Neshanic Microwave Circuit," Bell Telephone Lab., Rpt. MM-43-160-152, September 18, 1943.

Gough, M. W. " Microwave Line-of-Sight Propagation," Elec. Eng., 30, 237-247, May 1958.

Gudmandsen, P. and Larsen, B. F. "Statistical Data for Microwave Propagation Measurements on Two Oversea Paths in Denmark," Trans. IRE, AP-5, 255-259, July 1957.

Hancock, J. C., and Lucky, R. W. "Performance of Combined Amplitude and Phase-Modulated Communication Systems," Trans. IRE, CS-8, 232-237, December 1960.

Hathaway, S. D. and Evans, H. W. "Radio Attenuation of 11 kme and Some Implications Affecting Relay System Engineering," Bell Sys. Tech. J. 38, 73-89, January 1959.

Hay, D. R., and Fanski, F. M. "Experimental Technique for Studying Reflection Coefficients of Tropospheric Inhomogeneities," Can. J. of Phys., 41, 563-567, March 1963.

Hogg, D. C., Samplak, R. A. and Gray, D. A. "Measurement of Microwave Interference at 4 Gc due to Scatter by Rain," Proc. IEEE, 51, 500, March 1963.

Ikegami, F. "Estimation of Short Interruption due to Fading in Microwave Relay Systems" Proc. Microwave Seminar, Tokyo, I, Doc. No. 8, 59-71, 1961.

Ikegami, F. "Influence of an Atmospheric Duct on Microwave Fading," Trans. IRE, AP-7 252-257, July 1959.

Ikegami, F. "Radiometeorological Effects in Propagation over the Sea and Islands," Rev. Elect. Comm. Labor., NTT, 12, 5-6, 312-324, May-June 1964.

Kahn, L. R. "Radio Squarer," Proc. IRE, 42, 1704, 1954.

Kiely, D. G. "Some Measurement of Fading at a Wavelength of 8 mm over a Very Short Sea Path," J. Brit. IRE, 14, 89-92, 1954.

Kakito, K. "Space Diversity Reception in Microwave Relay Systems," Proc. Microwave Seminar, Tokyo, II, Doc. No. 9, 102-120, 1961.

Katzin, M., Bauchman, R. W. and Binnian, W. "Three-and Nine-Centimeter Propagation in Low Ocean Ducts," Proc. IRE, 35, 891-905, September 1947.

Kawazu, S. Kato, S. and Morita, K. "Over-Sea Propagation of Microwave and Anti-Reflected Wave Antenna," Reports of E. C. L., Japan, 7, 171-191, July 1959.

Kaylor, R. L. "Statistical Study of Selective Fading of Super-High Frequency Radio Signals," Bell Sys. Tech. J. 32, 1187-1202, September 1953.

Kerr, D. E. Propagation of Short Radio Waves, McGraw-Hill, New York, 1951.

Kiely, D. G., and Carter, W. R. "An Experimental Study of Fading in Propagation at 3-cm Wavelength over a Sea Path," Proc. IEE, Part III, 53, 1952.

Kirby, R. S., Rice, P. L. and Maloney, L. J. "Characteristics of Point-to-Point Tropospheric Propagation and Siting Considerations," NBS Tech. Note 95, 102 pp., October 1961

Klein, W. and Libois, L. J. "Essais de Transmission par Faisceau Hertzien sur un Long Trajet en Visibilite Optique entre la France et la Suizze," L'Onde Electrique, 33, 664, 1953.

LaGrone, A. H., Straiton, A. W. and Smith, H. W. "Synthesis of Radio Signals on Overwater Paths," Trans. IRE, AP-3, 48-52, April 1955.

Lane, J. A., and Bean, B. R. "A Radiometeorological Study, Part I; Existing Radiometeorological Parameters," NBS J. Res., 67D, 589-595, 1963.

Lewin, L. "Diversity Reception and Automatic Phase Correction," Proc. IEE, 109, Pt. B, 295-304, July 1962.

Mathur, L. S., and Kulshrestha, S. M. "On Superrefraction after the Passage of a Thunderstorm," Ind. J. Met. Geophysics, 12, 71-77, 1961.

Matsuo, S., Ugai, S., Kakita, K., Ikegami, F. and Kono, Y. "Fading of Microwaves," Elec. Comm. Lab. Tech. J., 2, 80-171, April 1953, see also Reports of ECL, Japan, 1, 38-47, November 1953.

McGavin, R. E. "A Survey of the Techniques for Measuring the Radio Refractive Index," NBS Tech. Note 99, 37 pp., May 1962.

McGavin, R. E. and Maloney, L. J. "Study at 1,046 Megacycles per Second of the Reflection Coefficient of Irregular Terrain at Grazing Angles," NBS J. Res., 63D, 235-248, 1959.

McPetrie, J. S., Starneck, B., Jarkowski, H. and Sicinski, L. "Oversea Propagation on Wavelengths of 3 and 9 Centimeters," Proc. IRE, 37, 243-257, March 1949.

Megaw, E. C. S. "Experimental Studies of the Propagation of Very Short Radio Waves," J. IEE, Part 3A, 93, 79-97, 1946.

Millar, J. Z., and Byam, L. A. "A Microwave Propagation Test," Proc. IRE, 38, 619-626, June 1950.

Millington, G. "The Reflection Coefficient of a Linearly Graded Layer," Marconi Rev., 12, 140-151, October-December 1949.

Misme, P. "Evanouissements d' Interferences Causés par des Discontinuités Frontales," L'Onde Electrique, 36, 43-47, 1956.

Montgomery, G. F. "Intermittent Communication with a Fluctuating Signal," Proc. IRE, 45 1678-1684, December 1957.

Morita, K. and Kakita, K. "Fading in Microwave Relays," Reports of ECL, Japan, 6, 352-370, September 1958.

Muchmore, R. B. and Wheelon, A. D. "Line-of-Sight Propagation Phenomena – I: Ray Treatment," Proc. IRE, 43, 1437-1449, October 1955.

Norton, K. A. "The Calculation of Ground-Wave Field Intensity over a Finitely Conducting Spherical Earth," Proc. IRE, 29, 623-639, December 1941.

Norton, K. A., Barrows, E. C., Thompson, M. C. Jr. and Janes, H. B. "Variance of Radio Frequency Caused by Atmospheric Turbulence in Line-of-Sight Transmissions," Trans. IRE, I-11, 153-155, December 1962.

Oguchi, T. "Attenuation of Electromagnetic Wave Due to Rain with Distorted Raindrops," J. Radio Res. Labs., Tokyo, 7, 467-485, Part II, ibid., 19-37, January 1964.

Omori, T. and Sato, R. "Multipath Propagation of Microwaves," Tech. J. of ECL, Japan, 6, 1-11, January 1958.

Oxenhufwud, A. "Tests Conducted over Highly Reflective Terrain at 4,000, 6,000 and 11,000 Mc," Trans. Amer. IEE, Part I, 78, 265-270, 1959.

Pierce, J. N., and Stein S. "Multiple Diversity with Nonindependent Fading," Proc. IEE, 48, 89-104, App. III, January 1960.

Rainey, R. J. Jr., and Thorn, D. C. "A Refraction Correction Technique which includes Nonsymmetric Index of Refraction," Trans. IEEE, AP-11, 446-450, July 1963.

Rice, S. O. "Distribution of the Duration of Fades in Radio Transmission: Gaussian Noise Model," Bell Sys. Tech. J., 37, 581-635, May 1958.

Rivet, P. "Essais de Diversité et étude de l'effect Defocalisation sur les Liaisons Longues en Visibilité," L'Onde Electrique, 36, 24-31, 1956.

Saxton, J. A. "Propagation à Travers la Troposphere," L'Onde Electrique, 40, 505-514, 1960.

Schelleng, J. C., Burrows, C. R. and Ferrell, E. B. "Ultra-Short-Wave Propagation," Proc. IRE, 21, 427, March 1933.

Siddiqui, M. M. and Weiss, G. H. "Families of Distributions for Hourly Median Power and Instantaneous Power of Received Radio Signals," NBS J. Res., 67D, 753-762, November-December 1963.

Smith-Rose, R. L. "A Preliminary Investigation of Radio Transmission Conditions over Land and Sea on Centimetre Wavelengths," J. IEE, Part III, A, 93, 98-100, 1946.

Staras, H. "The Statistics of Combiner Diversity," Proc. IRE, 44, 1057-1058, August 1956.

Suzuki, M. "Problems Concerning the Variations of (Equivalent Reflection Coefficient) in Microwave Propagation over Snow-Covered Terrain," ETJ of Japan, 2, 104-107, 1956.

Suzuki, M. "Experimental Analysis of Equivalent Reflection Coefficient of Various Reflecting Rough Surfaces in Microwave Propagation," ETJ of Japan, 4, 3-6, 1958.

Tomlinson, H. T., and Straiton, A. W. "Analysis of 3-cm Radio Height-Gain Curves Taken over Rough Terrain," Trans. IRE, AP-7, 405-413, October 1959.

Turin, G. L., "On Optimal Diversity Reception," Trans. IRE, IT-7, 154-166, July 1961; see also CS-10, 22-31.

Thompson, M. C. Jr., and Janes, H. B. "Measurements of Phase Stability over a Low-Level Tropospheric Path," NBS J. Res., 63D, 45-51, July-August 1959.

Ugai, S. "Statistical Consideration of the Structure of Atmospheric Refractive Index," Reports of ECL, Japan, 7, 253-289, August 1959.

Ugai, S. "Studies on Microwave Propagation within Line-of-Sight," Proc. Microwave Seminar, Tokyo, I, Doc. No. 6, 30-43, 1961.

Ugai, S. "Characteristics of Fading Due to Ducts and Quantitative Estimation of Fading," Rev. of ECL, Japan, 9, 319, May-June 1961.

Wheeler, B. F. and Mathwich, H. R. "Use of Distribution Curves in Evaluating Microwave Path Clearance," Trans. IRE, PGI-4, 31, October 1955.

Wheelon, A. D. "Near Field Corrections to Line-of-Sight Propagation," Proc. IRE, 43, 1459-1466, October 1955.

Wilkerson, R. E. "Defocusing of Radio Rays by the Troposphere," NBS J. Res., 66D, 479-485, 1962.

Willis, F. H. "Microwave Propagation Measurements, Report presented at NDRC Conference of February 10-11, 1944.

Wong, M. S., "Refraction Anomalies in Airborne Propagation," Proc. IRE, 46, 1628-1638, September 1958.

Note: The above list of references has been included for the convenience of the researcher in this area. A comprehensive NBS Technical Note by H. T. Dougherty, entitled "Bibliography of Fading on Microwave Line-of-Sight Tropospheric Propagation Paths and Associated Subjects," is in the final stages of publication at NBS. This note contains abstracts on over 200 items; the author should be contacted directly since there is no NBS number available at this time.

FINDINGS AND RECOMMENDATIONS OF THE NATIONAL ACADEMY OF SCIENCE "PANEL ON TRACKING DATA ANALYSIS" IN THE AREA OF TROPOSPHERIC PROPAGATION AND REFRACTION

Dr. A. T. Waterman, Jr. *

The Panel dealt with a variety of problems at the Eastern Test Range, (ETR), of which propagation was one. My role was only in connection with the propagation aspects.

Everyone else who has spoken here has said something about what he has actually done. The remarks that I have to make refer just to giving advice to people on how to do things. I might mention also (I think it's entirely appropriate to do so) a report that was put out a couple of years ago by the National Academy of Sciences Ad Hoc Panel on Electromagnetic Propagation of which Dr. Straiton was a member. Most of the technical investigations of propagation problems associated with missile guidance and tracking were comprehensively summarized in that report. As a result, the actual amount of work of that nature remaining to be covered by our Panel was relatively small.

There are two basic questions, I think, with regard to propagation and its relationship to the role of tracking accuracy. One is the question of what should be done to improve certain errors; the other is the question of the ultimate limit of accuracy set by the atmosphere. Now, it seems to me highly important to recognize that these two questions are of a different nature. The first question is one which can be answered by engineering techniques: by taking existing knowledge and turning it, through one approach or another, to best advantage in

---

*Stanford University, Stanford, California

working out a methodology for estimating errors. The second question, the ultimate limit of accuracy, is more a scientific than an engineering question – the sort of thing one should be quite cautious in answering, since new and unforeseen developments could lead to a substantial improvement in the future.

I think it is also worth noting (it is perfectly obvious to everyone here) that there have been a couple of schools of thought on how best to approach this basic propagation problem. One places emphasis on the spectral description of the atmosphere and, to a large extent, uses statistical techniques. The other is more deterministic. It thinks of the atmosphere in terms of the physical processes taking place. It is faced with more serious measurement problems, but, perhaps in the long run, might hold hope for greater advances because of a more profound eventual understanding of the processes at work. The viewpoint taken by the Panel, or at least by me in my role as a member, has been that these two approaches are not necessarily in conflict, but, rather, that they can be used in a complementary fashion.

I'll try and outline briefly the recommendations that relate most nearly to the propagation problems involved. These fall into three general categories. One is meteorological; the other is basically radio; the third is organizational.

Meteorologically, there were three recommendations; they are fairly obvious sorts of things, and are, in fact, being implemented to a certain extent. The first has to do with vertical soundings in the Cape Kennedy region. The recommendation is that these soundings be used to develop insight into what a sampling error is in a sounding. In this regard, it was quite gratifying to see the records which D. L. Ringwald showed. I think there is also, by implication, a need for a multiplicity of soundings and, therefore, of any improvement in cheaper methods of obtaining accurate soundings. In this regard, there is a possibility of further development of the concept of an expendable type of

refractometer as distinct from one in which the entire instrument has to be flown in a plane and, therefore, is expensive enough to have to be preserved.

Second, still in the meteorological vein, there is a recommendation that a surface network of refractive index measurement sites be set up in the region of the two MISTRAM stations, with spacings ranging from the order of antenna sizes to distances comparable with the largest baseline anticipated in guidance systems, and over time intervals of a length comparable with that required for the air to drift across the instrumentation range. (This recommendation relates to the approach adopted by the National Bureau of Standards).

The third recommendation with regard to meteorologic measurements is just that; with a large amount of instrumentation, the opportunity of obtaining as comprehensive a measure of atmospheric characteristics as possible should be fully exploited on some occasions.

Now, with regard to the recommendations relative to radio measurements, there were several things that were considered. Some of them were discarded for reasons that were not wholly related to propagational or meteorological problems, but to other practical considerations. Some of the things considered were (a) the establishment of fixed-path measurements in the range area, (b) a continuation of measurements obtained in the past in which location by optical means of a beacon in a plane is compared with the operation of the MISTRAM system with a transponer in the same plane, and (c) a satellite specially outfitted with a MISTRAM transponder, which could then serve as a means of calibrating the system. For one reason or another, none of these received the full support of the Panel. The concept of fixed-path measurements has limits in the range area. Most fixed paths would be relatively flat, and at low angles, and in situations which would not be pertinent as far as missile tracking is concerned. There is also the problem of surface reflections which would

complicate the situation considerably. The concept of the plane flights was argued as not being an effective means of calibrating the system, apparently because of problems pertaining to ballistic cameras: the accuracy and cost of reducing data. The idea of using a satellite equipped with a MISTRAM transponder was argued only to the extent that special satellite should be used. On the other hand, the concept of putting a transponder on a satellite that did have some extra room on it received favorable response, and constituted one of the recommendations. The most important recommendation in connection with calibrating the propagation errors, however, was that measurements obtained during a missile launch should be continued during the free-flight portion of the missile trajectory. The orientation of the missile would be stabilized, and this free-flight portion could then be used as a more accurate means of calibrating propagational errors.

Finally, with regard to the organizational recommendations of the Panel, it was felt that the amount of effort and manpower that was being placed on the problems related to propagation was small relative to its overall importance. The propagational problem itself will be one that continues to be emphasized and, therefore, its importance might be reflected in an organizational set-up in which there is greater centralization of control, authority and responsibility for refractive and propagational measurements, as well as for the analysis of propagational data.

Now, in this connection there are some advantages that have not been utilized, and the discussion in the recommendations includes mention of these. Work done in other places and the methods developed by other groups, such as the Cambridge Research Labs., the National Bureau of Standards and The MITRE Corporation, could be, perhaps, more fully utilized in the reduction of actual missile flight data. One possibility would be to furnish the data from some of

the flights directly to these concerns. They could perform their own analysis of the data; and the range would then be in a position to compare the relative merits of each type of analysis.

Finally, I think it is important in this field to keep abreast of all new developments. Certainly, equipment such as the line integral refractometer should be exploited quite fully in order to ascertain its ultimate merits. Undoubtedly, other ideas will arise. It is important to remain constantly alert to such new suggestions.

SPACED REFRACTOMETER EXPERIMENT

C. F. Martin*

Before discussing what the spaced-refractometer experiment is all about and what we hope to get out of it, I would like to briefly review the refractometer background, particularly in regard to calibration problems. Besides, it should also be of some interest in its own right and will, I hope, perhaps prompt some helpful suggestions from those of you who have been involved with similar problems.

REFRACTOMETER CALIBRATION

As most of you probably know, the AFETR now has in operation two precision electronic missile trajectory measurement systems which are commonly referred to as MISTRAM I and MISTRAM II. MISTRAM I, located at Valkaria, Florida, about 35 miles south of Cape Kennedy, consists of a central range-measuring station, a North-South baseline and an East-West baseline, each with range-difference measuring stations at 10 K feet and 100 K feet from the central station. MISTRAM II, located on the island of Eleuthera, about 300 miles southeast of Cape Kennedy, is a similar system except that it lacks the short baseline stations and the baselines intersect at about 120-degree angle. Specifications for these systems call for a range measurement accuracy of 0.4 foot and a range difference accuracy of 5 ppm. Although such specifications can be met by the system electronics, the current state of knowledge of (tropospheric) propagation effects is such that such accuracies cannot now be met.

*Pan American World Airways/GMRD, Patrick AFB, Florida

In designing the MISTRAM systems, it was recognized that propagation effects would likely be the limiting factor in final system accuracy, so provision was made for including as an integral part of the system at each measurement station the finest refractometer that money could buy. Originally, it was planned to record each refractometer reading 20 times per second just as the range and range differences were measured 20 times per second. For various reasons, including the state of calibration of the refractometers and the fact that the data channel was needed for other purposes, this rate of refractive index recording has long since been discontinued. Nevertheless, we still have the 5 Valkaria refractometers and the 3 Eleuthera refractometers for use with the MISTRAM systems in whatever manner will give us the maximum benefit in accounting for atmospheric effects on MISTRAM data.

I am not quite sure of the reasons for the selection of ground-level refractometers by General Electric as the basis for MISTRAM refraction corrections. No doubt they were influenced to a considerable extent by the work of Bean and Thayer of NBS, even though they reportedly were somewhat less than pleased by the refraction correction accuracies estimated by Bean and Thayer. Perhaps it was also felt that with $100,000 worth of microwave refractometers at the MISTRAM I site, highly accurate refraction corrections would be automatically insured. If this were the case they were certainly overly optimistic. Almost equally as certain, however, is the fact that the refractometers can be put to greater use than they have been until now.

Several months ago, Dr. A. J. Mallinckrodt, who is a consultant on radio propagation problems, to Pan American Airways/GMRD, proposed an experiment which would utilize the MISTRAM refractometers for obtaining information on the space-time structure of the refractive index near ground level in the MISTRAM area. The performance of this experiment would require that at least 6 refractometers be in operating condition, that all have almost identical performance,

but not necessarily that the zero point of each refractometer be determined. In other words, the experiment would require only relative refractive index measurements. But since considerable effort was necessary in order to verify satisfactory relative operation, and since absolute operation is certainly desirable, inasmuch as it is essential for use in any refraction correction procedure for MISTRAM tracking data, it was decided that the first order of business would be to put all eight MISTRAM refractometers into operational condition and then install them on site after the conclusion of the spaced-refractometer experiment. As a matter of fact, the MISTRAM I refractometers would be installed on site for the experiment itself.

The type of refractometer that we have been talking about was designed at the National Bureau of Standards and is commonly referred to as the Vetter refractometer. The ones that we have were built by Colorado Research Corporation which, I understand, is now defunct; but presumably this has no connection with our calibration difficulties. The design of the Vetter refractometer system is such that its accuracy of operation is relatively insensitive to the electronics involved and we need concern ourselves only with the two resonant cavities which are used.

One cavity, referred to as the reference cavity, is sealed and has a servo-controlled probe for varying the resonance frequency of the cavity. The resonance frequency of this cavity must be calibrated as a function of probe position, since the only readout of the instrument is really nothing more than probe position.

The other cavity is called the sampling cavity and is the one which is exposed to the atmosphere whose refractive index is to be measured. If we can establish the resonance frequency of the sampling cavity at a time when we know

the true refractive index of the atmosphere in the cavity, then we can obtain the refractive index with some other atmosphere by measuring the cavity's resonance frequency and using the relation

$$\frac{\Delta f}{f} = - \frac{\Delta n}{n} \quad .$$

The resonance frequency of the sampling cavity we measure by the use of the reference cavity; the servo-loop positions the probe of the reference cavity such that the two cavities have the same resonance frequency, and the probe-position calibration then gives the sampling-cavity resonance frequency. The atmosphere of a known refractive index is most accurately obtained by placing the sampling cavity in a bell jar and evacuating it. Since the refractive index of even a poor vacuum deviates from unity by an insignificant amount for our purposes, we have an absolute calibration of the instrument.

This all sounds rather simple and straightforward, but it really doesn't turn out to be that way. That this might be so we might suspect by considering what we are actually measuring and what affects our measurements. The resonance frequencies are dependent only upon geometry and we are interested in obtaining an overall accuracy of better than 1 N unit over a period of days. Over short periods of time we expect to detect changes of 0.1 N unit. When we realize that 1 N unit corresponds to a change in cavity dimensions of 1 ppm and that the sampling cavity must be open to the atmosphere along with its fluctuating temperature and, especially in Florida, its numerous varieties of flying and crawling pests, we can appreciate the possibility of difficulties arising. As a matter of fact, even before going out into an uncontrolled environment we have encountered some problems.

The calibration of the reference cavities, or at least finding a workable routine for it, can be considered successfully accomplished after considerable

effort. Since each reference cavity is a little bit different from any other, and the cavity resonance frequency is not quite a linear function of probe position in any case, each one must be calibrated individually and its own calibration curve of probe position versus resonance frequency drawn up. In a typical case, the error incurred by taking the refractometer readout to be true N-unit reading amounts to about 5 N units. Without this correction we might as well not use the refractometer at all, since standard meteorological measurements made with a little care give better results.

The calibration curve is obtained by replacing the sampling cavity by a sealed calibration cavity. This cavity also has a probe which is positioned by a vernier dial on the end of the cavity. Its calibration of resonance frequency versus vernier reading was performed by the Bureau of Standards Calibration Services.

Some difficulty has been encountered with a rather long-term drift in one or two of the reference cavities. This I understand is most likely due to the type of seal material used and should stabilize after a warmup of several hours.

An apparent instability of the sampling cavities which has been encountered in attempts to measure their temperature coefficients is causing more concern at the moment. I use the word apparent because I don't actually believe that they are as real as indicated. In going through a temperature cycle, a hysteresis loop is expected due to the lag in the temperature compensating device of the cavity, but the loop should close instead of being 3 to 4 N units away from the initial reading as has been found to be the case.

In order to insure both adequate ventilation of the sampling cavity and to help prevent the intrusion of undesired pests, a forced ventilation shelter (with screens) is being designed for use at the refractometer operating sites. The

shelter is designed so that it may be readily sealed for air evacuation. The evacuation process is necessary in order to check the refractometer zero set, but the frequency at which it will be required is not yet known.

SPACED REFRACTOMETER EXPERIMENT

The motivation behind the spaced-refractometer experiment lies in the current paucity of information on refractive index fluctuations over long periods of time at widely separated spatial points. Considering the at least potential availability of accurate refractometers at the already rather widely separated MISTRAM stations, it is proposed to use these instruments -- together with one of the Eleuthera refractometers as an extension of one of the baselines -- to record the near ground level index of refraction at a rate of about 6/minute for a period of 1 week. The current plan is to locate the extra refractometer at the Azusa Mark II site on Cape Kennedy, giving a maximum spatial separation between refractometers of about 55 miles. The Azusa location was selected, in preference to earlier suggestions of Tampa or Lakeland, Florida, partly because of its accessibility and partly because I found it very difficult to believe that atmospheric conditions at either of these towns had any relation to conditions high out over the Atlantic ocean.

This experiment is scheduled to be carried out as soon as the refractometers are calibrated. At the present time, it's impossible to say when this will be, but a crude guess would be sometime in September.

We might now briefly consider how we are going to treat the data and how it will be useful. Primarily, we are interested in obtaining a space-time correlation function for refractive index fluctuations. As a matter of definition, this function is given by

$$C(\bar{\rho}, \tau) = \langle \delta N(\bar{r}, t)\, \delta N(\bar{r} + \bar{\rho}, t + \tau) \rangle$$

where the <> indicates a time and spatial average. How we handle the data depends partly upon what we expect. Measurements made at a single point have supposedly indicated that the time correlation function is approximately exponential,

$$C(\tau) = e^{-\tau/\tau_0} \quad .$$

If the atmospheric inhomogeneities really were frozen, then they should drift by the measurement station which would then really be measuring spatial inhomogeneities. The resulting form for the space-time correlation function is then

$$C(\rho, \tau) = e^{-\frac{1}{\tau_0} \left| \tau - \rho/v \right|}$$

if v is the drift velocity of the inhomogeneities. Even on physical grounds, there are several things wrong with this reasoning. First, one should not expect perfect, or even near perfect, correlation of space and time fluctuations except over very short periods of time. When the wind direction changes many times during the data sampling period, one could hardly expect the data from spaced refractometers to yield a well defined wind velocity. In the Cape Kennedy area, the wind direction changes from a predominantly southeasterly direction during the day to a predominantly northwesterly direction in the evening, so a 7-day test would cover at least 14 major changes in wind direction.

A further source of difficulty is that even a simple time correlation function will not necessarily have the above simple form. An analysis of some refractive-index data obtained at the MISTRAM sites for Mr. Ringwalt shows that the function goes to zero at about 18 hours, and then to a negative value of $\sim$0.35 at around 28 hours. After this period, it again approaches zero, although rather slowly.

Such behavior is somewhat disconcerting and not at all what we would like. The reason we suspect to be a rather large daily fluctuation. Some of Mr. Ringwalt's data is now being analyzed after first taking out the daily mean. Hopefully this procedure will yield correlation functions which die off more rapidly and have better behavior. If so, we will then feel that, for the one week data period, we can adequately represent the refractive index fluctuations of the atmosphere as the sum of a sinusoid of a 1-day period plus a random component.

The use to which a space-time correlation function can be put will, we hope, lie in the area of improving the accuracy of the refraction corrections used in MISTRAM data reduction. In addition, an assessment can be made of the residual errors in the refraction correction. This possibility arises in the following way. Suppose that a mean range refraction correction for a certain period -- perhaps several hours or even several days -- is known but that it is desired to improve upon this accuracy. Such a mean correction could be based upon ground level measured values of index refraction, but this is not necessarily so.

Now let us suppose that the improvement in the range correction which we shall make will be proportional to some time-filtered function of δN_s, the deviations of the surface value of index of refraction about its mean during this period. Thus, we propose to make the additional range refraction correction

$$\delta R(t) = \int G(t' - t)\, \delta N_s(t')\, dt' \quad ,$$

with $G(t' - t)$ some, at present unkown, filter function. It seems logical that this function should be chosen in such a manner that the resulting range error will be a minimum, at least in a statistical sense. With the introduction of the space-time correlation function defined above, this may indeed be done.

If we demand that G be the function which minimizes the spectrum of the refraction correction errors (assuming the mean correction to be without error), then we are led to a G which has the Fourier transform

$$Y(\omega) = \frac{1}{\Phi_s(\omega)} \int_0^R \Phi(s, \omega)\, ds \quad ,$$

where $\Phi(s, \omega)$ is the Fourier transform of $C(s, \tau)$, $\Phi_s(\omega)$ is the Fourier transform of $C(0, \tau)$, and the integration is along the ray path from the tracking station to the space vehicle. The spectrum of the remaining range error is then

$$W(\omega) = -\frac{1}{\Phi_s(\omega)} \left[\int_0^R \Phi(s, \omega)\, ds\right]^2 + 2 \int_0^R (R - s)\, \Phi(s, \omega)\, ds$$

It is of interest to note that all the spectra which enter the above equations are cross spectra of refractive index fluctuations between different points along the actual ray path to the tracked vehicle. Thus, the use of spectra obtained from ground level measurements implies certain assumptions about the isotropy of the space-time correlation function. However, it is not presently feasible to make long-period refractive index measurements along an approximate ray path.

THE FABRY-PEROT REFRACTOMETER AND THE PRECISION NRL LYMAN-ALPHA HUMIDIOMETER

F. C. MacDonald, D. L. Randall, and D. Stillwell*

INTRODUCTION

The measurement of microcells of atmospheric moisture, which are believed to be responsible for transhorizon tropospheric radio propagation at VHF and UHF by the scattering mechanism, has been a challenge to the scientist because of inadequate meteoroligcal instrumentation. An aircraft is the most convenient platform for mounting these instruments, but, unless the time response of the sensing instruments is very rapid, the speed of the aircraft permits only large-scale measurements.

DISCUSSION

To make fine-grained meteorological measurements from an aircraft, NRL is developing two basic instruments: The Fabry-Perot Refractometer; and the Precision NRL Lyman-Alpha Humidiometer.

THE FABRY-PEROT REFRACTOMETER[1]**

The Fabry-Perot refractometer is similar to the conventional Pound stabilized refractometer except that it uses a much faster sampling cavity. This new resonator (Figs. 1 and 2) consists of two equal radii spherical caps hollowed from 1-inch-thick aluminum plates. These concave reflecting surfaces

*U. S. Naval Research Laboratory, Washington, D. C.
**Numbers in brackets denote References on page 193.

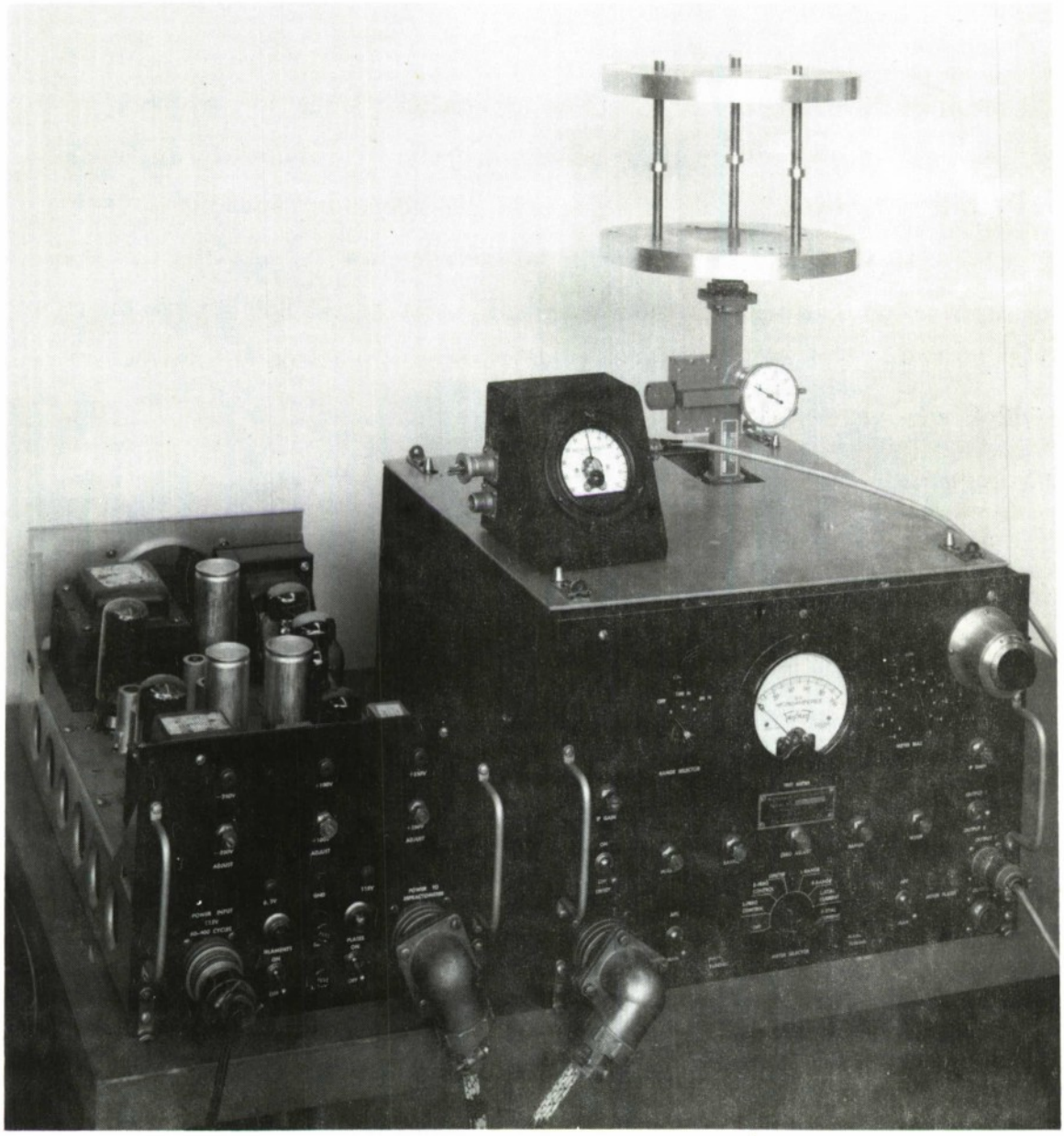

Fig. 1. Fabry–Perot Refractometer

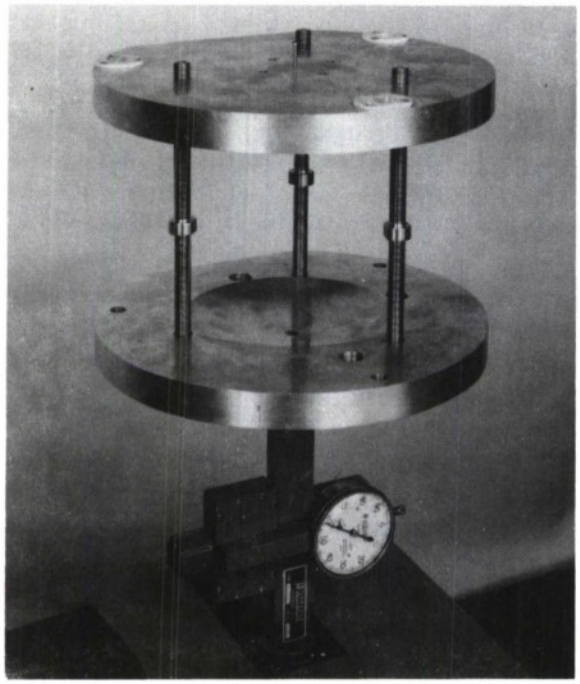

Fig. 2. Open-Sided Spherical Cavity Resonator

of 7 inches radii of curvature are spaced 5.5 inches apart by three alloy rods (Weinschel LA 685). Unlike the cylindrical (TE01) cavity, this cavity has no perforated end-plates to slow down the ventilation rate and to introduce errors in refractive index resulting from dynamic temperature and pressure changes in the measured sample. The selection of spherical surfaces over parabolic or plane surfaces was made because of the relative insensitivity of Q and frequency to lateral displacements of the plate axes. This configuration has the advantage that any condensation on the spherical surfaces will be rapidly removed by the air flow across the surface. In addition, corrosion of the surface has a minimal effect on cavity Q and manifests itself primarily in a long-term frequency drift of the resonator. For this reason it is not necessary to gold or silver plate the reflecting surfaces to obtain high Q as in the case of the cylindrical

cavities. The loaded Q of this aluminum cavity is about 10,000, which is comparable to the conventional cylindrical cavity. Accurate data is not yet available to state the affect of temperature on the performance of the cavity, though preliminary measurements indicate compensation to within ± 2 N-units over the range -20°C to +40°C. This variation will not adversely affect the use of the instrument for the study of fast refractive-index changes measured from an aircraft.

THE PRECISION NRL LYMAN-ALPHA HUMIDIOMETER[2]

The Precision NRL Lyman-Alpha Humidiometer is an improvement over the basic instrument described in the International Symposium on Humidity and Moisture, held in Washington, D. C., May 20-23, 1963, and in "The Report of NRL Progress," June 1963, in that an alternating-current recording channel has been added for recording fast fluctuations between 5 to 100 cps.

The block diagram in Fig. 3 shows the principal parts of the basic instrument. When energized by the high-voltage power supply, the hydrogen lamp emits Lyman-alpha radiation at 1216 A which passes through the lithium-fluoride window in the lamp, across a measuring path, and through a lithium-fluoride window of the detector tube which is filled with nitric-oxide gas. By photoionization processes, the radiation from the hydrogen lamp causes a current to flow in the detector tube which is connected to an electrometer, a metering circuit, and a recording system. This current is a logarithmic function of the water vapor density in the measuring path. The absorption coefficients of the different atmospheric gases at Lyman-alpha have been mentioned in previous papers[2] and will not be repeated, except to mention that there is a window which permits selective absorption of water vapor.

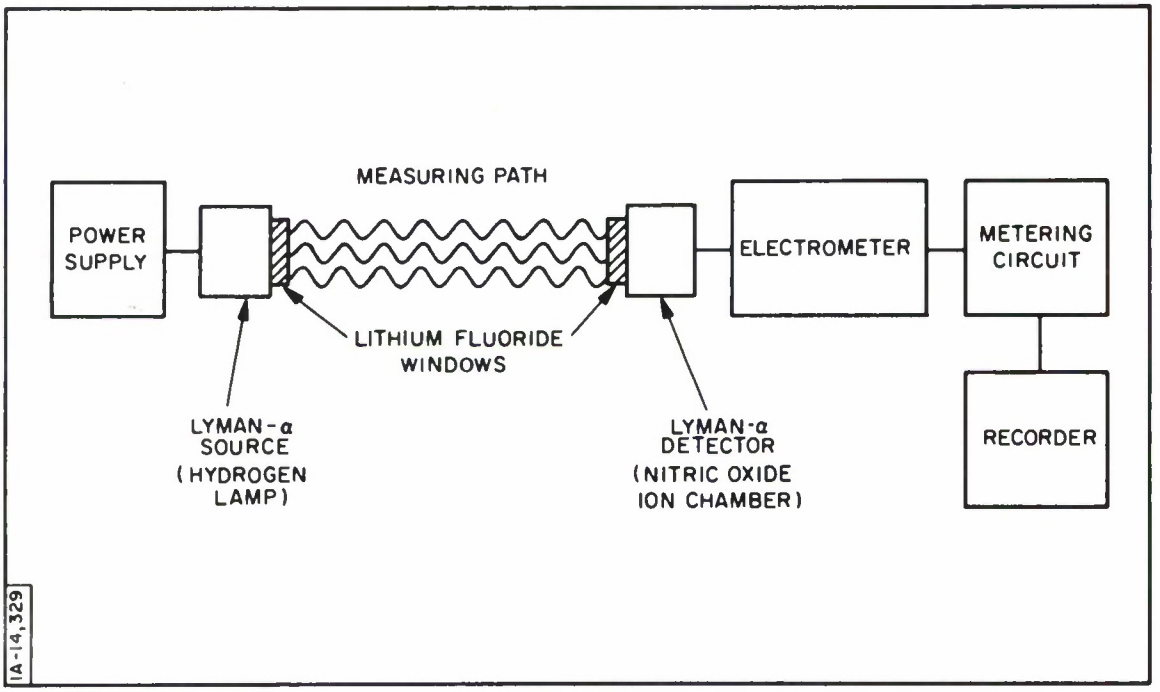

Fig. 3. NRL Lyman-Alpha Humidiometer (Block Diagram)

Figure 4 illustrates the basic humidiometer components shown in Fig. 3. The hydrogen lamp is mounted opposite the nitric-oxide ion chamber and potted electrometer with a plastic spacing block between them. For the humidiometer used in the measurements we shall later discuss, the measuring path spacer block is 3/4 inch and the air intake diameter is 5/8-inch.

Figure 5 is a view of the probe in which this unit is mounted. The probe is then attached to the side of the aircraft redome. From the outside of the radome surface to the air intake is 12 inches for this particular probe. The connections on the base of the probe are for the hydrogen lamp power, the power to the electrometer, and the output of the electrometer.

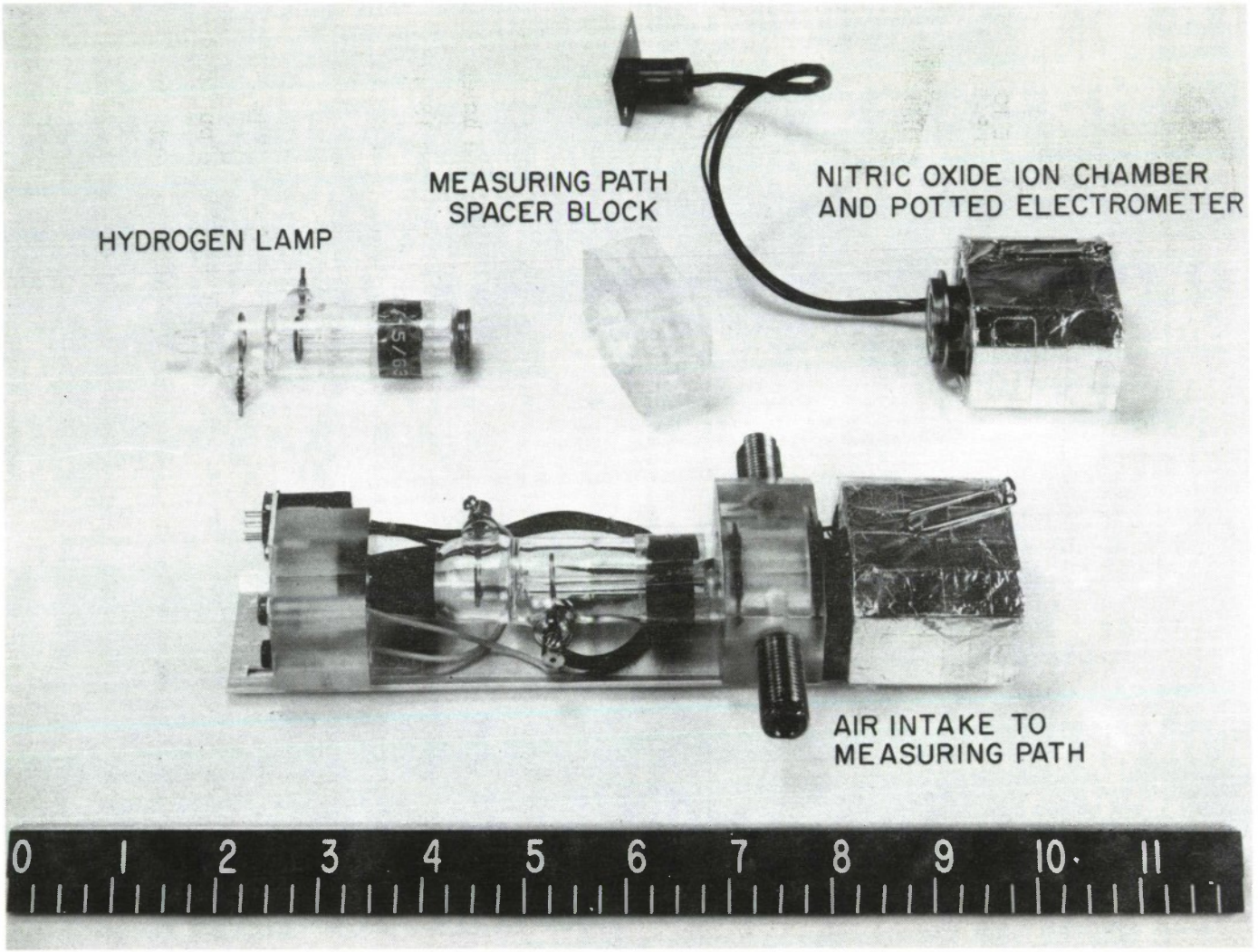

Fig. 4. Components of Humidiometer

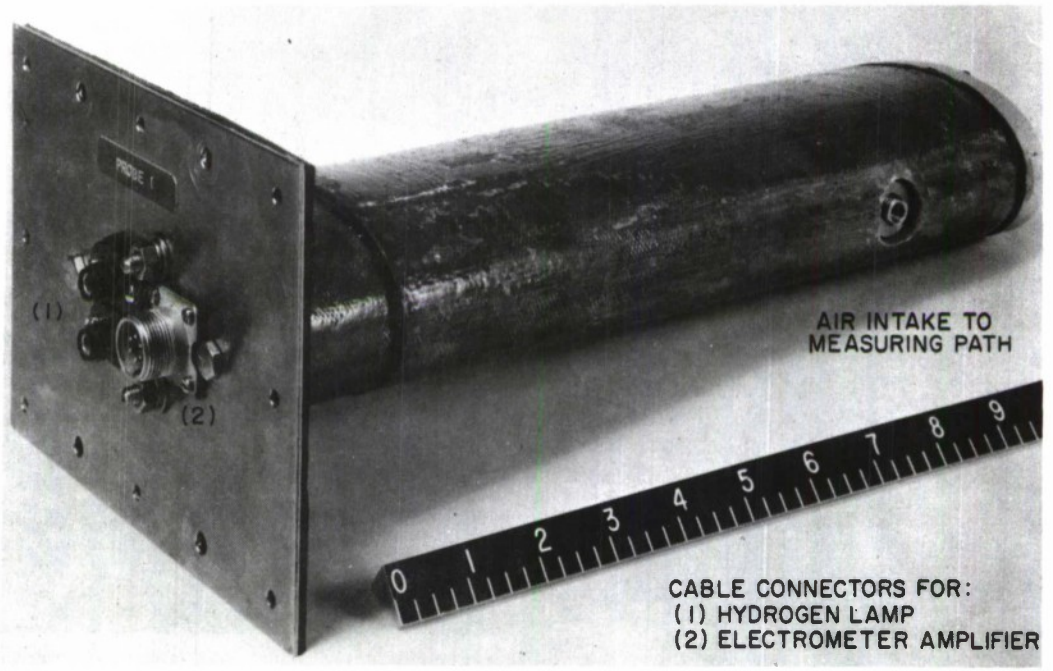

Fig. 5. Humidiometer Probe Assembly

Figure 6 shows two of these probes mounted on the top radome of a Navy Lockheed Constellation aircraft. The distance between the air-intake holes of the two humidiometers is 6 feet. The air intake of the top probe is 18 inches from the outside of the radome. This places the two air intake holes in a vertical line. Figure 7 is a forward view of the two humidiometer probes.

Figure 8 is a schematic diagram of the humidiometer. Tube V5 is the hydrogen lamp, and tube V4 is the nitric-oxide ion chamber. The output of the ion chamber is dropped across a 4.7×10^9 ohm resistor in this circuit. In order to achieve faster time response in the electronics, this resistor has been changed to 1.0×10^9 ohms. The cathode follower electrometer output goes to a logarithmic amplifier and then to the recorders. Tube V7 is used to control the current flowing through V5. For frequency calibration of the humidiometer,

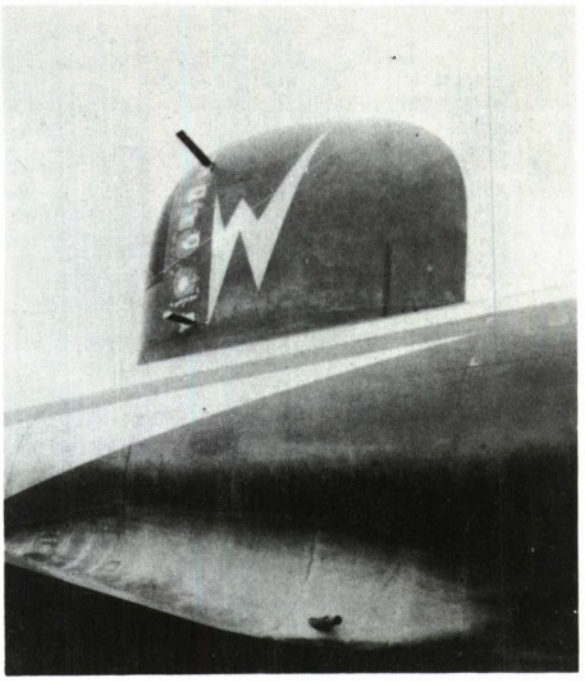

Fig. 6. Humidiometer Probes Mounted on Radome

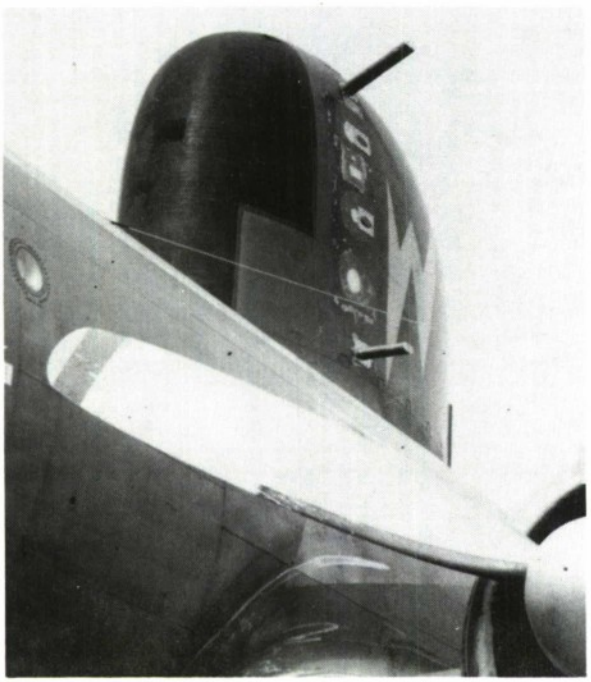

Fig. 7. Forward View of Probes Mounted on Radome

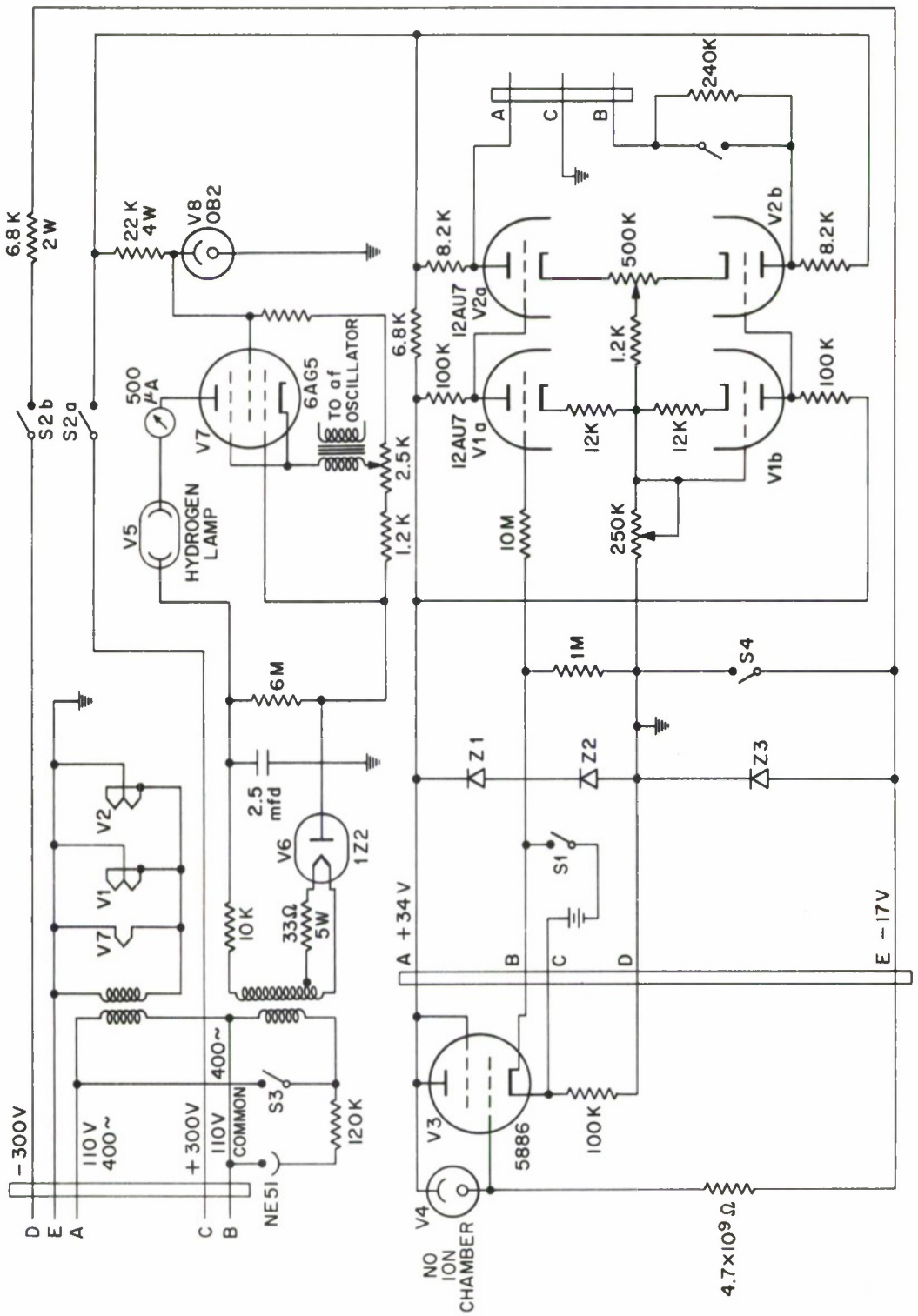

Fig. 8. Schematic Diagram of Humidiometer

the secondary of an audio frequency transformer is connected in series in the cathode circuit, and a signal generator is used to modulate the hydrogen Lyman-alpha beam received by the nitric-oxide ion chamber.

Figure 9 shows the basic humidiometer components plus the recording system. The DC recording system is a presentation on a photoelectric Visicorder. The AC recording system consists of an audio-signal generator, a variable-gain amplifier, a chopper, and a tape recorder. The magnetic tape is played into a Packard-Bell 250 computer.

DC Recording System

The DC recording system makes it possible to get absolute values for plotting soundings as is customarily done for refractive index, temperature, and humidity. Figure 10 presents a portion of mission 12. Here you see plots of temperature, dew-point temperature, total-refractive index, and moist-refractive index. In this case, the dew-point-temperature curve is used to compute the moist-refractive-index values. Notice that the differences in the moist-refractive index are slightly greater than for the total refractive index measured with the refractometer. This is probably due to the fact that in a layer of increasing temperature, the temperature term of the refractive-index equation subtracts from the moisture term. The DC recording channel will observe changes in refractive index and moisture to the order of 10 cps.

AC Recording System

As shown in the block diagram (Fig. 9), a capacitor blocks the DC from the AC channel. This cut off frequency is about 1/2 cps. The AC channel is designed to cover a range from 1/2 to 100 cps. This makes it possible to sense refractive-index fluctuations heretofore unmeasurable by our system. The moist component of refractive index is the dominant term in the refractive-index

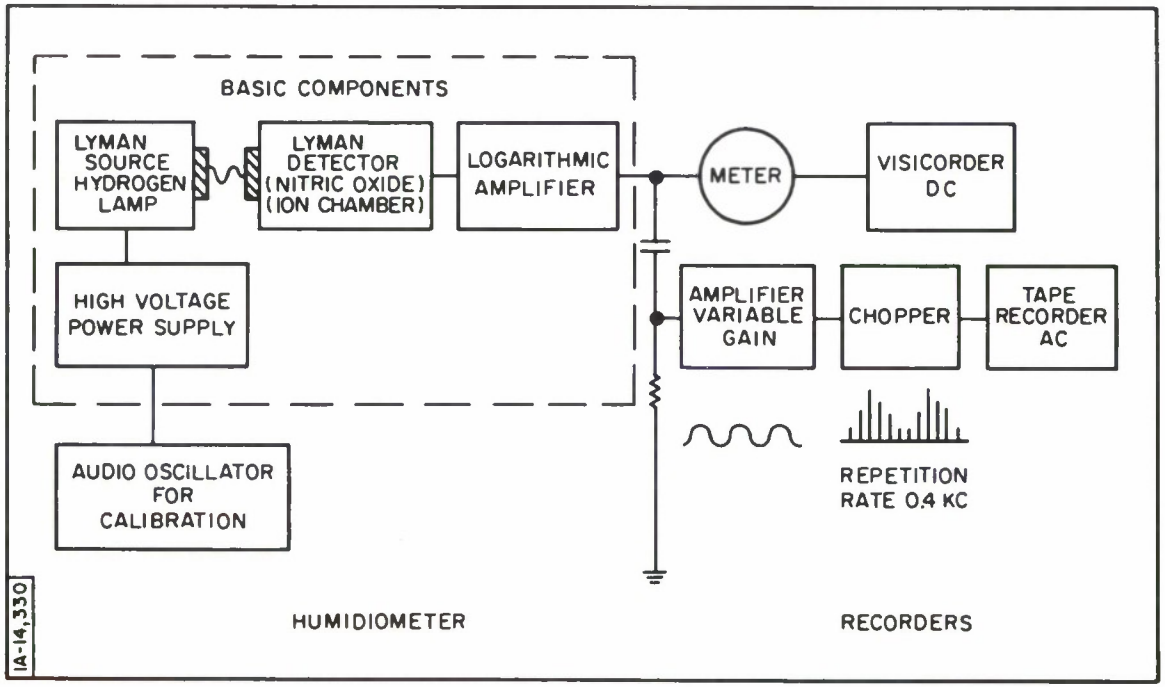

Fig. 9. NRL Lyman-Alpha Humidiometer and its Recording System

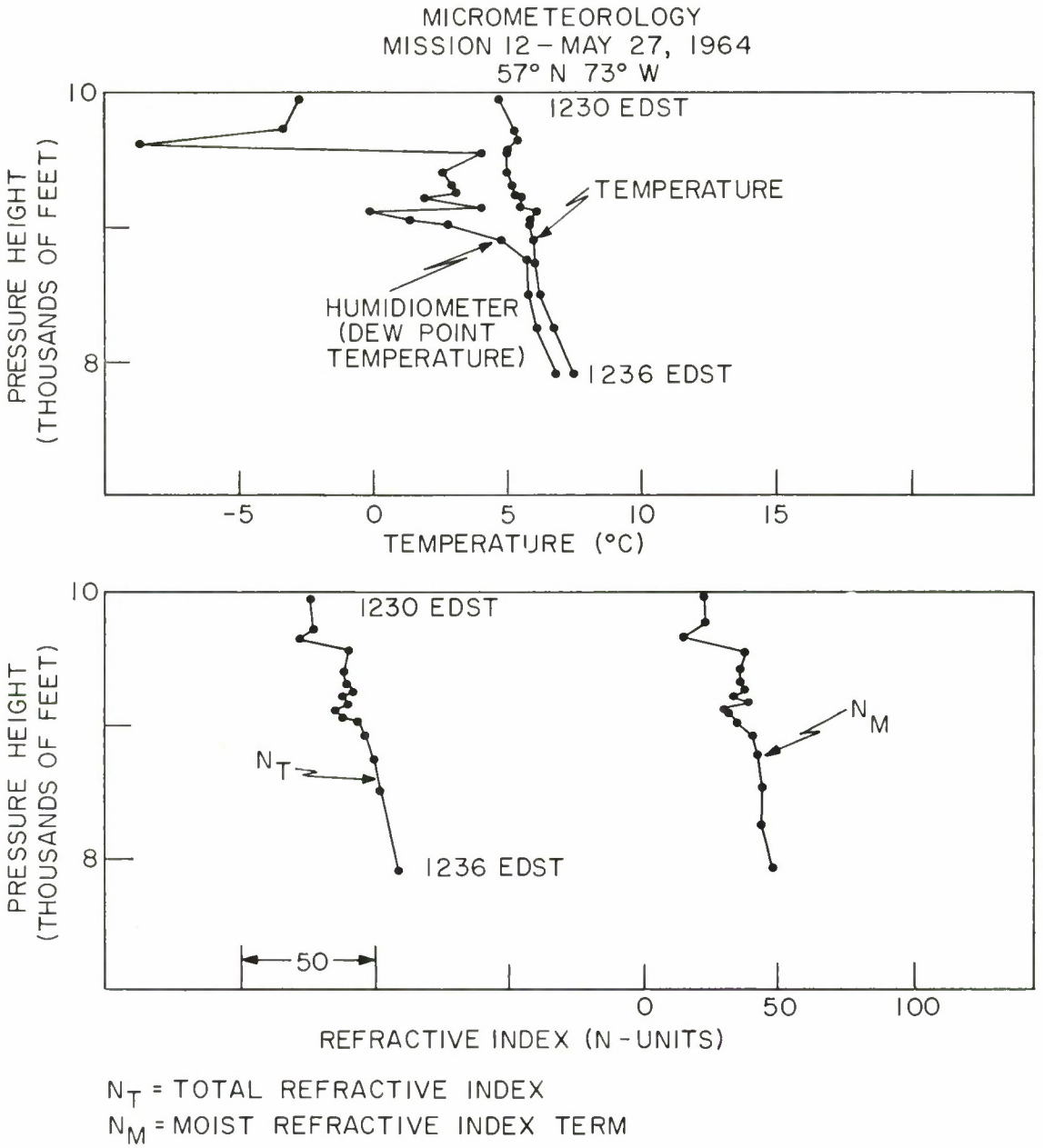

Fig. 10. Sample DC Record from Sounding

equation, having a weight of 4.14 for a 1-millibar change in water vapor, while the temperature term has a weight of -0.89 for a 1-degree change in temperature over the same height interval. Of course, this presupposes an atmosphere of 1000 millibars total pressure, a temperature of 300°K, and a water vapor pressure of 10 millibars.

Figure 11 depicts a typical humidiometer calibration curve made with a humidiometer having a measuring path of 3/4 inch and a drop resistor of 1×10^9 ohms. The slope of this curve between 2 to 10 millibars is 13.9 microamperes

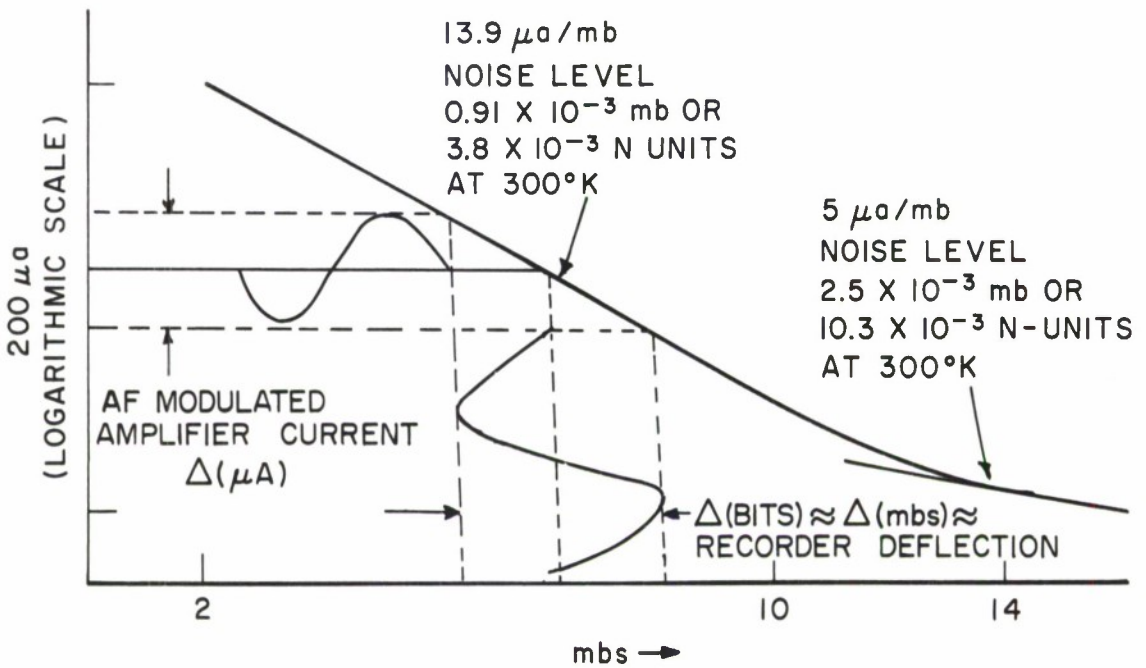

Fig. 11. Typical Humidiometer Calibration Curve

per millibar. Above 10 millibars there is a knee in the curve, and at 14 millibars, the slope has lessened to 5 microamperes per millibar. At 7 millibars, in the straight portion of the curve, the noise level is 0.9×10^{-3} millibars, or

3.8×10^{-3} moist N-units at 300^{o}K. At 14 millibars the noise level is 2.5×10^{-3} millibars or 10.3×10^{-3} moist N-units at 300^{o}K. These are the basic sensitivity values for this type humidiometer. The sensitivity can be increased by increasing the value of the drop resistor, but this increases the time constant so that high frequencies cannot be measured.

Figure 11 also presents the method of calibrating the water-vapor variation indicated by the system. The Lyman-alpha source is modulated by a 10-cps sine wave of fixed amplitude in microamperes. The tape recorder shows this variation in bits (1 volt equals 62 bits) which are directly proportional to the amplitude of the sine wave. The calibration curve is then used to convert this output to a fluctuation in millibars of water-vapor pressure.

With the basic sensitivities quoted, it is possible to amplify the incoming signals so that they will always fall within the 0- to 2-volt input range of the tape recorder. Four gain steps are provided so that weak signals can be amplified to fit the capabilities of the input to the tape machine.

Figure 12, curves No. 1, No. 2, No. 3, and No. 4, displays the modulating frequency at different gain settings. To keep the output of the amplifier within the 2-volt range of the tape recorder it is necessary to attenuate the input of the hydrogen lamp. In curve No. 1 of Fig. 12, the amplifier is set for gain position 1. Notice that there is very little noise on the envelope of the sine wave. For this setting, 0.3 millibars equals 1.2 moist N-units, or 62 bits. In curve No. 2 of Fig. 12, there is a slight increase in noise superimposed on the 10-cps modulating frequency with the amplifier set in gain position 2. For this position, 0.15 millibars equals 0.62 moist N-units, equals 62 bits. Curves No. 3 and No. 4 of Fig. 12 describe the same type of information. In curve No. 4 of Fig. 12, it is very obvious what would happen if the noise equaled the amplitude of the incident signal.

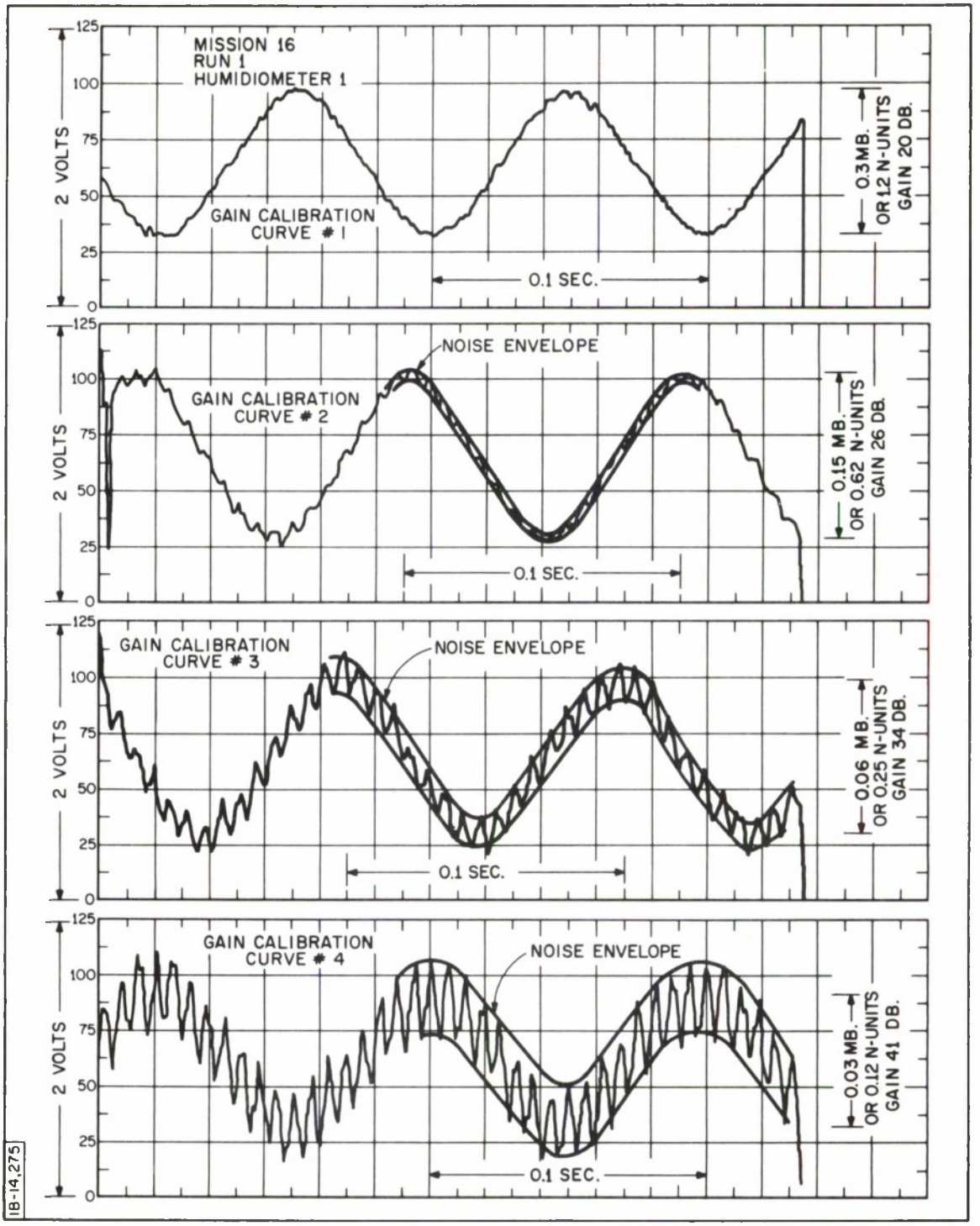

Fig. 12. Gain Calibration Curves

Figure 13 presents the frequency response of the system in terms of the amplitude at 10 cps, which is 100 percent.

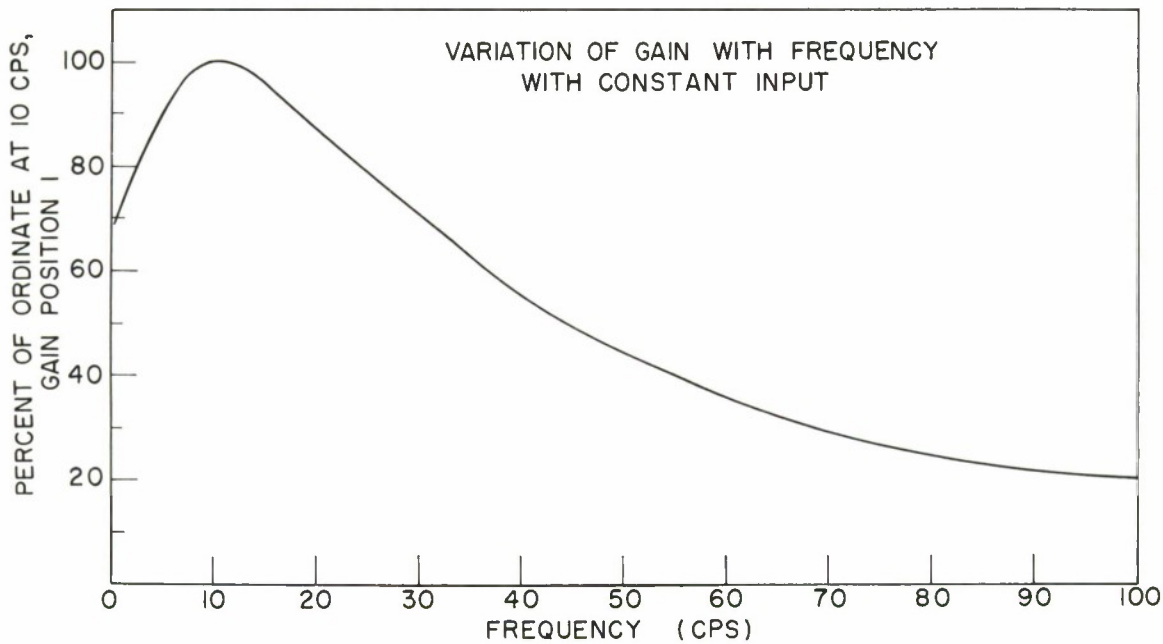

Fig. 13. Variation of Gain with Frequency

Some Experimental Results

Now that humidiometer calibration procedures have been worked out for both the DC and AC channels some measurements will be considered.

On Mission 16, made July 7, 1964, the aircraft was slowly descending through the top of a haze layer. The zone of greatest change was between 8550 to 7880 feet, a layer 670 feet thick. The refractive index gradient as measured by the refractometer was 52 N-units/1000 feet, and the temperature gradient was + 2.7^{o} C/1000 feet. The oscilloscope presentations for the two humidiometers

were fluctuating in unison as they normally do, but then a layer was encountered at 8250 feet in which the oscilloscope presentations of the probe fluctuations were out of phase.

The right-hand portion of Fig. 14 is a sketch of what was seen on the oscilloscope. Part of the time the two presentations were 180 degrees of arc out of phase. This condition lasted intermittently for about a minute, and then,

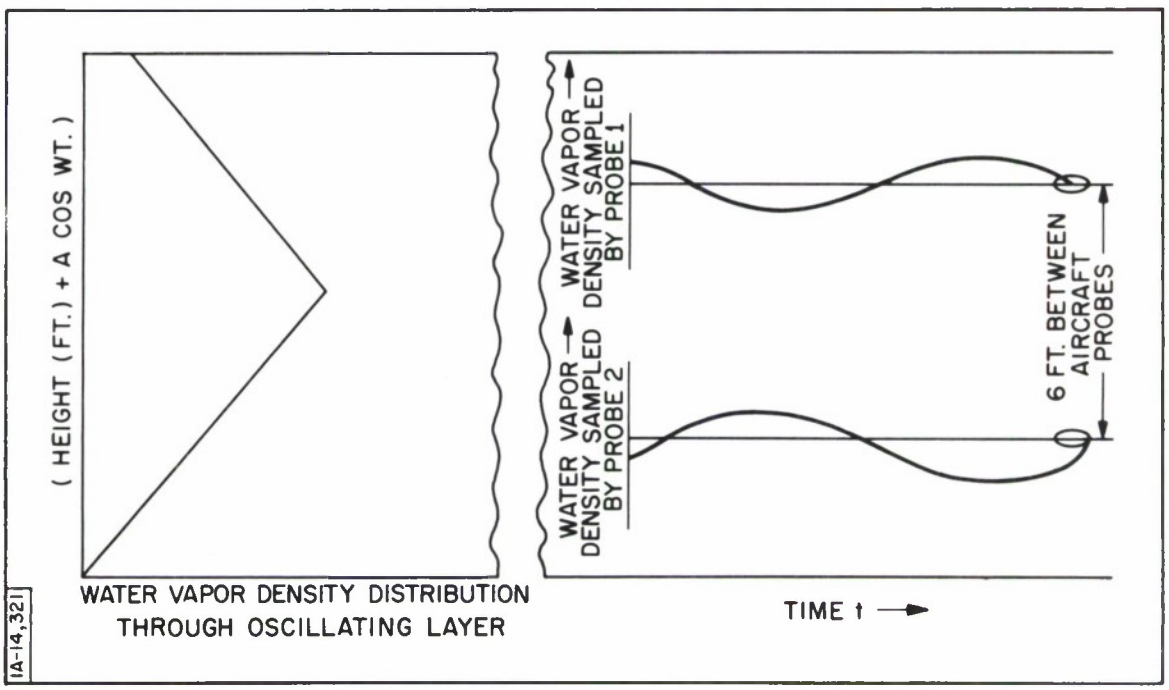

Fig. 14. Out-of-Phase Variation of Humidiometer Probe Sensors

as the aircraft lost altitude, the humidiometer fluctuations were in unison again. When the aircraft ascended, the layer was found, and the fluctuations were still out of phase. This lasted for nearly 5 minutes.

The left-hand portion of Fig. 14 is a possible explanation of this phenomenon. Suppose that there was a filament-like layer of moisture below which the moisture gradient was increasing, and above which the moisture was decreasing. Suppose also that this layer had travelling waves of a sinusoidal form. This would then account for the out-of-phase variation of the two humidiometers. This would mean that the filament must be very thin because the probes are only 6 feet apart.

To get more information about this phenomenon, a portion of this record was printed out by the PB-250 computer and some actual values measured. This is shown in Fig. 15. The assumption was made that the mean water vapor density of the fluctuations for either probe was the same. Then by using the gain and frequency calibrations described in Fig. 12, moist values of refractive index

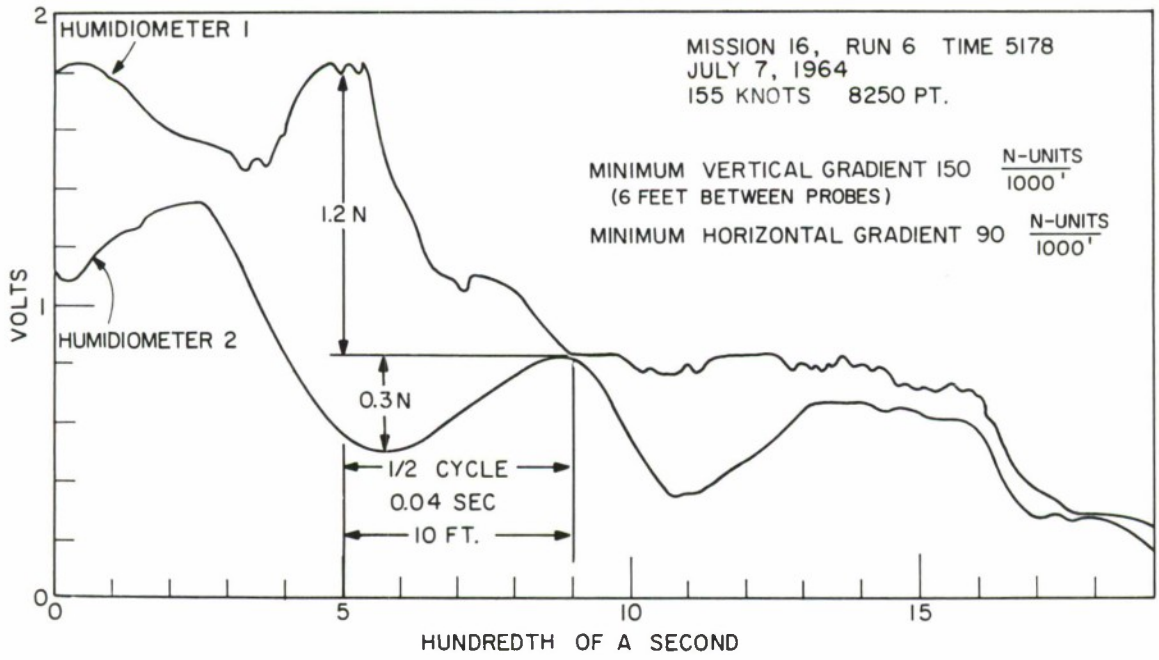

Fig. 15. Dimensions of a Microcell of Moisture

were assigned to the deflections. Consider the half cycle between 5 and 9 hundredths of a second. For humidiometer 1 there was an excursion of 1.2 N-units, and for humidiometer 2 there was an excusion of 0.3 N-units. Now if the lower probe was in a region where the refractive index gradient was increasing, and the upper probe in a region where the refractive index gradient was decreasing we have a minimum refractive index gradient of 0.9 N-units/6 feet or 150 N-units/1000 feet. By knowing the horizontal speed of the aircraft we can compute a minimum horizontal gradient of 90 N-units/1000 feet. Of course, one microcell of moisture in itself does not mean much, but when there is a thin layer covering many square miles with variations of refractive index as noted in this cell, then the problem becomes more meaningful.

Figure 16 is a power spectra of a 6-second sample made 233 seconds before the measurements shown in Fig. 15. The magnitudes of the cells are

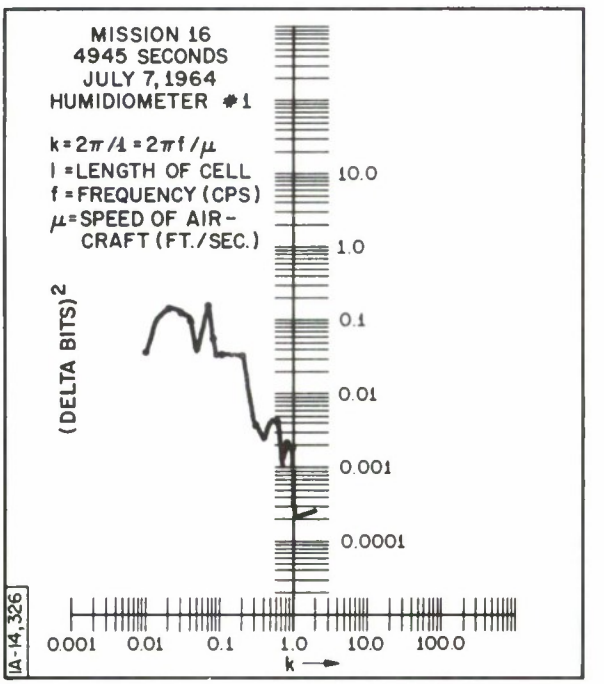

Fig. 16. Power Spectra of Moisture Fluctuations

read from the abscissa. Consider the maximum for k equal to .08. This states that the size of the cells at this particular maximum were 78.54 feet. Consider the maximum at k equal to 0.8. This gives a cell size of 7.8 feet.

The ordinate in Fig. 14 is (delta bits)$^{[2]}$. In Fig. 12, the gain calibration curves show the equivalent of bits in moist refractive index units. This 6-second sample was made on gain position 2. Using this information, the delta N in moist refractive index units was about 6.1×10^{-3} for the 78-foot cell, and 1.3×10^{-4} for the 7.8-foot cell. These are horizontal gradients made from one humidiometer. The sample from which these illustrations are computed was 6 seconds in length and covered a horizontal distance of about 1500 feet.

CONCLUSION

The results cited above are a beginning of things to come. The Fabry-Perot Refractometer when calibrated and tested will be recorded on the visicorder and the tape recorder in the same manner as the two humidiometer probes. The tape recording technique and the Packard-Bell 250 computer make it possible to print out fast fluctuations of the instrument up to 100 cps which were heretofore not discernible from the visicorder record, and to make power spectra of samples of 3 or 6 seconds in length.

So far the humidiometer is a fair weather measuring instrument because it loses sensitivity for water vapor pressure above 8 millibars. Plans are under study for making an all-weather humidiometer.

The object of the fast response instrument development program is to make studies of microcells in all types of weather conditions so that the meteorologist will have some basis for forecasting radio scattering conditions from a weather map and meteorological soundings of temperature, dew point, and refractive index.

REFERENCES

1. Zimmerer, R.W., et al., "Millimeter Wavelength Resonant Structures, IEEE Transactions on Microwave Theory and Techniques," Vol. MTT-11, Number 2, pp. 142-149, March 1963.

2. Randall, D.L., Hanley, T.E., and Larison, O.K., "The NRL Lyman-Alpha Humidiometer," "Report of NRL Progress," pp. 1-13, June 1963.

INSTRUMENTATION FOR LOWER TROPOSPHERIC SOUNDINGS OF REFRACTIVITY

D. R. Hay*

This paper describes one aspect of our tropospheric refraction studies at the University of Western Ontario. We are concerned with special instrumentation for sounding the lower troposphere. The region of interest lies between the ground and 3000 feet above, the so-called layer of frictional influence.

The motivation for this work stems from our research on radar angels. These are clear-air reflections which are observed on sensitive microwave radars. We have been studying microwave angels for several years with a special 7000-mc radar which has two 10-foot antennas spaced 15 feet apart and pointing in the vertical direction. Our attempts to interpret the anomalous clear-air reflections lead us to conclude that they arise from very thin strata of contrasting temperature and humidity injected into the environment.[1, 2]** Further, it appears that they must be of the order of radar wavelength in depth. This means that we are looking for changes in refractivity of the order of one or two parts per million, through a vertical height interval of only a few centimeters. This type of structure may be related to turbulence and other well-known weather features.

Direct evidence of air microstructure with this degree of fineness is very meager. Instruments which will measure temperature and water vapor pressure with sufficient precision and time or spacial resolution are generally not

*University of Western Ontario, London, Canada.
**Numbers in brackets designate References on page 205.

commercially available. We have been working on a program on instrument development to aid us in obtaining these measurements for some time.[3, 4, 5, 6]

The measurements are made from a ground station which is adjacent to our microwave radar, and which permits the same volume of air to be examined simultaneously by different techniques. Two types of instruments are used. One is a smoke generator in the nose of a rocket which deposits an instantaneous vertical column that is studied for wind shear. The second instrument is a combination which measures air refractivity and air temperature simultaneously, with a rapid speed of response and a high degree of spatial resolution. The information from these instruments will be used not only to deduce the detailed profiles of temperature and water vapor pressure, but also to obtain the local Richardson numbers to describe the regime of turbulence in this lower part of the troposphere.

The remainder of my talk will be on the details of these instruments. Figure 1 shows the rocket-borne smoke generator which deposits the vertical smoke trail. The rocket vehicle commercially known as a "Cricket," is propelled by carbon dioxide in both liquid and gaseous form. The launching device is readily portable. It will be seen that the man on the left is holding a launching tube extension, which is about 10 feet long. After launch, the rocket vehicle ascends for about 12 seconds and then turns over to begin its descent under parachute. Figure 2 shows the nose cone being fitted into the rocket vehicle. This smoke generator is not commercially available; it is similar to one described and used by Gill at the University of Michigan.[7] Figure 3 is a close-up of the smoke-depositing nose cone. It is 10 inches in length and has a pressure chamber, in the upper-half, for gaseous carbon dioxide at 70 psi. The clear lower section contains titanium tetrachloride which is ejected through fine nozzles to produce titanium oxide when in contact with moisture in the air.

Fig. 1. Cricket Rocket Being Lowered into the Launching Tube

Fig. 2. Fitting the Nose Cone on the Rocket Vehicle

Fig. 3. Smoke-Generating Nose Cone

It is necessary to perform two tasks after the ascent of the rocket, as shown by Figs. 4 and 5. Since the rocket is recoverable and reusable, the impact point must be determined by tracking the rocket during descent. This is done with the aid of an optical range finder at the launching site and an astro-compass at a remote location (see Fig. 4). The second task involves photographic recording of the smoke trail during its 10-second lifetime. Two cameras are used for this purpose. One is a photo-theodolite with a telephoto lens to observe fine details in the trail deformation. The other has a wide-angle lens; here the film advances at 1-second intervals to record the time sequence in the position of the whole smoke trail. These cameras are located normal to the plane of drift of the trail as determined from a preliminary pilot balloon ascent. Figure 5 shows the two cameras at a field site.

Fig. 4. Optical Ranging Instruments

Fig. 5. Photographic Equipment for Observing the Smoke Trail

The second instrument for airborne soundings measures air temperature and refractivity simultaneously. It is launched on a manner similar to a standard radiosonde, with balloon and parachute (see Fig. 6). It will be seen that the trailer contains a winch for controlling the height of ascent; the ascent rate normally is about 1000 feet per minute. The response of the instrument is adequate to follow changes in temperature or refractivity within a height of interval of only a few centimeters. Figure 7 shows the mobile ground station with a 4-foot paraboloid antenna on its roof for receiving and recording the signal from the airborne instrument.

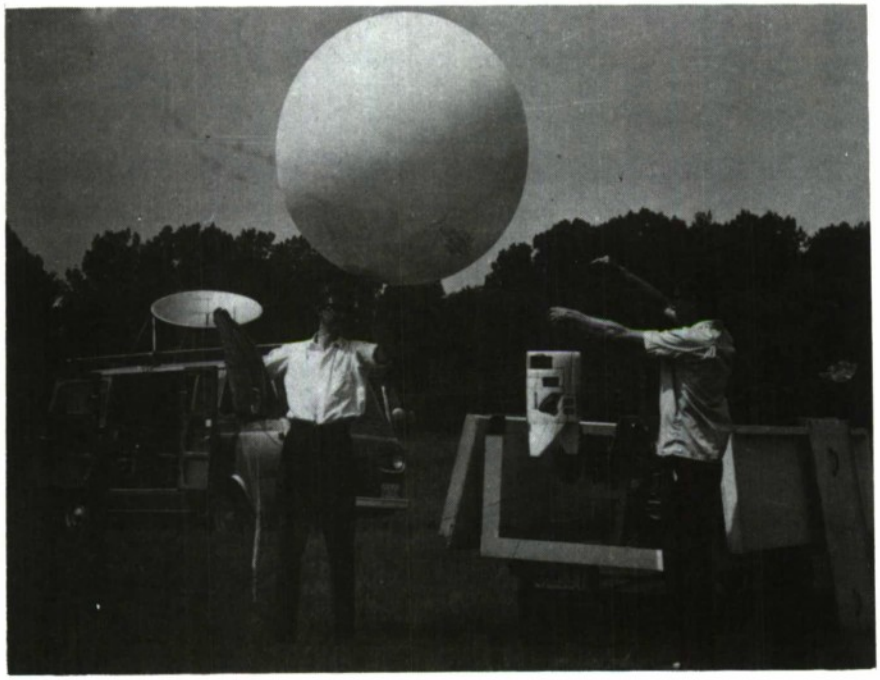

Fig. 6. Launching the N-T Sonde

Fig. 7. Recording-Receiver Van

Two views of the N-T sonde are found in Figs. 8 and 9. This device weighs about 4 pounds and is built in modular form. It contains two 400-mc transmitters; one carries the temperature information and the other the refractivity modulation. The section above the transmitters contains the temperature sensor, which uses a very fine element of platinum wire. It can detect changes in temperature of a fraction of a degree with a response time of one millisecond. At the top is the capacitor-type (Hay) refractometer. The sensing element is a ring-type air capacitor with a vertical depth of 1 cm. for the desired spatial resolution. All of the circuits of this dual instrument have been transistorized, with the exception of the 400-Mc transmitters.

Figure 10 is a block diagram of the N-T sonde. The upper section represents the refractometer circuit; the lower section, the temperature circuit, and the middle, a common control circuit. The air capacitor on the left which is the

Fig. 8. N-T Sonde, Side View

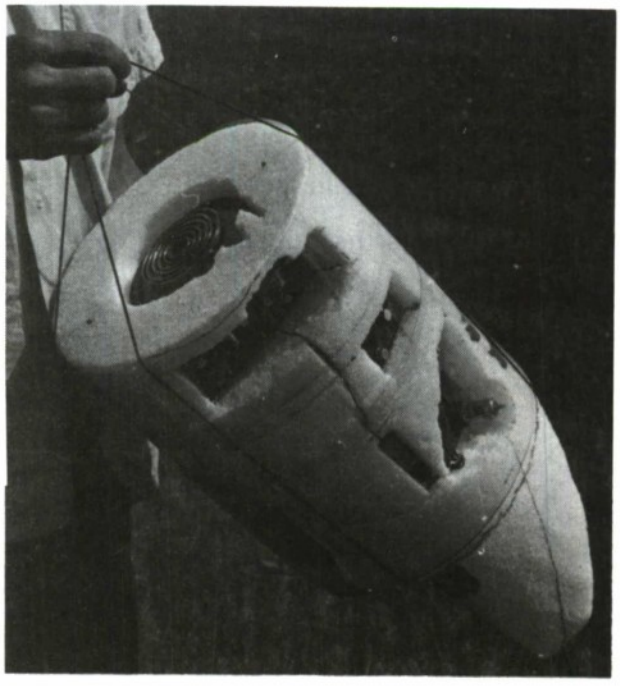

Fig. 9. N-T Sonde, Showing
Refractometer Sensing Capacitor

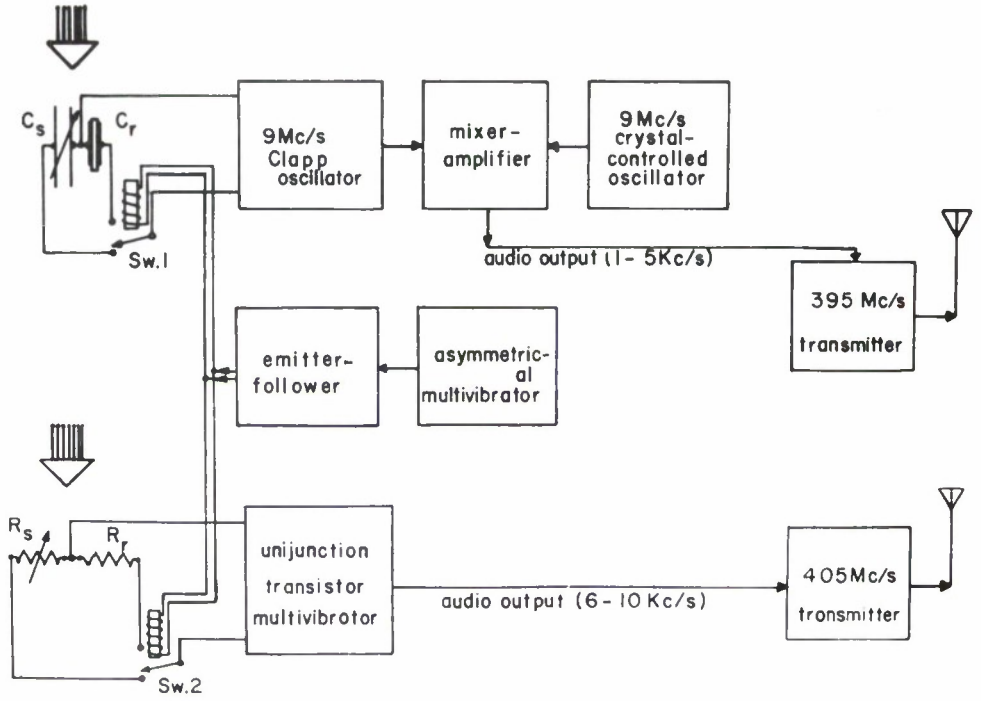

Fig. 10. Block Diagram of the N-T Sonde

refractivity-sensing element, forms part of the resonant circuit of a 9-mc Clapp oscillator. Changes in this capacitance, which are due to changes in the dielectric constant of the air passing through it, result in variation of the oscillator, and the audio difference output used to modulate one of the 400-mc transmitters. The temperature sensing element is platinum resistance wire, having a diameter of 2.5 microns. It is part of the circuit of a unijunction transistor multivibrator. The output of this circuit also is an audio signal which is used to modulate the second 400-mc transmitter. In each case, the sensing element is replaced periodically by a reference element, for a brief interval, for calibration purposes. *

*The calibration includes temperature compensation of the sensing element for the ambient air temperature. It should be noted that the simplicity of construction has been an important factor in the design of the N-T sonde, and that circuit complexity is similar to that of the conventional radiosonde. This suggests its possible use as an expendable instrument.

At present, we are studying the photographic techniques for smoke-trail observation, and the calibration of the refractometer sensor. Examples of the temperature profile in the lower troposphere that were obtained with the temperature sonde are shown in Fig. 11; the small fluctuations superimposed upon the slowly varying background are apparent.

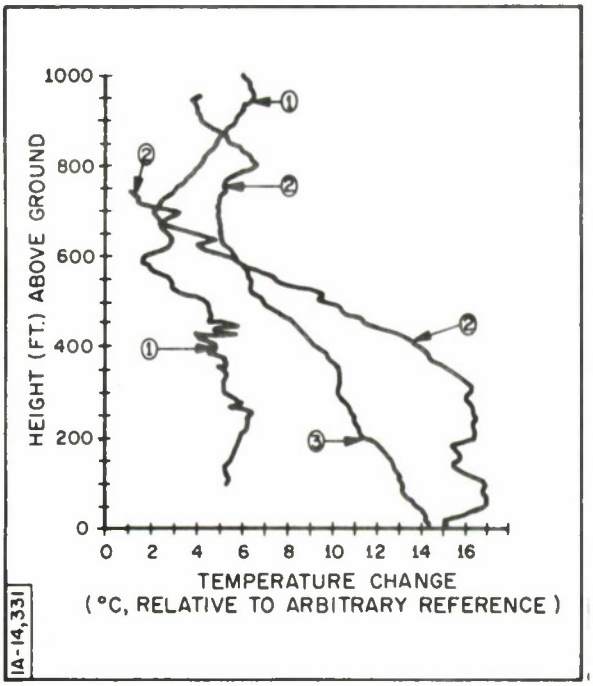

Fig. 11. Profiles of Air Temperature Obtained with the T Sonde

A number of preliminary soundings with the instruments have been carried out in the field. The separate components have been tested individually, and reports on part of this work have been published elsewhere.[4, 6]

The research and development of the two airborne instruments described in this paper have been supported in part through a subcontract from the Northern Electric Company of Canada, under Contract DDP 9 PC 1-436.

REFERENCES

1. D. R. Hay, W. M. Reid, "Radar Angels in the Lower Troposphere," Can. J. Phys., 40, 128, Jan. 1962.

2. M. B. Bell, D. R. Hay, R. W. Johnston, "Observations Upon Clearair Stratification in the Lower Troposphere," Can. J. Phys, 42, 273, 1964.

3. D. R. Hay, H. C. Martin, H. E. Turner, "A Light-weight Refractometer," Rev. Sci. Instrum., 32, 693, June 1961.

4. H. E. Turner, D. R. Hay, "Fine Structure of Temperature and Refractivity in the Lower Troposphere," Can. J. Phys., 41, 1732, Oct. 1963.

5. D. R. Hay, F. H. Fanaki, "An experimental Technique for Studying Reflection Coefficients of Tropospheric Inhomogeneities," Can. J. Phys., 41, 563, 1963.

6. D. R. Hay, H. E. Turner, "Refractometer Measurements at High Relative Humidities" Proc. Int'l Symposium on Humidity and Moisture, Washington, 1963 (in publication).

7. G. C. Gill, E. W. Bierly, J. N. Kerawalla, "An Inexpensive Rocket Technique for Obtaining Low Level Wind Profiles" J. Appl. Meteorol. 2, 457, 1963.

BIBLIOGRAPHY

L. J. Galbiati

This listing is an extension of the Bibliography which appeared in the Proceedings of the Second Tropospheric Refraction Effects Technical Review Meeting. * The previous Bibliography contained 409 entries; this listing cites an additional 223 publications.

ESD-TDR-64-103, Volume III.

BIBLIOGRAPHY

Ament W. S. and Katzin M. "Signal Fluctuations In Long-Range Overwater Propagation," IRE Trans. Comm. Sys., Vol. CS-4, No. 1.

Anderson, L. J. Calculator for Atmospheric Refractive Index, U. S. N. Electronic Lab, Rept. No. 279, March 1959.

Anderson, L. J. and Abbott, F. R. The Rapid Reduction of Meteorological Data to Index of Refraction at Radar Frequencies, Navy Electronics Labs, San Diego, Calif., Rept. WP-8, December 1943.

Anderson, W. L. Beyers, N. J. and Rainey, R. J. Comparison of Experimental with Computed Tropospheric Bending, UNM Exp. Sta. Rept. EE28., AD 287 498; Trans. IRE, AP-8 pp. 456-461, September 1960.

Anderson, W. L. and Fannin, B. M. Comparison of Computed with Observed Atmospheric Refraction, UNM Tech. Rept. EE14, AD 203 893.

Anderson, W. and Fannin, B. H. Discussion of Radar Errors Due to Propagation Effects, U. of New Mexico, Tech. Rept. EE16, AD 203 894, August 1958.

Anderson, L. J., Morgan, L. A, Weisbrod, S. and Loucks, H. D. Tropospheric and Ionospheric Radar Refraction Effects, Smyth Research Associates Rept. No. SRA-91.

Anderson, L. J., Trolese, L. G. and Huges, L. R. Refraction Errors in Space Positioning of High Flying Objects, Smyth Research Assoc. Rept. SRA-74, AD 148 887.

Anderson, L. J., Trolese, L. G. and Smyth, J. B. Experimental Determination of Tropospheric Bending Part I & II, SRA-6 SRA-7, April 1956.

Arvola, W. A. Refractive Index Profiles and Associated Synoptic Patterns, Navy Electronics Labs, San Diego, Calif., NEL Rept. 793, AD 143 768, 1957.

Bailin, B. and Colin, L. Tropospheric Refraction Effects on Height-Finding Radars, Rome Air Development Center, AD 208 284, Tech Note 59-1, February 1959.

Barbery, T. B. Correction of Radar Data for Refraction Errors, WSSA Tech. Rept. 22, December 1954.

Barnett, K. M., Bomba, S. J. Heil T. W. and Kirchner, E. K. A Review of the Calculation of Radar Refraction Errors, USAERDAA-MET-7-64, DA Task 1AO-13001-A-039/14, May 1964.

Barnett, K. M. An Objective Procedure for Planning Meteorological Observations Needed to Calculate Radar Refraction Errors, Interim Report, USAERDAA-MET-9-64, DA Task 1-A-O-50212-A-127-01A/01, June 1964.

Bean, B. R. Survey of the National Bureau of Standards Application of Atmospheric Refractivity Measurements to Radio Propagation Studies, NBS Rept. No. 5007, August 1956.

Bean, B. R. A Study of the Three-Dimensional Distribution of the Radio Refractive Index, NBS Rept. 6042, February 1959.

Bean, B. R. "Atmospheric Bending of Radio Waves," Electromagnetic Wave Propagation, (edited by M. Desirant and J. L. Michiels,); (Academic Press,) 1960, pp. 163-181.

Bean, B. R. "Concerning the Bi-Exponential Nature of the Tropospheric Radio Refractive Index," Beiträge zur Physik der Atmosphäre, 34, No. 1/2, January - February 1961, pp. 6-91.

Bean, B. R. "Comparison of Observed Tropospheric Refraction with Values Computed from the Surface Refractivity," Trans. IRE, PGAP, AP-9, No. 4 July 1961.

Bean, B. R. Comparison of Observed Tropospheric Refraction with Values Computed from the Surface Refractivity, NBS Rept. 6753; see Periodical P33, March 1961.

Bean, B. R., Horn, J. D. and Riggs, L. P. Telecommunications Performance Standards: 1. Introduction; 2. Radio Refractive Index Climatology, NBS Memo Rept., DM-83-30-1 & 2, 3 & 4, AD 255 332L and 33L; 334L and 335L.

Bean, B. R. and Dutton, E. J. "On the Calculation of the Departures of Radio Wave bending from Normal," J. Res., NBS, 64D, (Radio Prop.), No. 3, May - June 1960, pp. 259-263.

Bean, B. R. and Dutton, E J. (Nov., 1961). "Concerning Radiosondes, Lag Constants, and Radio Refractive Index Profiles," J. Geophys. Res., 66, No. 11, November 1961, pp. 3717-3722.

Bean, B. R. and Horn, J. D. On the Climatology of the Surface Values of Radio Refractivity of the Earth's Atmosphere, NBS Rept. No. 5559, March 1958.

Bean, B. R., Horn, J. D. and Riggs, L. P. "Refraction of Radio Waves at Low Angles Within Various Air Masses," J. Geophys. Res., 65, No. 4, April 1960, pp. 1183-1187.

Bean, B. R. and Horn, J. D. "On the Average Atmospheric Radio Refractive Index Structure over North America," Beiträge zur Physik der Atmosphäre, 34, No. 1/2, January-February 1961, pp. 92-104.

Bean, B. R. and Ozanich, A. M. Jr. Climatology of the Radio Refractive Index near the Ground for the United States, NBS Rept. 6030, December 1958.

Bean, B. R. and Riggs, L. P. "Synoptic Variation of the Radio Refractive Index," J. Res. NBS, 63 D, (Radio Prop.), No. 1, July - August 1959, pp. 91-97.

Bean, B. R. Riggs, L. P. and Horn, J. D. "Synoptic Study of the Vertical Distribution of the Radio Refractive Index," J. Res. NBS, 63D, (Radio Prop.), No. 2, September - October 1959, pp. 249-258.

Bean, B. R., Thayer, G. D. and Cahoon, B. A. Methods of Predicting the Atmospheric Bending of Radio Waves, NBS Report 6056, May 1959.

Bean, B. R. and Thayer, G. D. (1963). "Comparison of Observed Atmospheric Radio Refraction Effects with Values Predicted Through the Use of Surface Weather Observations," J. Res. NBS, 67D, No. 3, 1963, pp. 273-285.

Becker, G. E., and Autler, S. H. "Water Vapor Absorption of Electromagnetic Radiation in the Centimeter Wavelength Range," Phys. Rev., 70, Nos. 5 and 6, 1946, pp. 300-307.

Bell, M. B., Hay, D. R. and Johnston, R. W. "Observations upon Clear-Air Stratification in the Lower Troposphere," Can. J. Phys., 42, No. 2, 1964, pp. 273-286.

Beyers, N., Hinds, B. and Hoidale, G. An Elevation of Radar Corrective Systems, WSMR MGD Progress Rept. No. 7, June 1959.

Boileau, A. R. Correlation Between Measured Path Function and Relative Humidity, U. of California, Visibility Lab., S10 Rept. No. 59-5 February 1959.

Boudouris, G., "On the Index of Refraction of Air, the Absorption and Dispersion of Centimeter Waves by Gases," J. Res. NBS, (Radio Prop.), 67D, 6, November-December 1963, pp. 631-684.

Braham, R. R. and Harrington, E. Cloud Refractive Index Studies: Part I, Gradient Distributions; Cloud Physics Lab., U. of Chicago, Tech. Note No. 11 March 1958.

Braham, R. R. Jr., Harrington, E. L. and Hoffer, T. E. Cloud Refractive Index Studies: Part II. Use of Distribution of ΔN vs. ΔS for Estimating Mechanical Turbulence, Cloud Physics Lab., U. of Chicago, Tech. Note No. 77, August 1958.

Bremmer, H. Terrestrial Radio Waves, Theory of Propagation, Elsevier Publishing Co., 1949.

Brocks, K., Fengler, G. and Jeske, H. Radiometeorological Papers, Bericht No. 7 (1963) and No. 8 (1964), Institute for Radio Meteorologie and Maritime Meteorologie Univ. of Hamburg, Hamburg, (1963).

Brooks, F. E. Final Report of Radio Results for 1955 Gulf of Mexico Propagation Tests, EERL Rept. 3-21, U. of Texas, March 1957.

Brown, D. C., Bush, N. and Sibol, J. L., Study of the Feasibility of Rocket and Satellite Approaches to the Calibration of Tracking Systems, Air Force Cambridge Research Laboratory, Document No. 64-789, Final Report, 23 October 1963.

Bull, G. Untersuchungen uber Autokorrelations-funktionen von Brechungsindex-Variationen Kleinheubacher Tagungsberichte, 1963.

Bull, G. "Untersuchungen uber Autokorrelations-funktionen von Brechungsindex-Variationen;" will be published in: Gerlands Beitruge zur Geophysik.

Carlson, A. V. Analysis of the Precision of Atmospheric Refractivity Corrections to Radar Tracking Measurements, USAERDAA-MET-8-64, DA Task 1AO-13001-A-039/14, July 1964.

Carr, T. Tropospheric Propagation Study Progress Report for 1955, 56, 57, U. S. Naval Air Missile Test Center, TM Rept. 102, 106, July 1956, May 1957, June 1958.

Chegwidden, R. E. and Wright, S. F. Tropospheric Propagation Study Progress Report for 1958, Point Mugu, Calif., NAMTC TM 60-15, AD 237 801, May 1960.

Cheng, D. K. "Relations Concerning Refracting Surfaces, Wavefronts, and Phase Errors," J. Franklin Inst., Vol. 269, pp. 184-95.

Colin, L. and Engleman, A. An Analysis of the Time and Space Scale Problems in Radio Meteorology, Tech. Rept. No. RADC-TN-57-394, RADC, Griffiss AFB, N. Y., AD 131 392, December, 1957.

Counter, V. A. Propagation of Radio Waves Through the Troposphere and Ionosphere, Lockheed Corp., AD 211 504, December 1956.

Cowan, L. W. Computing the Index of Refraction of the Atmosphere, Colorado Springs, Colo., Air Defense Command Forcast Center, 3rd Weather Group, Tech. paper No. 1, AD 58 892, May 1952.

Cowan, L. W. Interpreting Refractive Index Profiles in Terms of Radar Coverage, Colorado Springs, Colo., Air Defense Command Forecast Center, Tech. Paper No. 3, AD 23 234, October 1955.

Crain, C. M. Atmospheric Refractive Index Measurements, Ph. D. Dissertation, U. of Texas, June 1952.

Crain, C. M. Airborne Measurements of Atmospheric Refractive Index Micro-Variations up to 20,000 ft. MSL over Southeastern Colorado, EERL Rept. No. 5-11, December 1955.

Crain, C. M. Further Airborne Measurements of Atmospheric Refractive Index Microvariations, EERL Rept. No. 5-18, September 1956.

Crain, C. M. Low-Level Overwater Refractive Index and Water Vapor Fluctuation Measurements, U. of Texas, EERL Rept. No. 5-22, March 1957.

Crain, C. M. and Chapman, H. Characteristics of Tropospheric Refractive Index Fluctuations Observed During a 1955 Measurement Program in the Colorado and Florida Areas, EERL 6-12, U. of Texas, AD 79 979, October 1955.

Crain, C. M., Deam, A. P. and Gerhardt, J. R., A Preliminary Study of the Variations in Refractive Index Over a 5000-Foot Height Interval above the Earth's Surface, Univ. of Texas, EERL No. 53, June 1951.

Cramer, H. E., Record, F. A., Tillman, J. E., Vaughan, H. C. Studies of the Spectra of the Vertical Fluxes of Momentum, Heat and Moisture in the Atmospheric Boundary Layer, Annual Report, 15 December 1960, 130 pages, 61 illus.

Cramond, W. R., Leeman, J. E. and Thorn, D. C. Radar Elevation Angle Errors and Refraction Corrections, Univ. of New Mexico, EE-79, AD 287 231, September 1962.

Cramond, W. R. and Thorn, D. C. An Analog Computer for Calculating Atmospheric Density and Refractive Index, UNM Exp. Sta. EE58, AD 287 233, July 1961.

Cramond, W. R. and Thorn, D. C. An Approach to Azimuth Angle Refraction Corrections UNM Tech. Rept. E E72, AD 287 230, April 1962.

Crozier, A. L. Micrometeorological Data Taken over the Arizona Desert, Report No. 386, U. S. Naval Electronics Lab. San Diego, Calif., 5 October 1956.

Dixon, H. M. Study of Refraction Errors in Radar Propagation, White Sands Signal Corps Agency, Tech. Rept. 18A, April 1956.

Dixon, H. M. Microwave Refractive Index Profiles for the Atmosphere over WSPG From Radiosonde Data, WSPG Tech. Rept. 18b, October 1956.

Dixon, H. M. A First Order Approximation Correction of Radar Elevation Angles for Tropospheric Refraction, WSPG Tech. Rept. 18E, January 1957.

Dotts, W. and Miggantz, E. B. Microwave Tropospheric Study-Progress Report for 1959, U. S. Naval Missile Center, Port Nugu, AD 260 025, July 1961.

Duncan, D. B. On the Simultaneous Estimation of a Missile Trajectory and the Error Components Including the Error Power Spectra of Several Tracking Systems, (Preliminary Report given at the Ninth Conference on the Design of Experiments in Army Research Development and Testing), Huntsville, Ala., 23-25 October 1963.

Duncan, D. B., and Carroll, C. L. Jr. Studies in the Simultaneous Estimation of a Trajectory from Several Tracking Systems, No. 1. Estimates of Error Spectra Derived from Estimates of the Spectra of Residuals Technical Staff Technical Memo No. 4, MTV-TM-62-13, Air Force Systems Command, Patrick Air Force Base, Florida, 7 September, 1962.

Durst, C. S. Meteorological Factors in Radio Wave Propagation, Physical Society London and Royal Meteorological Society; Rept. of 1947 Radio Climatology Conf. April 46; Royal Institution. London, 1947, pp. 193-212.

Edmonds, F. N. A Comparison of Observed Amplitudes of Tropospheric Index of Refraction Fluctuations with those from Observed Median Transmission Losses, U. of Texas, EERL 6-27, AD 160 831, August 1958.

Edmonds, F. N. Jr., Bostick, F. X. Jr. and Gerhardt, J. R. Power Spectra Evaluation for Selected Airborne Microwave Refractometer Readings, U. of Texas, EERL 6-24, August 1958.

Edmonds, F. N. "An Analysis of Airborne Measurements of Tropospheric Index of Refraction Fluctuations" Statistical Methods of Radio Wave Propagation, Pregamon Press, 1960, pp. 197-211.

Englemann, A. and Colin, L. Preliminary Study of Tropospheric Microwave Refraction at Rome, N. Y., RADC-TN-57-257, AD 131 187, September 1957.

Epstein, R. A. Analysis of Refractive Index Errors, AF Tech. Rept. No. 2, AFMTC Patric AFB, March 1951.

Ewen Knight Corp., Investigation of a Method for Precision Measurement of Atmospheric Refractive Index at Microwave Frequencies, Doc. No. 862, Contract AF 19(628)-4142, July 1964.

Faulds, A. H. and Brock, R. H. An Analysis of Atmospheric Refraction, Syracuse U. Res. Institute, AD 272 586, March 1960.

Fannin, B. M. Field Strength Determination by Ray Tracing Techniques for Horizontally Stratified Layers, EERL Rept. 6-04, U. of Texas, August 1953.

Fannin, B. M. and Jehn, K. H. Radar Elevation Angle and Range Errors in a Representative Air Mass, U. of Texas, EERL NR7-01, June 1954.

Fine, T. I. and Rodrick, T. L., Global Calibration Study, Appendix 3, TRW Space Technology Laboratories, Doc. No. 4108-6002-RU000, February 1964.

Fukushima, M., Iriye, H., Akita K. and Miura S. "Preliminary Study of Spatial Distribution of Atmospheric Refractive Index from Aircraft Observation," J. of Radio Res. Labs., March 1964, pp. 75-87.

Fukushima, M., Iriye, H. and Akita, K "Spatial Distribution Characteristics of Atmospheric Refractive Index from Helicopter and Kytoon Observation," J. Radio Res. Labs., Vol. 9, No. 45, September 1962, pp. 369-383.

Furry, W. H. Theory of Characteristic Functions in Problems of Anomalous Propagation, M. I. T. Rad. Lab. Rept. 680, February 1945.

Furutsu, K. "Propagation of Electro-Magnetic Waves Over Flat Earth Across Boundary Separating Different Media and Coastal Refraction," J. Radio Res. Labs., Vol. 2, No. 7, January 1955, pp. 1-49.

Freiesleben, H. C. "Refraction Occurring Immediately Above the Water Surface Inter. Hydrographic Rev. Vol. 28, No., 2

Gerhardt, J. R. Measurements and Analyses of Index of Refraction of the Atmosphere, U. of Texas, EERL Rept. 619, March 1957.

Gerhardt, J. R. Errors in the Measurement of Angle-of-Arrival Resulting from Overwater Refraction, U. of Texas, EERL Rept. 3-01, July 1951.

Gerhardt, J. R. (Editor) Summary of the December 1957, Radar Refraction Meeting, U. of Texas AD 154 629, EERL Rept. 97, January 1958.

Gilmer, R. O., Cramond, W. R. and Byrd, M. R. Survey of Papers on Tropospheric Refraction, Tech. Report EE-86, February 1963.

Gifford, F. "The Relation Between Space and Time Correlations in the Atmosphere," J. Meteor, 13, 1956, pp. 289-294.

Gjessing, D. T. Determination of Permittivity Variations in the Troposphere by Scatter-Propagation Methods, IEE (England) Monograph No. 510E, 1962; also Proc. IEE, Part C, 109, 447.

Gjessing, D. T. "An Experimental Study of the Variation of the Tropospheric Scattering Cross Section and Air Velocity with Position in Space, " IEEE Trans., PTGAP, AP12, No. 1, 1964.

Gjessing, D. T. "Determination of Isotropy Properties of the Tropospheric Permittivity and Wind Velocity Fields by Radio-Propagation Methods" J. Geophys. Res. 69, No. 4, 1964.

Gjessing, D. T. "An Experimental Determination of the Spectrum of Permittivity and Air Velocity Fluctuations along a Vertical Direction in the Troposphere using Radio Propagation Methods," J. Atmos. Terr. Phys., 26, No. 2, 1964.

Gjessing, D. T. "On the Scattering of Electromagnetic Waves by Nonisotropic Inhomogeneities in the Atmosphere," J. Geophys. Res., 67 No. 3, 1017, 1962.

Gjessing, D. T. and Irgens, F. " On the Scattering of Electromagnetic Waves by a Moving Tropospheric Layer having Sinusoidal Boundaries," IEEE Trans., PTGAP, AP12, No. 1, 1964; Int. Rept. R-124, NDR.

Glass, B. V. Generalized Earth's Curvature Correction, AD 122 260.

Goldie, A. "Waves at an Approximately Horizontal Surface of Discontinuity in the Atmosphere," Quart. J. Res. Met. Soc., 51, pp. 239-246.

Gordon, W. E. and Waterman, A. T. "Angle-of-Arrival Aspects of Radio Meteorology, U. of Texas, EERL-1, March 1946.

Gordon, W. E. Inhomogeneities in the Troposphere and Stratosphere, Cornell U., Astia, AD 136 840.

Gossard, E. E., "Power Spectra of Temperature, Humidity and Refractive Index from Aircraft and Tethered Balloon Measurements," IRE. Trans., AP-8, No. 2, March 1960, pp. 186-201.

Gossard, E. E. "The Reflection of Microwaves by a Refractive Layer Perturbed by Waves," Trans. IRE, A. Pr., AP-10, 1962, pp. 317-325.

Gossard, E. E. and Munk, W. "On Gravity Waves in the Atmosphere," J. Met., 11, No. 4, 1962, pp. 259-269.

Gossard, E. and Michaelis, J. Distribution of Refractivie Layer Over the North Pacific and Arctic, USN Electronics Lab., Rept. No. 841, AD 205 224

Gossard, E. "Power Spectra of Temp Humidity and Refractive Index from Aircraft and Tethered Balloon Measurements," IRE Trans., PGAP, March 1960, p. 186.

Gracely, F. R. An Investigation of the Wave-Propagation Aspects of Surface-Based Surveillance Radar Performance, Air Force Operations Analysis Div., AD 6122, TM No. 39 January 1953.

Hadeen, K. D. Microwave Potential Refractivity Distribution over the Gulf of Mexico, Texas A. & M., AD 249 243, January 1961.

Hamilton, G. D. Subsidence Inversions and Associated Refractive Index in the Pacific High Pressure Cell, AD 230 566, 1959.

Hamlin, E. W., Gordon, W. E. and Lagrone, A. H. X-Band Phase Front Measurements in Arizona During April 1946, U. of Texas, EERL Rept. 6, February 1947.

Haragan, D. R. Moist-Term Refractivity as an Aid in Forecasting Tropospheric Refractivity Fields, Texas A. & M., MS Thesis, August 1960.

Harrington, E. L. Cloud Refractive Index Studies, Part II, U. of Chicago, Cloud Physics Lab., Tech. No. 21, AD 239 789, May 1960.

Hay, D. R. and Reid, W. M. 1962 "Radar Angels in the Lower Troposphere," Can. J. Phys., 40, No. 1, 1962, pp. 128-138.

Hay, D. R. and Turner, H. E. "Refractometer Measurements at High Relative Humidities," Proceedings of the International Symposium on Humidity and Moisture, Washington, D. C. May 1963.

Hay, D. R. and Turner, H. E. Investigation of Refractometer Measurements in the Atmosphere at High Relative Humidities and Temperatures, Final Report AFCRL-63-631 on Contract AF 19(628)-444. Dept. of Physics, U. of Western Ontario, London, Canada, 1963.

Herman, E., Rentschler, M., Russell, W. and Dodds, B. Radio Propagation Study Interim Engineering Report, AD 234 345.

Herzberger, M. "Automatic Ray Tracing; Formulas for Refraction or Reflection," Opt. Soc. Am. J. 47:736-9, August 1957.

Hinds, C. A. Data for Predicting Dependable Air-to-Air Radar Range, WADC Tech. Rept. No. 56, AD 101 277, April 1956.

Hines, C. A. Study of Propagation Conditions at Vero Beach, AD 118 200, April 1957.

Hines, C. A. and Tobias, J. J. Tropospheric Refractive Index Measurements in Eastern Colorado During August 1954, Wright Air Development Center, TM-55-482, AD 89 093, November 1955.

Hoidale, G. B. Index of Refraction Data Procurement and Reduction (Microwave), Missile Geophysics Program, WSPG Prog. Report No. 3, February 1957.

Hoidale, G. B. and Glenn, B. Microwave Refractive Conditions Over WSMR, July Through December 1957, WSMR, TM 610, Progress Report NR6, February 1959.

Hooper, A. H. and Taylor, A. P. Radio Refraction in the Free Atmosphere, Meteor. Research Comm., Rept. MRP 1021; SC 1/121, AD 139 540.

Horn, J. D., Bean, B. R. and Riggs, L. P. Some Meteorological Aspects of the Radio Refractive Index, NBS Boulder Labs., Rept. 6066.

Hunt, Wade T. Catalogue of Ray Tracing Patterns through a Nonstandard Atmosphere, Wright Air Development Division, USAF, AD 265 029.

Hunter, C. Proceedings of the First Joint NRD-ESD Calibration Conference, September 1 and 2, 1964, ESD-TDR-64-611, to be published.

Jehn, K. H. The Use of Potential Refractive Index in Synoptic-Scale Radio Meteorology, U. of Texas, EERL Rept. 6-29 (see Periodical P186), September 1959.

Jehn, K. H., Koscielski, A. and Fannin, B. M. Further Studies of the Variations of Radar Elevation Angle Errors for Selected U. S. Locations, U. of Texas, EERI. Rept. No. 7-07, October 1955.

Jehn, K. H. Refractive Index Distribution Associated with the Texas Gulf Cyclone and the Central U. S. Cold Outbreak, U. of Texas, EERL Rept. 7-10, AD 154 626, April 1957.

Jehn, K. H. Variability of Microwave Refractive Index at the Surface and at 850 MBs over Canada and Alaska in April and October, U. of Texas, EERL Rept. 7-17, August 1958.

Johannessen, K. R. Computation of Atmospheric Refractivity on the USAF Skew T, Log P Diagram, AWS Tech. Rpt. No. 169, 1963, 7 pp.

Katzin, M., Bauchman, R. W. and Binnian, W. "3-and 9-Centimeter Propagation in Low Ocean Ducts," Proc. IRE, Vol. 35, No. 9 , September 1947.

Kiely, D. G. and Carter, W. R. An Experiment Study of Substandard Propagation over an Optical Sea Path at 3 CM Wavelength, ASRE Tech. Rept. No. TX-51-1, AD 42 366, January 1951.

Kennedy, J. T., Rossoni, J. W. "The Use of Solar Radio Emission for the Measurement of Radar Angle Error," Bell Sys. Tech. J., November 1962.

LaGrone, A. H. Doppler Errors Caused by Variations in the Electromagnetic Properties of the Atmosphere, U. of Texas, EERL Rept. No. 7-12, AD 148 443 September 1957.

Landry, P. M. and Parks, L. D., Atmospheric Refraction Effects on Tracking System Data, APGC TDR No. 63-28, Air Proving Ground Center, Eglin Air Force Base, Florida, September 1963.

Lukes, G. D. Meteorological Analysis of the Propagation of Microwaves with an Application to the Angle-of-Arrival Measurements", Evans Signal Lab., Tech. Memo No. TM-GE-10, May 1945.

Manasse, R. An Analysis of Angular Accuracies from Radar Measurements. MIT Lincoln Lab. Ground Rept. 32-24, AD 236 166, December 1955.

Mann, H. P., The Accuracy of AMR Instrumentation, AFMTC Technical Document Report, MTC-TDR-63-3, Air Force Missile Test Center, Patrick Air Force Base, Florida, December 1962.

Mann, H. P., The Accuracy of AMR Instrumentation RCA Systems Analysis TR No. 23, MTC-TDR-63-3, ASTIA Doc. No. AD-270800, Air Force Missile Test Center, Patrick Air Force Base, Florida, 17 December 1962.

Martin, C. F. and Carroll, C. L. Tropospheric Refraction Corrections and Their Residual Errors, MTC-TDR-64-3, February 1964.

Matschlie, Arnold Bibliography on Electromagnetic Wave Propagation, Sylvania, AD 216 404, April 1959.

McClure, R. M. and Smith, H. W. Statistical Analysis of Selected Tropospheric Microwave Refractive Index Recordings, U. of Texas, EERL Rept. 6-22, July 1957.

McDowell, C. I. Frequency Diversity, 6 and 12 GC, Conf. Paper CP-63-1158, June 1963.

Metcalf, D. F. The Requirement for Refractive Index Observations in Radar Evaluation Programs, U. of Texas, EERL Rept. 6-10, AD 71 930, July 1955.

Meteorological Aspects of Radio-Radar Propagation U. S. Navy Weather Research Facility AD 243 191, June 1960.

Meteorological Factors in Radio-Wave Propagation, The Physical Society, London, April 8, 1946.

Millman, G. H. An Analysis of Tropospheric Ionospheric and Extra-Terrestrial Effects on VHF and UHF Propagation, GE Company, Electronics Div., AD 137 969, October 1956.

Moler, W. F. and Gossard, E. E. Atmospheric Refraction Error in Radar Elevation Angles, USN Elec. Lab., No. 795, AD 205 22, July 1957.

Moyer, V. E. A Preliminary Synoptic Analysis of the Atmospheric Refractive Index Climatology of Alaska, U. of Texas, EERL Rept. No. S-06, AD 58 923, February 1955.

Moyer, V. E. Meteorological Analysis of Selected Offshore California Refractive Index Profiles, U. of Texas, EERL Rept. 6-09 AD 71 929. June 1955.

Moyer, V. E. Correlation of Tropospheric Refractive Index Fluctuations with Synoptic Meteorological Data, U. of Texas, EERL Rept. No. 6-14, May 1956.

Moyer, V. E. Further Synoptic Analyses of The Atmospheric Refractive Climatology of Alaska, U. of Texas, EERL Rept. No. 5-16, September 1956.

Moyer, V. E. and Gerhardt, J. R. A Preliminary Climatology of Refractive Index Layer Characteristics, I. Southwest Ohio and the Washington Coastline, U. of Texas, EERL Rept. 6-26, AD 160 841, November 1958.

Moyer, J. E. and Gerhardt, J. R. Survey of Microwave Refractive Index Analysis and Forecasting Techniques, U. of Texas, EERL Rept. No. 6-18, May 1957.

Muchmore, R. B. and Wheelon, A. D., "Line-of-Sight Propagation Phenomena–I. Ray Treatment;" Proc. IRE, 43, 10 October 1955, pp. 1437-1449; " II. Scattered Comp.," op. cit., pp. 1450-1458.

Naito, K. A. Method of Forecasting the Refractive Index of the Elevated Layer, Cornell Univ. Elec. Engr. Research Rept. No. EE 280, AD 90 390.

National Academy of Sciences. Final Report of the Panel on Tracking Data Analysis, June 1964.

Norton, K. A., "Recent Experimental Evidence Favouring the $\rho K_1(\rho)$ Correlation Function for Describing the Turbulence of Refractivity in the Troposphere and Stratosphere," J. A. T. P., 15, Nos. 3/4, 1959, pp. 206-227.

Ocura, Y. "The Relation between the Space- and Time-correlation Functions in a Turbulent Flow," J. Meteor. Soc., Japan, 31, 1953, pp. 1-10.

Ogura, Y. "Temperature Fluctuations in an Isotropic Turbulent Flow," J. Meteor., Soc., 15, 1958, pp. 539-546.

Page, R. M. and George, S. F. Errors in Altitude Triangulation Caused by Variation in Index of Refraction, NRL Rept. 3844, June 1951.

Pearson, K. E., Kasparek, D. D. and Tarrant, L. N. The Refractive Correction Developed for the AN/FPS 16 Radar at White Sands Missile Range, WSMR Tech. Memo 577, November 1958.

Pierson, A. L. III. Analysis of Wave Equations for Radio Propagation in Over-Water Ducts, U. of Texas, Master's Thesis, May 1949.

Plank, V. G. Spurious Echoes on Radar, A Survey, A. F. Cambridge Research Center, Geophysical Res. Paper 62 AD 215 470, May 1959.

Plank, V. G. Convection and Refractive Index Inhomogeneities, Pergamon Press Ltd., Ireland, 1959.

Proceedings of the Second Tropospheric Refraction Effects Technical Review Mecting (3 Volumes), March, April, May 1964; ESD-TDR-64-103; AD 435 973 (Vol. I); AD 441 576 (Vol. II); AD No. 442 626 (Vol. III).

Prosser, S. J. Microwave Refractive Index Profile for the Atmosphere over V from Radiosonde Data, WSPG Sup. to Tech. Report 18D, January 1957.

Prosser, S. J. Radio Climatology of the WSPG Area, Electromagnetic Radiation Through the Atmosphere Pr-Nr5, April 1958.

Riggs, L. P. and Bean, B. R. Radio Meteorological Data Available as of April 1, 1958, NBS Rept. 5565, April 1958.

Rainey, R. J. and Thorn, R. C. A Radar Refraction Correction for Symmetric and Nonsymmetric Tropospheric Index Distributions, Tech. Report EE-43, Engineering Exp. Station, U. of New Mexico, Albuquerque, New Mexico, AD 287 484, February 1961.

Ring, R. M., A Theoretical Study of Tropospheric Radiowave Propagation, AFCRL-63-713, May 1963.

Ringwalt, D. L., Instrumentation to Measure the Effect of Meteorological Parameters on the MISTRAM System and Preliminary Data Reduction, MR No. CLI-11/3, Electromagnetic Research Corporation, College Park, Maryland, 7 November 1963.

Richardson, D. J. The Estimation of Atmospheric Refraction from Azimuth and Elevation Data, Royal Aircraft Establishment (Gt. Brit.), AD 7829, February 1953.

Riggs, L. P. and Bean, B. R. Radio Meteorological Data Available as of April 1, 1958, NBS Rept. 5565, April 1958.

Root, L. W. Jr. Improved Microwave Phase Measurement Techniques, Directorate of Research and Development, U. S. Army Missile Command, Redstone Arsenal, Alabama, RE-TR-63-35; June 1963.

Schunemann, R. and Bull, G. "Uber die Abhangigkeit der Fluktuationen des atmospharischen Brechungsindex von den meteorologischen Parameters. Ergebnisse von Messungen mit einem Mikrowellen-Refractometer," Hochfrequenztechnik u. Blektroak, 70, 1961, pp. 104-111.

Schipper, R. J., Niemi, P. et al. Refraction Correction and Height Accuracy for Radar Height Finders, AVCO Mfg. Corp. Cincinnati, Ohio, Rept. No. EW 9929-TN-04-60, AD 319 110, September 1960.

Schmid, H. An Analytical Treatment of the Problem of Triangulation by Stereo-photogrammetry, Ballistic Research Laboratories Report 961, October 1955.

Schulze, A. E., and Tolbert, C. W., "Shape, Intensity, and Pressure Broadening of the 2.53-Millimeter Wavelength Oxygen Absorption Line," Nature, No. 4908, 1963, pp. 747-750.

Solem, R. J. and Marion, T. M. First Quarterly Report for Electromagnetic Propagation Study, WMEC Motorola, Inc., Reference Systems Lab. AD 157 751, December 1957.

Schmid, H. H. Accuracy Aspects of a World-Wide Passive Satellite Triangulation System, U. S. Coast & Geodetic Survey, Washington, D. C.

Schulkin, M. Determination of Microwave Atmospheric Absorption Using Extraterrestrial Sources, NRL Report 3843, 1941.

Seielstad, G. A., Morris D., Radhakrishnan, Y. and Wilson, R. W. Linear Polarization Measurements of the Decimeter Wavelength Radiation from Small Diameter Radio Sources, California Inst. of Technology, 1963.

Smith, E. D. and Fletcher, R. D. Tropospheric Weather Factors Likely to Affect Superrefraction of VHF-SHF Radio Propagation as Applied to the Tropical Western Pacific, Weather Bureau, Washington, D. C., Rept. No. RP-1, AD 64 589, July 1944.

Smith, H. W. and Straiton, A. W. Three-Centimeter Radio Wave Propagation in a Surface Duct over the Gulf of Mexico, U. of Texas, EERL Rept. No. 26, July 1949.

Steffen, W. Über ein batteriegespeistes Microwellen-Refraktometer geringer Grübe, Hochfrequenztechnik u. Blektroak, 70, 1961, pp. 47-54.

Stickland, A. C. "Refraction in the Lower Atmosphere and Its Application in the Propagation of Radio Waves," Phys. Soc. Royal Me. Soc., April 1956, pp. 253-67.

Straiton, A. W., Deam, A. P. and Walker, G. B. "Spectra of Radio Refractive Index Between Ground Level and 5000 Feet above Ground," IRE. Trans., AP-10, No. 6, November 1962, pp. 732-737.

Straiton, A. W. "An Extension of McFarlane's Method of Deducing Refractive Index from Radio Observations," Appl. Phys., Vol. 20, No. 2, February 1949, p. 228.

Straiton, A. W., Gerhardt, J. R., Gordon, W. E. and Williams, C. E. Horizontal Microwave Angle-of-Arrival Measurements along the Coast Line near Corpus Christi, Texas, U. of Texas, EERL Rept. No. 7, December 1946.

Straiton, A. W. and LaGrone, A. H. Determination of Modified Index of Refraction Profiles and Wave Attenuation from Radio Data, U. of Texas, EERL Rept. No. 25, April 1949.

Strand, K. J. Investigation of Atmospheric Refraction at Low Altitudes, Maxwell AFB, AD 6452, February 1958.

Strandberg, M. W. P., Meng, C. Y. and Ingersoll, J. G. The Microwave Absorption Spectrum of Oxygen, Tech. Rept. No. 87, Research Laboratory for Electronics, M. I. T., 1948.

Swanson, L. W. Logistics and Time Schedules for a World-Wide Satellite Triangulation Program, U. S. Coast & Geodetic Survey, Washington, D. C.

Taylor, P. B. Atmospheric Effects on Microwave Radio Propagation, WADC Tech. Rept. 54-549, AD 64 927, December 1954.

Temple, E. Equation Designed to Correct Radar Range and Angle Information for Errors Caused by Atmospheric Refraction, Rept. No. TM-1072, RCA Electronics & Controls Div., April 1960.

Texas, University of, Final Report on Refraction Measurements, EERL Rept. No. 6-19, AD 117 023, March 1957.

Texas, University of, Catalogue of Microwave Refractive Index Recordings on File, EERL Rept. No. 6-17, 25-26, AD 133 769, August 1956.

Thayer, G. D. "A Formula for Radio Ray Refraction in an Exponential Atmosphere," J. Res. NBS, (Radio Prop.), 65D, No. 2, October 1960, pp. 181-182.

Thayer, G. D. and B. R. Bean "Systematic Atmospheric Refraction Errors of Baseline-Type Radio Tracking Systems and Methods for Their Corrections;" to be published in the Proceedings of the First Space Congress, Cocoa Beach, Fla., 1964.

Thompson, M. C. Jr. and Freethey, F. E. Hourly Correlation of Radio Path Lengths and Surface Refractivity Index from Maui, T. H., Phase Stability Program, NBS Report 5579, Project 8360-12-8865, 24 June 1958.

Thompson, M. C. Jr. and Janes, H. B., Preliminary Measurements of Phase Stability over Low-Level Tropospheric Paths, NBS Report 6010 Project 8300-11-8805, 20 September 1958.

Thompson, M. C. Janes, H. B. and Freethey, F. E. Atmospheric Limitations on Electronic Distance Measuring Equipment, NBS Report 6060, May 1959.

Thompson, M. C., et al. Final Report on Phase Stability Studies of Ground-to-Ground Microwave Links, NBS Report 6702, June 1960.

Turner, H. E. and Hay, D. R. "Fine Structure of Temperature and Refractivity in the Lower Troposphere," Can. J. Phys., 41 No. 10, 1963, pp. 1732-1737.

VonRosenberg, Charles E. An Analysis of Atmosphere Refractive Index Fluctuation as Recorded by An Airborne Microwave Refractometer, U. of Texas, Master's Thesis, January 1953.

Vysokovskie, D. M. Some Problems in Long Range Propagation of Microwaves in the Troposphere, Academy of Science, USSR, AFCRC-TR-59-151, AD 216 238, 1958.

Wagner, N. K. Microwave Index of Refraction Fluctuations Associated with Certain Meteorological Situations in the East and Central U. S., U. of Texas, EERL Rept. No. 6-17, September 1956.

Wagner, N. K. A Preliminary Climatology of Refractive Index Layer Characteristics. II. Southern California Coastal Areas, U. of Texas, EERL Rept. No. 6-28, May 1959.

Wagner, N. K. An Analysis of Radiosonde Effects on the Measured Frequency of Occurrences of Ducting Layers, U. of Texas, EERL Rept. No. 6-31, AD 229 858, December 1959.

Wait, J. R. On Radio Wave Propagation in an Homogeneous Atmosphere, NBS Report 6035, August 1959.

Waldron, C. G. Some Examples of Exponential Refractivity Distribution, U. S. N. Postgraduate School, Monterey, Calif., 1960.

Walker, G. B. Power Spectrum and Correlation Function Evaluation of Selected Tower Refractometer Measurements, U. of Texas, EERL Rept. No. 6-43, December 1961.

Waterman, A. T. and Strohbehn, J. W. "Reflection of Radio Waves From Undulating Tropospheric Layers," J. Res. NBS, (Radio Prop.) 67D, No. 6, 1963, pp. 609-616.

Weickmann, H. K. Review of Interactions Between Atmosphere and Wave Propagation, United States Army, Electronics Research and Development Laboratories, Fort Monmouth, N. J., USAELRDL-TR-2437, March 1964.

Weisbrod, S. and Heritage, J. L. Ionospheric Refraction and Faraday Effect at Frequencies above 100 MC, AD 138 621, March 1956.

Wexler, R. Theoretical Analysis of Errors in Radar Due to Atmospheric Refraction, Rept. No. TM-GE-6, US Signal Corps Ground Signal Agency, Fort Monmouth, N. J.,

Wheelon, A. D. "Near-Field Corrections to Line of Sight Propagation," Proc. IRE, Vol. 43, 1955 p. 1460.

Wheelon, A. D., "Radio-Wave Scattering by Tropospheric Irregularities," J. Res. NBS, (Radio Prop.), 63 D, 2, September-October 1959, pp. 205-233.

Woodring, M. J. A Compilation of Papers Presented at the Fifth Joint AFMTC/ Range User Data Conference, MTC-TDR-64-5, April 1964.

Yates, H. W. Atmospheric Refraction over Water, Naval Research Lab., AD 105 380, July 1956.

Zinichev, V. A., Ryzkov, IU. A. and Iudin, O. I. Method of Investigating Radio Waves in the Troposphere under Large Angles, Morris D. Friedman, Inc., W. Newton, 65, Mass., AD 262 415, May 1961.

LIST OF ATTENDEES

THIRD TROPOSPHERIC REFRACTION EFFECTS MEETING, 28-30 JULY 1964

Held at

The MITRE Corporation

Bedford, Massachusetts

Preston H. Allen
Gemini Program Office, NASA-MSC,
Houston, Texas

Dr. Edward Altshuler
AFCRL, Bedford, Massachusetts

Jorge L. Alvarez
NASA, Goddard Space Flight Center
Code 525, Greenbelt, Maryland

Byron Bailin
Rome Air Development Center
Griffiss Air Force Base, New York

Dr. J. G. Barry,
The MITRE Corporation, D-08
Bedford, Massachusetts

David K. Barton
Raytheon Company
Wayland, Massachusetts

Richard T. Brown
Sperry Rand Research Center
Sudbury, Massachusetts

Maj. R. Burnham,
ESD, Range Measurements
L. G. Hanscom Field
Bedford, Massachusetts

Arthur V. Carlson
U. S. A. Electronic Research &
Development Activity
Fort Huachuca, Arizona

Dr. Charles L. Carroll
M. U. 844 Pan American Airways
Patrick Air Force Base, Florida

James H. Chisholm
MIT Lincoln Lab.
Lexington, Massachusetts

Maj. James F. Church
AFCRL (CRHC),
L. G. Hanscom Field
Bedford, Massachusetts

Maj. John R. Clark,
ESD Staffmet Office (ESTW),
L. G. Hanscom Field
Bedford, Massachusetts

Gary T. Coats
AFCRL (CRDT), Hanscom Field
Bedford, Massachusetts

Raymond J. Connolly
Electronic News
Boston, Massachusetts

Dr. H. E. Cramer
Geophysics
Burlington, Massachusetts

R. K. Crane
The MITRE Corporation, D-81
Bedford, Massachusetts

Lt. John A. Cribbs, Jr.
HQ AFETR,
Patrick Air Force Base, Florida

Dr. Robert M. Cunningham
AFCRL (CRHC),
L. G. Hanscom Field
Bedford, Massachusetts

Harold T. Dougherty
National Bureau of Standards
Boulder, Colorado

Dr. Warren A. Dryden
RCA/AMR,
Patrick Air Force Base, Florida

Capt. E. G. Eames HQ ESD ESRIM,
L. G. Hanscom Field
Bedford, Massachusetts

Kathryn Erat
The MITRE Corporation, D-73
Bedford, Massachusetts

Dr. Harold I. Ewen
Ewen-Knight
Natick, Massachusetts

Vincent J. Falcone
AFCRL, Microwave Physics
L. G. Hanscom Field
Bedford, Massachusetts

William A. Farone
USA-ERDA SELWS-MA
White Sands Missile Range,
White Sands, New Mexico

Dr. Louis J. Galbiati
The MITRE Corporation, D-82
Bedford, Massachusetts

Colin Gardner
Code 3201-5 Box 8, HQ Pacific
Missile Range, Pt. Mugu, California

Dr. Paul Z. Gast
AFCRL, Hanscom Field
Bedford, Massachusetts

Dr. Ernest Gehrels
MIT Lincoln Lab.
Lexington, Massachusetts

Lt. Kenneth W. Graham
Space Systems Division
AF Unit PO
Los Angeles, California

B. M. Hadfield, D-80
The MITRE Corporation
Bedford, Massachusetts

Oscar T. Halley
The MITRE Corporation, D-62
Bedford, Massachusetts

Joseph F. Hannigan
U. S. Army Corps of Engineers
GIMRADA Ft. Belvoir, Virginia

Dr. Fred S. Hanson
Range Operations Directorate
White Sands Missile Range,
New Mexico

Patrick J. Harney
AFCRL CRES (Aerospace Instrumentation)
Bedford, Massachusetts

Dr. Donald R. Hay
University of Western Ontario
London, Canada

Louis G. Hayden
Pan American Airways
Patrick Air Force Base, Florida

E. W. Heinzerling
General Electric Company
Syracuse, New York

Dr. George K. Hess
National Range Division, AFSC
Patrick Air Force Base, Florida

Dr. Donald M. Hill
General Dynamics/Astronautics
(Mail zone 036-10), Box 1128
San Diego 12, California

Theodore E. Johnson
The MITRE Corporation, D-82
Bedford, Massachusetts

Paul M. Kalaghan
Ewen-Knight Corporation
Natick, Massachusetts

Martin Katzin
Electromagnetic Research Corp.
5001 College Avenue
College Park, Maryland

Lt. Col. William H. Lake
HQ NRD (SCGRH),
Andrews Air Force Base,
Washington, D. C.

Donald S. Luczak
Rome Air Development Center
Griffis Air Force Base, New York

Dr. J. R. Meyer-Arendt
National Bureau of Standards
Boulder, Colorado

J. H. Meyer
Technical Operations, Inc.
Burlington, Mass.

Sheldon Newman
The MITRE Corporation, D-82
Bedford, Massachusetts

Kenneth A. Norton
National Bureau of Standards
Boulder, Colorado

Byron C. Potts
Rand Corporation
1700 Main Street
Santa Monica, California

Richard A. Profio
Technical Operations, Inc.
Burlington, Massachusetts

Col. R. D. Ragsdale
ESD L. G. Hanscom Field
Bedford, Massachusetts

Dwight L. Randall
U. S. Naval Research Lab.
Code 5273
Washington, D. C.

Harold M. Richardson
The MITRE Corporation, D-82
Bedford, Massachusetts

David Ringwalt
Electromagnetic Research Corp.
5001 College Avenue
College Park, Maryland

James F. Roche
Raytheon Company
Norwood, Massachusetts

Lyall G. Rowlandson
The MITRE Corporation, D-81
Bedford, Massachusetts

Stanley Sharenson
The MITRE Corporation, D-82
Bedford, Massachusetts

Dr. Dale Sheckels
University of Massachusetts
Amherst, Massachusetts

Spurgeon E. Smathers
U. S. Department of Commerce,
Coast and Geodetic Survey
Washington, D. C.

George J. Stiles
Ballistic Research Labs.
U. S. Army Aberdeen Proving Ground,
Maryland

Dr. A. W. Straiton
University of Texas, Box 7789
Austin, Texas

John F. Sullivan
The MITRE Corporation, D-82
Bedford, Massachusetts

Lt. Col. T. L. Summers,
ESD, L. G. Hanscom Field
Bedford, Massachusetts

William G. Tank
Boeing Company
Seattle, Washington

Dr. John O. Taylor
Northern Electric
Ottawa, Canada

Dr. Moody C. Thompson
National Bureau of Standards
Boulder, Colorado

James E. Tillman
Lincoln Lab., MIT Round Hill
South Dartmouth, Massachusetts

Dr. A. C. Traub
The MITRE Corporation, D-81
Bedford, Massachusetts

William W. Vickers
Technical Operations, Inc.
Burlington, Massachusetts

H. A. von Biel
Cornell Aero Labs.,
Buffalo, New York

Hillard M. Wachowski
Aerospace Corporation
Los Angeles, California

Dr. Alan T. Waterman
Stanford Electronics Lab.
Stanford University
Stanford, California

Brude F. Watson
Naval Weather Research Facility
NAS Norfolk, Virginia 23511

John Whipple
The MITRE Corporation, D-73
Bedford, Massachusetts

John T. Willis
The MITRE Corporation, D-82
Bedford, Massachusetts

Thomas H. Witherby
The MITRE Corporation, D-82
Bedford, Massachusetts

Lt. Col. Robert S. Wood
1370th Photomapping Wing,
Staff Weather Advisor,
Turner Air Force Base, Georgia

George R. Woodring
1370th Photomapping Wing,
Turner Air Force Base, Georgia

Dr. Joseph W. F. Ye
The MITRE Corporation, D-72
Bedford, Massachusetts

Security Classification

DOCUMENT CONTROL DATA - R&D

(Security classification of title, body of abstract and indexing annotation must be entered when the overall report is classified)

1. ORIGINATING ACTIVITY *(Corporate author)*

The MITRE Corporation
Bedford, Massachusetts

2a. REPORT SECURITY CLASSIFICATION

Unclassified

2b. GROUP

3. REPORT TITLE

Proceedings of the Third Tropospheric Refraction Effects Meeting
Vol. I Results and Status of Tropospheric Effects Measurement Programs

4. DESCRIPTIVE NOTES *(Type of report and inclusive dates)*

6. REPORT DATE	7a. TOTAL NO. OF PAGES	7b. NO. OF REFS
November 1964	252	339

8a. CONTRACT OR GRANT NO.	9a. ORIGINATOR'S REPORT NUMBER(S)
AF 19(628)-2390	
b. PROJECT NO. 705.1	ESD-TDR-64-148, Vol. I (of two volumes)
c.	9b. OTHER REPORT NO(S) *(Any other numbers that may be assigned this report)*
d.	

10. AVAILABILITY/LIMITATION NOTICES

Qualified requestors may obtain from DDC
DDC release to OTS authorized

11. SUPPLEMENTARY NOTES	12. SPONSORING MILITARY ACTIVITY
	Directorate of Aerospace Instrumentation Range Measurements Division, L. G. Hanscom Field, Bedford, Massachusetts

13. ABSTRACT

Publication covers the presentations made at the Third Tropospheric Refraction Effects Meeting, sponsored by the Electronic Systems Division of The Air Force Systems Command. The Meeting was held at The MITRE Corporation on July 28, 29 and 30, 1964. The Proceedings are being published in two volumes for ease in handling. Papers covering the work on tropospheric refraction, sponsored by the Electronic Systems Division in support of metric instrumentation on the national missile ranges, are contained in Volume I. While these papers are complete in themselves, many of the specific details on the work covered in the Proceedings of the Second Refraction Meeting (ESD-TDR-64-103) have not been repeated. The first volume also contains papers on the findings and recommendations of the National Academy of Science's "Panel on Tracking Data Analysis" in the area of tropospheric propagation and refraction, refractometer and humidiometer development of the Naval Research Laboratory, the spaced refractometer program of the Eastern Test Range and Canadian tropospheric measurement activities. Presentations on certain refraction activities at the Pacific Missile Range, the National Bureau of Standards, Ft. Huachuca, Ballistic Research Laboratory, M.I.T. Round Hill, and Cold Lake, Canada, on new measurement techniques and on tropospheric and Ionospheric effects on interferometer systems, are included in Volume II.

DD FORM 1 JAN 64 1473

Security Classification

14 KEY WORDS	LINK A		LINK B		LINK C	
	ROLE	WT	ROLE	WT	ROLE	WT
Angle of Arrival (electromagnetic waves) Electromagnetic Waves Ionospheric Propagation Multipath Transmission Phase Measurement Interferometers Polariscopes Refractometers Tracking Telescopes						

INSTRUCTIONS

1. ORIGINATING ACTIVITY: Enter the name and address of the contractor, subcontractor, grantee, Department of Defense activity or other organization *(corporate author)* issuing the report.

2*a*. REPORT SECURITY CLASSIFICATION: Enter the overall security classification of the report. Indicate whether "Restricted Data" is included. Marking is to be in accordance with appropriate security regulations.

2*b*. GROUP: Automatic downgrading is specified in DoD Directive 5200.10 and Armed Forces Industrial Manual. Enter the group number. Also, when applicable, show that optional markings have been used for Group 3 and Group 4 as authorized.

3. REPORT TITLE: Enter the complete report title in all capital letters. Titles in all cases should be unclassified. If a meaningful title cannot be selected without classification, show title classification in all capitals in parenthesis immediately following the title.

4. DESCRIPTIVE NOTES: If appropriate, enter the type of report, e.g., interim, progress, summary, annual, or final. Give the inclusive dates when a specific reporting period is covered.

5. AUTHOR(S): Enter the name(s) of author(s) as shown on or in the report. Enter last name, first name, middle initial. If military, show rank and branch of service. The name of the principal author is an absolute minimum requirement.

6. REPORT DATE: Enter the date of the report as day, month, year; or month, year. If more than one date appears on the report, use date of publication.

7*a*. TOTAL NUMBER OF PAGES: The total page count should follow normal pagination procedures, i.e., enter the number of pages containing information.

7*b*. NUMBER OF REFERENCES: Enter the total number of references cited in the report.

8*a*. CONTRACT OR GRANT NUMBER: If appropriate, enter the applicable number of the contract or grant under which the report was written.

8*b*, 8*c*, & 8*d*. PROJECT NUMBER: Enter the appropriate military department identification, such as project number, subproject number, system numbers, task number, etc.

9*a*. ORIGINATOR'S REPORT NUMBER(S): Enter the official report number by which the document will be identified and controlled by the originating activity. This number must be unique to this report.

9*b*. OTHER REPORT NUMBER(S): If the report has been assigned any other report numbers *(either by the originator or by the sponsor)*, also enter this number(s).

10. AVAILABILITY/LIMITATION NOTICES: Enter any limitations on further dissemination of the report, other than those imposed by security classification, using standard statements such as:

(1) "Qualified requesters may obtain copies of this report from DDC."

(2) "Foreign announcement and dissemination of this report by DDC is not authorized."

(3) "U. S. Government agencies may obtain copies of this report directly from DDC. Other qualified DDC users shall request through _____."

(4) "U. S. military agencies may obtain copies of this report directly from DDC. Other qualified users shall request through _____."

(5) "All distribution of this report is controlled. Qualified DDC users shall request through _____."

If the report has been furnished to the Office of Technical Services, Department of Commerce, for sale to the public, indicate this fact and enter the price, if known.

11. SUPPLEMENTARY NOTES: Use for additional explanatory notes.

12. SPONSORING MILITARY ACTIVITY: Enter the name of the departmental project office or laboratory sponsoring *(paying for)* the research and development. Include address.

13. ABSTRACT: Enter an abstract giving a brief and factual summary of the document indicative of the report, even though it may also appear elsewhere in the body of the technical report. If additional space is required, a continuation sheet shall be attached.

It is highly desirable that the abstract of classified reports be unclassified. Each paragraph of the abstract shall end with an indication of the military security classification of the information in the paragraph, represented as *(TS)*, *(S)*, *(C)*, or *(U)*

There is no limitation on the length of the abstract. However, the suggested length is from 150 to 225 words.

14. KEY WORDS: Key words are technically meaningful terms or short phrases that characterize a report and may be used as index entries for cataloging the report. Key words must be selected so that no security classification is required. Identifiers, such as equipment model designation, trade name, military project code name, geographic location, may be used as key words but will be followed by an indication of technical context. The assignment of links, rules, and weights is optional